SUPERCRITICAL PROCESSING OF ELECTRICALLY CONDUCTING POLYMERS

A Dissertation
Presented to
The Academic Faculty

By

Shutaro Kurosawa

In Partial Fulfillment
Of the Requirements for the Degree
Doctor of Philosophy in Chemical Engineering

Georgia Institute of Technology

May 2004

SUPERCRITICAL PROCESSING OF ELECTRICALLY CONDUCTING POLYMERS

Approved:

Dr. Amyn S. Teja, Chairman

Dr. Laren M. Tolbert

Dr. John D. Muzzy

Dr. Sue Ann Bidstrup-Allen

Dr. J. Carson Meredith

May 12, 2004

ACKNOWLEDGMENTS

I would like to gratefully acknowledge the advice and guidance of my advisor, Professor Amyn S. Teja, who always encouraged me to work hard and joyfully during this work. I would also like to express my appreciation for the numerous suggestions provided by the committee members: Dr. Laren M. Tolbert, Dr. Sue Ann Bidstrup Allen, Dr. J. Carson Meredith, and Dr. John D. Muzzy.

I would like to state my gratitude to all those who contributed their expertise to this work: to Dr. Janusz Kowalik and Dr. Tolbert's group members for continuous input and collaboration and for the use of their four-point probe and multimeter; to Dr. Yolande Berta for her assistance during the SEM measurements; to Dr. Charles A. Eckert, Dr. James S. Brown, Dr. Jason P. Hallett, and Dr. Jie Lu for the use of their high-pressure vessel, UV-Vis spectrometer, and fluorescence photometer; to Dr. David M. Collard and Mr. Ling Li for providing per/semi-fluorinated polythiophenes; to Dr. Christopher W. Jones and Mr. Benn C. Wilson for the surface area measurement of my porous substrate via their BET equipment; to Dr. Haskell W. Beckham and Mr. Christopher A. Hubbell for the use of TGA equipment in the TFE thermal analysis center; to Dr. Z. John Zhang and Ms. Christy R. Vestal for the conductivity measurement using their SQUID system; to Dr. Robert E. Guldberg and Ms. Angela S. P. Lin for mechanical testing; to Mr. Karsten G. Bartling for use of his optical imaging system. I am grateful to the Molecular

Design Institue/ the Office of Naval Research and Georgia Research Alliance, FPRI, and the Specialty Separations Center for funding assistance during this project.

I appreciate the friendship and support of the following people who helped me while I was studying in the Teja research group: Dr. Tongfan Sun, Dr. Takeshi Furuya, Dr. Kimberly Abbett, Dr. Linda Cote, Dr. Kerry Bullock, Dr. Hirohisa Uchida, Dr. Zhi Yun, Dr. Jeong Woo Lee, Ibrahim Ozkan, Chunbao Xu, Nantida Thamanavat, Michael Beck, Rebecca Shiels, James Fallabella, Myrna Guow, Yalin Hao, and Abel Zuniga-Moreno. I wish to express my sincere thanks to Dr. Ronald W. Rousseau and his group members, Dr. Kunio Arai, Dr. Hiroshi Inomata, and Dr. Richard Lee Smith, Jr. in Tohoku University, Dr. Hiroshi Ishida and Yukie Ishida from Tokyo Institute of Technology, and all the rest of my friends in Atlanta, Georgia and Japan.

Finally, and most importantly, this thesis is dedicated to my parents, Dr. Hideo Kurosawa and Chikako Kurosawa, my parents-in-law, Kunio and Mariko Akiba, and my family whose continuous backing and encouragement made this possible. Especially, I would never have finished this work without unceasing support given by my wife, Izumi.

TABLE OF CONTENTS

Page

LIST OF TABLES

Page

LIST OF FIGURES

Page

LIST OF SYMBOLS

a	distance between localized states
A_{SP}	specific surface area
d	film thickness
D	diameter of pores, diffusivity
D_{eff}	effective diffusivity,
e	electronic unit charge
E_A	activation energy
k	Boltzmann's constant
K	temperature-dependent constant
$M(t)$	mass gain at time t
M_W	mass of water in samples
M_∞	maximum mass gain
n	dimensionality of electrical conduction process
$N(E_F)$	density of states at Fermi energy
N_P	total number of pores per unit volume
P	probability of a hop per unit time
P_c	critical pressure
r	distance
$R,\ \overline{R}$	hopping distance

s	probe spacing
t	time
T	temperature
T_0	characteristic temperature of thermally assisted hopping
T_c	critical temperature
V_P	volume of polymer strips
W	activation energy
α	decay factor
λ	constant in equation (2-9)
ν_0	jump rate factor
ρ, ρ^*	density of solid materials and foams, resistance
ρ_P	polymer density
ρ_W	density of water
σ	conductivity
σ, σ^*	yield stress of solid materials and foams
$\sigma(T)$	conductivity at temperature T
σ_0	pre-exponential factor in equation (2-1)

SUMMARY

Thick composites (~ 3 mm in thickness) of polypyrrole with electrically insulating porous (polystyrene) and nonporous (polymethyl methacrylate) substrates were prepared using a two-step batch method. In the two-step method, impregnation of volatile (iodine) or nonvolatile (ferric chloride) oxidant in the substrate is followed by in-situ polymerization of pyrrole. Conductivities as high as 10^{-1} S/cm were obtained in this work in the case of composites of polypyrrole and porous, crosslinked polystyrene. Use of the nonvolatile oxidant (ferric chloride) resulted in higher conducting polymer yield, as well as composites having a higher conductivity, thermal stability, and mechanical strength. However, the volatile oxidant (iodine) could be transported to the substrate using supercritical carbon dioxide as the solvent. As a result, partitioning of the oxidant between the solvent phase and the polymer substrate, and hence the distribution of the oxidant in the substrate, could be controlled by manipulation of the pressure.

The amount of polypyrrole-oxidant complex produced in the in-situ polymerization step was linearly proportional to the amount of oxidant impregnated in the substrate. Since this amount is related to the level of conductivity in the composite, this work shows that the manipulation of pressure during the impregnation step can potentially be used to control the level of conductivity of the composite.

A disadvantage of using iodine as the oxidant is that it tends to diffuse out of the substrate because of its volatility, a process that is accelerated in the presence of

supercritical carbon dioxide. Thus, iodine was observed to diffuse out of the substrate when carbon dioxide was used to transport pyrrole to the substrate prior to the polymerization step of the process. This counter-diffusion led to the formation of a conducting surface layer, and hence a nonuniform distribution of polypyrrole, even at low polypyrrole concentrations. The nonuniform distribution of polypyrrole was verified by the measurement of a new property – the volume conductivity. When coupled with bulk and surface conductivity measurements, this property provides a good measure of the spatial distribution of conducting polymer in the composite. The volume conductivity data of this work were also consistent with morphological observations, which suggests that this property may be a useful characterization variable to consider in future investigations of electrical conductivity in thick composites.

Non-porous substrates such as polymethyl methacrylate (PMMA) require a solvent that is able to swell the polymer appreciably in order for the oxidant to dissolve/diffuse in the substrate. Although carbon dioxide is an excellent swelling agent for PMMA, the limited diffusivity of the monomer and oxidant in the PMMA did not allow the desired interconnected network of conducting polymer throughout the composite to be attained in this work. Furthermore, the plasticization effect of supercritical carbon dioxide on the thermoplastic PMMA induced foaming during depressurization, leading to low integrity of the surface conducting phase of the composite. Therefore, a porous substrate offers the best means for obtaining thick conducting composites with a specified level of conductivity.

The hypothesis that the distribution of the oxidant controls the level of conductivity of a composite was verified. As a result, the two-step batch method in which supercritical carbon dioxide is used to facilitate transport and as a solvent for the oxidant was found to be an effective method for the production of thick composites with uniform conductivity, thermal stability, and mechanical strength. Such composites are desired in important practical applications such as rechargeable battery electrodes and electromagnetic interference shielding materials.

CHAPTER 1

INTRODUCTION

Electrically conducting polymers such as polyacetylene, polyaniline, polythiophene, and polypyrrole have received much attention in the literature because they are known to have unique properties such as low density, versatility in methods of production (Ruckenstein and Park, 1991), high anisotropy of electrical conduction, and non-metallic temperature dependence of conductivity (Kaiser, 2001a). Their potential applications include rechargeable battery electrodes (Chandrasekhar, 1999b; Beck and Ruetschi, 2000), antistatic coatings (Defieuw *et al*., 1993), capacitors (Liu *et al*., 2003), electromagnetic interference shielding materials (Wong *et al*., 1992), electrochromic windows (Arbizzani *et al*., 1991), sensors for chemicals and biomolecules (Selampinar *et al*., 1995; Onoda *et al*., 1995; Brahim *et al*., 2002), recording materials (Falcao and DeAzevedo, 2002), nonlinear optical devices (Ghoshal, 1989), field-effect transistors (Koezuka and Tsumura, 1989), light-emitting diodes (Gao *et al*., 1996), separation membranes (Tishchenko *et al*., 2000; Singh *et al*., 2000), reinforced fibers for aircraft (Bhattacharya and De, 1996), printed circuit boards (Saurin and Armes, 1995), and drug delivery devices (Kontturi *et al*., 1998).

Conducting polymers for these applications are expected to have high performance and stability in terms of electrical, magnetic, optical, thermal, and

mechanical properties. For example, static charges such as those generated by walking across a synthetic fiber carpet or sitting in an armchair with polyurethane cushioning require shielding materials to withstand well over 10,000 V (Jonas and Heywang, 1994). Note that modern electronic components can be permanently damaged by a 100 V discharge. For shielding against electromagnetic interference, the Federal Communication Commission (FCC) requirements for commercial applications require conducting polymers with a shielding effectiveness greater than 40 dB at 1 GHz for use in electronic housings (Shacklette *et al*., 1992). Requirements for military applications are significantly higher, ranging between 80 and 100 dB. In mobile electronic devices, low-cost and low-weight plastics with sufficient conductivity for shielding are required to replace conventional internal metal shrouds (Huang, 1995).

For practical applications, stable and processable forms of the conducting polymers are required (Kossmehl and Engelmann, 1999). It has been reported that the properties of conducting polymers depend strongly on the processing conditions such as temperature, concentration, and stoichiometry as well as on the type of monomer, oxidant, dopant, and solvent used (Myers, 1986). Conducting polymers also tend to be brittle, infusible, and intractable because of the presence of conjugated double bonds and crosslinked covalent bonds, leading to strong inter- and intra-molecular interactions. Furthermore, such double bonds are easily oxidized, resulting in decomposition before melting, formation of covalent bonds or defects, and reduction in electrical conductivity along the main chain. Many attempts have therefore been made to overcome these limitations by designing new monomers, by developing new polymerization mechanisms

for conventional monomers, and by blending existing polymers (Brunswick *et al*., 1998). An example is the addition of alkyl side chains onto heterocyclic rings, yielding a polymer that is more soluble in conventional solvents and, can therefore be easily processed (Elsenbauer *et al*., 1986; Jen *et al*., 1986; Sato *et al*., 1986; Hotta *et al*., 1987; Kowalik *et al*., 2001). Chemical synthesis of polypyrrole soluble in organic solvents using acidic or polymeric dopants has also been studied (Lee *et al*., 1995; Lee *et al*., 1997a; Lee *et al*., 2000).

Composites of conducting polymers with insulating polymers are often used to impart synergistic effects such as mechanical strength, environmental stability, and processability to the materials (Park and Ruckenstein, 1992). The word 'composite' consists of the Latin prefix 'com' meaning 'together' and 'posit' meaning 'to put or place', which means 'put together or made up of separate parts' (Bhattacharya and De, 1996). At earlier stages of development, conductive composites were made by dispersing conductive particles such as carbon black, graphite fibers, and metals in insulating polymer matrices (Jagur-Grodzinski, 2002). More recently, interest has focused on composites of conductive and insulating polymers because of the versatility of their methods of production (Park and Ruckenstein, 1992). Conventional preparation methods such as melt mixing, solution casting, and fiber spinning have been used to obtain conducting polymer composites with desired properties. However, post-processing steps such as injection molding or compression molding often result in lower degree of network connectivity of conductive components by thermal degradation and/or mechanical distortion (Pionteck *et al*., 1999).

A composite will not require further post-synthesis steps if the conductive component is introduced in a suitably pre-molded host substrate (Roberts and Schulz, 1986). Coating of host substrates with conducting polymers is therefore an effective production method to build electrical conductive paths in the composite while retaining the mechanical properties of the host polymer (Nikpour *et al*., 1999). Furthermore, it has been reported (Martin, 1994; Wallace and Innis, 2002) that the use of open-pore structured templates enhances electrical conductivity by many orders of magnitude due to alignment of conducting polymer chains along pores as the diameter of the pore decreases to molecular scale. Unfortunately, organic and aqueous solvents containing various salts, complexes, by-products, and non-reacted residuals must be handled in most steps in polymer synthesis and processing, and economic and environmental objectives may have to be balanced in such processes (Mellor *et al*., 2001).

Environmental concerns related to the use of toxic organic solvent have led to a search for environmentally benign alternatives to conventional solvents in polymer processing (Subramaniam *et al*., 2002). Among candidate solvents, carbon dioxide (Tc=304.2 K, Pc=7.38 MPa) in both liquid and supercritical states has been favored because it is non-flammable, inexpensive, and environmentally benign. Supercritical carbon dioxide ($scCO_2$), especially, has been proposed as a solvent with 'tunable' properties for various applications such as extraction, purification, particle production, materials processing, and analysis (Teja and Eckert, 2000). The feasibility of a process to synthesize electrically conducting polymers and their composites with host substrates in $scCO_2$ has been demonstrated by Webb (2001), Abbett *et al*. (2003), and others (Kerton

et al., 1997; Fu *et al*. ,1997; DeSimone, 1998; Shenoy *et al*. ,2001; Weiss et al., 2002; Anderson *et al*., 2002; Tang *et al*., 2003a; Tang *et al*., 2003b; Shenoy *et al*. ,2003). However, such processes suffer from non-uniform distribution of the conductive component in the composite, resulting in relatively low conductivity. Figure 1-1 is an optical micrograph of a cross-section of a composite sample prepared in $scCO_2$ by Abbett *et al*. (2003). Thick black layers of a conductive complex of poly(3-undecylbithiophene) and ferric triflate can be seen up to a certain depth in the porous, crosslinked polystyrene substrate. Such a non-uniform distribution of the conducting polymer in the substrate probably is one of the reasons why the highest conductivity of the composite was of the order of 10^{-4} S cm^{-1}. The non-uniformity may be ascribed to limited diffusion of ferric triflate near the surface of the substrate because of its low solubility in $scCO_2$ (Shenoy *et al*., 2001).

It has been suggested that both the yield of the in-situ polymerization and the conductivity of the composite depend primarily on the amount of oxidant (ferric triflate in the above case) impregnated in the substrate (Fu *et al*., 1997). A sufficient amount of oxidant must therefore be partitioned evenly between the solvent and the host substrate in any process for the preparation of uniformly conductive composites.

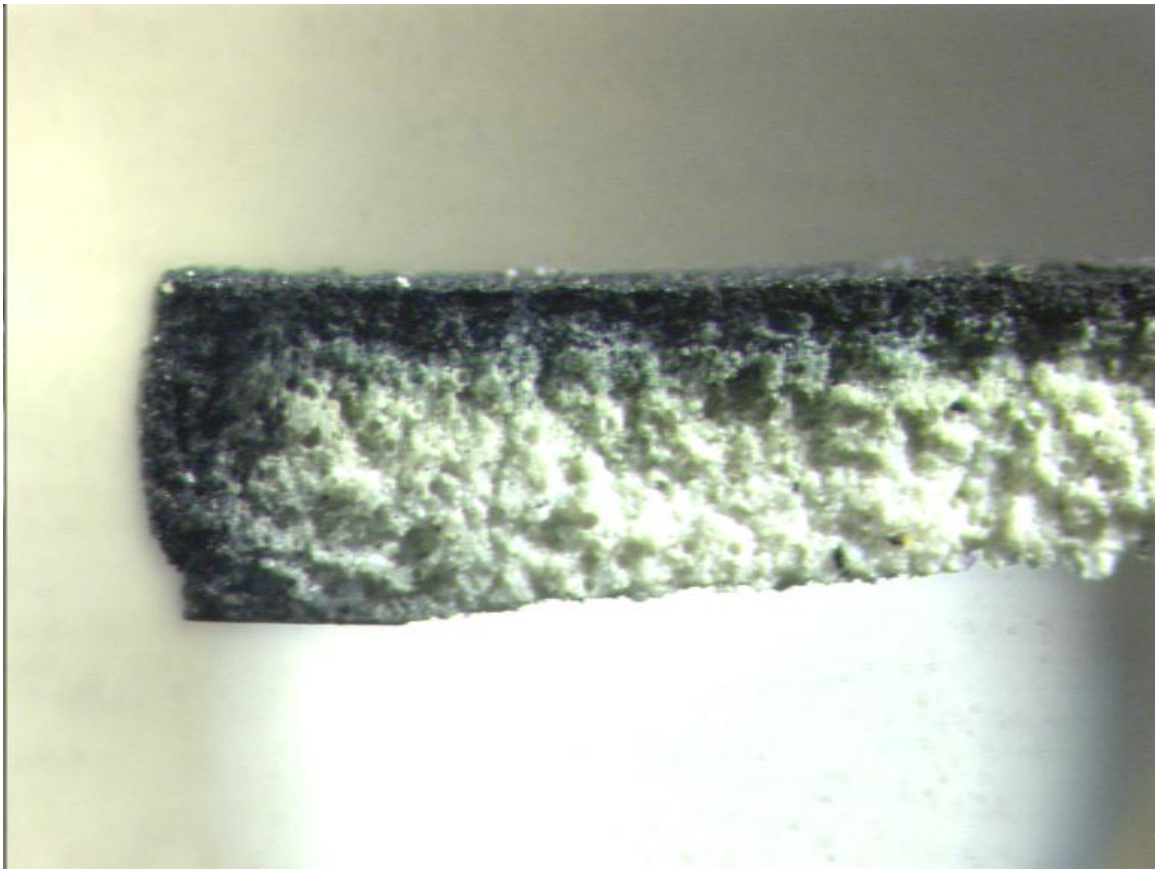

Figure 1-1. Optical micrograph of the cross-section of a poly(3-undecylbithiophene) composite in porous, crosslinked polystyrene synthesized in supercritical carbon dioxide by Webb (2001).

It should also be noted that most literature studies report the preparation of *thin* films of conducting polymers or composites, with very few studies of *thick* conducting materials. Thick films (thickness greater than 3 mm) are likely to suffer from non-uniform distribution of the conducting component that could very well affect the conductivity. Therefore, an objective of the present work is to identify key variables in the preparation of thick (3 mm) conducting composites for practical applications such as shielding materials. Conductivity in such composites is likely to be affected by the type of substrate, oxidant, and solvent, the distribution of oxidant and polymer in the substrate, and the preparation procedure. Among these variables, the oxidant solubility and diffusivity in the solvent are expected to have a significant impact on the level and uniformity of the conductivity. A hypothesis that will be tested is that uniform distribution of the oxidant in the host substrate leads to a composite with high conductivity.

Polypyrrole was chosen as a model conducting polymer in this research because it shows both good conductivity and relatively good environmental stability (Thieblemont *et al*., 1993). It also has the unique ability to form stable and uniform coherent films on hydrophobic surfaces (Kuhn and Child, 1998). Furthermore, Avlyanov *et al*. (1997) have shown that polypyrrole deposited on a hydrophobic polymeric substrate exhibits high conductivity. The host substrate chosen was porous, crosslinked polystyrene because it is easily prepared and provides a three-dimensional template (Ruckenstein and Park, 1991). The open-pore structure of the substrate is expected to enhance the diffusivity of reactants in the substrate. For comparison, poly(methyl methacrylate) will also be used as

a non-porous substrate in order to study the effect of substrate structure on the properties of the composites. Iodine was selected as an oxidant because it has appreciable solubility in $scCO_2$ (Fang *et al*., 1997) and ability to form charge transfer complexes with polypyrrole (Kang *et al*., 1987). For comparison, ferric chloride will also be used as a conventional Lewis acid oxidant to react with the weakly basic pyrrole monomer (Myers, 1986; Webb, 1998). The electrical conductivity and morphology of the resulting composites will be investigated in this work. Furthermore, electrical, thermal and mechanical properties will be studied to evaluate the composites for practical use. The ultimate goal of this research is to identify and thus control the properties of conductive composites. Potential applications for the type of conductive composites studied might be as rechargeable battery electrodes (Boinowitz *et al*., 1995; Beck and Ruetschi, 2000), antistatic packaging (Kuhn and Child, 1998), or electromagnetic interference shielding materials (Wong *et al*., 1992; Huang, 1995).

The organization of this thesis is as follows: In chapter 2, the literature on electrically conducting polymers and their composites is reviewed. In chapter 3, the preparation and characterization of porous, crosslinked polystyrene are described. In chapter 4, details related to the preparative procedures and characterization methods of polypyrrole composites with ferric chloride and iodine in porous and non-porous substrates are given. In chapter 5, the experimental results are discussed, and the effects of selected variables on the final properties of the composites are considered with theoretical models. Finally, in chapter 6 the conclusions of this research are outlined and recommendations for further study are listed.

CHAPTER 2

BACKGROUND

In 1977, Shirakawa *et al*. reported that the oxidation of trans-polyacethylene films with iodine vapor increased the conductivity of the films by seven orders of magnitude relative to their conductivity at room temperature. Since then, the intrinsic electrical, optical, thermal, and mechanical properties of conducting polymers have been extensively investigated (Kumar and Sharma, 1998; Wessling, 1998). Indeed, the Nobel Prize in Chemistry for 2000 was awarded to A. J. Heeger, A.G. MacDiarmid, and H. Shirakawa "for the discovery and development of electrically conductive polymers."

In this chapter, the literature on conducting polymers and their composites is reviewed, with emphasis on the synthesis, processing, and characterization of polypyrrole (PPy).

2-1 ***Electrically Conducting Polymers***

Electrically conducting polymers are generally comprised of C, H, and simple heteroatoms such as N and S. What differentiates electrically conducting polymers from other insulating polymers is their extended π-conjugation, in which π-electrons form delocalized conjugated bonds (Chandrasekhar, 1999a). Several examples of electrically conducting polymers such as polyacetylene, polyparaphenylene, polypyrrole, polyaniline,

and polyperinaphthalene are depicted in Figure 2-1. The conjugated structure allows mobility of charge carriers along polymer chains via a rearrangement of double bonds. Note that these polymers are “intrinsically” conducting and do not require any conducting fillers such as metal or carbon particles to impart conductivity. It should also be pointed out that other polymers such as polyesters, polyimides, and polyamides, have π-electrons, but they are all insulating as they lack extended conjugation.

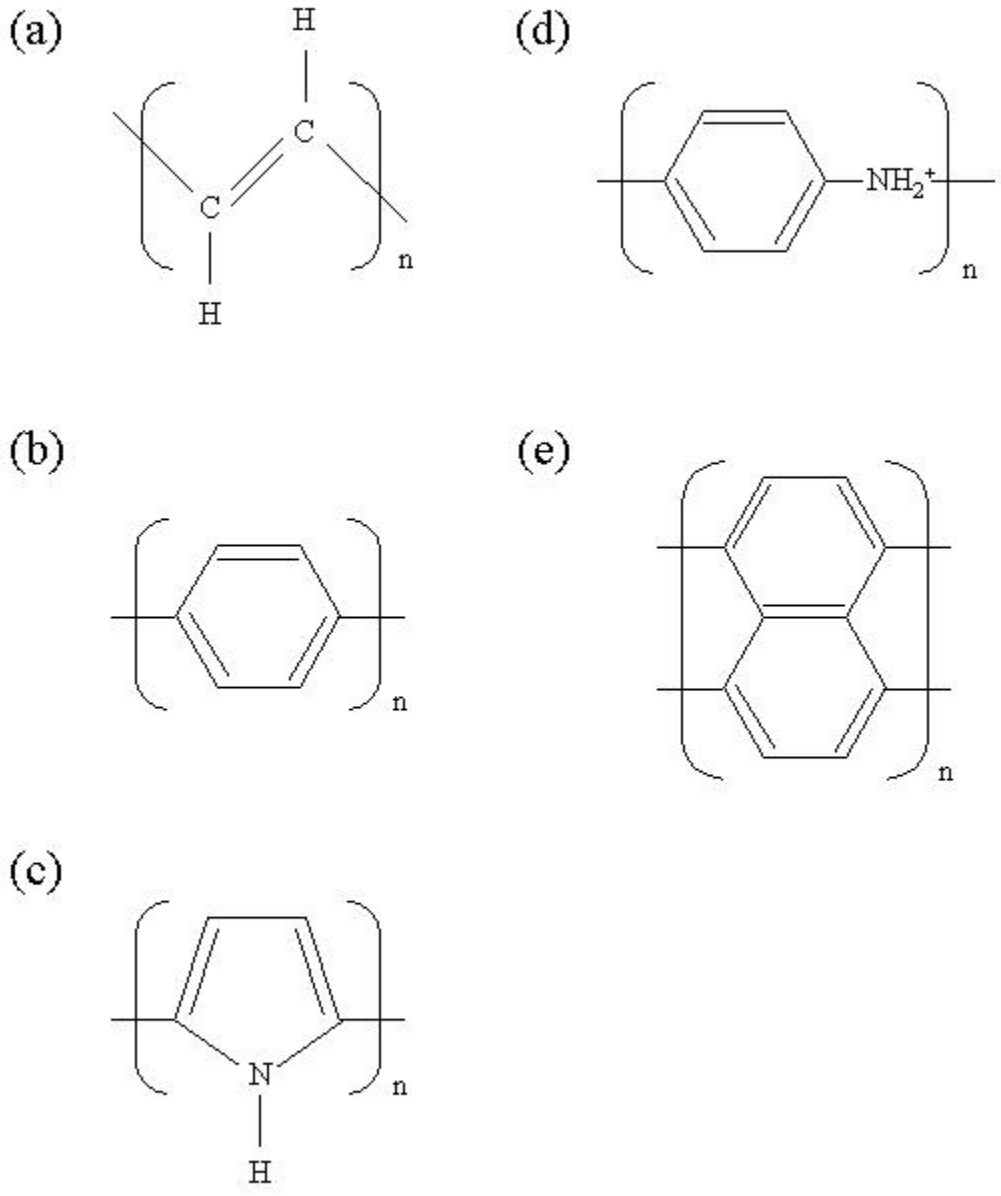

Figure 2-1. Electrically conducting polymers: (a) polyacetylene, (b) polyparaphenylene, (c) polypyrrole, (d) polyaniline, and (e) polyperinaphthalene.

2-1-1 **DC Conductivity**

Polymer conductivity depends strongly on their redox state. For example, the room-temperature dc conductivity of PPy in its oxidized state can exceed the upper limit of the semiconducting range, whereas the polymer conducts poorly in its reduced state (Saunders *et al*., 1995). In order to maintain the oxidized or reduced state, addition of electron acceptors or donors has been utilized in the literature (Walker *et al*., 1988; Chandrasekhar, 1999a). This is referred to as doping, a term borrowed from the semiconductor field. Note, however, that the concentration of dopant in conducting polymers is orders of magnitude greater than typical doping concentrations for semiconductors (Kaiser, 2001a), and that doping is a process of oxidation or reduction in the chemical and electronic sense, not in the inorganic semiconductor sense (Chandrasekhar, 1999a).

Upon doping of PPy by addition of an oxidant (dopant), for instance, both a positive charge and an unpaired electron associated with a quinoid structure over 4 to 5 rings are formed as a result of the removal of an electron from a polymer chain (Bredas *et al*., 1984a). The resulting p-doped structure is referred to as a polaron, and the unpaired electron occupies a bonding state with a spin of one-half. Further oxidation of a PPy chain containing a polaron forms a bipolaron, which is doubly charged and diamagnetic. The formation of a bipolaron is energetically favorable by 0.45 eV over that of two polarons at higher oxidation level according to the tight-binding Huckel theory (Bredas *et al*., 1984b). The positive charges may move via a rearrangement of the conjugated bonds

along polymer chains. Therefore, the bipolaron is a major charge carrier in doped PPy, which is confirmed by the absence of an electron spin resonance signal in electrochemically cycled highly conducting films (Scott *et al*., 1983). Figure 2-2 represents such charge carriers in an idealized PPy polymer chain. In spite of the fact that PPy has a lower degree of crystallinity and greater disorder compared to polyacetylene and polyaniline, the highest room-temperature conductivity of doped PPy is comparable to that of polyaniline (~ 10^3 S cm^{-1}), and can be higher than that of plastics with conducting filler (Kumar and Sharma, 1998). This 'quasi-1D' picture of *inter*-chain metallic conduction becomes less dominant than a hopping mechanism of *intra*-chain conduction as disorder is increased, which is indicated by the conductivity data as a function of temperature in conducting polymers (Kaiser, 2001a). This is discussed in the following section.

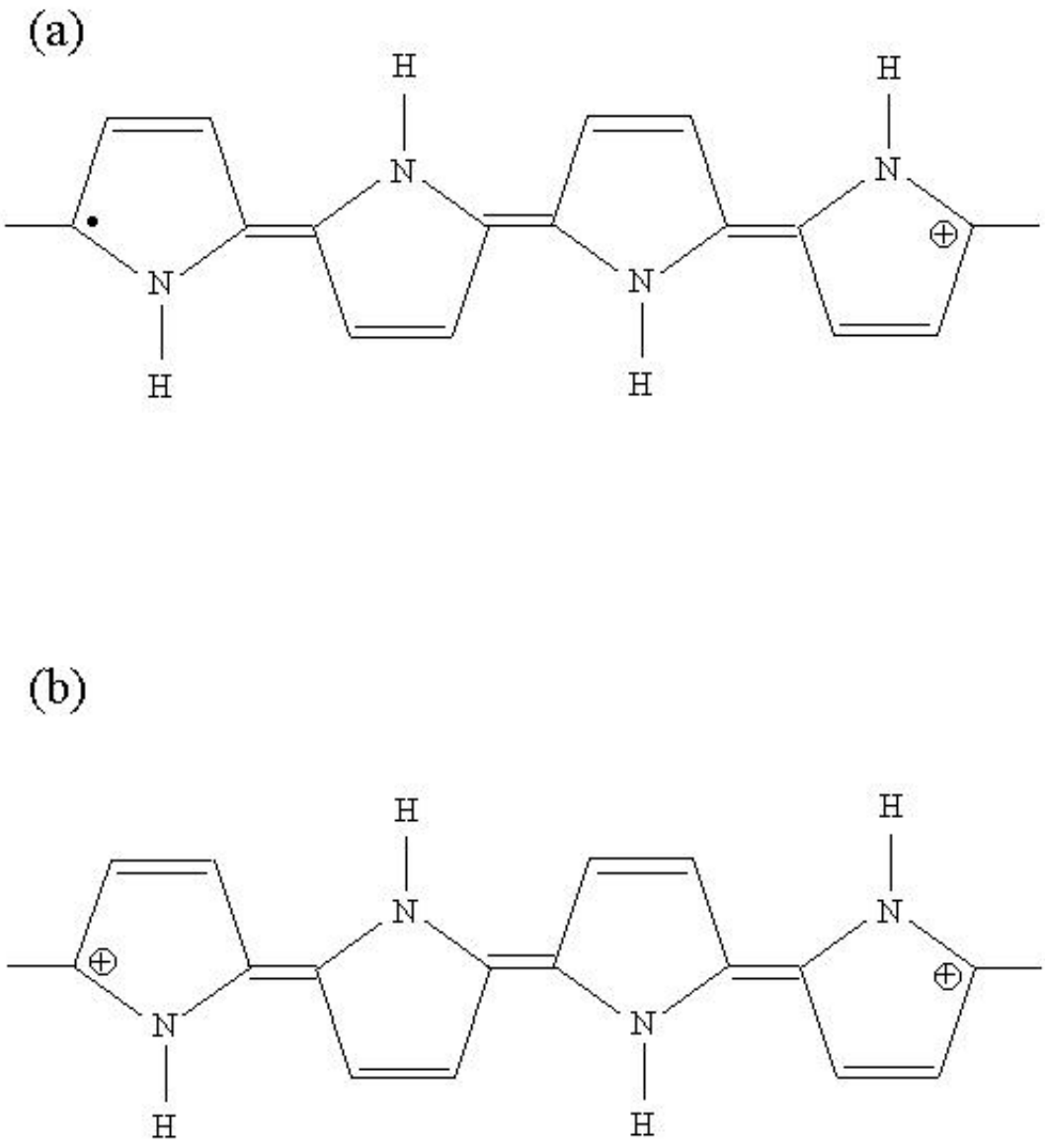

Figure 2-2. Charge carriers in polypyrrole: (a) polaron, and (b) bipolaron.

2-1-2 **Temperature Dependence of Conductivity**

The conductivity of the most highly conducting polymers is as high as those of traditional metals at room temperature. However, the temperature dependence of conductivity of typical organic conducting polymers exhibits non-metallic sign (conductivity increases with temperature), which has been a challenge for conventional ideas of metallic charge transport (Kaiser, 2001a; Kaiser, 2001b).

The temperature dependence of conductivity of electrically conducting polymers is often interpreted using Mott's law for variable-range hopping (VRH). The model was derived based on amorphous semiconductors in which charge carriers such as electrons, holes, and ions move between localized states whose energies are compatible to the Fermi energy (Saunders *et al*., 1995). More specifically, Mott's law is based on Miller-Abrahams hopping or nearest-neighbor hopping at sufficiently low temperatures (Mott and Davis, 1979). The localized energy states correspond to structural disorder arising from imperfect crystallinity, lower degree of conjugation, and the presence of impurities. As temperature decreases, thermal energy kT decreases, and there are fewer neighbor states with accessible energies, so the mean range of hopping of charge carriers increases. This leads to the following expression for the conductivity:

$$\sigma = \sigma_0 \exp\left[-\left(\frac{T_0}{T}\right)^{1/(n+1)}\right] \tag{2-1}$$

where σ_0 is a pre-exponential factor, T_0 is the characteristic temperature of thermally assisted hopping, and n is the dimensionality of the process (n = 1, 2, or 3). If n equals three in equation (2-1), the so-called "$T^{-1/4}$" law is obtained, denoting a three-dimensional

transport process. This is the most often observed temperature behavior in conducting polymers (Aguilar-Hernandez and Potje-Kamloth, 2001). In the three-dimensional hopping description, an electron in a Fermi glass (a degenerate electron gas in a highly disordered medium) will normally hop to a site at a hopping distance R smaller than the distance "a" between localized states at a temperature T. This implies that the electron will have available $4\pi(R/a)^3/3$ sites. It will normally jump to a site for which the activation energy W is as low as possible, and for this site:

$$W = \frac{3}{4\pi R^3 N(E_F)} \tag{2-2}$$

where $N(E_F)$ is the density of states at the Fermi energy.

The average hopping distance is:

$$\overline{R} = \frac{\int_R r^3 dr}{\int_R r^2 dr} = \frac{3R}{4} \tag{2-3}.$$

So, the probability of a hop per unit time is:

$$P = \nu_o \exp\left(-2\alpha\overline{R} - \frac{W}{kT}\right) \tag{2-4}$$

where ν_o is a jump rate factor, and k is Boltzmann's constant. Here α is defined so that $\exp(-\alpha r)$ is the rate at which the atomic wavefunction on a single potential well falls off with distance r. Assuming that ν_o varies little with R or T, the maximum value of P is obtained when the derivative of equation (2-4) with respect to R is zero:

$$\frac{3}{2}\alpha = \frac{9}{4\pi R^4 N(E_F) kT} \tag{2-5}$$

giving for the optimum value of R:

$$R = \left(\frac{3}{2\pi\alpha N(E_F)kT} \right)^{1/4} \tag{2-6}.$$

Therefore, the hopping probability becomes

$$P = \nu_o \exp\left(-\frac{3}{\pi R^3 N(E_F)kT} \right) \tag{2-7}.$$

The conductivity will be obtained by:

$$\begin{aligned} \sigma &= e^2 N(E_F) \overline{R}^2 P \\ &= K_0 T^{-1/2} \exp\left(-\left(\frac{T_0}{T} \right)^{1/4} \right) \end{aligned} \tag{2-8}$$

where e is electronic unit charge,

$$T_0 = \frac{\lambda\alpha^3}{kN(E_F)} \tag{2-9}$$

and

$$K_0 = \left(\frac{3e}{4} \right)^2 \left(\frac{3N(E_F)}{2\pi\alpha k} \right)^{1/2} \nu_o \tag{2-10}.$$

In the original description, $\lambda = 24/\pi$ in equation (2-9); however, $\lambda = 16$ (Epstein *et al*., 1983; Roy *et al*., 1991) or $\lambda = 18.1$ (Paul and Mitra, 1973; Singh *et al*., 1991a; Singh *et al*., 1993) has been generally used since Ambegaokar *et al*. (1971) have shown its lower limit to be 16 from a percolation concept.

One alternative model is the charge-energy-limited tunneling (CELT) model (Sheng and Abeles, 1972; Sheng *et al*., 1973). The model was proposed to account for the

charge transport in a system where metallic particles were embedded in an insulating matrix. The temperature dependence of conductivity in the composite can be written as:

$$\sigma = \sigma_0 \exp\left(-\left(\frac{T_0}{T}\right)^{1/2}\right) \qquad (2\text{-}11)$$

where σ_0 and T_0 are constants.

2-1-3 **Polypyrrole**

PPy has been a subject of many studies because it exhibits relatively high electrical conductivity, good environmental stability, and versatility of synthesis. For instance, it has been shown experimentally that PPy is stable both in air at ambient conditions and in an inert atmosphere at high temperatures (Arca *et al*., 1987). The stability of PPy in air comes from its lower oxidation potential (Diaz *et al*., 1981) and has led to its use in commercial applications such as electrolytic capacitors, static dissipation wrist rests, and electronic noses (Saunders *et al*., 1995).

Pyrrole (Py), the monomer of PPy, has been polymerized via electrochemically anodic oxidation or chemically oxidative polymerization in the presence of oxidant, as well as dehalogenative polycondensation (Yamamoto *et al*., 1993), photochemical polymerization, and other techniques used in organic chemistry (Kumar and Sharma, 1998). When Py is polymerized by either electrochemical or chemical means, ideally, the polymerization of Py requires 2.25 equivalents of an oxidant per mole of Py (Walker *et al*., 1988). However, excess amount of oxidant is often consumed upon polymerization due to doping or further oxidization of PPy that gives rise to charge carriers such as

polarons and bipolarons in π-conjugated bonds. Lewis acid catalysts have been widely used as polymerization catalysts and oxidants for Py. One of the commonly used oxidizing chemicals is ferric chloride ($FeCl_3$) (DeJesus *et al*., 1997a).

Electrochemical preparation of PPy has been widely conducted since Diaz *et al*. (1979) found a free-standing film deposited on a platinum electrode. One of the advantages of electrochemical polymerization is that the instantaneous growth rate of the resulting film is proportional to the current. Therefore, the thickness of the film can be controlled, and is proportional to the integral of the current over the polymerization period (Saunders *et al*., 1995). The electrical conductivity of such electrochemically synthesized PPy films can be enhanced via physical stretching by a factor of 2.2 (~10^3 S cm^{-1}) due to the formation of a more ordered structure under stress (Ogasawara *et al*., 1986). However, a highly oriented texture along the direction of stretching results and is associated with anisotropy of the conductivity. Furthermore, it is technically and economically difficult to prepare uniform films electrochemically on a large scale (Walker *et al*., 1988; Balci *et al*., 1997; Omastova *et al*., 1997). Finally, since electrochemical polymerization is limited to conducting electrodes, no conducting films can be obtained on insulating surfaces (Malinauskas, 2001).

Chemical oxidative polymerization of Py has the advantage of shorter reaction times and large-scale production (Ruckenstein and Park, 1991a). The first chemical polymerization of Py is believed to date back to 1888 and was achieved by Dennestedt and Zimmermann (Myers, 1986). However, the resulting materials were low-molecular-weight oligomers. A series of improvements ws proposed and chemically synthesized

PPy powders and films can now be obtained with electrical conductivities as high as ~10^3 S cm^{-1} in the oxidized state (Kaiser, 2001b). For example, Myers (1986) polymerized Py with iron and copper salts, including anhydrous $FeCl_3$, in various solvents and was able to produce PPy powder with conductivity as high as 10^2 S cm^{-1}, which is comparable to that of electrochemically-synthesized PPy. A reactant mole ration of 4:1 ($FeCl_3$/Py) in diethyl ether was found to be optimal in obtaining high conductivity, suggesting that the oxidant plays dual roles as an initiator and dopant to induce the oxidative polymerization and to increase the level of conductivity. Chen *et al*. (1995) also showed that the monomer-to-oxidant ratio determines electrical conductivity and morphology of the resulting PPy. The high oxidation potential of $FeCl_3/FeCl_2$ at a low Py/$FeCl_3$ ratio can induce the formation of a highly doped PPy, whereas a high Py/$FeCl_3$ ratio favors the depletion of the oxidant, leading to lower doping levels and lower conductivity. Additionally, degradation of conjugated bonds is possible at very high $FeCl_3$ concentrations because of the formation of covalent carbon-chloride bonds. Consequently, it was concluded that a maximum conductivity is obtained at a 2:1 monomer-to-oxidant ratio (Chen *et al*., 1995).

The oxidizing agent for synthesis of conducting polymers is not limited to transition metal complexes. Other chemicals such as halogens, noble gas fluorides, and protonic acids have also been used for this purpose (Przyluski *et al*., 1982). Simultaneous polymerization and oxidation of Py with halogenic electron acceptors in organic solvents has been reported by Kang *et al*. (1987). An environmentally stable black granular complex was obtained at a ratio of four Py units to one molecule of halogen. The electrical conductivities were 2 and 5 S cm^{-1} for the iodine and bromine complexes,

respectively. Further exposure of the precipitate to halogen vapor did not increase the conductivity. Moreover, elemental analysis revealed that a C:H:N ratio was close to the theoretical value corresponding to a linear chain of Py rings without defects. It was suggested that both samples have highly conjugated structures upon oxidative polymerization.

Kang *et al*. (1987) also suggested that the polarity of the solvent impacts the polymerization because of the ionic nature of the process. For example, a yield of 20-30 % was obtained for Py polymer with iodine and 50-60 % with bromine in acetonitrile, while only traces of precipitate were obtained for polymerization in methanol. Myers (1986) indicated that the presence of water in the reaction solvent influences morphology and molecular weight of the polymer, and the reactivity of the dopant species. The density of PPy, for instance, was ~ 0.03 g cm^{-3} in aqueous medium, which is much less than 1.4-1.5 g cm^{-3} under anhydrous reaction conditions. The most highly conducting PPy samples were formed only in solvents having substantial solubility of $FeCl_3$, although the solubility was not directly related to the yield and conductivity. The solvent dependence of yield was attributed to the extent of the interaction of $FeCl_3$ with the solvent relative to the interaction of $FeCl_3$ with Py. For example, no PPy was formed in strong donor solvents in which extensively solvated $FeCl_3$ cannot initiate the polymerization reaction with the weakly basic Py monomer. The choice of reaction medium also affects the composition of the PPy powders. For instance, elemental analysis and infrared spectra suggested that acetonitrile promotes the formation of a

complex between a PPy cation and the chloride counterion, whereas the counterion is $FeCl_4^-$ in diethyl ether.

The reaction temperature also determines the type of the counterion in PPy that affects the electrical conductivity. It has been shown (Ogiwara et al., 1985; Myers, 1986) that higher temperatures result in a decrease in electrical conductivity of PPy, especially at longer reaction times, due to the oxidation of double bonds. The polymerization reaction may also be more favorable at lower temperatures because the oxidation reaction and competing side reactions such as non α-α' coupling are suppressed, leading to more ordered and highly conjugated structures (Myers, 1986).

In terms of morphology, chemical oxidative polymerization usually produces PPy powders called "pyrrole black." The powder is brittle, infusible, and insoluble in most solvents, and compression molding is used to mold it into pellets or films to characterize its properties. In order to prepare compact, thin conducting films directly, Lu *et al*. (1998) polymerized Py at the interface between two immiscible solutions – a chloroform solution of Py monomer and an aqueous solution of ammonium persulfate. The conductivity and thermal stability of the PPy film decreased slightly as the monomer-oxidant molar ratio increased, probably due to overoxidation of PPy (Yin *et al*., 1998a). When $FeCl_3$ was used as an oxidant, the rate of polymerization was faster. However, only thick porous PPy cake was formed. Interfacial polymerization was also used in the formation of PPy thin films of 50 – 100 nm thickness (Sree *et al*., 2002).

2-2 ***Composites of Electrically Conducting Polymers***

As discussed in chapter I, some of the mechanical limitations of conducting polymers may be overcome by incorporating the polymers in composites with a host substrate. The substrate can either be electrically insulating or conducting for chemical oxidative polymerization. In the case of insulating substrates, sufficient concentration of the conducting polymer is required to attain a percolation threshold for an insulator-to-conductor transition (Scher and Zallen, 1970). The percolation threshold is theoretically predicted to be at a volume fraction of 0.154 for globular agglomerates in a three-dimensional insulating medium (Scher and Zallen, 1970), and 0.183 for randomly packed hard spheres (Powell, 1979). In reality, the percolation threshold is strongly influenced by the size and shape of the conducting species, as well as by processing methods such as solution casting, compression and injection molding, chemical modification, or chemical deposition.

2-2-1 **Solution Casting**

In solution casting, both substrate and particles of pre-synthesized conducting polymer are dispersed in a solvent and then cast into a film. The type of substrate impacts the mechanism of electrical conduction in the composite. For example, the presence of PMMA chains can induce the one-dimensional electronic transport process due to the alignment of polymer chains and the reduction of inter-chain hopping while the conducting and insulating components dominate equally in the composite (Dutta and De, 2003).

Castillo-Ortega *et al*. (2001) prepared PPy composites using two casting methods. In one method, PPy powders were synthesized with a dispersant, and mixed with various thermoplastics in tetrahydrofuran. In the other method, PPy powders formed without the dispersant were mixed with thermoplastics and dispersant in tetrahydrofuran. The conductivities ranged from 10^{-9} to 10^{-3} S cm^{-1}, depending on the PPy content and the choice of substrates, dispersant, and the powder formation methods. SEM pictures showed that the former method formed smaller agglomerates than the latter whereas the former method was worse in terms of the conductivity and homogeneity of the films. The investigators claimed that such smaller agglomerates are hard to interconnect, leading to lower electrical conductivity. Cassignol *et al*. (1999) also reported that epoxy composites mixed with smaller PPy powders synthesized via dispersion polymerization reach the percolation threshold at a higher PPy concentration compared to composites with larger PPy powders formed by suspension polymerization. Similarly, thermoset composites were produced by mixing an epoxy pre-polymer with pure PPy powders and hardeners to investigate percolation behavior in the composites (Fournier *et al*., 1997). The percolation threshold was about 3 vol. %, much less than that of corresponding composites with carbon black. A proposed model of electrical conduction based on the Fermi-Dirac distribution was able to fit all the results.

Conducting composites can also be produced via *in situ* polymerization during processing. For example, Gulsen *et al*. (2001) prepared PPy composites with polycarbonate for gas separation membranes by mixing an electrolyte-$FeCl_3$-acetonitrile solution with a polycarbonate-chloroform solution, followed by dropwise addition of Py

to the mixture. The mixture was then transferred immediately to a glass plate to evaporate the solvent. Although the PPy content of the resulting film was 3-4 wt. % and its electrical conductivity was 10^{-8} S cm^{-1}, the permeability and selectivity were greater than those of a dense flat sheet of polycarbonate. The authors claimed that the type and concentration of supporting electrolyte are important factors in the separation performance of the PPy composite. Composites with hybrid biomaterials were also prepared via *in situ* polymerization of PPy (Khor *et al*., 1995). Py or its derivative, sodium 4-(3-pyrrolyl) butanesulfonate, was imbibed in an animal tissue (porcine pericardium), and then placed in $FeCl_3$ solutions. The polymer of the derivative appeared to penetrate further into the tissue than PPy due to its solubility, although the penetration was limited near the surface.

2-2-2 **Compression and Injection Molding**

Compression molding at high temperature has been used to convert surface-modified composite particles into conducting films (Omastova and Simon, 2000). Thus poly(methyl methacrylate) (PMMA) particles were immersed in $FeCl_3$ aqueous solution, and contacted with a Py aqueous solution at 493 K to obtain 0.2 mm thick composite films via compression molding. The conductivity of the molded composite increased by seven orders of magnitude as the PPy concentration increased from 0.25 to 10 wt. %. The surfaces of the composite particles were rough reflecting the morphology of virgin PMMA, and the typical granular morphology of PPy was not observed. XPS analysis of the composites showed that the PPy content at the surface of the particles was smaller than that calculated from elemental analysis, indicating that PPy was formed in the

interior of the host particles. Imaging technique employing low-voltage scanning electron microscopy revealed the connectivity of the conducting polymer network in the composite (Omastova *et al*., 1998). The higher PPy content composites were thermally stable at higher temperatures (Omastova *et al*., 1997). Surface discharge experiments suggested that the threshold concentration of PPy was 1.5 wt. % corresponding to an electrical conductivity of 10^{-8} S cm^{-1} when any static charge is removed from the surface immediately. Yin *et al*. (1994) showed that the percolation threshold increases with decreasing length of polypyrrole-coated nylon fibers when they are hot-pressed with polyethylene spheres.

The electrical and mechanical properties of PPy composites can be affected by the choice of molding methods (Omastova *et al*., 1996a, b, 1997, 1999; Pionteck *et al*., 1999). The conductivity of PPy composites processed by injection molding was seven orders of magnitude lower than compression-molded composites with the same PPy content. This was attributed to the deterioration of PPy connectivity at high shear. In contrast to the samples processed by injection molding, all compression-molded composites were brittle and heterogeneous owing to the PPy network coating on polypyrrole particles resistive to mixing. When chemically synthesized PPy was mechanically mixed with pure polypyrrole particles, the conductivity did not exceed 10^{-7} S cm^{-1} even with a PPy content of 34 wt. %.

2-2-3 **Chemical Modification in Non-Porous Polymer Substrates**

The incorporation of conducting polymers into non-porous polymeric matrices has been implemented via surface polymerization, in which polymerization takes place

almost exclusively on the surface of the substrate; therefore, any competitive polymerization reactions in the solution are suppressed (Malinauskas, 2001). In this chemical modification method, the substrate surface is impregnated either with a monomer or oxidant, and then exposed to an oxidant or monomer, respectively. The surface conductivity of the composite depends strongly on the thickness of the conducting film. Kim *et al*. (2003) deposited a thin PPy film on poly(ethylene terephthalate) that was pretreated with 1-4 wt. % solution of $FeCl_3$ hexahydrate in methanol, and found that the conductivity was 10^{-1}-1 S cm^{-1} for 20-100 nm thick films and 10^2 S cm^{-1} for 600 nm thick films. The penetration of the conducting layer in the composite can be controlled by adjusting the diffusion of the oxidant and/or monomer into the substrate (DeJesus *et al*., 1997). The percolation threshold in the composites occurs at lower volume fractions than values predicted by classical percolation theory when specific interactions between PPy and substrates are involved (Wang *et al*., 1990; Wang and Fernandez, 1992), or when an interpenetrating network of conducting polymers is formed (Mandal and Mandal, 1996).

A PMMA substrate has been utilized for chemical deposition of PPy (Ratcliffe, 1990; Guernion *et al*., 2002). The composite synthesis involves a two-step method (adsorption followed by oxidation) as well as a one-step procedure (dipping in a polymerizing solution). The coating of PPy on PMMA consists of a layer of spheres of 50 nm in diameter. Poly(vinyl alcohol) or PVA has also been investigated due to its high solubility in water. The resulting composite is known to have a very low percolation threshold (molar ratio of PPy to PVA ~ 5×10^{-3}) (Makhlouki *et al*., 1992). PVA powders

were dissolved in water containing $FeCl_3$, followed by evaporation to form free-standing films. The films were suspended over a Py solution in ethanol under reduced pressure for a week to polymerize Py (Ojio and Miyata, 1986; Pron *et al*., 1987; Benseddik *et al*., 1995). The same approach was also applied to make PPy composite films with poly(vinyl chloride) (Mano *et al*., 1996), flexible crosslinked copolymers (Yin *et al*., 1997; Yin *et al*., 1998b), or copolyesters (Baik *et al*., 1998). The electrical conductivity of the resulting PVA-PPy composites was measured over a wide range of temperatures in order to investigate the mechanism of electrical conduction in the composites. The temperature dependence of the conductivity was expressed as a sum of two contributions: that due to hopping between bipolaronic clusters within polypyrrole domains (Zuppiroli *et al*., 1994), and that due to thermally induced tunneling through small insulating host polymer barriers (Sheng, 1980).

Low penetration of PPy into dense substrates often limits the applicability of the chemical modification method. However, introduction of ionic groups (such as sulfonic) can be used to enhance the miscibility of PPy and insulating polymer phases (Liu *et al*., 1996; Lee *et al*., 2001). DeJesus *et al*. (1997b) prepared a surface layer of PPy on sulfonated polystyrene ionomer films. Thin polystyrene films sulfonated up to 17.3 mol % were subsequently immersed in Py and $FeCl_3$ aqueous solutions for 5 to 72 and 24 hours, respectively. PPy yield was linearly proportional to square root of the time of immersion in Py solution, suggesting diffusion of Py in polystyrene substrate was the limiting step. The sulfonated glassy microdomains of a poly(styrene-*b*-(ethylene-*alt*-propylene)) triblock copolymer were used as a template for preparing an anisotropically

conducting nanocomposite with the same procedure described above (DeJesus *et al*., 1997c; DeJesus *et al*., 1998). The incorporation of PPy resulted in enhanced mechanical strength above the grass transition temperature of the host substrate. The polymerization of Py was restricted to the hydrophilic microdomains due to the preferential absorption of Py and $FeCl_3$ aqueous solution into the sulfonated polystyrene phase. The micrographs revealed that the PPy was intercalated within the 10-20 nm thick polystyrene lamellae of the triblock copolymer. The highly anisotropic structure of the composites was reflected in the degree of anisotropy in electrical conductivity: conductivity parallel to the film surface was 1-2 orders of magnitude higher than that normal to the surface.

2-2-4 **Chemical Deposition in Porous Polymer Substrates**

The potential advantage of porous composites is that PPy can be dispersed throughout the pore structure while the mechanical properties of the host polymer are retained (Nikpour *et al*., 1999). Furthermore, the electrical conductivity can be enhanced due to regular alignment of PPy chains via stretching or crystallization along pores as the diameter of the pore decreases to molecular scale (Martin, 1994; Wallace and Innis, 2002). Production of composites in such porous structures has been attempted via chemical oxidative polymerization within host porous polymers (Cai and Martin, 1989; Cepak and Martin, 1999), glass (Warren *et al*., 1986; Newman *et al*., 1986; Kamada *et al*., 1994; Zarbin *et al*., 1999), and zeolites channels (Bein and Enzel, 1989; Ikegame *et al*., 2003); and also via diaphragmatic polymerization (Martin *et al*., 1993), electrochemical polymerization within hydrogels (Brahim *et al*., 2002), or electro-deposition on platinised porous poly(vinylidene fluoride) (Zhou *et al*., 2000). Electrochemical deposition of PPy

and its derivatives on polymer membranes has been summarized by Sarrazin *et al*. (2002). A review of chemical deposition methods of polyaniline, polythiophene, PPy, and their derivatives on various substrates is also available (Malinauskas, 2001). In the following section, the chemical oxidative polymerization of Py within host porous polymers is reviewed.

Lee and Hong (2000) dip-coated a number of porous substrates, such as nylon membranes, track-etched polycarbonate, cellulose fiber filters, and silanized alumina membranes, with PPy and found that the composites with nylon or alumina membranes gave good adhesion, and smooth coating surfaces due to their hydrophilicity (Avlyanov *et al*., 1997), whereas polycarbonate pores were barely coated with PPy. The filter paper was found to contain a fair amount of PPy with poor mechanical strength in wet conditions. The electrochemical and thermal stability of the nylon composite was improved by an acid treatment, which was attributed to the increased ordering of the PPy structure by ion exchange (Cheah *et al*., 1998). Nikpour *et al*. (1999) produced PPy composites with porous PMMA substrates in which polypropylene glycol or sodium chloride was used to control the porosity of the host polymer. As the porosity increased, more Py monomer was imbibed into the host film, resulting in conductivities up to 19.8 S cm^{-1}. Although the pore shape of the host and composites was not uniform, the composite membranes exhibited selective permeability of amino acids and proteins.

Ruckenstein and Park (1991a) synthesized porous crosslinked polystyrene through a condensed emulsion polymerization (Ruckenstein and Park, 1988) and used it as a host substrate to produce PPy composites. The substrate has the capacity to hold

liquids greater than 3-9 times its own weight. The composite prepared with anhydrous $FeCl_3$ gave higher electrical conductivity by two orders of magnitude than the composite prepared with $FeCl_3$ hexahydrate. It was also demonstrated that the procedure in which the host absorbs an oxidant solution followed by contact with Py solution resulted in higher conductivity by an order of magnitude compared with a host subjected to the reverse procedure, while the yields were similar in both cases. The lower penetration of monomer into the host substrate due to the formation of PPy film at the reaction front may lead to non-uniform distribution of PPy, resulting in lower conductivity. A similar method was adopted to produce composites with poly(3-alkylthiophene)s (Pomerantz *et al*., 1991; Isotalo *et al*., 1993; Morsli *et al*., 1996).

Park and Ruckenstein (1992) produced PPy composites with different porous substrates, such as cotton fiber, non-woven polypropylene and porous crosslinked polystyrene. Owing to the interaction between the substrate and PPy, the electrical conductivity and amount of conducting polymer deposited in the composites depended on the morphology and the nature of the substrate. Porous crosslinked polystyrene exhibited the highest conductivity and good compatibility between the host and conducting polymer. Electron microscopy showed that the host substrate provides a macroscopic structure for a uniform network of the conducting polymer, as well as mechanical strength as a reinforcing material. Park and Ruckenstein also showed that the rate of reaction of Py with $FeCl_3$ depends on the solvent used for oxidant imbibition, and that the presence of water enhances the conductivity and productivity. The rate of decrease in conductivity of composites prepared with $FeCl_3$ was less than that of composites prepared

with copper perchlorate, indicating that a thermally driven undoping process depends on the nature of the oxidant in the conducting complex.

Bleha *et al*. (1999) polymerized Py vapor with $FeCl_3$ adsorbed on the surface of a thin microporous polyethylene film. Electron micrographs revealed a rough layer of PPy covering the smooth surface of the polyethylene host. Studies indicate that there are three stages of the polymerization: (1) formation of a thin layer of PPy in the pores and on the surface of the substrate (~ 15 wt. % of PPy); (2) filling of the host pores with PPy (~ 35 wt. %); (3) formation of rigid chains of PPy. The PPy-polyethylene composite doped with an HCl solution was highly permeable to anions and poorly permeable to cations, and may act as an anion-exchange membrane because of the presence of the positively charged PPy network with negatively charged chloride counter-ions. The elastic modulus of the composite increased monotonously with the formation of PPy while the strength of the composites increased with PPy content up to 20 wt. %, and then decreased due to the orientation of the PPy layer.

The vapor phase polymerization of Py and its derivative was also carried out in polyurethane foams of different densities (Fu *et al*., 1998). The foams incorporated with $FeCl_3$ hexahydrate in methanol were dried in air, and then exposed to monomer vapor under reduced pressure. In the case of Py only, a transition from insulator to conductor occurred at low concentrations of 3-5 wt. % due to a PPy layer on the pore walls. However, the copolymerization of Py and n-methylpyrrole resulted in conductivities of 10^{-7} S cm^{-1} if the mole fraction of Py in the vapor phase was less than 0.5 due to the lower conductivities of N-alkyl substituted PPy (Kim and Elsenbaumer, 1997).

*2-3 **Development of More Environmentally Benign Methods***

2-3-1 **Solvent-Less and Liquid Carbon Dioxide Methods**

The conventional processing methods described above generally require significant amounts of harmful organic solvents and/or high temperatures. However, high temperatures are known to have adverse effects on the electrical conductivity because of twisting of main chains (Iwasaki *et al*., 1994). Therefore, efforts have been devoted to develop environmentally benign methodologies that can reduce or eliminate the amount of waste and energy in polymer synthesis and processing. One environmentally benign technique is a solvent-free method developed by Shenoy *et al*. (2002). In this method, iodine was impregnated in polyurethane foams by sublimation, and the impregnated foam was then exposed to Py vapor. The PPy-polyurethane composites prepared at 313 K exhibited electrical conductivities ranging from 10^{-6} to 10^{-1} S cm^{-1} with the corresponding concentration of the PPy-iodine complex from 6 to 50 wt. %. The conductivities followed a power law function of the PPy concentration. Scanning electron micrographs revealed that the PPy was granular in texture and contained within the polymer-rich regions of the foam, and that some PPy was embedded on the inside PU surfaces of the pores. However, the sorption of iodine by the foam was slow due to limitation of the sublimation process (27 wt. % after 54 hours of exposure). The diffusion process was facilitated at higher temperature (343 K) although the foam was found to have lost its porosity due to oxidation at this temperature.

The same synthesis method was adopted by Wang *et al*. (2003) for the preparation of polyetherurethane open-cell foams with low densities (0.045 g cm^{-3}). Foam strips were

impregnated with iodine in a desiccator, then transferred to another desiccator containing Py vapor. The amount of PPy-iodine complex that formed was directly related to the mass of iodine impregnated in the first step. The electrical conductivity of the conducting foams followed a power law relationship with the mass of the complex. The foams were then exposed to dilute triethylamine vapor to test their capability as chemical gas sensors. The response was reversible for the alternative flow of amine vapor, although a hysteresis was observed at the onset of exposure.

Liquid carbon dioxide has also been utilized as a solvent for making electrically conducting polymers (Desimone, 1998). $FeCl_3$ hexahydrate was dispersed by mechanical agitation in CO_2 at 25 ^oC, 1500 psia. The color of the solution in the cell turned black immediately after Py monomer was flashed. The electrical conductivity of a pressed film of the thus-obtained black powders was on the order of 10^{-5} S cm^{-1}. Other combinations of monomers and oxidants also showed similar results, indicating that CO_2 is an effective reaction medium for the synthesis of conducting polymers.

2-3-2 **Polymer Synthesis and Processing in Supercritical Fluids**

Processing methods using supercritical carbon dioxide ($scCO_2$) include fractionation, extraction, purification, impregnation, dyeing, heterogeneous chemical modification, coatings, lithography, and formation of microcellular materials or polymeric particles (Cooper, 2000). The feasibility of polymerization using $scCO_2$ has been demonstrated by many investigators (Webb, 1998; Webb, 2001; Abbett *et al*., 2003; Watkins and McCarthy, 1994, 1995; Kung *et al*. 1998, 2000; Rajagopalan and McCarthy, 1998; Arora *et al*. 1999; Muth *et al*. 2000). Polymeric reactions in $scCO_2$ include free

radical, cationic, transition metal catalyzed, melt-phase condensation, sol-gel, or oxidative coupling polymerizations (Kendall *et al*., 1999).

Although $scCO_2$ has a limited ability to dissolve most polymers (except silicones or fluorinated polymers), it is able to plastisize thermoplastic polymers with a reduction in the glass transition temperature that could lead to processing with less energy (Wang *et al*., 1982; Wissinger and Paulaitis, 1987; Condo *et al*., 1992). Moreover, the development of new fluorinated polymers and surfactants that can be dispersed in the gas phase have enhanced the applications of carbon dioxide as an environmentally benign solvent in polymer synthesis and polymer processing (DeSimone *et al*., 1992; Canelas *et al*., 1996). It should also be added that hydrocarbon copolymers with Lewis base functionality, high flexibility, and large free volume were found to be more CO_2-philic than expensive fluorinated polymers (Sarbu *et al*., 2000). Reviews on polymer synthesis and processing are also available elsewhere (Kendall *et al*., 1999; Kirby and McHugh, 1999; Cooper, 2000).

2-3-3 **Synthesis of Electrically Conducting Polymers in Supercritical Fluids**

There are a few studies related to synthesis of electrical conducting polymers in $scCO_2$. Electrochemical synthesis of PPy in $scCO_2$ was reported by Anderson *et al*. (2002). Py was polymerized by repeated potential cycling on indium tin oxide glass electrodes in $scCO_2$ containing acetonitrile as modifier and tetrabutylammonium hexafluorophosphate as electrolyte. The electrical properties were comparable to those of PPy prepared electrochemically on indium tin oxide in aqueous solution. However, scanning electron micrographs of the films showed totally different morphologies. The

film prepared in $scCO_2$ consisted of small (0.5-3.0 μm) granular nodules on a flat PPy surface (0.167 μm of average thickness), whereas the film prepared in non-aqueous solutions typically exhibited a wrinkled texture.

Kerton *et al*. (1997) reported the first example of chemical synthesis of PPy in $scCO_2$. Py monomer was generated *in situ* by decarboxylation of pyrrole-2-carboxylic acid precursor at high temperature, and reacted with $FeCl_3$ or ferric triflate in carbon dioxide. The resulted PPy powder showed fibrillar morphology in contrast to the globular morphology obtained when the powder was prepared by conventional methods. The electrical conductivities of the PPy pellets were of the order of 5×10^{-2} S cm^{-1}. The lower conductivities were attributed to overoxidation at the elevated temperature. Webb (1998) conducted chemical oxidative polymerization of Py in $scCO_2$ in a continuous manner by flowing a saturated monomer mixture into a high-pressure vessel containing $FeCl_3$. Webb (2001) and Abbett *et al*. (2003) also synthesized an electrically conducting polymer, poly(3-undecylbithiophene), in $scCO_2$ using ferric triflate as an oxidant. The polymer was designed to possess processability with retained electrical conductivity (Narayan, 1999; Kowalik *et al*., 2001). The resulting polymer was comparable to the polymer synthesized in nitrobenzene in terms of yield, molecular weight, optical properties, and electrical conductivity.

A composite of PPy with non-porous polystyrene was prepared in $scCO_2$ (Tang *et al*., 2003a). Py monomer was absorbed into polystyrene specimens at 313 K and 10.5 MPa for 24 hours using CO_2. The host polymer was then soaked in a 2.25 M $FeCl_3$ aqueous solution to carry out the polymerization. Although less than 3 wt. % of PPy was

obtained in the composite, the conductivity was as high as 1.12×10^{-2} S cm^{-1}, mostly because PPy was concentrated on the surface of the composite. They also reported the effect of doping conditions on electrical conductivity of the composites (Tang *et al*., 2003b). $FeCl_3$ in water resulted in higher conductivity than $FeCl_3$ in acetonitrile because of its higher solubility and protonation in water (Machida and Miyata, 1989). The composites polymerized with iron salts exhibited an anion dependence of the maximum conductivity in the order: chloride > sulfate > perchlorate > nitrate. The authors attributed the dependence to the lower rate of polymerization of Py with $FeCl_3$, leading to a higher bulk density and less porous morphology.

Fu *et al*. (1997) showed that an open-porous substrate could be impregnated with ferric triflate to prepare conducting composites of polyurethane foams and PPy. The solubility of ferric triflate in carbon dioxide at 45 °C and 24 MPa was reported to be about 0.01 wt. %. The oxidant mass uptake increased linearly with the square root of time, indicating Fickian diffusion. It was also confirmed that an *in situ* polymerization occurred in the polymer matrix when the impregnated foams were exposed to Py vapor (at 1 Torr) for four hours. The conductivity measured by a four-point probe was linear with the period of impregnation and attained values up to 3×10^{-2} S cm^{-1}. An increase in the oxidant uptake correlated with an increase in conductivity. The average content of PPy in the composite was estimated to be 3 wt. % by a thermal gravimetric method. However, a relatively thick layer was found to be deposited near the surface of the foam due to the low solubility of ferric triflate in $scCO_2$. Shenoy and coworkers (2001) tried to improve the above process by the addition of ethanol as a cosolvent to increase the

amount of ferric triflate impregnated in the foam. The amounts of the oxidant and PPy increased with the addition of ethanol at 312 K and 17.2 MPa. However, the oxidant concentrations near the surface layer of the foam were less than those without the cosolvent for a given soaking time, resulting in lower surface conductivities.

In the search for oxidants that are more soluble in $scCO_2$ than ferric triflate, Weiss et al (2002) used iodine to prepare PPy-polyurethane composites (Weiss *et al*., 2002). The mass uptake of iodine into polyurethane foams after 4-6 hours of soaking in saturated $scCO_2$ was 10 wt. % greater than that of foams exposed to iodine vapor for 4 days. The corresponding PPy uptake approximately doubled. Although the electrical conductivity of the foams increased by 3 to 4 orders of magnitude to 10^{-4}-10^{-3} S cm^{-1}, inhomogeneous distribution of iodine resulted in less uniformity of the conducting foam. It suggests that uniform distribution of oxidant is required to form uniform conducting composites.

Porous, crosslinked polystyrene has also been used to prepare composites of poly(3-undecylbithiophene) in $scCO_2$ (Webb, 2001; Abbett *et al*., 2003). The effective diffusivity of $scCO_2$ in the substrate was high (Webb and Teja, 1999); hence, enhanced mass transfer of reactants in the host substrate was expected. It was found that the morphology and electrical conductivity of the composites were greatly influenced by experimental conditions, the highest conductivity being obtained in composites formed at low temperature and moderate pressure. The conductivity of the composites was increased by more than an order of magnitude via iodine doping in $scCO_2$. However, the structural analysis of the composites and optimization of the process were not demonstrated conclusively.

CHAPTER 3

PREPARATION AND CHARACTERIZATION OF THE HOST SUBSTRATE

The preparation of porous, crosslinked polystyrene, the host substrate used in this work, is described in this chapter. The procedure employs a surfactant to disperse water in a condensed emulsion solution of monomer and crosslinking agent, resulting in a crosslinked network of polystyrene and divinylbenzene around the water droplets and yielding a porous structure after drying. The porous structure was characterized in terms of porosity, specific surface area, and distribution of pore sizes as well as liquid sorption behavior.

3-1 ***Materials***

Styrene (99+ %), divinylbenzene (80 % of isomers mixture, technical grade), sorbitane monooleate (Span®80), and 2,2'-Azobis(2-methylpropionitrile) (AIBN, 98 %) were purchased from Aldrich (Milwaukee, WI). Acetonitrile (HPLC) and water (HPLC) were procured from Fisher Scientific (Hampton, NH). High purity grade nitrogen cylinder was obtained from Air Products and Chemicals (Allentown, PA). All chemicals were used as received.

3-2 ***Preparation of Host Substrate***

Porous, crosslinked polystyrene (denoted as PCPS in this thesis) was prepared according to a procedure originally reported by Ruckenstein and Park (1988). AIBN to act as an initiator (0.05 g), and divinylbenzene (1.0 g) as a crosslinking agent, were mixed under nitrogen flow in a 250-mL three-necked round-bottom flask equipped with a magnetic stirrer (Figure 3-1). Sorbitan monooleate (1 mL) as a surfactant and styrene monomer (5 g) were added to the flask, followed by 25-mL water in a dropwise fashion. The mixture was stirred for 4 hours at room temperature. The polymerization reaction was then accomplished by heating the emulsion for 24 hours in four covered petri dishes. Afterwards, excess water was removed by keeping uncovered petri dishes on a hot plate at 373 K for 3 days. If any pores of the film contained residual surfactant (visually confirmed by spots near the surface), then the film was discarded. The resulting PCPS wafers were then cut into strips with dimensions of 1.0 cm × 2.5 cm.

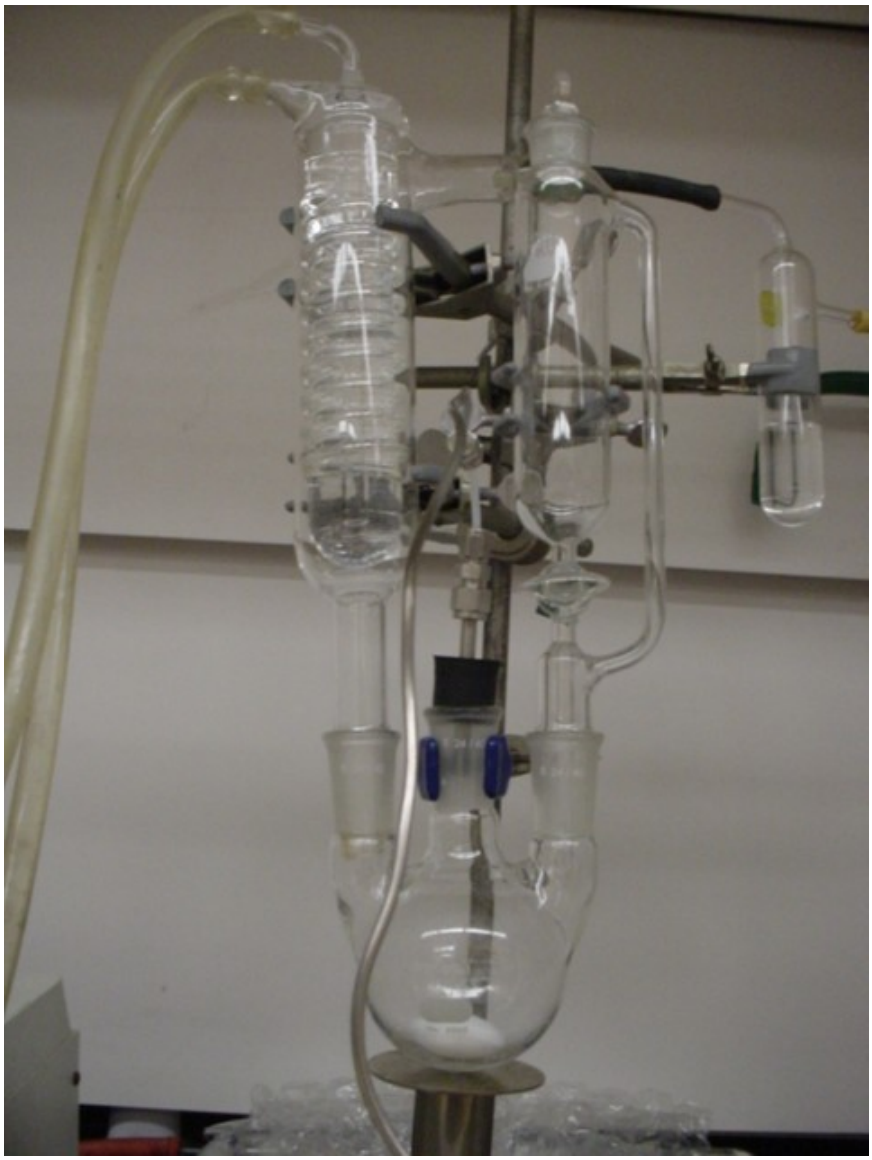

Figure 3-1. Apparatus used in the preparation of porous, crosslinked polystyrene (PCPS).

3-3 Characterization of Porous, Crosslinked Polystyrene

Characterization of the synthesized PCPS was carried out to measure porosity, specific surface area, and distribution of pore sizes. The porosity of the substrate was measured by the water displacement method using a vacuum system. The specific surface area was obtained using an isothermal gas absorption measurement with nitrogen as an adsorbent. Pore sizes were observed by SEM pictures of the cross-sections of the host substrate, and compared with the results from BET measurements. Absorption and desorption behaviors were also observed at room temperature.

3-3-1 **Porosity Measurement**

It is important to select an appropriate solvent to estimate porosity by liquid displacement because the porosity calculation is based on assumptions that the volume of a solvent absorbed corresponds to the volume of accessible voids in a sample, and that all the accessible voids are filled with the solvent. According to Park and Ruckenstein (1992), the amount of toluene absorbed by PCPS prepared by their method is 5.06 g per g of the host substrate. The large liquid uptake should be ascribed to the absorption of the solvent into the polystyrene. This absorption leads to the overestimation of porosity. If water is chosen as the solvent in this method, liquid absorption in the polymer phase is not likely to happen due to the hydrophobic nature of the polystyrene surface. Therefore, the porosity of the substrate was measured by water displacement.

A strip of PCPS was dried, and its dimensions were measured with a caliper with accuracy of ± 0.005 cm to calculate the volume of the polymer strip. The strip was then immersed in 50 mL of HPLC grade distilled water in a 120-mL fast-freeze vacuum flask (Labconco, Kansas City, MO) as shown in Figure 3-2. A piece of stainless steel was used as a weight to ensure that the polymer strip was completely under water. A vacuum pump was used to maintain vacuum inside the flask until there was no evolution of bubbles out of the strip. The water-saturated strip was weighed after wiping water off the surface to obtain the mass of the absorbed water. The porosity was calculated using the following equation:

$$\text{Porosity} = \frac{\text{Volume of Water Absorbed}}{\text{Volume of the Polymer Stip}} = \frac{M_W / \rho_W}{V_P} \qquad (3\text{-}1)$$

where M_W is the mass of water in the sample, ρ_W is the density of water, and V_P is the volume of the polymer strip.

3-3-2 **Specific Surface Area Measurement**

The isothermal gas sorption of PCPS was measured using an ASAP 2000 (Micromeritics Instrument, Norcross, GA) with nitrogen as an adsorbent. A sample was dried overnight under a vacuum of 4×10^{-3} Torr at 323 K. Data processing was conducted using a Micromeritics ASAP 2010 Version 5.02 software. The software can produce an analysis report including the raw data, isotherm plot, Brunauer-Emmett-Teller (BET) and Langmuir plots, t-plot, and Barrett-Joyner-Halenda (BJH) adsorption and desorption pore distributions. The analysis reports are presented in Appendix B.

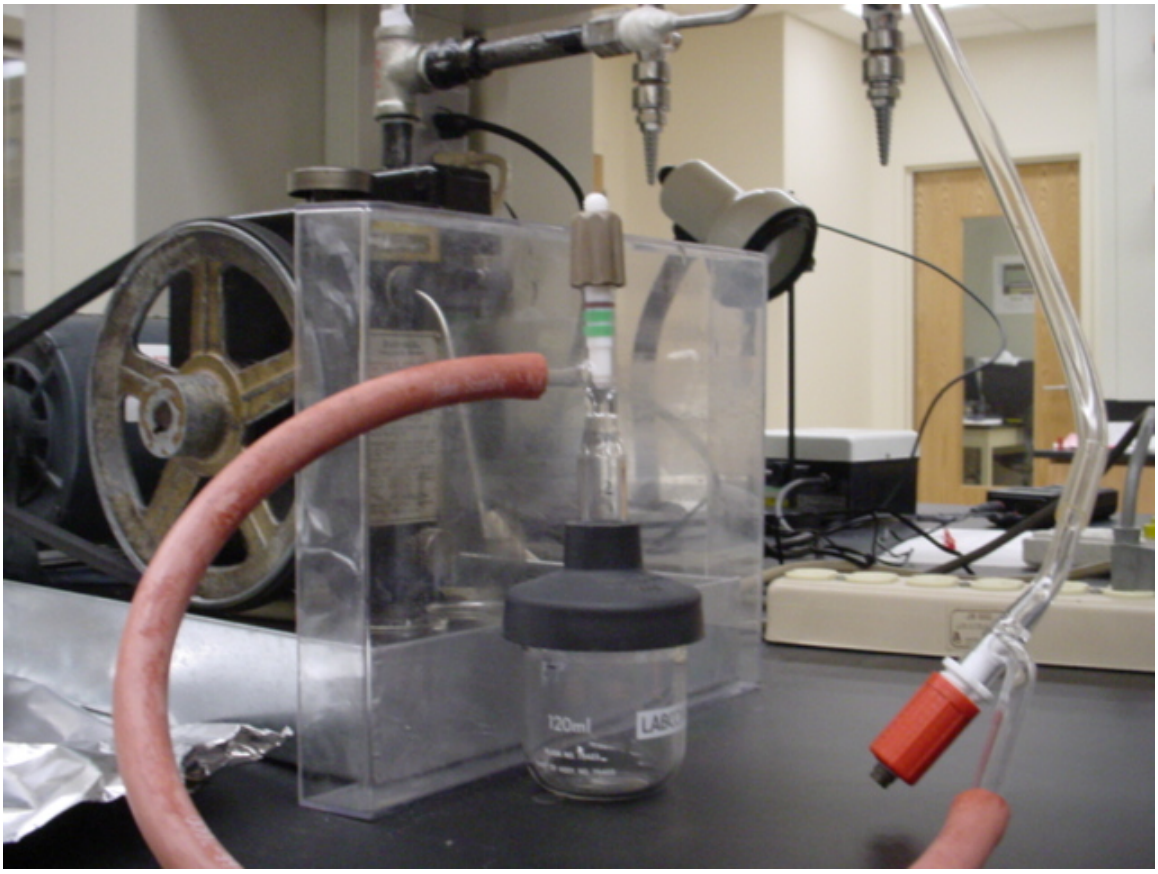

Figure 3-2. Apparatus used in the porosity measurement.

3-3-3 **Distribution of Pore Sizes**

The actual pore sizes were observed by scanning electron microscopy (SEM). The direct observation of the porous structure in the substrate can also confirm the reproducibility of the synthetic method. Details of the SEM imaging are described in Chapter 4. Briefly, fractured pieces of a host substrate were secured on a sample holder with double-sided adhesive, then sputter-coated with gold, and their surfaces and cross-sections were examined using an S800 SEM (Hitachi, Tokyo, JP).

3-3-4 **Absorption and Desorption Measurement**

The absorption and desorption behavior of acetonitrile in PCPS was observed by immersing a sample in acetonitrile at room temperature for one hour. The rate of desorption of the solvent out of the substrate to air was measured periodically on a balance (Model AE 163, Mettler Instrument, Hightstown, NJ). The glass covers of the balance were closed throughout the measurement in order to reduce convection.

*3-4 **Experimental Results***

3-4-1 **Porosity Measurement**

The expulsion of air bubbles from the substrate took about two hours in this experiment. The experimental and calculation results are listed in Table 3-1. The substrate exhibits an absorption capacity of water as high as 380 wt. %. The value is consistent with the result reported by Ruckenstein and Park (1991). The volume of water absorbed corresponds to the volume of voids accessible to water molecules. The porosity of the substrate was 77 vol. % using equation 3-1, which is comparable to 0.74 – the volume fraction of the most compact arrangement of spheres (Higgins, 1994). The high porosity indicates that the host substrate has an open-pore structure with a large internal area in which most of the pores are connected by channels. The connected-pore structure favors the generation of a network of conductive phases throughout the substrate, and thus can lead to a highly conductive and uniform composite (Park and Ruckenstein, 1992).

Table 3-1. The porosity of PCPS film.

Dimensions (cm)	2.595 × 1.065 × 0.355
Volume (cm^3)	0.981
Dry Weight (g)	0.20023
Density of Polymer (g cm^{-3})	0.204
Weight (g)	0.95750
Mass of Water Absorbed (g)	0.75727
Density of Water (g cm^{-3})	1.00
Porosity %	77

3-4-2 **Specific Surface Area Measurement**

The isothermal gas sorption of PCPS was measured at 77.19 K using nitrogen as an adsorbent. The mass of the sample was 0.1100 g after drying overnight under a vacuum of 4×10^{-3} Torr at 423 K. The specific surface area of PCPS calculated by the BET method was 23.7639 ± 0.2562 m^2 g^{-1}, but was 55.7056 ± 1.5451 m^2 g^{-1} from the Langmuir method. Negative values were obtained from the t-plot method. The variation in the data suggests that the nitrogen absorption method is not suitable for the surface area measurement of a substrate with large pores. The BET surface area could be reliable because the correlation coefficient in the BET plot is closest to 1. The BJH analyses on pore distribution indicate that the substrate does not contain pores that are sub-micron in diameter.

In order to estimate the average pore size from the BET surface area, the host substrate was assumed to have a uniform, hexagonal, closed-packed (hcp) structure with a uniform pore size (Rodeheaver, 1999; Higgins, 1994). This assumption may be valid because the experimental value of the porosity of the substrate (77 vol. %) is very close to the hcp packing fraction (74 vol. %). If pores are impinged to create a thin-walled foam structure, the specific surface area can be calculated using the following equation where A_{SP} is specific surface area [m^2 g^{-1}], D is the diameter of a pore [μm], N_P is the total number of pores per unit volume [pores μm^{-3}], and ρ_P is the polymer density [g cm^{-3}]:

$$A_{SP} = \frac{\pi D^2}{\rho_P} \cdot N_P = \frac{\pi D^2}{\rho_P} \cdot \frac{6}{3\sqrt{2}D^3} = \frac{\sqrt{2}\pi}{D \cdot \rho_P} \qquad (3\text{-}2)$$

The calculated result is plotted in Figure 3-3. The plot shows significant increase in specific surface area when the diameter is below one micron. The figure also indicates that the pore size of the host substrate should be on the order of 1 μm in diameter if the experimental value of the BET surface area is true. In order to confirm this hypothesis, the pores were observed under a microscope as described below.

3-4-3 **Distribution of Pore Sizes**

The actual pore sizes of PCPS were observed by scanning electron microscopy (SEM). The SEM pictures are shown in Figures 3-4 and 3-5.

The results show that PCPS has an open-cell structure consisting of pores of various diameters connected by small channels. This can be clearly seen in the pictures, in spite of the fact that some of the pores collapsed due to mechanical stresses during SEM preparation. The average pore diameter was estimated to be between 1-10 μm, or approximately the same as the value determined by BET measurement.

3-4-4 **Absorption and Desorption Measurement**

The absorption capacity of PCPS was observed by immersing a sample in a solvent at room temperature. Acetonitrile was chosen as the solvent because it is the solvent that was used in the preparation of electrically conducting composites with ferric

chloride described in the next chapter. The weight change of the sample with time is plotted in Figure 3-6.

The amount of acetonitrile absorbed by the sample after one hour at room temperature reached 225 wt. %, which is consistent with the result (256 wt. %) of Park and Ruckenstein (1992). The expulsion of the solvent took about an hour, close to the value of 40 minutes reported by Park and Ruckenstein (1992). The difference in desorption time may be ascribed to the difference in specimen dimensions, temperature, and atmosphere in the balance. The negligible weight loss of the substrate after the test indicates that the substrate is intact after exposure to acetonitrile.

3-5 ***Summary***

A summary of the density, porosity, specific surface area, pore size of the PCPS substrate are tabulated in Table 3-2.

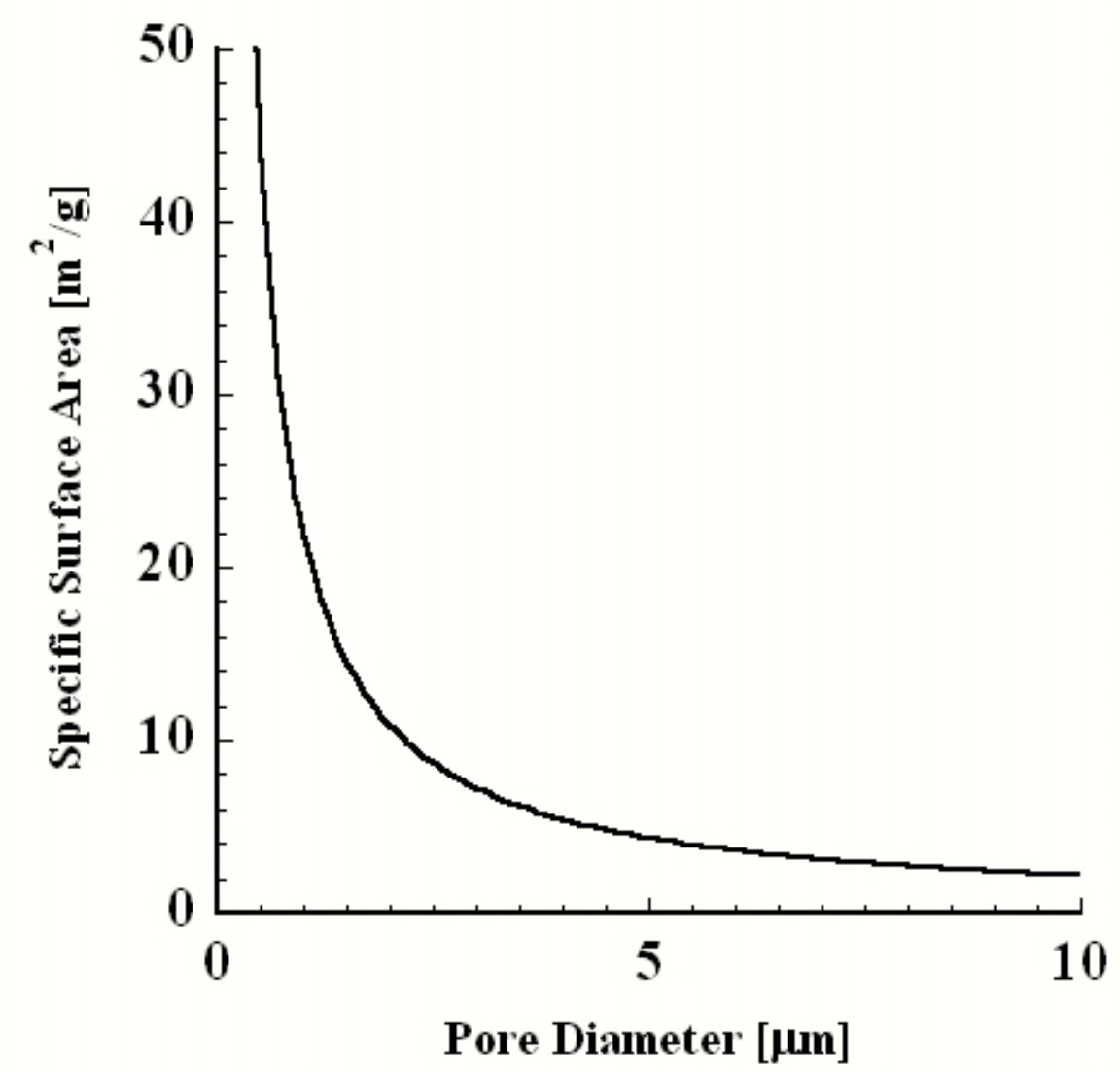

Figure 3-3. Specific surface area as a function of the diameter of hexagonal, closed-packed spheres with a density of 0.204 g cm^{-3}.

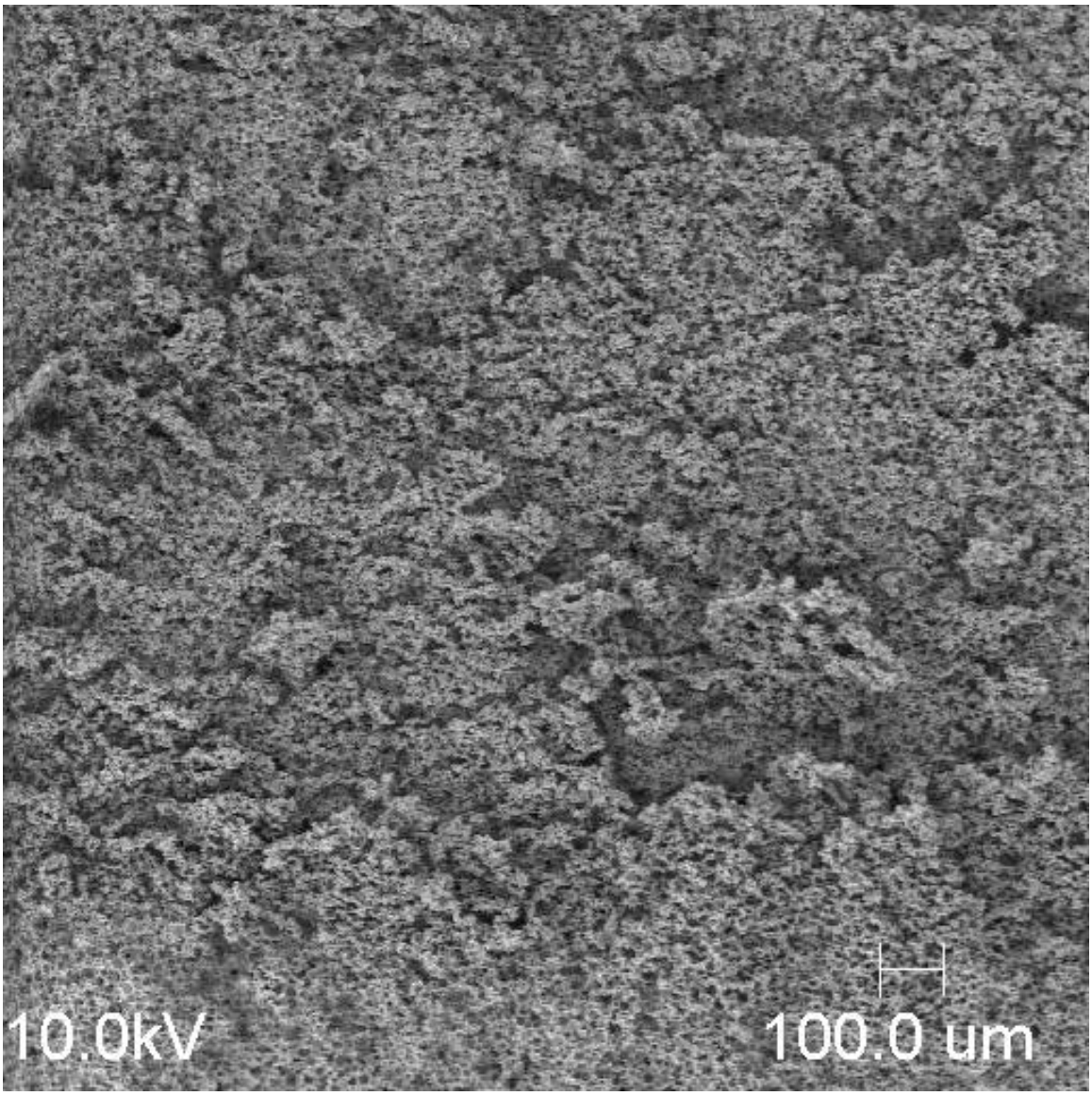

Figure 3-4. SEM micrograph of the surface of PCPS (×400).

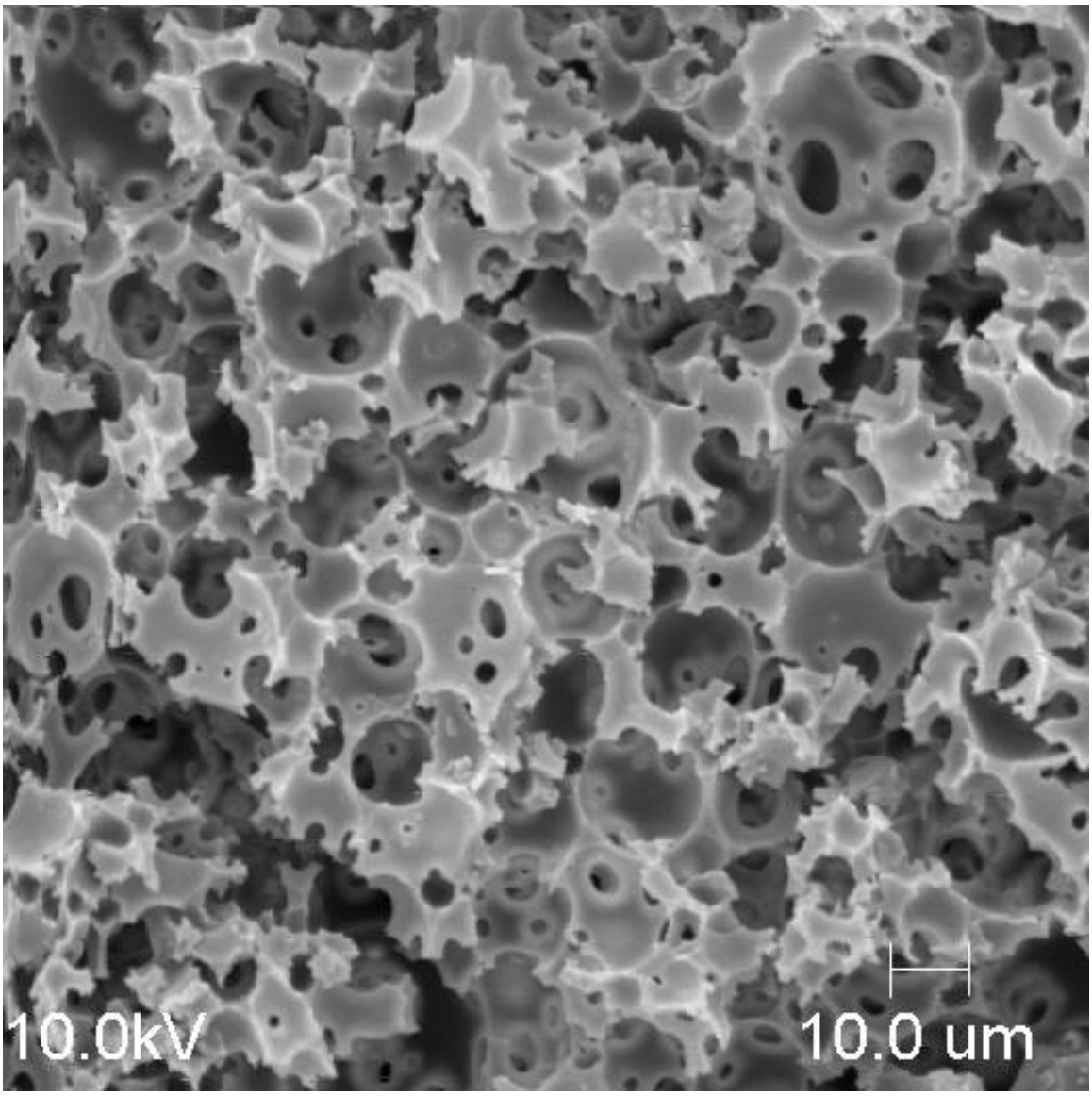

Figure 3-5. SEM micrograph of the cross-section of PCPS (×5000).

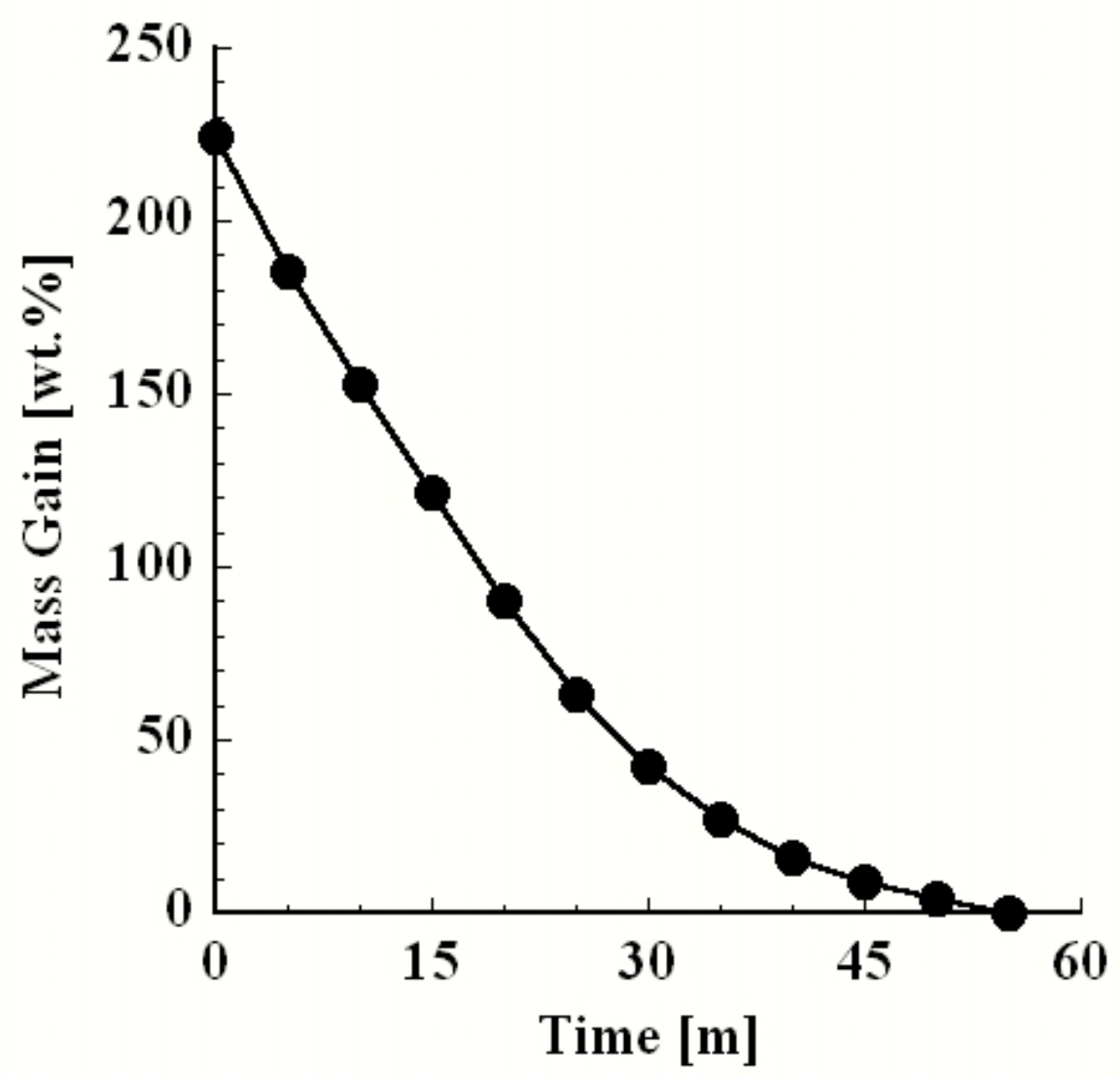

Figure 3-6. Amount of acetonitrile in PCPS against time during drying in air at room temperature.

Table 3-2. Characterization of PCPS substrate.

Density [g cm^{-3}]	0.204
Porosity [vol. %]	77
Specific surface area [m^2 g^{-1}]	23.7639 (BET) 55.7056 (Langmuir)
Actual pore size [μm]	1-10

CHAPTER 4

EXPERIMENTAL DESIGN AND PROCEDURES

Details regarding the preparation of electrically conducting composites of polypyrrole with porous and non-porous substrates using supercritical carbon dioxide are presented in this chapter. A two-step batch process was adopted in this work in which impregnation of the oxidant and in-situ polymerization of monomer were achieved sequentially inside a host substrate. The effect of several parameters including typs of substrate, solvent, and oxidant used, pressure, concentration, soaking and polymerization time, and procedure, were studied. The parameters were systematically varied to investigate their effect on the final properties of the composite. The electrical, thermal, and mechanical properties of the composites were measured.

4-1 ***Materials***

Iodine (ACS grade, 99.8 % purity) was purchased from Aldrich (Milwaukee, WI). Ferric chloride anhydrous (Laboratory grade), pyrrole (Acros Organics, 99 % purity), and acetonitrile (HPLC) were procured from Fisher Scientific (Hampton, NH). Poly(methyl methacrylate) (Spartech Polycast Poly II, 0.254 cm in thickness) was purchased from Laird Plastics (Atlanta, GA). Coolant grade carbon dioxide (99.99 % purity) cylinder was obtained from Air Products and Chemicals (Allentown, PA). Pyrrole (Py) was stored in a

refrigerator to prevent undesired reactions before use. All chemicals were used as received.

4-2 ***Host Substrates***

Porous, crosslinked polystyrene (PCPS) wafers were prepared as described in Chapter 3. After drying, each wafer of PCPS was carefully cut into several pieces using a razor blade. The dimensions of the pieces were typically 1.0 cm × 2.5 cm × 0.25 cm. The thickness of the substrate was measured with an uncertainty of ± 0.005 cm by a caliper before use.

Poly(methyl methacrylate) (PMMA) was processed to obtain a non-porous thermoplastic substrate from a large stiff sheet using a cutting saw. The surfaces of the PMMA sheet were protected by double-face seals. After removing the seals off the sheet, a methanol-soaked paper was applied on both surfaces of the sheet in order to wipe off adhesive residuals.

Two samples are shown with a caliper for scaling in Figure 4-1. The PCPS piece (left) appears to be white due to light scattering of pore interfaces, while the PMMA substrate (right) is clearly transparent. All the samples were stored in a fume hood before use.

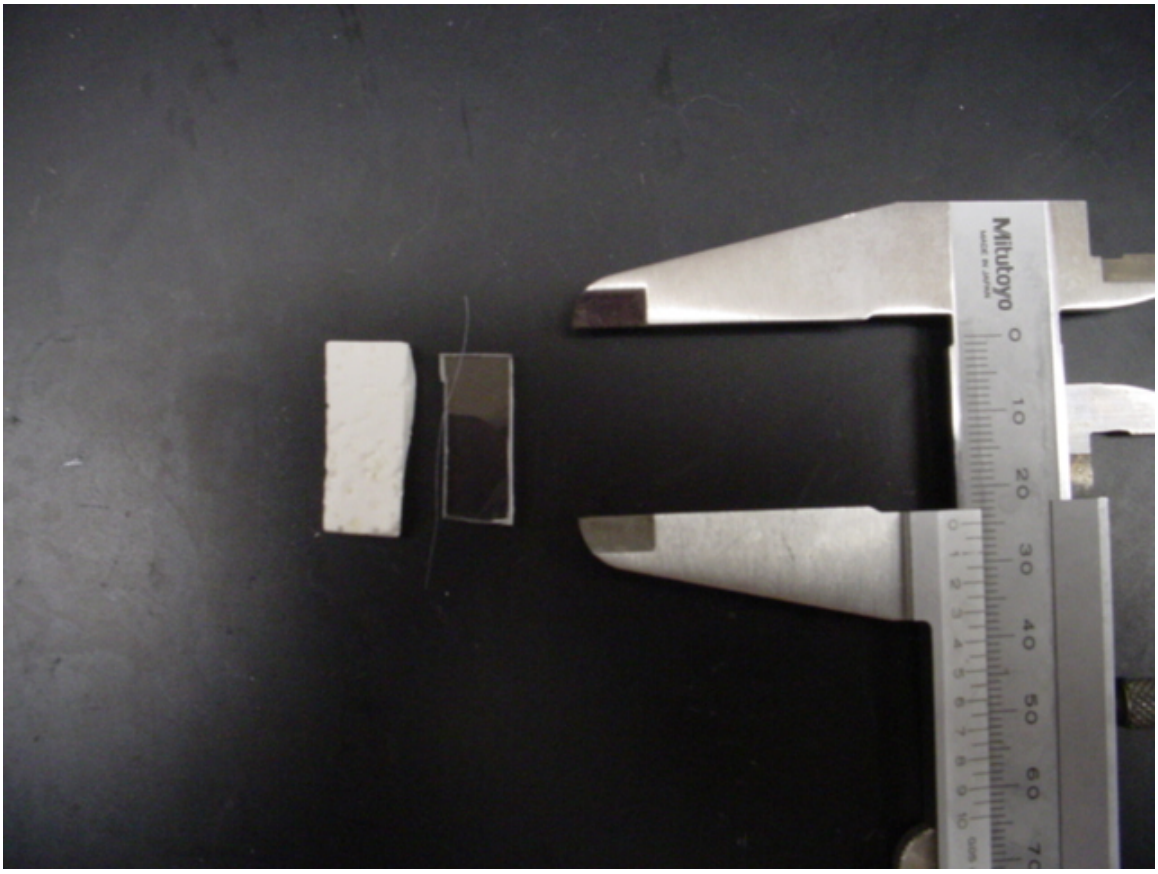

Figure 4-1. Porous, crosslinked polystyrene (left) and poly(methyl methacrylate) (right).

4-3 ***Composite Preparation by a Two-Step Batch Method***

Both Py monomer and oxidant ($FeCl_3$ or I_2) must be introduced separately to host substrates (PCPS or PMMA) since they react immediately upon contact according to the reaction depicted in Figure 4-2. A two-step batch process was employed to prepare composite. In the first step, the oxidant was imbibed in the host substrate. In the second step, the oxidant-impregnated host substrate was brought into contact with Py monomer to initiate the polymerization reaction. Figure 4-3 is a schematic description of the two-step batch process.

4-4 ***Experimental Apparatus for High-Pressure Experiments***

The high-pressure apparatus used in this work consisted of an ISCO SFX 2-10 extractor (Lincoln, NE) connected to an ISCO 100DX high-pressure syringe pump to control the CO_2 pressure in the system. A circulating pump with an immersion cooler (CC-100II, Neslab Instruments, Newington, NH) was used for circulating water to liquefy CO_2 at the pump head. The temperature in the extractor was controlled by a pre-installed temperature controller (Model PYZ4-TCY1-4V, Fuji Electric, Saddle Brook, NJ). The system pressure was measured by a pressure gauge (Model CM-51917, Heise, Newtown, CT) that was calibrated by a dead weight tester (Model 380 H, Budenberg Gauge, Manchester, UK). The calibration is presented in Appendix G. The experimental apparatus for the high-pressure experiments is shown in Figure 4-4.

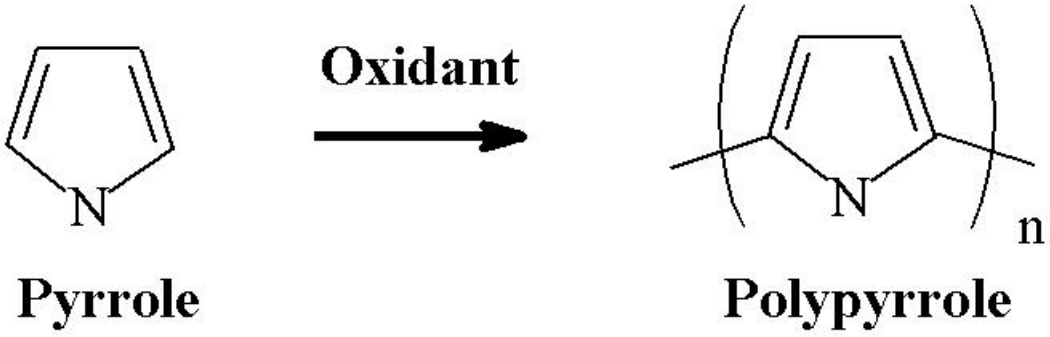

Figure 4-2. Synthesis of polypyrrole.

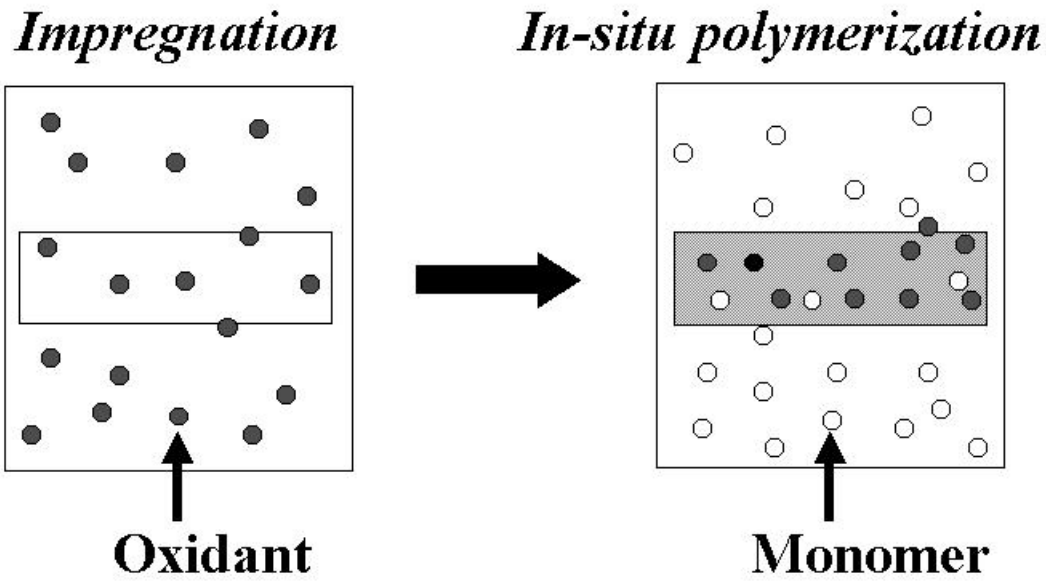

Figure 4-3. Schematic diagram of the two-step batch process.

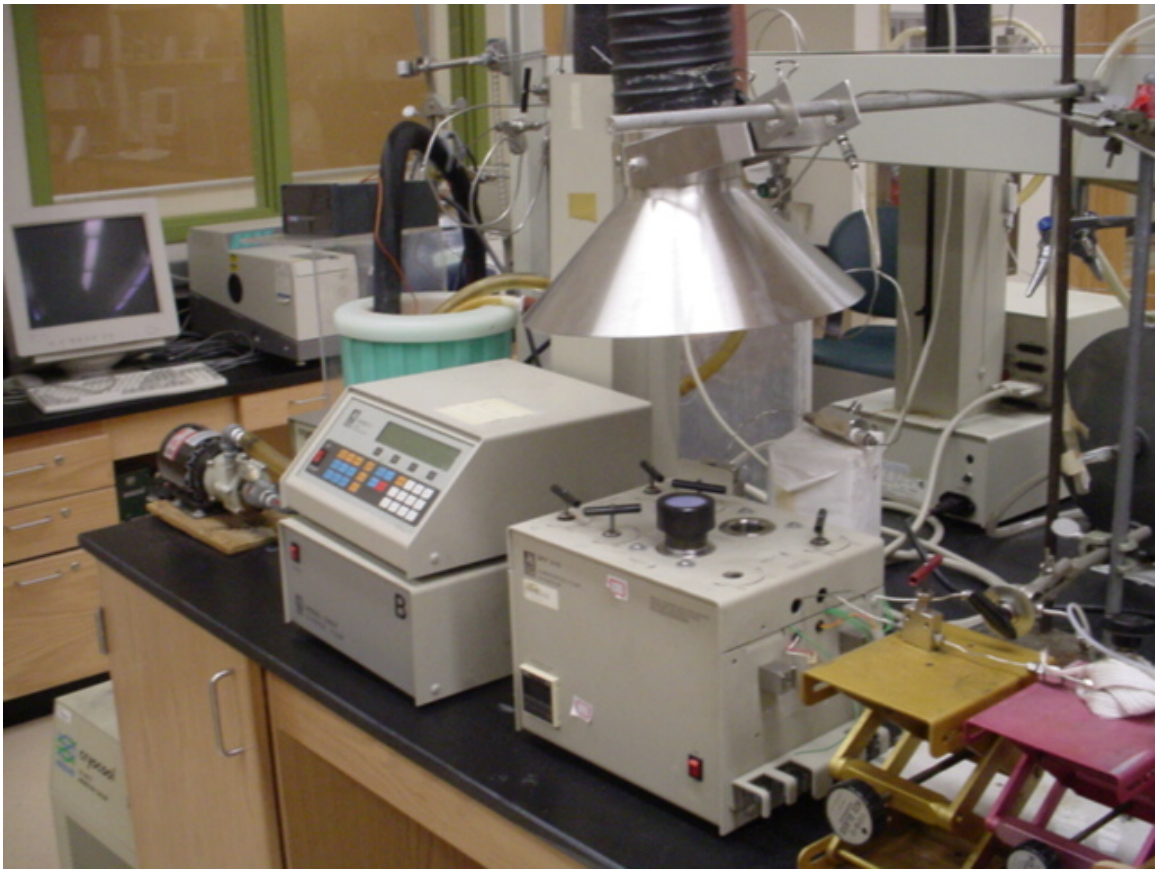

Figure 4-4. Experimental apparatus for the high-pressure experiments.

*4-5 **Impregnation of Oxidant***

4-5-1 **Impregnation of Ferric Chloride with Liquid CO_2 and Acetonitrile**

All $FeCl_3$ impregnation experiments were carried out using acetonitrile at ambient conditions except a trial run using liquid CO_2 because $FeCl_3$ is practically insoluble in either liquid or supercritical CO_2 (Kerton *et al*., 1997; DeSimone, 1998). The experimental procedure for the trial run is as follows: 1 g of $FeCl_3$ was placed in the bottom of a Parr reactor (No. 4575-76, Parr Instrument, Moline, IL). A plastic sieve was placed in the reactor to suspend a PCPS sample well above the reactor bottom and away from the $FeCl_3$. The reactor was sealed and connected to an ISCO 100DX high-pressure syringe pump. Liquid CO_2 was introduced slowly until a set pressure at 10.3 MPa was attained. The liquid mixture was subjected to mechanical agitation by a magnetic stirrer to disperse the oxidant in the reactor. After four days of soaking at room temperature, the system was depressurized slowly, and the substrate was removed. Subsequently, the in-situ polymerization of Py in the impregnated substrate was conducted at 313 K and 10.3 MPa for 24 hours. The amounts of $FeCl_3$ impregnated and PPy complex formed in the substrate were determined gravimetrically.

Acetonitrile was chosen as a solvent in the $FeCl_3$ impregnation process because PCPS is stable in acetonitrile containing $FeCl_3$ (Webb, 1998). A predetermined amount of $FeCl_3$ was dissolved in 25 mL of acetonitrile, and the solution was capped and left to dissipate the heat of dissolution. A PCPS film was immersed in the $FeCl_3$ solution for a specified period of time at room temperature. After drying under vacuum overnight in a

micro rotary evaporator (PN 421-4001, Labconco, Kansas City, MO) as shown in Figure 4-5, the substrate was weighed to determine the mass gain of $FeCl_3$ relative to the weight of the pristine host substrate.

4-5-2 **Impregnation of Iodine with and without Supercritical Carbon Dioxide**

The impregnation of I_2 was carried out by exposure of the substrates to a mixture of I_2 and CO_2 at high pressures. Most experiments were carried out at 313 K and 10.3 MPa where the partitioning of I_2 in the poly(3-undecylbithiophene) composites with PCPS over CO_2 phase is favorable (Webb, 2001).

In each run, a host substrate was loaded in a glass vial placed inside a 10-cm^3 stainless steel vessel as shown in Figure 4-6. In the glass vial, glass beads were used to prevent direct contact of the substrate with any solid I_2. Typically, 2 g of glass beads were mixed with 1 g of I_2, followed by the addition of 0.5 g of fresh beads. The vessel containing the substrate in the glass vial was set in the ISCO extractor for a predetermined length of time. The introduction and release of CO_2 in the high-pressure experiments were done slowly so that no convection currents were set up. After depressurization, the substrate was weighed to determine the mass uptake of I_2 relative to the weight of the pristine host substrate.

In order to study the diffusion kinetics of I_2 into the substrate under supercritical conditions, a series of sorption measurements with different soaking times at 313 K and 10.3 MPa were also conducted. For comparison, the solvent-free impregnation of I_2 in the PCPS substrate was also conducted in the ISCO extractor at 313 K.

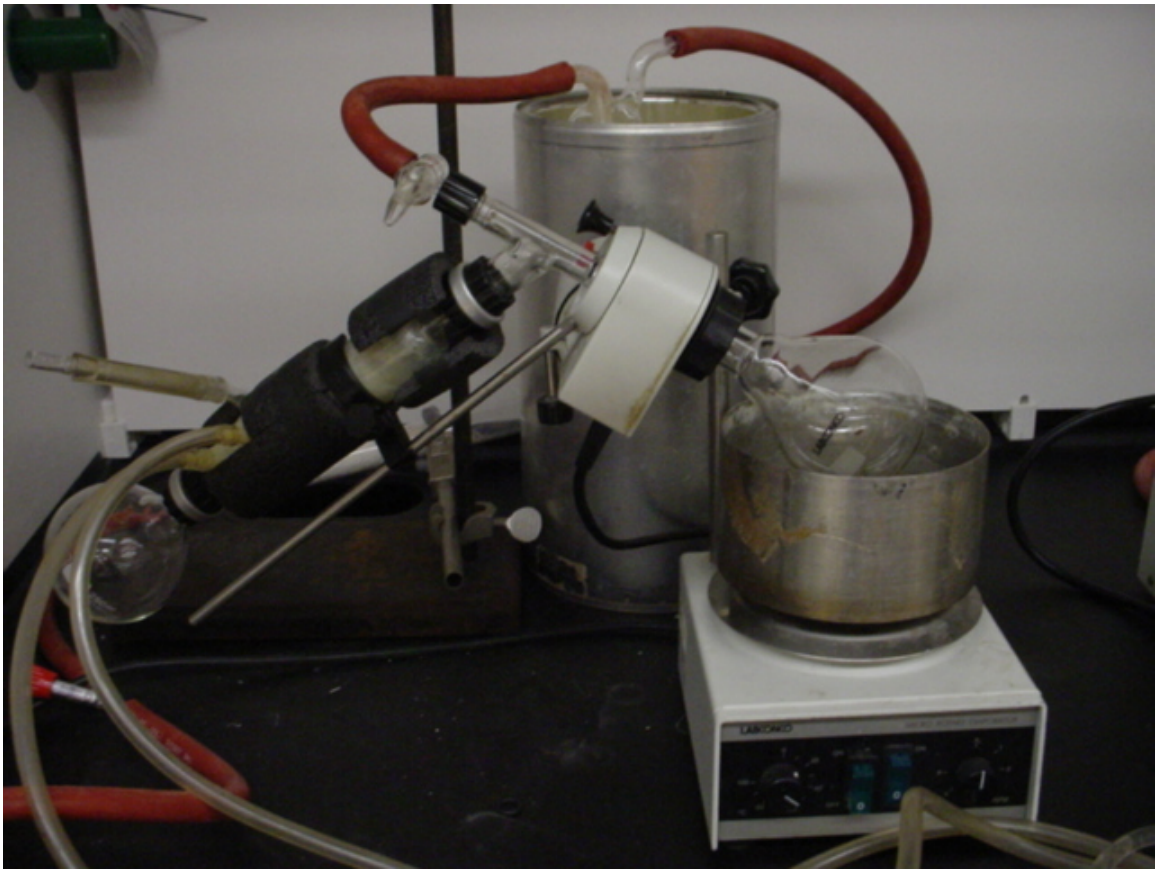

Figure 4-5. Rotary evaporator connected to a vacuum pump.

Figure 4-6. High-pressure vessel (left) and glass vial with a substrate on glass beads (right).

4-5-3 **In-Situ Polymerization of Polypyrrole with and without Supercritical Carbon Dioxide**

The substrates impregnated with an oxidant ($FeCl_3$ or I_2) were contacted with Py monomer in $scCO_2$. The impregnated substrate was transferred to a glass vial containing 2.5 g of fresh glass beads and Py monomer at the bottom. Care was taken not to exceed the liquid level of Py monomer above the top layer of glass beads. Py monomer dissolved in supercritical CO_2 was allowed to diffuse into the host substrate for a specified period of time. According to Myers (1986), the reactant stoichiometry is a primary factor that determines the rate of polymerization, yield, and conductivity. In the two-step batch method, the reactant stoichiometry can be calculated by the amount of oxidant impregnated in the first step and by the concentration of pyrrole (Py) monomer in the solvent at the second step. The concentration of Py monomer inside the reactor was maintained constant by the presence of an excess amount of liquid Py at the bottom of the glass vial at a fixed temperature, 313 K. Therefore, the polymer yield and electrical conductivity should be a function of the impregnated oxidant content in the impregnation step.

For comparison, a solvent-free polymerization of Py was also conducted. The polymerization of Py with $FeCl_3$ was carried out in the high-pressure extractor without CO_2 at 313 K for 24 hours. The impregnated sample was then transferred to a desiccator saturated with Py vapor using glass beads to separate the substrate and Py monomer. The desiccator was covered with a blanket and stored in a dark place in order to prevent side

reactions as a result of exposure to light. The solvent-free polymerization was carried out at room temperature for 48 hours.

In all the polymerization experiments, the resulting composites were left in a fume hood for a couple of days to remove unreacted oxidant and monomer before analysis. The mass gain due to the formation of PPy was calculated based on the weight of the pristine host substrate.

4-6 ***Electrical Conductivity Measurement***

Two methods were used to determine the electrical conductivity of the composites prepared in this research: a four-point-probe method for *surface* conductivity, and a two-point-probe method for *bulk* conductivity.

The surface resistance of the composite was measured with a four-point probe (Model C4S-64/00, Cascade Microtech, Beaverton, OR) connected to a multimeter (Keithley, Model 196 System DMM). The measured resistance ρ [ohm] was converted into the surface conductivity σ [S cm^{-1}] using the following expression for uniform films if the film thickness d [cm] is much less than half the probe spacing (Uhlir, Jr., 1955):

$$\sigma = \frac{\ln 2}{\pi d} \cdot \frac{1}{\rho} \qquad (4\text{-}1).$$

Since the probe has the spacing of 0.155 cm, equation 4-1 is not valid for composites with a thickness of 2 ~ 3 mm. Therefore, the bulk conductivity was calculated using the following expression for thick materials (Uhlir, Jr., 1955):

$$\sigma = \frac{1}{2\pi s} \cdot \frac{1}{\rho} \tag{4-2}$$

where s [cm] is the probe spacing. However, the coefficients in equations 4-1 and 2 are similar and close to unity for a film thickness of 2 ~ 3 mm and probe spacing of 0.155 cm. This also means that the surface conductivity is approximately a reciprocal of the reading resistivity. In this work, the surface conductivity was calculated using equation 4-1.

The bulk resistance of the composite was measured by a two-wire probe (2-mm O.D., Fluke, Everett, WA) connected to a multimeter (Model 3458A, Hewlett-Packard, Houston, TX) using sandwich geometry. The configuration for the bulk conductivity measurement is shown in Figure 4-7. Silver paint (Ernest F. Fullam Inc., Latham, NY) was applied to contact points in order to reduce the resistance between the probes and the sample surfaces. The measured resistance ρ [ohm] was converted into the bulk conductivity σ [S cm^{-1}] of the film of thickness d [cm] and cross-sectional area of the probe S [cm^2]:

$$\sigma = \frac{d}{\rho S} \tag{4-3}$$

It should be noted that S is not the surface area of the sample, but the probe contact area. It is assumed in the analysis that electrical conduction is limited to a hypothetical column in the composite between the probe contacts as schematically depicted in Figure 4-8. This may overestimate the values of the bulk conductivity because electrical conduction may also occur through the other regions outside the hypothetical column. Therefore, the bulk conductivity may be higher than the surface conductivity because of the reduced resistance (silver paint) and conduction area (small S value).

A new measurement using the two-point-probe method was therefore developed in the present work. This measurement is termed the *volume* conductivity and is intended to measure electrical conduction in a thin volume element normal to the composite surface. In order to eliminate any contributions from side conductive layers of the composite, the four sides of the sample were sliced off with a razor blade to obtain a 0.5 cm × 0.5 cm square film. The removal of the side coating was confirmed by visible inspection of the sliced square films as shown in Figure 4-9. The volume conductivity was determined by the same method as the bulk conductivity except that S in Equation 4-3 is now the surface area of the square film measured with a caliper. The volume conductivity obtained in this work may be underestimated because the concentration of the conductive component in the composite is probably the smallest at the center. However, the change in volume conductivity with the total conductive polymer content should be a measure of the percolation process in the composite. Furthermore, comparison of the three conductivities provides information on the uniformity of electrical conduction in the composite.

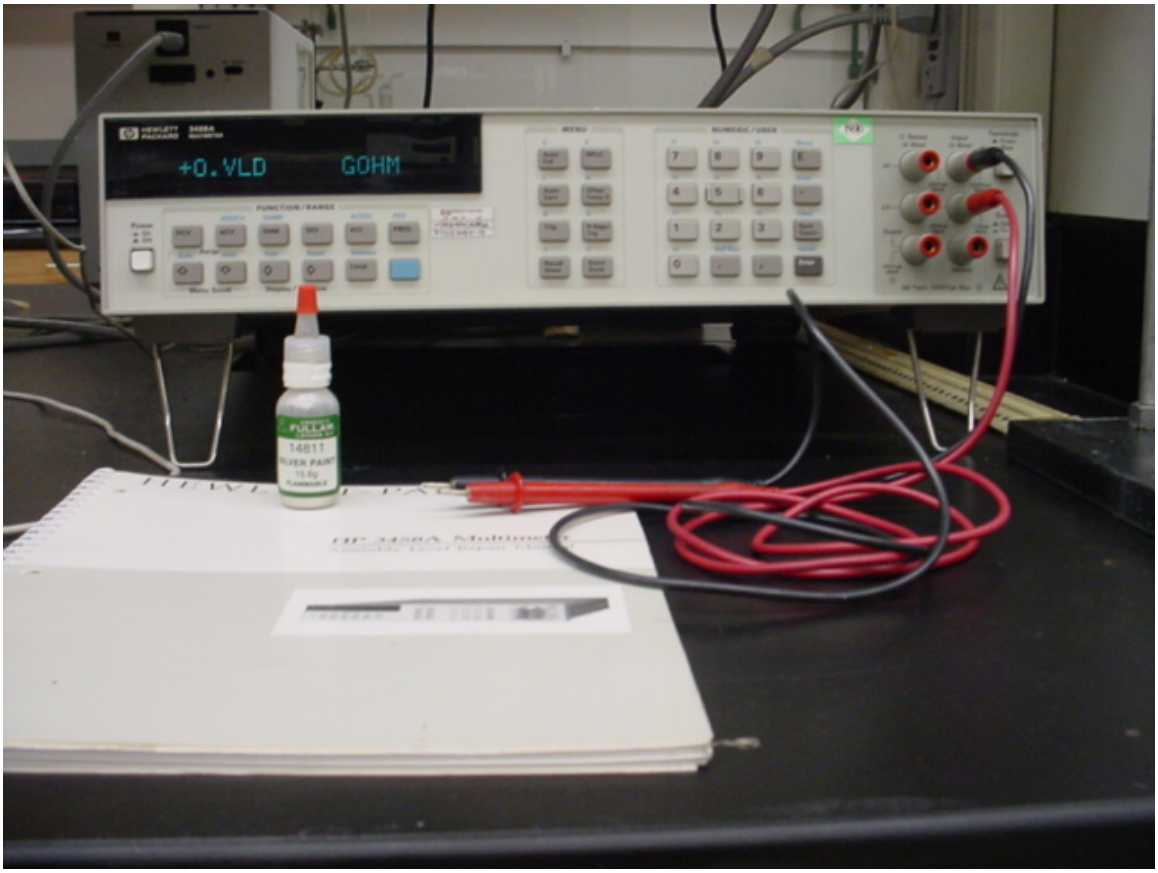

Figure 4-7. Experimental setup and silver paint for the two-point-probe method.

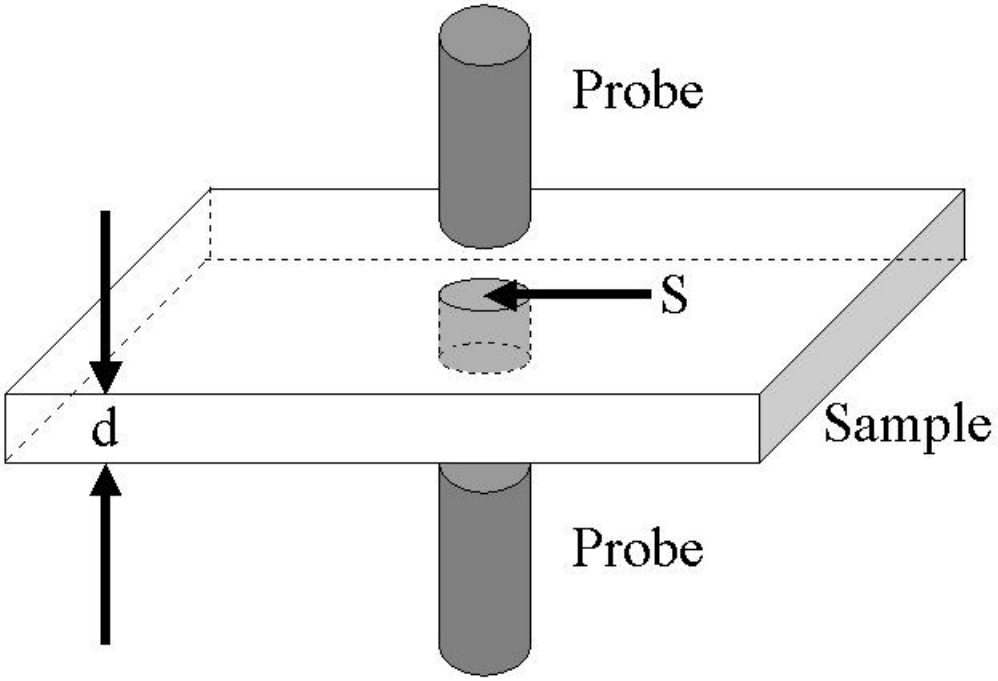

Figure 4-8. Schematic diagram of the two-point-probe method for bulk conductivity.

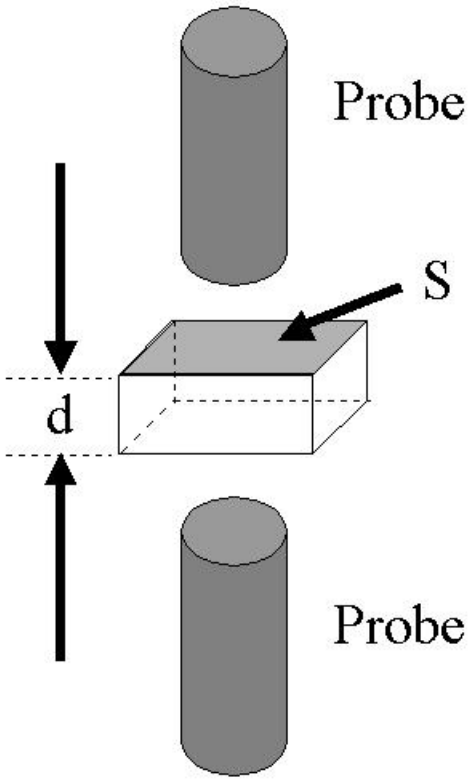

Figure 4-9. Schematic diagram of the two-point-probe method for volume conductivity.

4-7 ***Morphological Observation***

4-7-1 **Optical Microscopy**

Changes in color of the substrate were noted because they are indicative of the distribution of chemical species. For example, a white PCPS substrate becomes yellow with the absorption of ferric chloride, and transparent pyrrole becomes black upon polymerization. Optical microscopy was therefore used to obtain information regarding the distribution of chemicals and morphologies after each step.

Fractured pieces of samples were placed on glass slides of an optical microscope. The slides were mounted on the stage of a Leica DMLM microscope (Leica Microsystems, Bannockburn, IL) equipped with a Sony DKC-5000 CCD camera. The microscope had a 10× eyepiece and 5 FLUOTAR objective lenses for magnifications of 2.5×, 5×, 10×, 20×, and 50×. Reflected light sources were used to illuminate the samples. Images were captured and processed with an Image-Pro PLUS version 4.5 software. The setup is shown in Figure 4-10.

4-7-2 **Scanning Electron Microscopy**

Scanning electron microscopy (SEM) was also employed to investigate features of the host substrates during processing. A Hitachi S800 field emission gun scanning electron microscope (Tokyo, JP) shown in Figure 4-11 was used to image the surface and cross-section of the samples. The polymer sample was first cut to fit the size of a SEM

sample holder. The fractured pieces were then placed on the holder surface of the SEM with a double-face adhesive (05071-AB, SPI Supplies, West Chester, PA). The samples were gold-sputtered before the measurements. This prevented charge accumulation during the electron scans. The gold coating was applied with an International Scientific Instruments PS-2 Coating Unit shown in Figure 4-12. Samples were coated for 120 seconds at 20 mA and 1.2 kV under a specified pressure of argon flow. The gold-sputtered sample on the sample holder was placed in a vacuum section under the microscope. An acceleration voltage of 10 kV was used in all the SEM measurements. After focusing and adjustments, each digital image was captured through an iXRF Systems Iridium software with a scaling bar.

4-8 ***Thermogravimetric Measurement***

Thermal stability of the host substrates and PPy composites was determined using a thermogravimetric (TG) method. A TG curve is a plot of the mass change against temperature to characterize the decomposition and thermal stability of samples to examine the kinetics of the physicochemical processes (Hatakeyama and Quinn, 1999).

A Seiko Instruments Model TG/DTA 320 (Torrance, CA) was utilized under an inert atmosphere. The reference was an empty aluminum pan, and a flow of nitrogen was set at 250 mL min^{-1}. A small amount of fractured samples (5-15 mg) was placed in a sample aluminum pan. The temperature scan started from room temperature to 823 K, and the heating rate was set at 20 K min^{-1}. The onset temperature of decomposition is

defined as a cross point of tangent lines before and after a steep weight change is observed. All the data are presented in Appendix D.

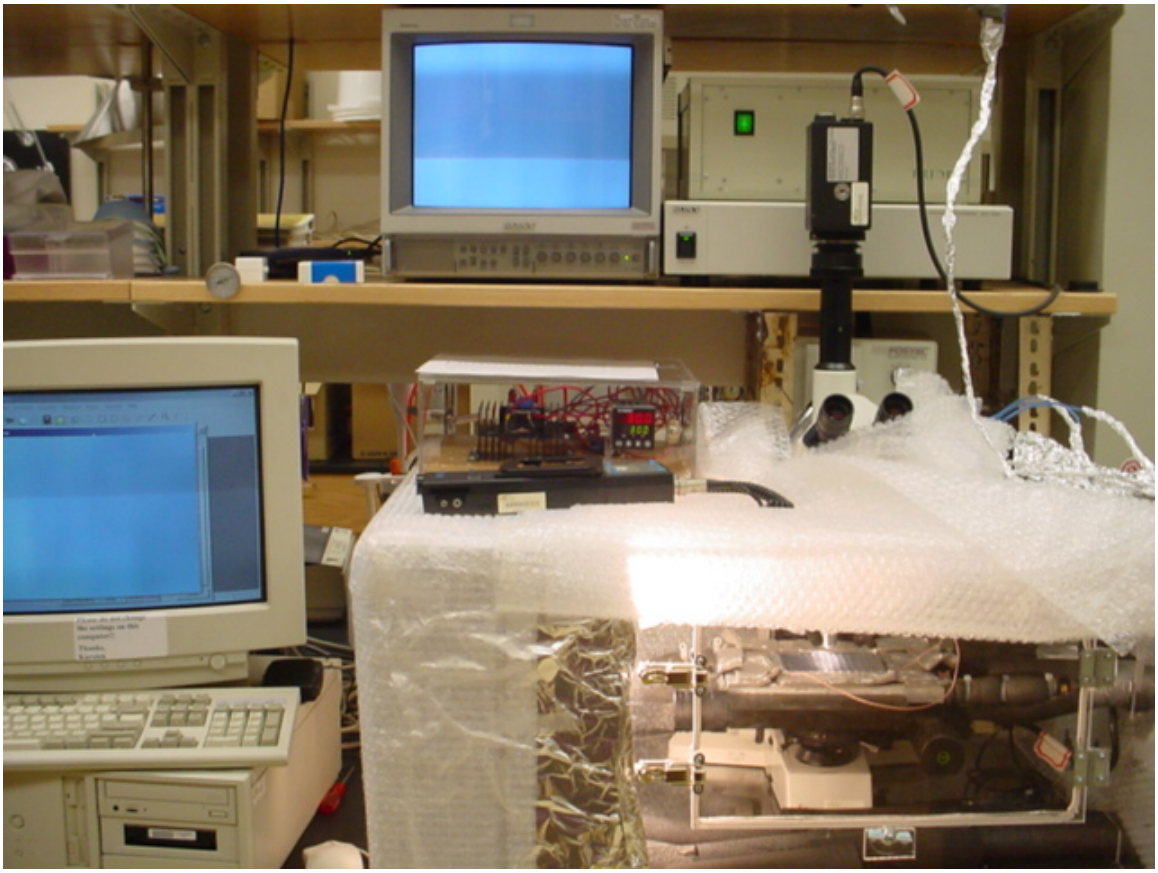

Figure 4-10. Imaging system including the optical microscope (right).

Figure 4-11. Hitachi scanning electron microscope.

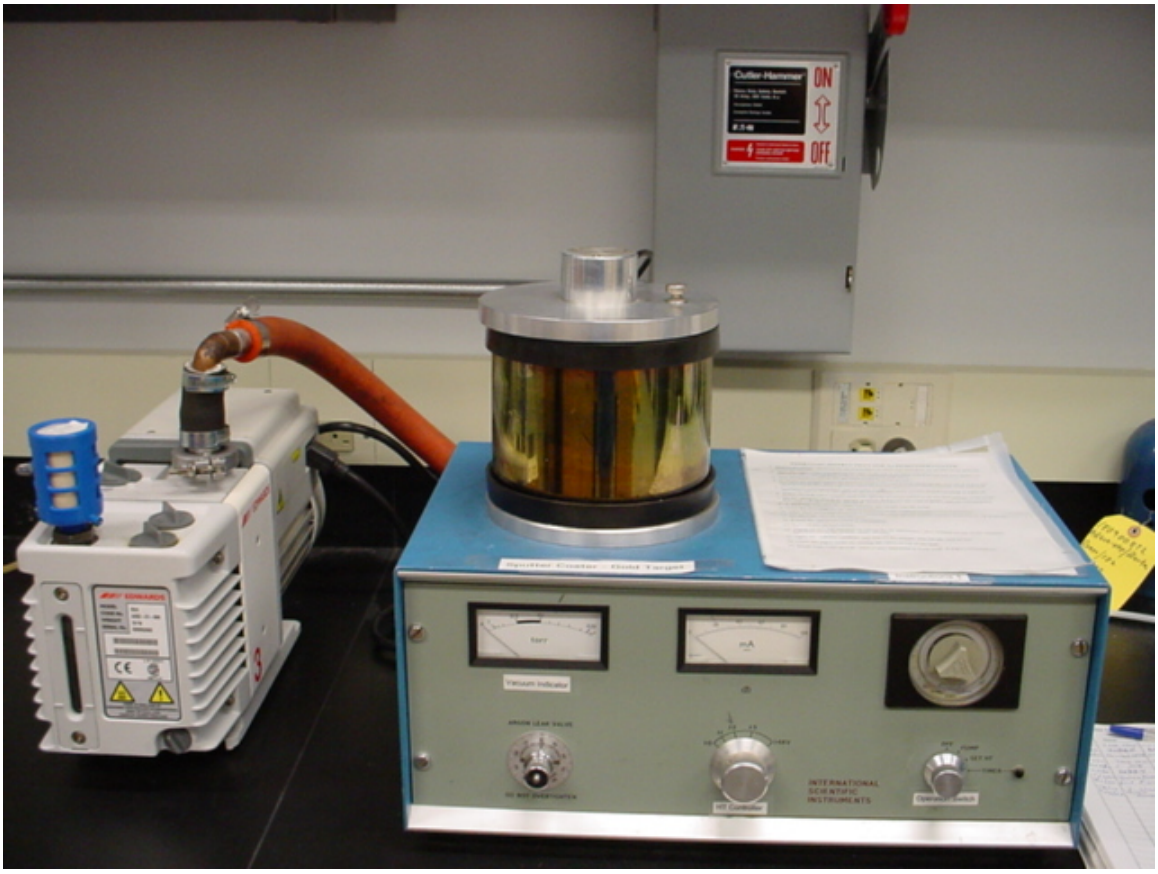

Figure 4-12. Gold sputter and vacuum pump.

4-9 ***Compressive Mechanical Testing***

The incorporation of PPy in the porous structure should affect the mechanical properties of the conductive composite. Typical elastic-plastic porous materials will show a compressive stress-strain curve with three distinct regions: elastic deformation, collapse plateau, and densification, in which a distinct yield point should be observed at the end of the elastic deformation (Arora *et al*., 1998). According to Gibson and Ashby (1988), the yield stress of open-porous foams can be related to a relative density by the following equation:

$$\frac{\sigma^*}{\sigma} = 0.23\left(\frac{\rho^*}{\rho}\right)^{3/2}\left[1+\left(\frac{\rho^*}{\rho}\right)^{1/2}\right] \qquad (4\text{-}4)$$

where σ^* is the yield stress of the foam, σ is the yield stress of the solid material, ρ^* and ρ are the densities of the foam and solid materials, respectively. The equation predicts that the yield stress of a foam (relative density of 0.204) is 0.92 MPa or 2.46 MPa if the corresponding solid material exhibits a yield stress of 30 MPa or 80 MPa, respectively. Notice that the range of reported yield strength data for polystyrene is between 30 MPa and 80 MPa (Arora *et al*., 1998).

Compressive mechanical testing was performed using a uniaxial electromechanical testing device (Model 650R, TestResources, Shakopee, MN). The device has been applied to oriented, biodegradable porous polymer scaffolds (Lin *et al*., 2003). Square specimens were cut out of a substrate or composite with a single-edged razor blade. Initial sample dimensions were measured using a caliper. Note that the

samples were square and smaller in size than recommended in ASTM Method D1621 due to limitations in the size of the reactor. A preload of 5 N was applied to the samples before initiating compression testing at a rate of 0.5 mm min^{-1}. Samples were tested to a strain endpoint of 50 % of initial thickness. The stress-strain relationship of the sample was calculated from the measured load-displacement data and sample dimensions. Compressive modulus was also determined from the largest slope in the linear elastic region of the stress-strain curve. All the data are presented in Appendix E.

4-10 ***The Effect of Temperature on Electrical Conductivity of Composite***

The temperature dependence of electrical conductivity has been measured in electrically conducting polymers (Masubuchi *et al*., 1995; Gilani *et al*., 1996; Lee *et al*., 1997b; Kemp *et al*., 1999; Yoshioka *et al*., 1999) and their composites (Makhlouki *et al*., 1992; Samir *et al*., 1995; Morsli *et al*., 1996; Omastova *et al*., 1996; Kaiser *et al*., 1997). Several models, including the variable range hopping model (Mott and Davis, 1979) and the fluctuation-induced tunneling model (Sheng, 1980), have been proposed and applied to the conductivity data to estimate the mechanism of electrical conduction in the semiconducting materials.

The change in electrical conductivity of the composites with temperature was measured using a constant-current van der Pauw method (van der Pauw, 1958). The measurement system consisted of a programmable current source (Model 220, Keithley, Cleveland, OH), autoranging picoammeter (Keithley, Model 485), multimeter (Keithley, Model 2000), and switch system (Keithley, Model 7001) with a computer for control and

data acquisition. A sample composite was cut into a 1-cm^2 film. Silver wires (0.127 mm in diameter, 99.9 % purity, Alfa Aesar, Ward Hill, MA) were attached at the four isolated corners of the sample. A silver-filled epoxy (410E, Epoxy Technology, Billerica, MA) was used to secure the contact between wire and sample by curing for three days at room temperature. The wires on the sample were then connected to electrodes on a sampling rod. The rod was inserted and evacuated in a superconducting quantum interference device (SQUID) magnetometer (Model MPMS-5S, Quantum Design, San Diego, CA). The rod was connected to the measurement system, and the connection was covered with aluminum foil to reduce electromagnetic interferences. After the system reached thermal equilibrium at 90 K, a program was executed to initiate the measurement. The measurement was repeated up to 300 K with a temperature increment of 5 K. At each temperature, a total of eight measurements were made around the sample, and the mathematical formula for the average resistance of the sample was adopted from ASTM Method F76. The electrical conductivity was calculated from the measured resistance and the thickness of the sample film. All the data are presented in Appendix C.

CHAPTER 5

RESULTS AND DISCUSSION

Experimental results obtained in this work are presented in this chapter. Composites containing polypyrrole (PPy) were made by the two-step batch method with non-porous poly(methyl methacrylate) (PMMA) or porous, crosslinked polystyrene (PCPS) substrates. The chemical oxidative polymerization of pyrrole (Py) monomer inside the substrates involved either ferric chloride ($FeCl_3$) or iodine (I_2) as an oxidant. The effects of the experimental parameters on electrical, thermal, and mechanical properties of the composite are discussed in the following sections.

5-1 ***Substrate: Non-Porous Poly(methyl methacrylate)***

Non-porous, thermoplastic PMMA strips were used as host substrates for comparison to the porous substrate, PCPS. It should be noted that PMMA is soluble in conventional organic solvents used for $FeCl_3$ impregnation such as acetonitrile, nitrobenzene, and chloroform. Webb (1998) found that $FeCl_3$ was deposited in a thin layer on the outer surface of the substrate when supercritical carbon dioxide ($scCO_2$) was used as a solvent. Although the $FeCl_3$-coated substrate was able to form PPy upon contacting with Py monomer in $scCO_2$, the penetration of the conductive PPy phase was limited to a small depth of the substrate where the oxidant was delivered in the

impregnation step. Therefore, $FeCl_3$ cannot be distributed uniformly inside the non-porous substrate using CO_2. I_2 was therefore used as an alternative oxidant since it is known to form charge transfer complexes with polypyrrole (Kang *et al*., 1987).

5-1-1 **Impregnation of Iodine**

The solvent-less method was carried out first to determine if I_2 molecules can penetrate the substrate without a solvent. After 24 hours of exposure to I_2 vapor at 313 K, no appreciable amount of I_2 could be detected in the substrate. As a result, the subsequent exposure to Py vapor did not form PPy. Furthermore, the bottom part of the PMMA substrate was partially dissolved because of the plasticization effect of Py monomer on the polymer. The non-uniform distribution of I_2 in the substrate indicates that a solvent that has a substantial solubility and diffusivity into the polymer is required for the impregnation step. Therefore, $scCO_2$ was utilized as a solvent because it dissolves an appreciable amount of I_2 (Fang *et al*., 1997) and plastisizes thermoplastic polymers to increase the diffusivity of additives (Wang *et al*., 1982; Wissinger and Paulaitis, 1987; Condo *et al*., 1992; Berens *et al*., 1992). The combination of high I_2 solubility and plasticization effect was expected to promote the mass transfer of I_2 into the PMMA substrate.

The sorption of I_2 in non-porous PMMA with CO_2 was measured at 313 K and 10.3 MPa for various soaking times as shown in Figure 5-1. The thick line represents a fitting curve using a Fickian diffusion model for the later stages of the sorption process in a plane sheet:

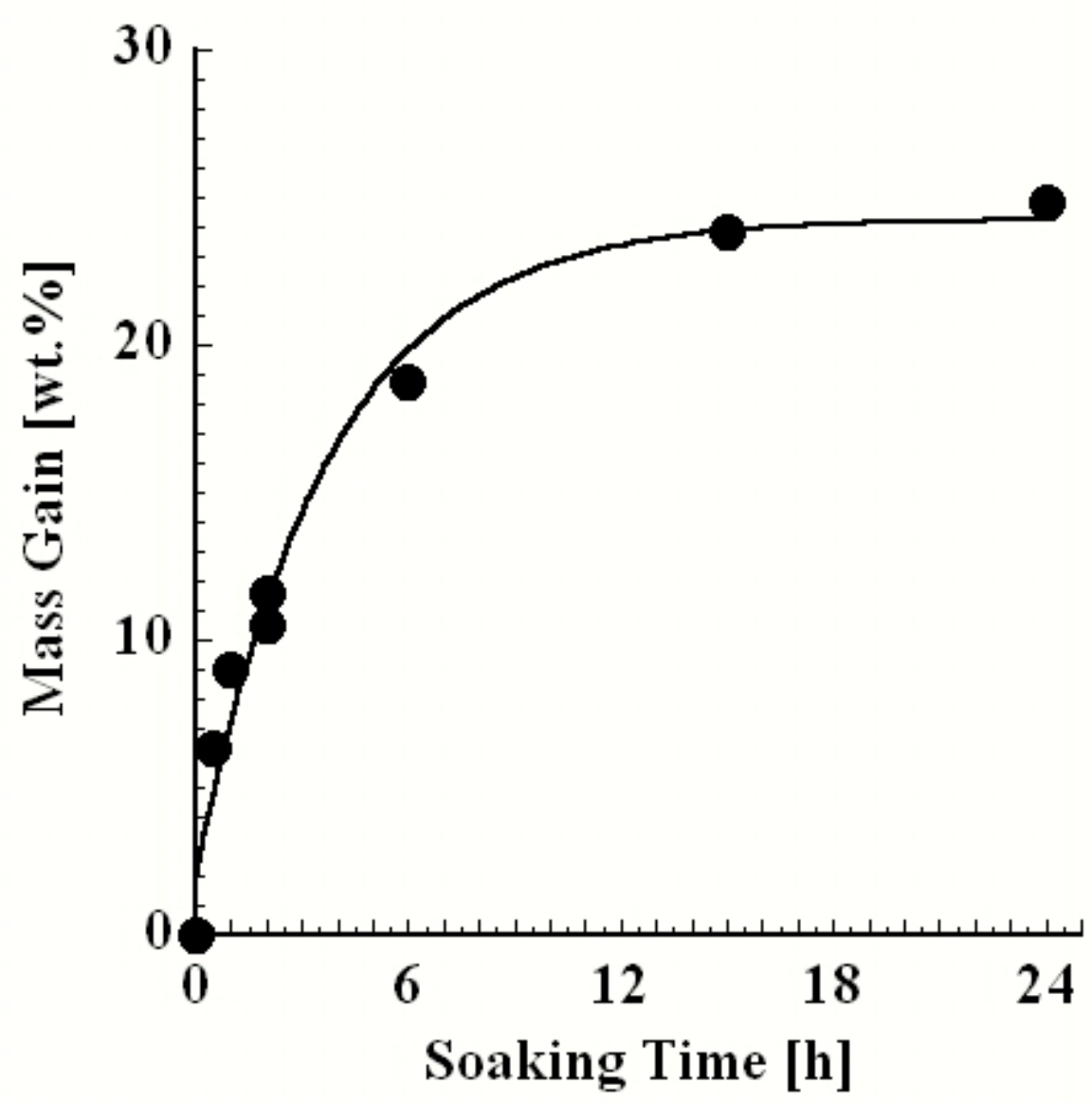

Figure 5-1. Sorption of I_2 in PMMA with CO_2 at 313 K and 10.3 MPa.

$$M(t) = M_\infty \left[1 - \frac{K}{\pi^2} \exp\left(- \frac{\pi^2 D t}{d^2} \right) \right] \tag{5-1}$$

where M(t) is the mass gain at time t, M_∞ the maximum mass gain, K is a temperature-dependent constant, and D is the diffusivity, and d is the sheet thickness. The mass uptake of I_2 in the PMMA substrate measured after depressurization was assumed to be the amount of I_2 incorporated into the substrate under high-pressure conditions because the weight loss due to desorption of I_2 from the impregnated substrates under ambient conditions was negligible. In all the experiments, an excess amount of I_2 was charged in the vial so that a distinct I_2 phase was present during the measurement. It should also be noted that no agitation was used in this work. Visual observation of the cross-sectional area of the non-porous substrate showed that I_2 was distributed evenly inside of the dense polymer substrate after a sufficient soaking time (~ 24 hours) although a small amount of I_2 was deposited on the surface of the substrates at high mass gains.

The diffusivity of I_2 in PMMA with CO_2 was calculated using the following equation for the rates of sorption in the early stages:

$$M(t)/M_\infty = 4\left(Dt/\pi d^2\right)^{1/2} \tag{5-2}.$$

The maximum mass gain of I_2 in PMMA is 24.8 wt. %, corresponding to a solubility of 19.9 wt. %. As shown in Figure 5-2, $M(t)/M_\infty$ is plotted against ($t^{1/2}/d$), where the linear curve indicates that the sorption of I_2 appears to follow a Fickian diffusion mechanism. The diffusivity of I_2 in PMMA with CO_2 was determined to be 3.54×10^{-7} cm^2 s^{-1} using equation (5-2) and the slope of the least-squares-fitting line in Figure 2. This value is

comparable to the diffusivity of CO_2 in PMMA, which is 1.04×10^{-6} cm^2 s^{-1} at 313 K and 10.5 MPa (Webb and Teja, 1999). It suggests that the impregnation of I_2 in PMMA is associated with the diffusion of CO_2 in the polymer matrix.

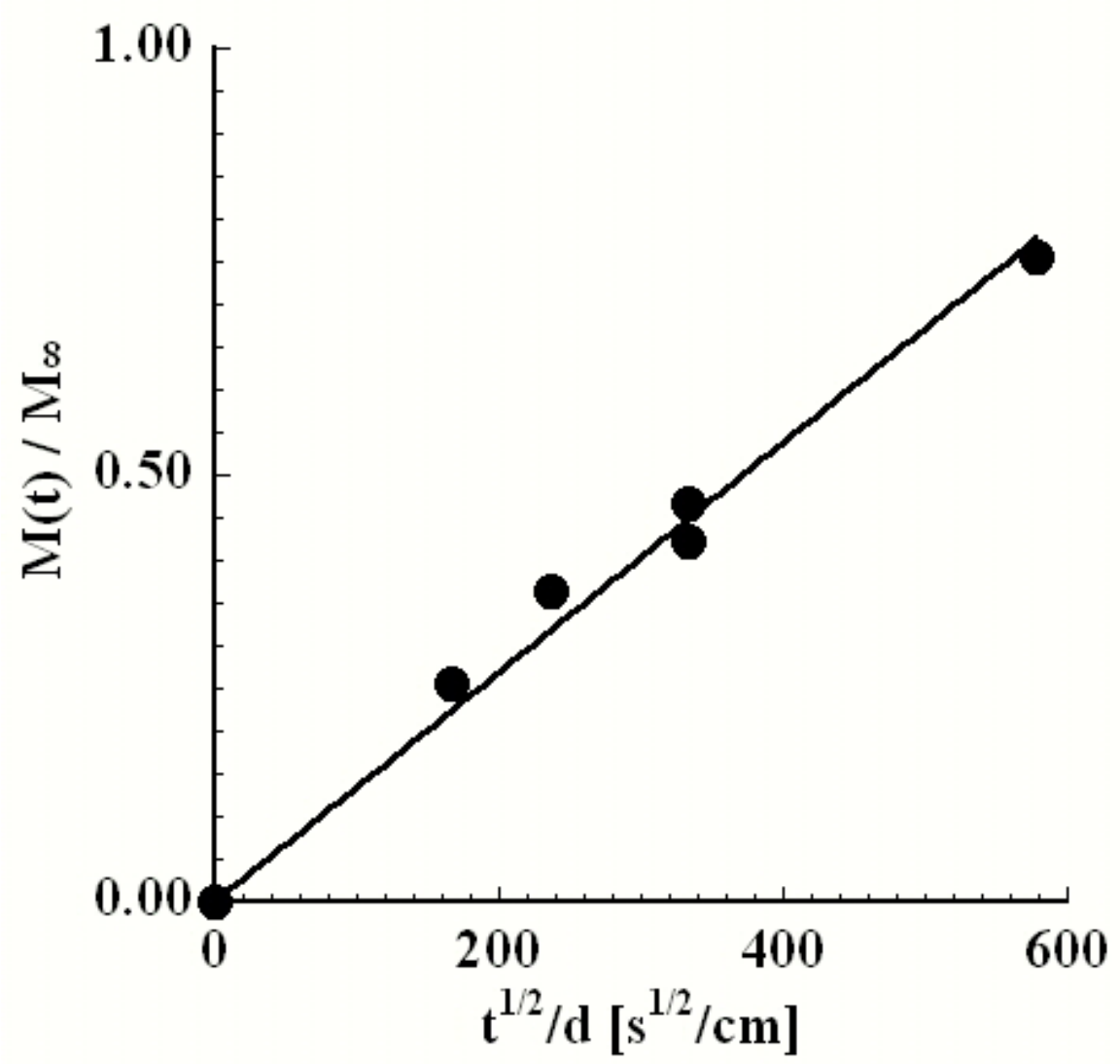

Figure 5-2. Diffusion of I_2 in PMMA with CO_2 at 313 K and 10.3 MPa.

5-1-2 **In-Situ Polymerization of Pyrrole**

The I_2-impregnated PMMA substrates were exposed either to Py vapor or to a mixture of Py and CO_2 to see the effect of CO_2 on the polymerization reaction in the substrate.

In the case of the Py vapor, an optical micrograph in Figure 5-3 reveals that a transparent phase of pure PMMA is encapsulated by a thick black-color phase, indicative of the presence of conductive PPy. Since the thickness of the substrate did not change as a result of polymerization, PPy is apparently fused into the PMMA matrix. SEM pictures show that PPy covers the surface smoothly in Figure 5-4(a), and that the composite has a clear phase boundary in Figure 5-4(b). The bulk and surface conductivities increase with the amount of PPy and I_2 complex (PPy + I_2) in Figure 5-5, and are comparable to the data reported in the literature (Wang *et al*., 2002).

In the case of the mixture of Py and CO_2, the composite shows higher mass gain and bulk conductivity as expected. However, the PMMA composite was foamed even at a moderate rate of depressurization of CO_2 as shown in Figure 5-6. It is mainly because the absorption of Py monomer is assisted by the presence of CO_2, and the absorbed monomer acts as a plasticizing agent, resulting in the enhancement of the deformation of the composite (Berens *et al*., 1992). The deformation also lowers the surface integrity of the conductive phase as indicated by the low level of surface conductivity. The bulk conductivity of the foamed composite is of the same order of magnitude as that of the non-foamed composites as shown in Figure 5-5, although the deformed sample has also

discrete phases of conducting and non-conducting polymers as shown in Figure 5-6. This may be due to the stiff chains of the conductive polymer as shown in Figures 5-7(a) and (b). It should be noted, however, that no volume conductivity was detected in the three samples.

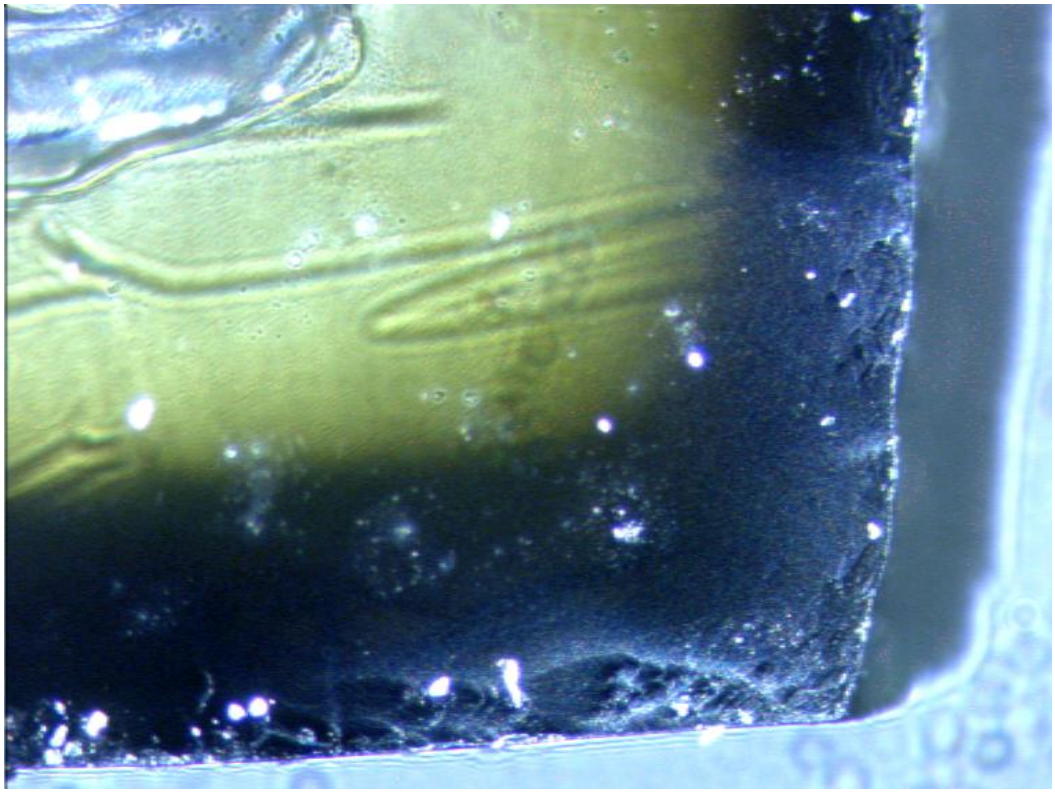

Figure 5-3. Optical micrograph of the cross-section of PMMA composite (×50).

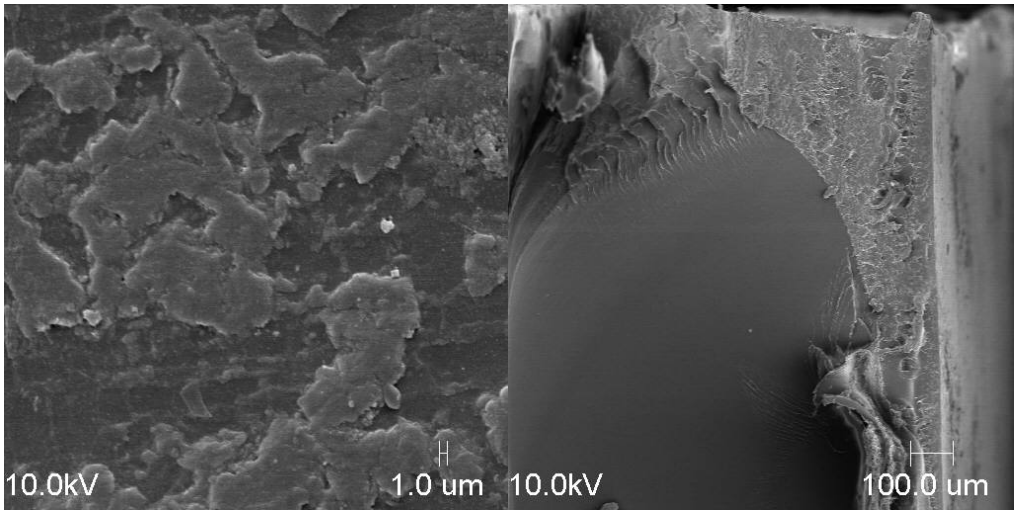

Figures 5-4(a) and (b). SEM pictures of the surface (×1000) and cross-section (×50) of PMMA composite.

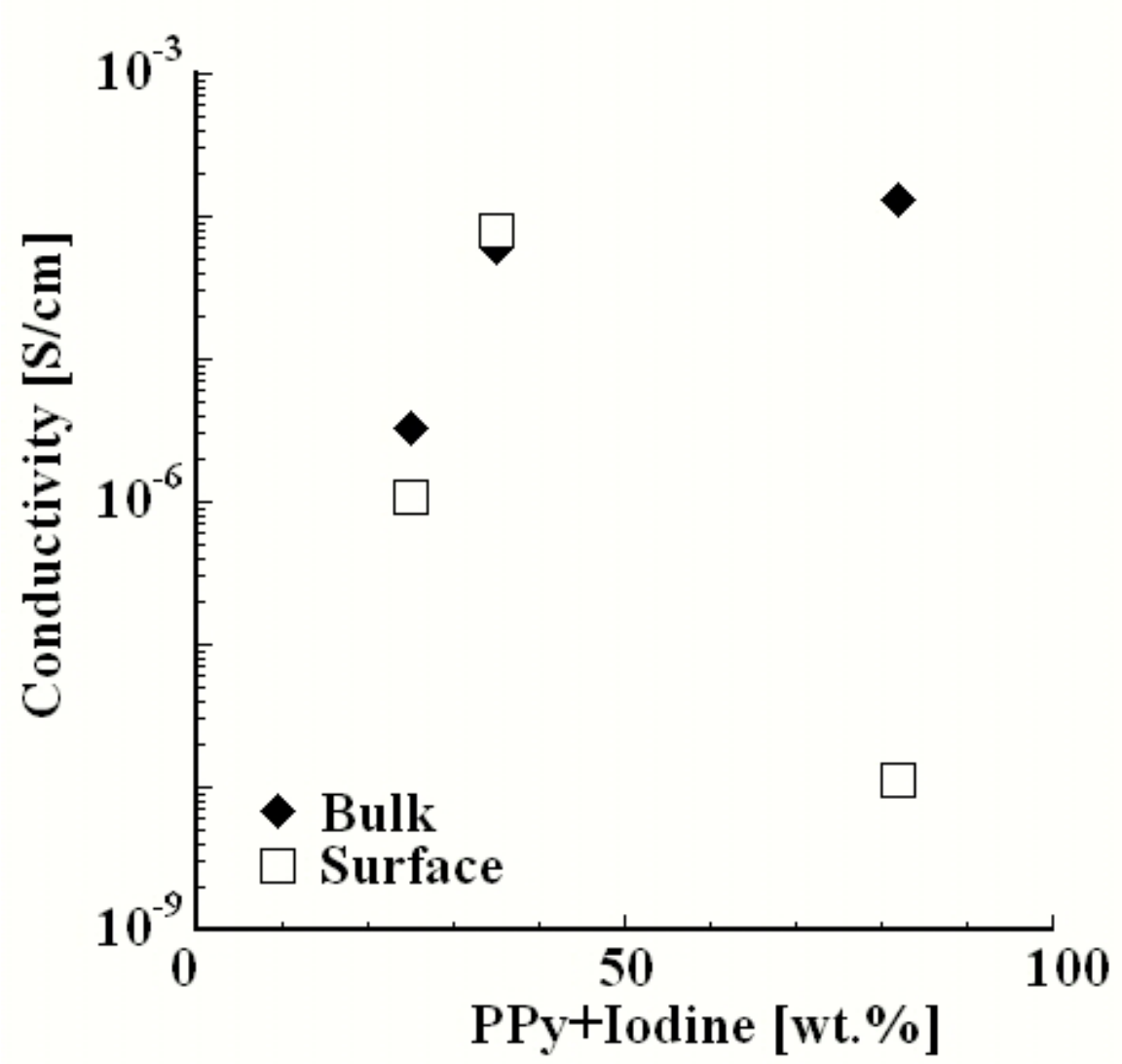

Figure 5-5. Conductivity of PMMA composite.

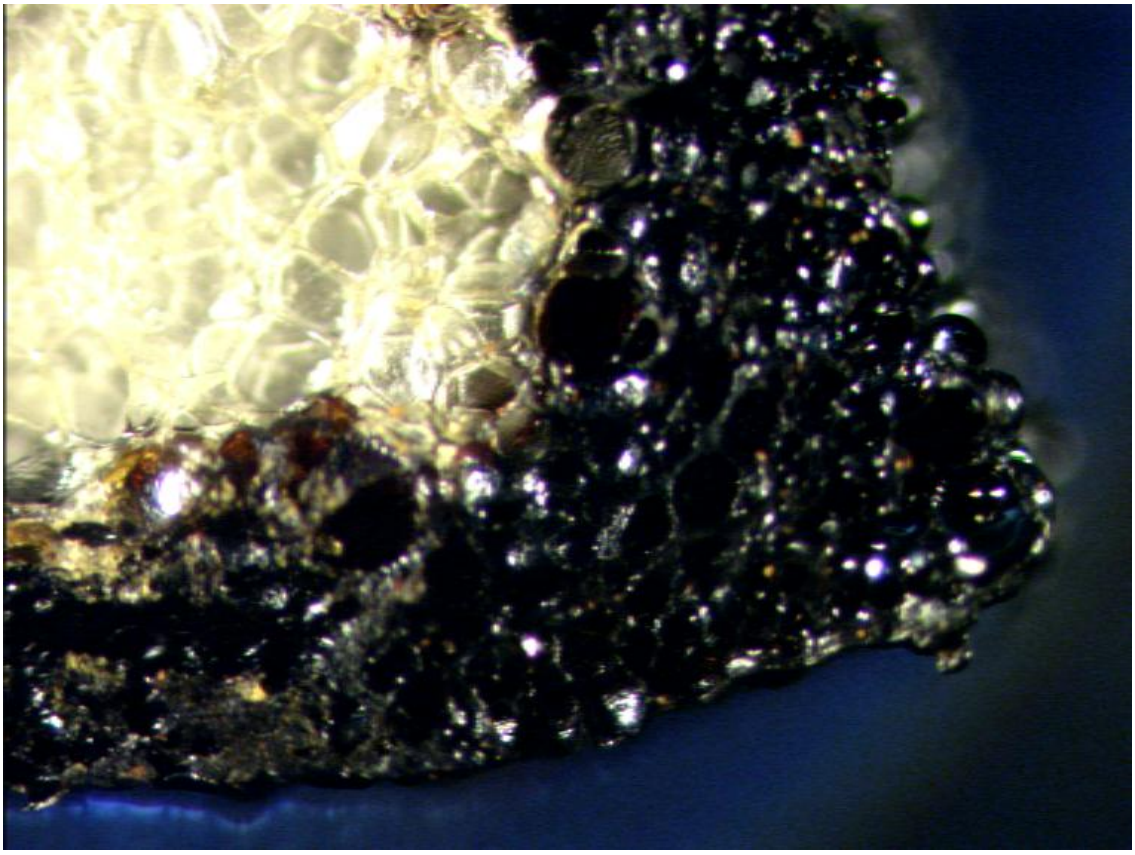

Figure 5-6. Optical micrograph of the cross-section of foamed PMMA composite (×50).

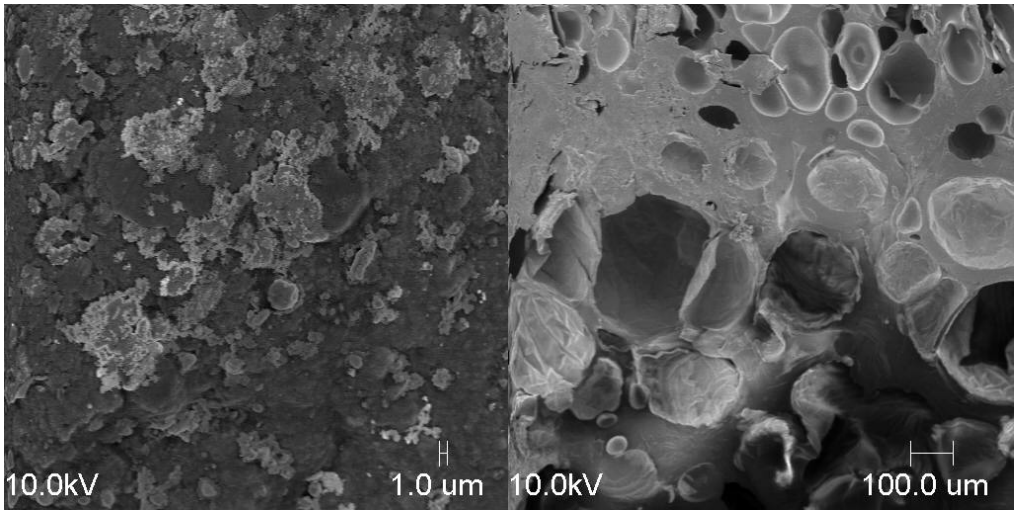

Figure 5-7(a) and (b). SEM pictures of the surface (×1000) and cross-section (×50) of foamed PMMA composite.

5-2 ***Substrate: Porous, Crosslinked Polystyrene***

Due to its open-pore structure, the PCPS substrate was expected to act as a template that allows an oxidant to distribute uniformly in the substrate, and hence result in a uniform distribution of PPy in the composite. $FeCl_3$ was used as a conventional Lewis acid oxidant that reacts with the weakly basic pyrrole monomer (Myers, 1986; Webb, 1998). According to Webb (1998), the use of acetonitrile as a solvent allows the substrate to be stable in the presence of $FeCl_3$. However, the amount of PPy in the composite was only 13 wt. % by elemental analysis, leading to electrical conductivity as low as 10^{-5} S cm^{-1}. In order to obtain a uniform composite with higher conductivity, it is necessary to facilitate the impregnation of the oxidant in the substrate. In this context, oxidant concentration and soaking time are expected to be the experimental variables that have a significant impact on the composite production. The effect of preparation order on the final properties of the composite was also investigated.

For comparison, I_2 was also used as an oxidant that is processable with CO_2. Since I_2 is soluble in CO_2 (Fang *et al*., 1997), CO_2 pressure is expected to provide an additional variable to control the properties of the conductive composite.

5-3 ***Oxidant: Ferric Chloride***

5-3-1 **Composite Production Using Organic Solvent**

Upon exposure of the oxidant-impregnated substrate to Py monomer in the second step, the color of the substrate surface changed from dark brown to black, indicating that

the polymerization takes place instantaneously. In Figure 5-8, the mass gain of the complex of PPy and $FeCl_3$ (PPy + $FeCl_3$) formed in the second step is plotted against the amount of $FeCl_3$ impregnated in the first step. As expected, after exposure either to Py vapor or to a mixture of Py and CO_2, the mass gain of the complex formed in the composite increases linearly with the oxidant impregnated.

The bulk, surface, and volume conductivities of the composite are plotted as a function of the amount of PPy complex in Figures 5-9, 10, and 11, respectively. Each conductivity appears to follow percolation behavior with the amount of complex formed in the composite. The uniform conductivity of the composite also indicates that the distribution of PPy is uniform throughout the composite. The fitting of the conductivity data to a classical percolation model reveals that the percolation threshold is about 4 wt. %. The calculated threshold is much smaller than that of randomly distributed conductive spheres in an insulating substrate (~ 16 vol. %). The low percolation threshold means that a high level of conductivity can be obtained with only a small amount of the conductive polymer formed in the composite, resulting in reduction of production cost, time, and waste. It also leads to an expectation that the mechanical strength of the composite is as strong as that of the substrate as the required amount of the conductive polymer decreases.

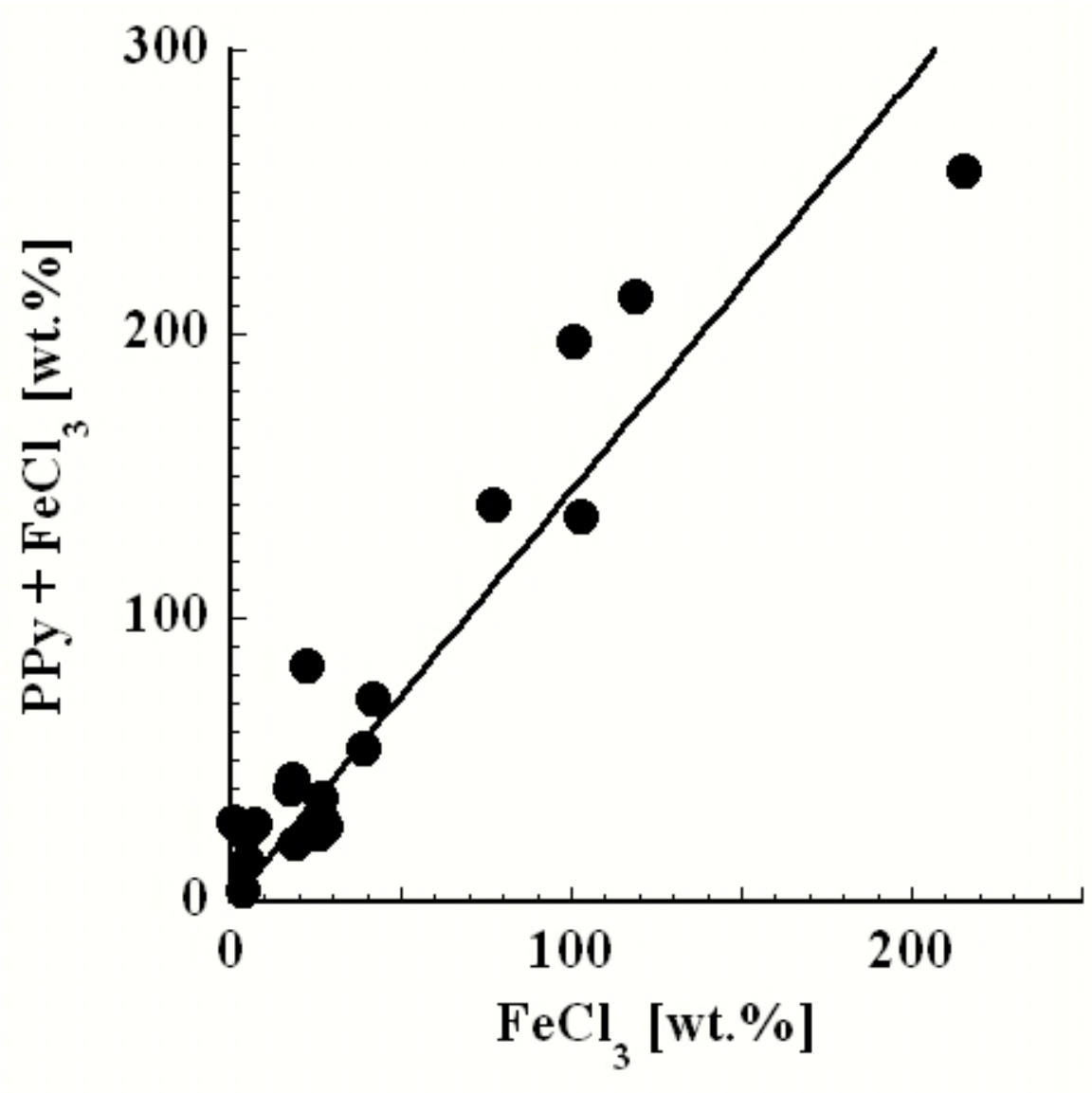

Figure 5-8. Amount of PPy formed as a function of amount of $FeCl_3$ impregnated.

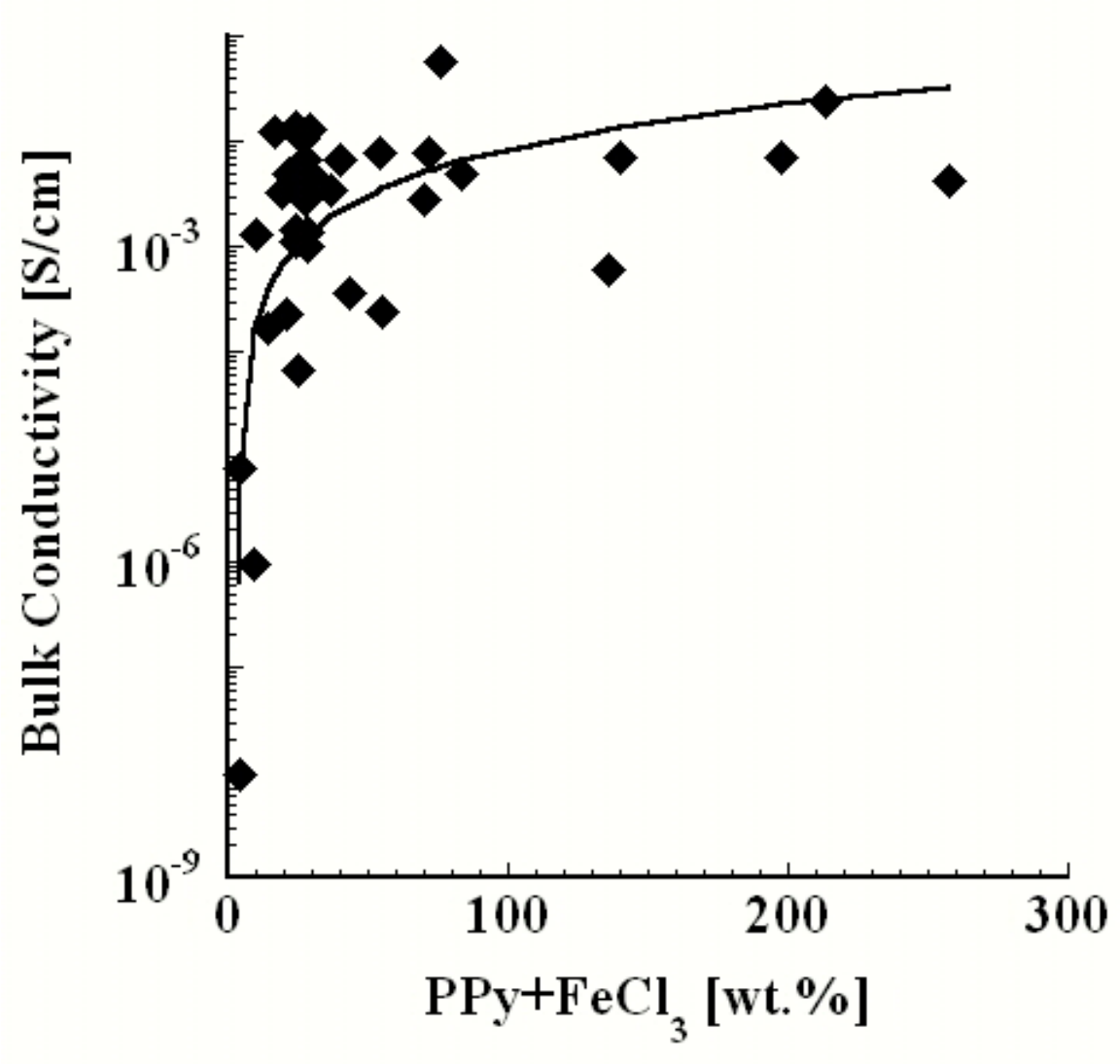

Figure 5-9. Bulk conductivity of PPy + $FeCl_3$ composite.

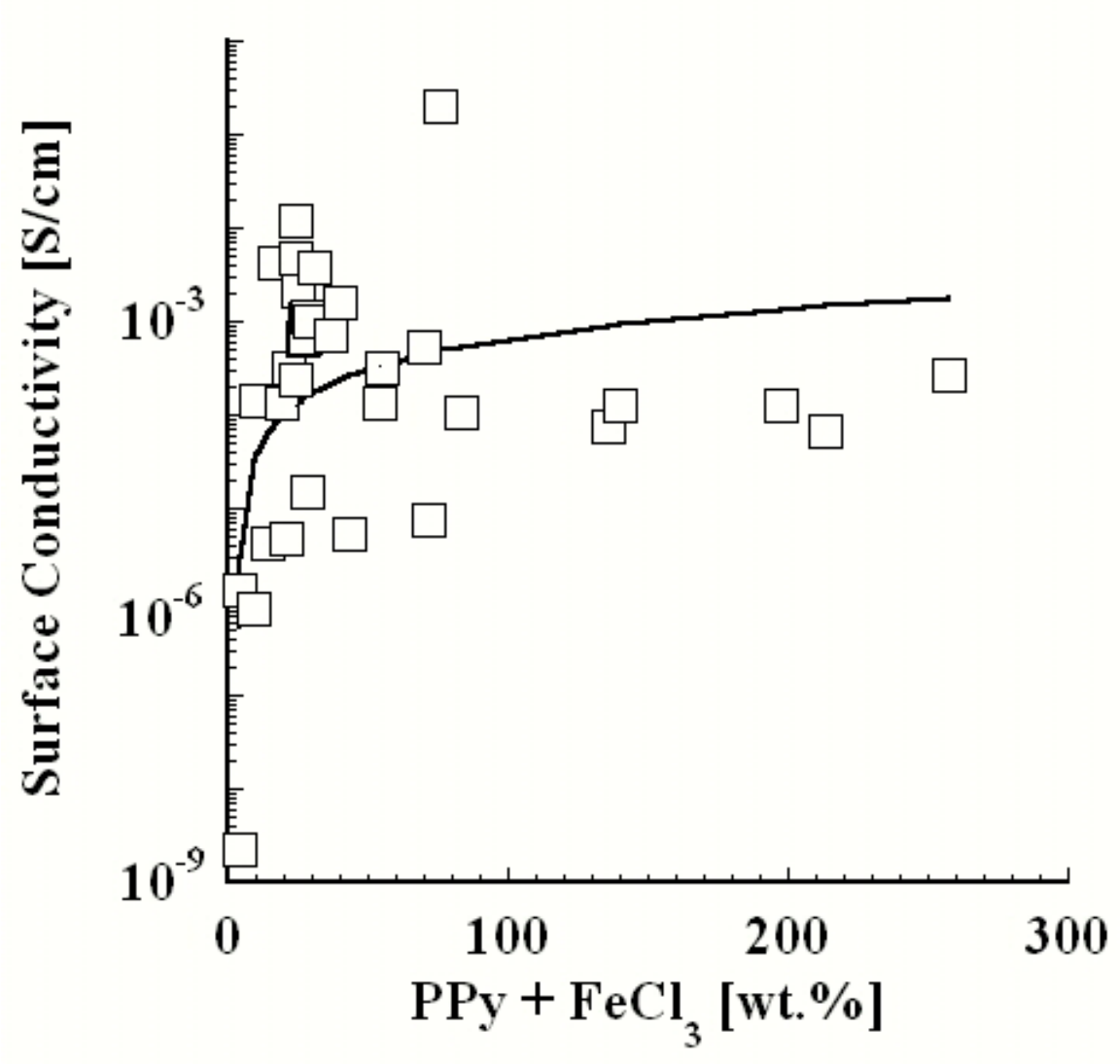

Figure 5-10. Surface conductivity of PPy + $FeCl_3$ composite.

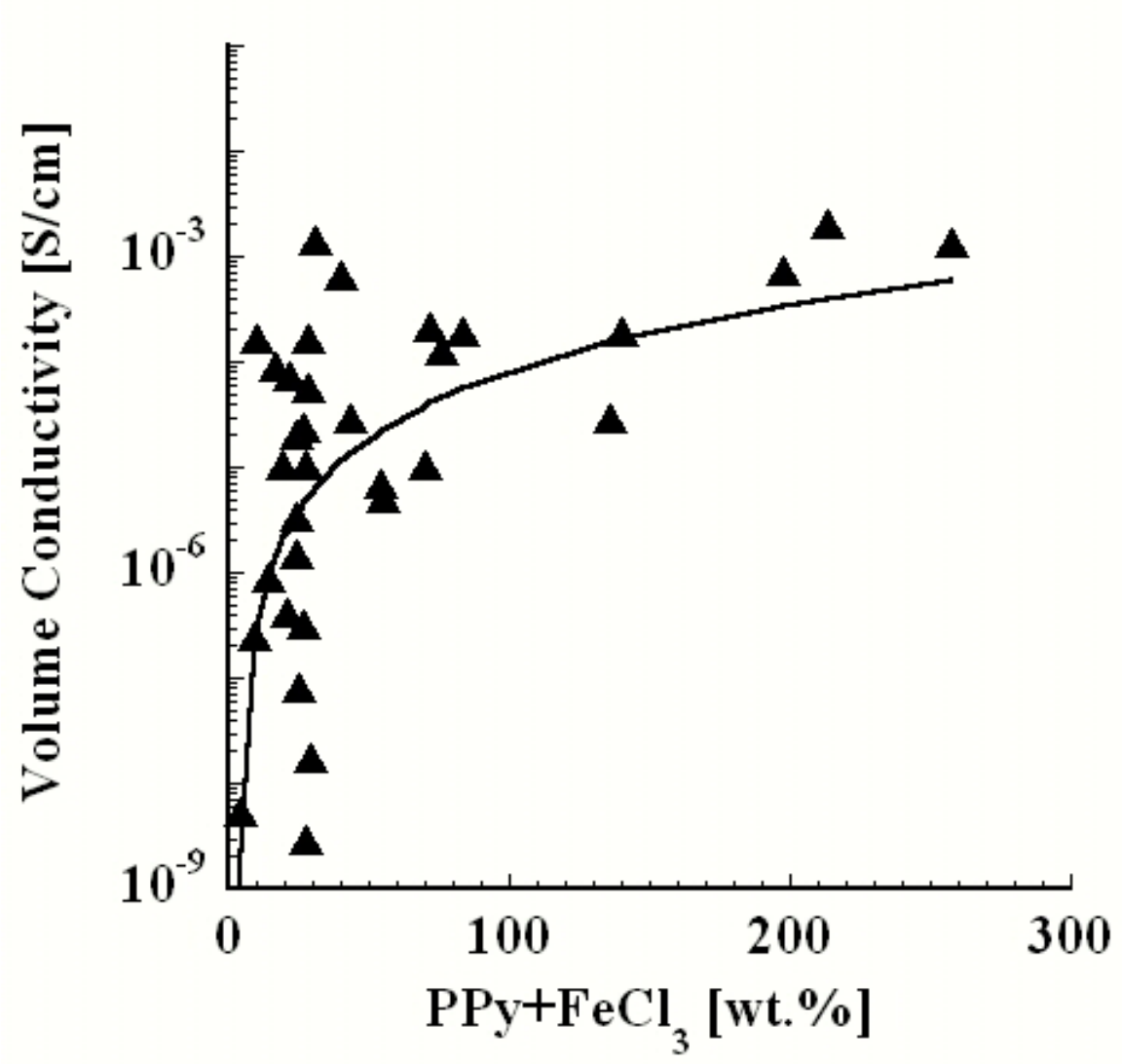

Figure 5-11. Volume conductivity of PPy + $FeCl_3$ composite.

5-3-2 **Composite Production in Carbon Dioxide**

In this trial run, liquid CO_2 was used as a solvent in the impregnation step, and the $FeCl_3$-impregnated substrate was then exposed to a mixture of Py monomer and CO_2 in the in-situ polymerization step. Liquid CO_2 was not chosen as a solvent in the second step because the liquid can re-dissolve the oxidant impregnated in the host substrate, leading to low yields of PPy.

The optical photograph of the composite prepared in this experiment is shown in Figure 5-12. It is clearly seen that thin layers of PPy are formed only on the surface of the substrate. The failure to obtain a uniform distribution of PPy in this experiment could be attributed to the large particle size of the oxidant. It is expected that impregnation depends on how finely the oxidant can be dispersed in the solution so that the oxidant particles can diffuse into μm-sized pores and channels in the substrate. A high oxidant concentration in the liquid phase can also lead to clogging of channels between pores.

Although the conductive layer is apparently limited to the composite surface, the electrical conductivities were as high as 10^{-3} S cm^{-1}. The high conductivity suggests that a certain thickness of conducting phase is enough to achieve a high level of electrical conductivity in the composite. Similar results have been obtained in porous and non-porous substrate experiments (Fu *et al*., 1997; DeJesus *et al*., 1997b; Bleha *et al*., 1999; Tang *et al*, 2003a; Tang *et al*, 2003b). It should be mentioned that volume conductivity in the composite was below detection limits, indicative of the lack of the interconnected network of PPy between the conductive surface layers.

Figure 5-12. Optical micrograph of the PPy + $FeCl_3$ composite processed in liquid CO_2 and scCO_2 (×25).

5-3-3 **Reverse-Order Preparation**

The reverse procedure was utilized to prepare conductive composite where Py monomer is first impregnated in the host substrate, and the Py-impregnated substrate is then placed in contact with a $FeCl_3$ solution in acetonitrile. At the moment when the substrate was immersed in the oxidant solution, evolution of bubbles at the interface was observed. A deformation of the substrate was also confirmed after polymerization. Those two phenomena can be ascribed to the exothermal polymerization reaction (Myers, 1986). CO_2 may be an effective solvent to remove heat of reaction since such deformation was not observed in the other preparation method. The mass gain of the PPy complex was in the range 20 – 70 wt. %; however, no correlation was found with contact time in the second step. Gel-like solids were found on the substrate and the bottom of the reactor. They may be Py oligomers that elute into the solution from the substrate.

The bulk and surface conductivities were comparable to those of the composite prepared in the other experiments; however, no volume conductivity was detected. This means that the interconnected network of PPy is limited to the composite surface if prepared in the reverse-order preparation. An optical micrograph of the cross-sectional area of the composite in Figure 5-13 shows that a surface layer of PPy exists near the surface with less PPy content in the bulk.

Figure 5-13. Optical micrograph of the PPy + $FeCl_3$ composite prepared in reverse order (×50).

5-4 ***Oxidant: Iodine***

The low solubility of $FeCl_3$ in CO_2 makes it difficult to accomplish the desired uniform distribution of oxidant (and of the conductive polymer) in the porous substrate. As the feature size of the substrate such as pore diameter and channel size decreases, it will be more important to use an oxidant that can diffuse easily in the substrate.

By analogy to the non-porous PMMA composite, I_2 was used as an alternative oxidant that can be distributed uniformly in the substrate. Due to the open-porous structure of the substrate, I_2 molecules were expected to penetrate the porous substrate with or without a solvent.

5-4-1 **Composite Preparation via a Solvent-Free Method**

The host substrate was first exposed to I_2 vapor for 24 hours, and subsequently to Py vapor for 24 hours in a closed vial at 313 K. During the contact of I_2 and Py in the substrate, the characteristic color change of the surface of PCPS from dark purple of I_2 to black of pyrrole was observed. The mass gains were 12 and 46 wt. %, respectively. The optical images of the host substrate after the I_2 impregnation (Figures 5-14(a) and (b)) clearly show the gradual distribution of I_2 from the bottom (more) to the top (less). The bulk and surface electrical conductivities were 3.24×10^{-7} and 1.31×10^{-8} S cm^{-1}, respectively. The low conductivities of the final composite in spite of the high PPy content may be ascribed to the low connectivity of the conducting polymer network through the sample as shown in Figures 5-15(a) and (b). This is supported by the fact that no volume conductivity was observed in the composite.

Figure 5-14(a) and (b). Optical micrographs of the cross-section of the bottom and top of PCPS sample exposed to I_2 vapor (×25).

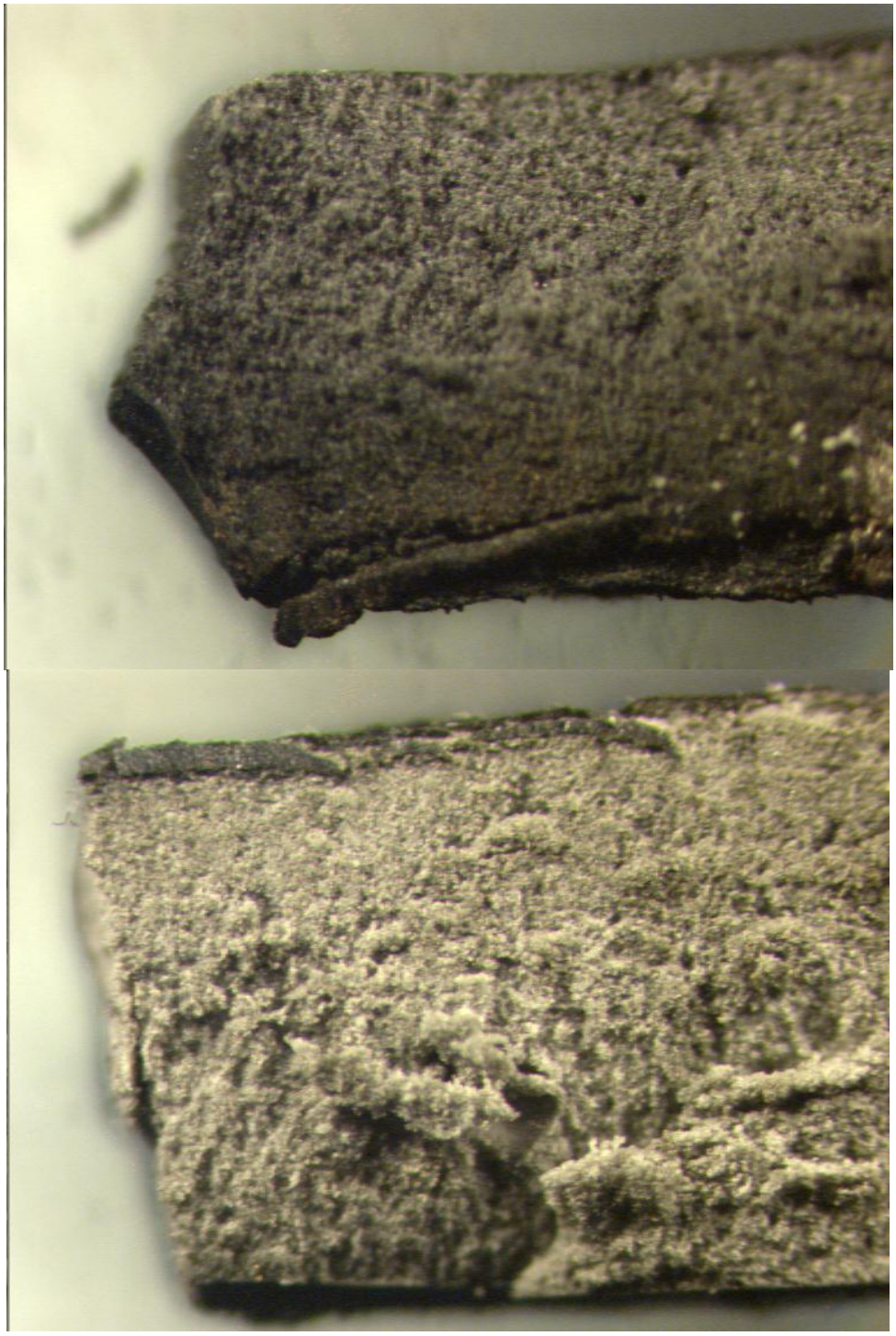

Figures 5-15(a) and (b). Optical micrographs of the cross-section of the bottom and top of PCPS sample exposed to Py vapor (×25).

The desired uniform distribution of I_2 in the substrate may be obtained by longer periods of contact. Therefore, the soaking times were extended to seven and two days for impregnation of I_2 and in-situ polymerization of Py, respectively. As expected, the longer processing times resulted in high mass gain and conductivity. The connectivity of the conducting polymer phase was confirmed by a volume conductivity that was as high as 5.43×10^{-6} S cm^{-1}. In Figures 5-16(a)-(d), a film texture consisting of large particles of PPy appears on the surface of the composite whereas small granular PPy nodules (~100 nm) can be seen on the surfaces of the pore walls. The nodule morphology of PPy has been observed in the composite prepared both chemically without solvent (Shenoy *et al*., 2002) and electrochemically in modified CO_2 with acetonitrile (Anderson *et al*., 2002).

For industrial applications, it is not realistic to spend more than a week to conduct the whole synthetic process. Therefore, the reduction in process time was intended in the following experiments involving supercritical fluid technology. Weiss and coworkers have used $scCO_2$ as a solvent only for the impregnation of I_2 in open-porous, polyurethane and polyetherurethane foams (Weiss *et al*., 2002; Shenoy *et al*., 2002; Wang *et al*., 2003; Shenoy *et al*., 2003). They successfully obtained the composite with a wide range of conductivity (10^{-7} – 10^{-2} S cm^{-1}) by controlling the amount of the oxidant impregnated in the first step. However, the composite often showed less uniformity in conductivity on the two parallel surfaces of the foam by an order of magnitude. The sources of the heterogeneity were not clearly explained, but they suggested that it might come from a consequence of a gradient in the I_2 or Py concentration in the vapor phase (Shenoy *et al*., 2003). The oxidant and monomer concentration gradients may be reduced

by the application of $scCO_2$ to both steps. However, the I_2 impregnated in the substrate may diffuse out at the in-situ polymerization step before the reaction takes place because of the presence of CO_2. Therefore, it is important to determine the diffusivity of I_2 and Py in the porous and non-porous substrates with $scCO_2$ in order to prepare conductive composite via the new process.

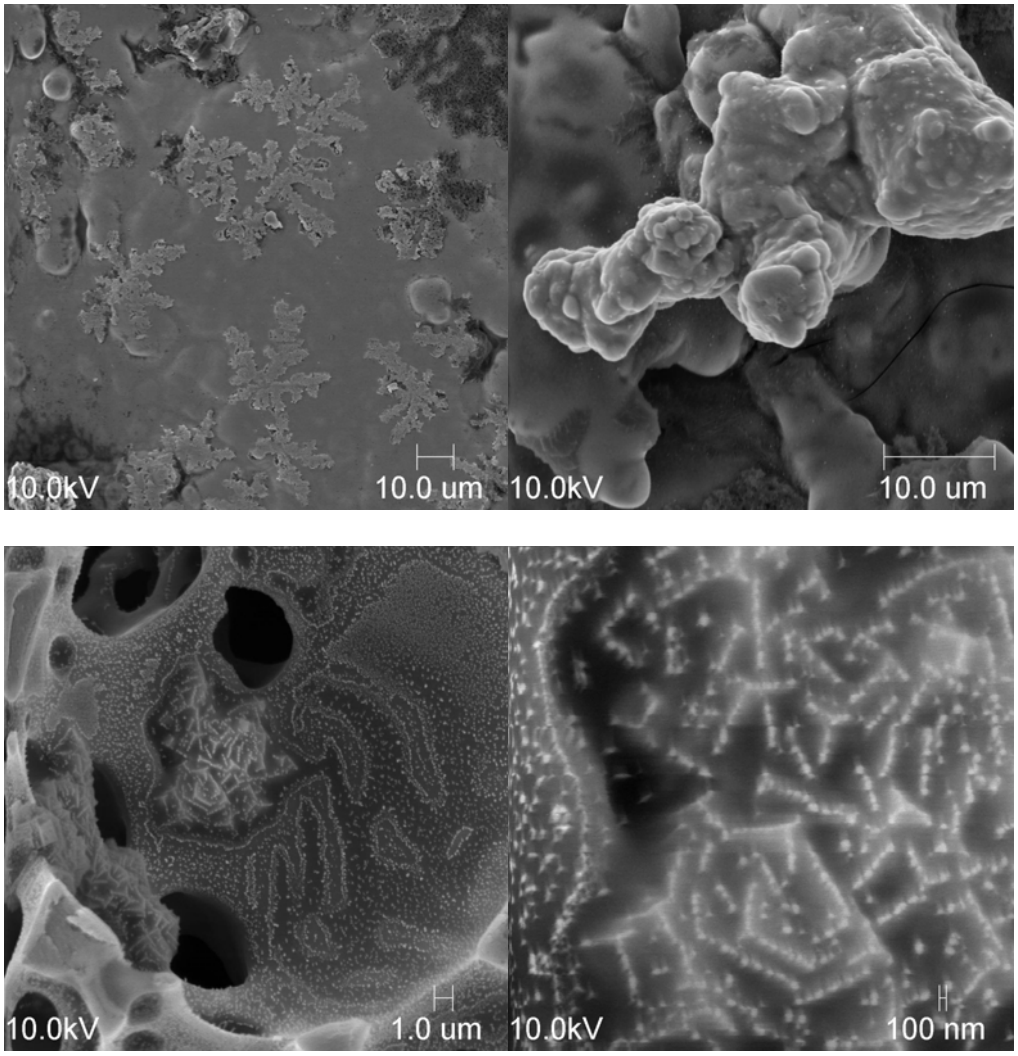

Figure 5-16(a)-(d). SEM pictures of the surface (×500, 1500) and cross-section (×2500, 3000) of PPy + I_2 composite in PCPS produced by the solvent-free method.

5-4-2 **Diffusivity of Iodine and Pyrrole in Supercritical Carbon Dioxide**

The sorption behavior of I_2 into PCPS at 313 K and 10.3 MPa is plotted as a function of soaking time in Figure 5-17. The dense line represents a fitting curve using equation 5-2. The mass uptake of I_2 in the PCPS substrate measured after depressurization was assumed to be the amount of I_2 incorporated into the substrate under the high-pressure conditions. This is because the weight loss due to desorption of I_2 from the impregnated substrates under ambient conditions was negligible. For comparison, the mass uptake of I_2 vapor into PCPS at 313 K for 24 hours is represented by a square symbol, and a sorption curve of I_2 vapor into polyurethane foams from the literature (Shenoy *et al*., 2002) is also plotted using a dashed line. The presence of CO_2 increases the diffusivity of I_2 in the substrate. The experimental errors in mass gain may come from the difference in thickness of each substrate, and/or from the deposition of solid I_2 on the surface during depressurization.

The diffusivity of I_2 in PCPS with CO_2 was calculated using the same expression as in equation (5-2) except that the diffusivity is replaced by the effective diffusivity, D_{eff}:

$$M(t)/M_\infty = 4\left(D_{eff}\, t/\pi d^2\right)^{1/2} \qquad (5\text{-}3).$$

The maximum mass gain of I_2 in PCPS is 52.4 wt. %, corresponding to a solubility of 34.4 wt. %. The high mass gain of I_2 in PCPS can be attributed to its large surface area. As shown in Figure 5-18, $M(t)/M_\infty$ was linear against ($t^{1/2}/d$), and the plot suggests a Fickian diffusion mechanism up to $M(t)/M_\infty \sim 0.75$. The effective diffusivity was determined from the slope in Figure 5-18 to be 9.79×10^{-8} cm^2 s^{-1}, which is of the same

order of magnitude as for the I_2 sorption in the non-porous PMMA with $scCO_2$. In the above calculation, it is not clear if the thickness of the substrate can be used as the film thickness due to the porous nature of the substrate. Therefore, an effective diffusion constant $D/d^2 = 0.0061\ h^{-1}$ was calculated instead, which is about 1.5 times larger than of I_2 in a polyurethane foam without CO_2 (Shenoy *et al*., 2002).

In terms of morphological observation, all the trials to take SEM pictures of the host substrate after gold-sputter coating failed because of intense emission of electrons from I_2. The optical micrograph of the cross-section of the I_2-impregnated substrate at 313 K and 10.3 MPa for 24 hours illustrates that I_2 was distributed throughout the sample using $scCO_2$ as shown in Figure 5-19. Deterioration of the substrate due to the presence of I_2 (Shenoy *et al*., 2002) was not observed in any of the samples tested. The absence of oxidation may be ascribed to the low experimental temperature and the nature of crosslinked substrate.

When it comes to the measurement of Py in PCPS, continuous weight loss was observed after depressurization. Therefore, desorption behavior was monitored as a function of time to determine the equilibrium mass gain (Berens *et al*., 1992). In Figure 5-20, the desorption curve is not linear with square root of time as required by the Fickian diffusion model. Similar results were obtained at various soaking times ranging from 10 minutes to 24 hours. The non-linear behavior is probably due to the high diffusivity of Py compared to that of CO_2. Additionally, the surface of the sample appeared to be covered by a thin layer of ice produced from ambient moisture by the Joule-Thomson effect. It

suggests that this method may be inadequate to determine the diffusivity and solubility of Py in PCPS.

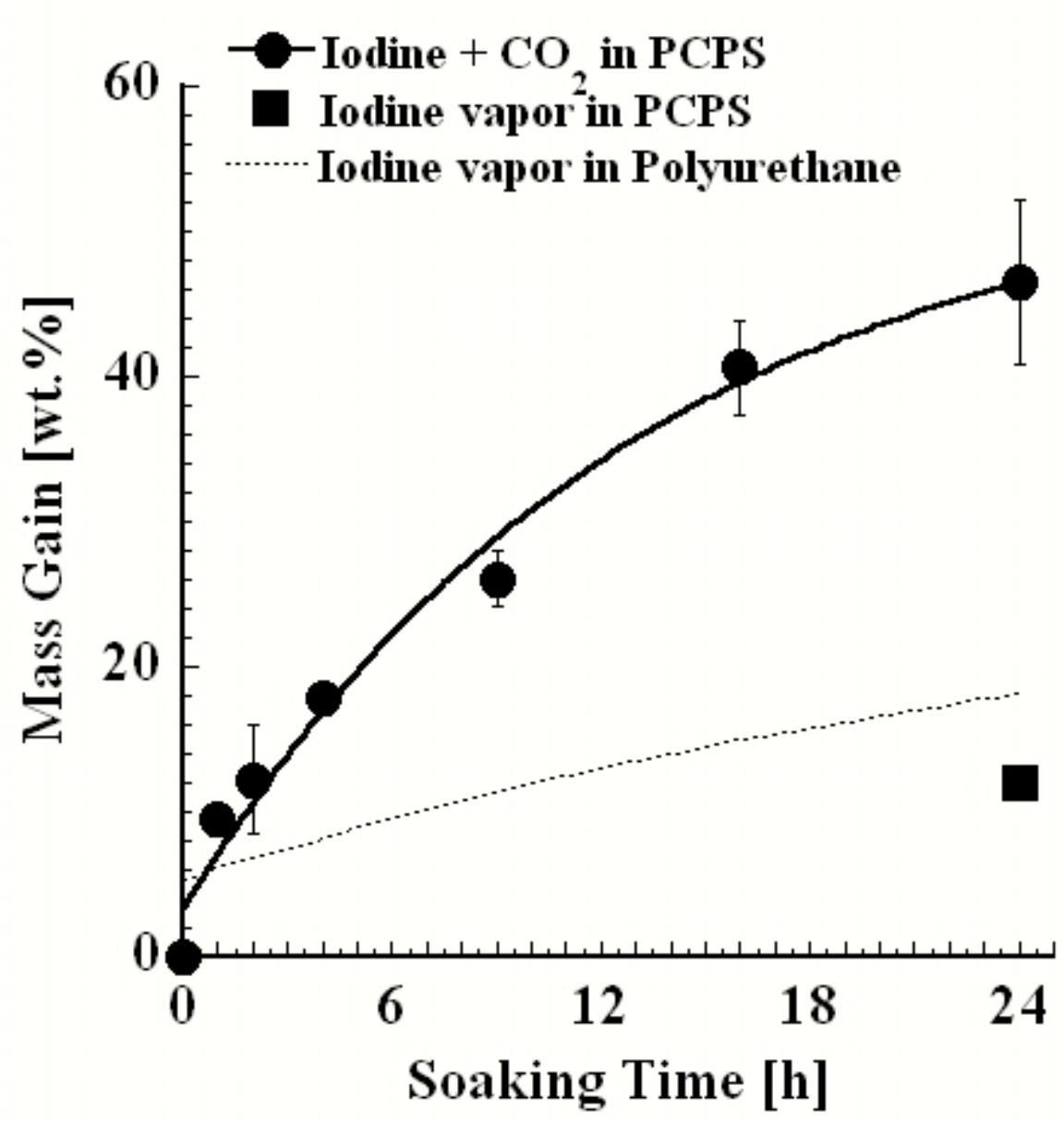

Figure 5-17. Sorption of I_2 in PCPS with and without CO_2 at 313 K and 10.3 MPa. Also shown is the sorption curve of I_2 in a polyurethane foam without CO_2 obtained by Shenoy et al. (2002).

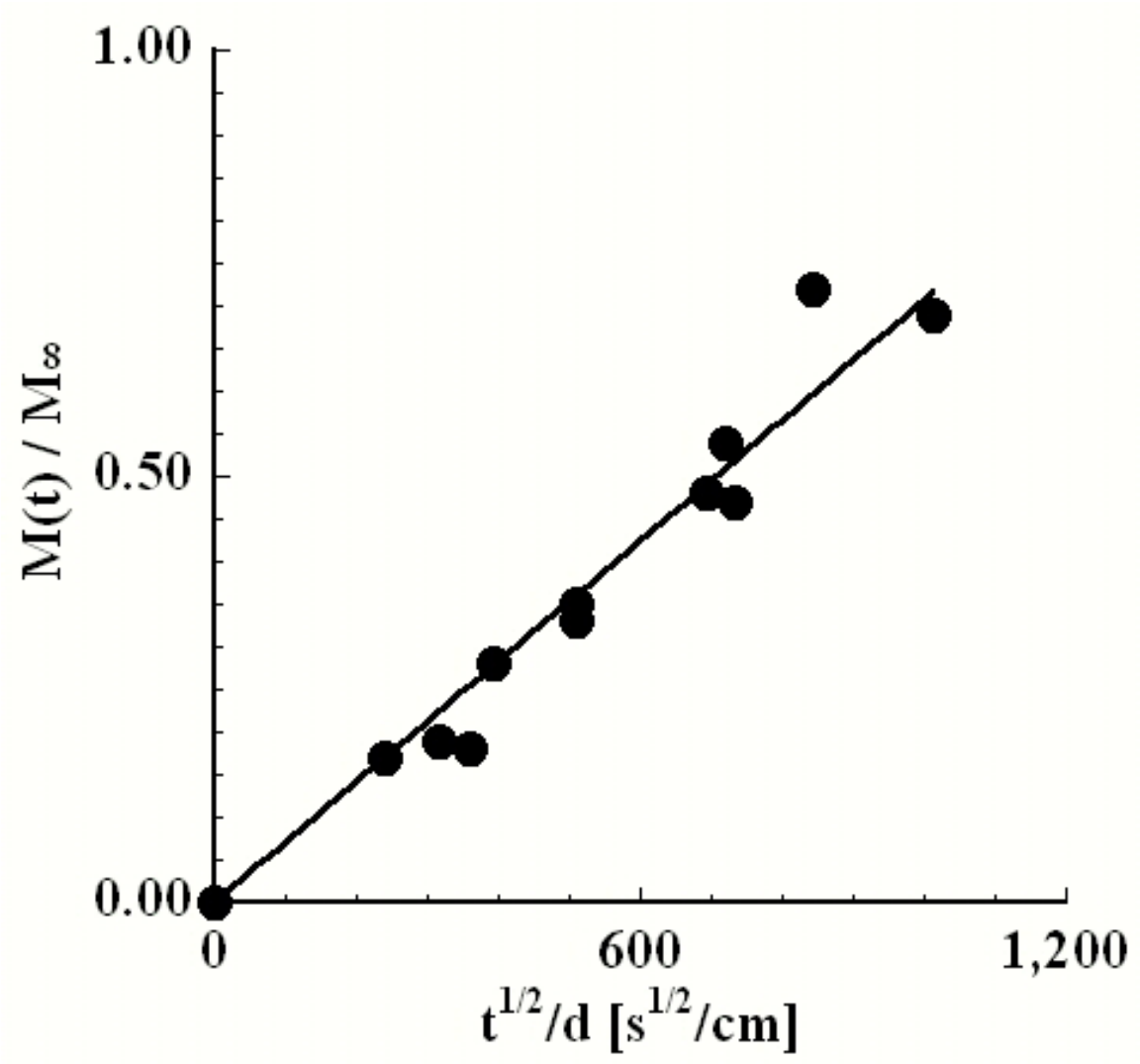

Figure 5-18. Diffusion of I_2 into PCPS at 313 K and 10.3 MPa.

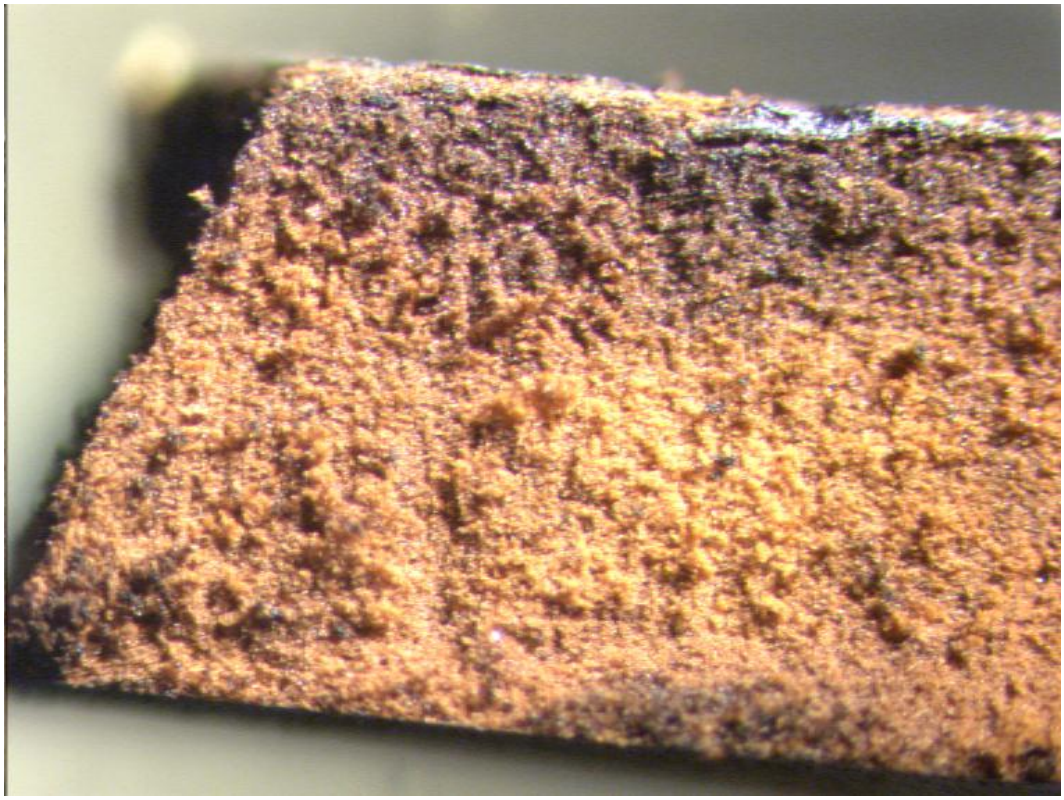

Figure 5-19. Optical micrograph of the cross-section of PCPS impregnated with I_2 in CO_2 (×25).

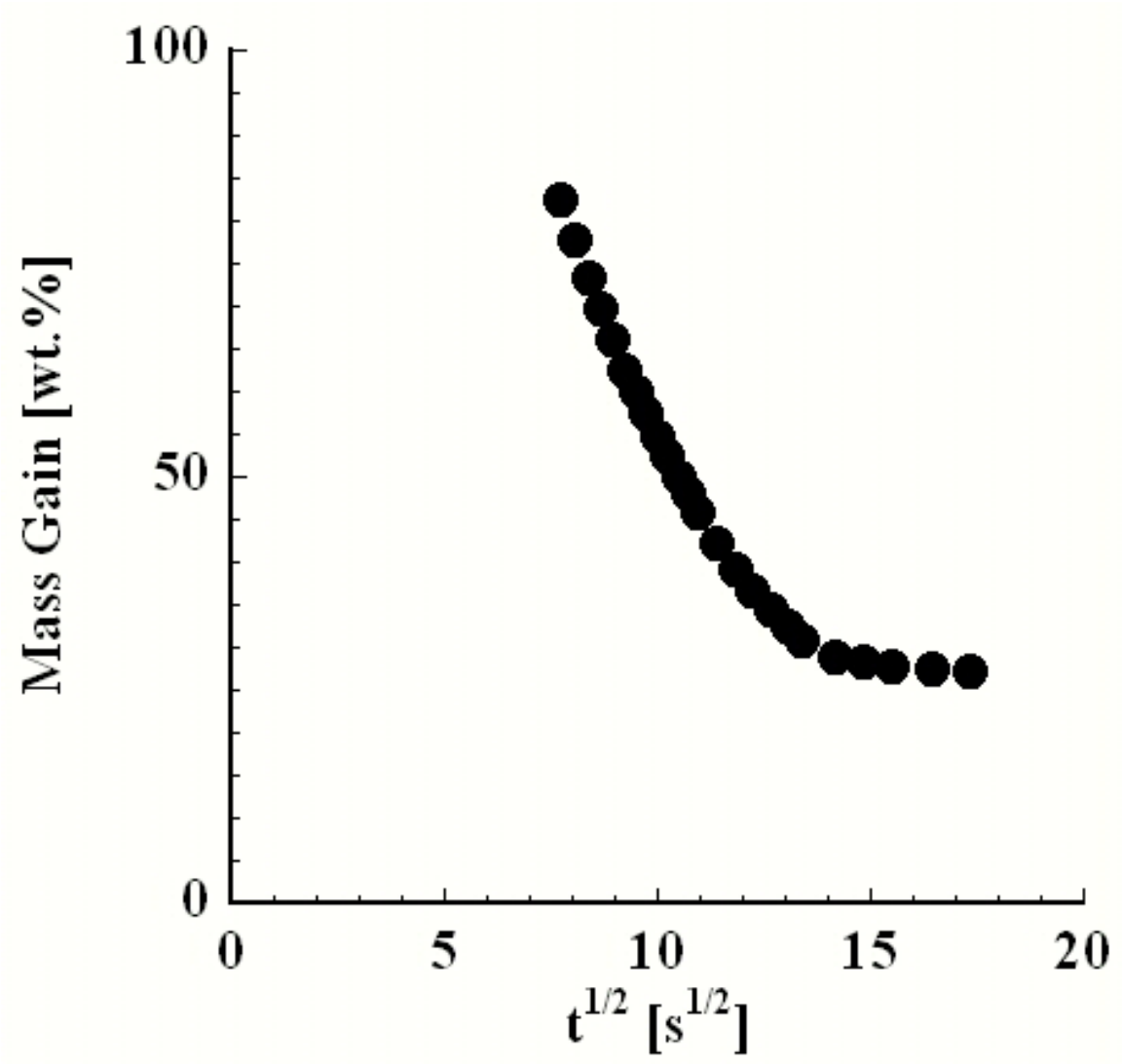

Figure 5-20. Desorption curve of Py out of PCPS substrate.

5-4-3 **Composite Preparation Using Supercritical Carbon Dioxide**

The I_2-impregnated PCPS substrates were transferred either to a desiccator saturated with Py vapor or to the high-pressure reactor to contact a mixture of Py and CO_2. The mass of PPy + I_2 complex formed by the in-situ polymerization is plotted with the amount of I_2 impregnated in Figure 5-21. The linear relationship indicates that the polymer yield depends only on the amount of the oxidant impregnated in the substrate. It also suggests that the in-situ polymerization proceeds with a constant molar ratio of Py to I_2. In order to determine the stoichiometry, an assumption was made that all the amount of I_2 impregnated in the impregnation step is incorporated in the substrate in the form of a PPy charge transfer complex (Shenoy *et al*., 2002; Shenoy *et al*., 2003). This assumption allows the estimation of the amount of PPy formed by the in-situ polymerization. The slope in Figure 5-21 corresponds to the stoichiometry of Py to I_2 in the complexes, which is about 4.5. This value is in agreement with the value determined from elemental analysis where about four Py units are complexed to one I_2 molecule in the PPy complexes synthesized in acetonitrile (Kang *et al*., 1987). Shenoy and cowokers have also reported similar values for PPy complexes obtained in polyurethane foams by the solvent-free method (Shenoy *et al*., 2002; Shenoy *et al*., 2003).

The bulk, surface, and volume conductivities of the PPy + I_2 composite are plotted as a function of the amount of PPy complex in Figures 5-22, 23, and 24, respectively. Although the bulk and surface conductivities exhibit percolation behavior with the amount of the complex, the percolation threshold is higher (~ 10 wt. %). And the

bulk and surface conductivities are lower by one or two orders of magnitude than those of the PPy + $FeCl_3$ composite at similar PPy concentrations. The volume conductivity shows a stepwise transition around 100 wt. % of PPy complex with respect to the substrate weight, at which the degree of connectivity of the PPy network is sufficient to have uniform conductivity in all directions. Therefore, there should be a non-uniform distribution of PPy in the composite below the transition point. In Figure 5-25, the color of the cross-section of the composite shows a gradual distribution of PPy from the surface to the center although the total mass gain is relatively high. The results are consistent with the hypothesis that the volume conductivity provides a good measure of the spatial distribution of the conductive component in the composite. Figures 5-26 (a) and (b) are the SEM micrographs that reveal the composite also has a smooth surface with many globules of PPy. Small nodules were also deposited on the pore walls in the composite shown in Figures 26 (c) and (d).

In the case of a mixture of Py and CO_2, continuous weight losses were observed in all the PCPS composites after depressurization of CO_2. Hence, the composite prepared in this work may retain its porous structure of PCPS after the in-situ polymerization. This observation was also supported by the optical and scanning electron micrograph images of the composite, and suggests that non-reacted Py molecules are left in pores. Additional contact of such a composite with the oxidant could be expected to produce more conducting polymer within the substrate. Therefore, a composite was produced by the two-step batch method, followed by immersion of the composite in a mixture of I_2 and CO_2 for four hours in order to induce further polymerization. It turned out that the extra

addition of I_2 did not increase the mass gains and conductivities. This result indicates that the effective diffusion of Py in the porous substrate under pressure is so fast that most of non-reacted monomer molecules trapped in the pores have diffused out before the polymerization reaction takes place. However, the volume conductivity of the post-treated composite is one or two orders of magnitude higher than that of the composite with similar PPy content. This suggests that the additional step acts as further oxidation of existing PPy network to produce charge carriers (or doping). Depletion of oxidant during polymerization may reduce the degree of oxidation and the number of charge carriers in the composite.

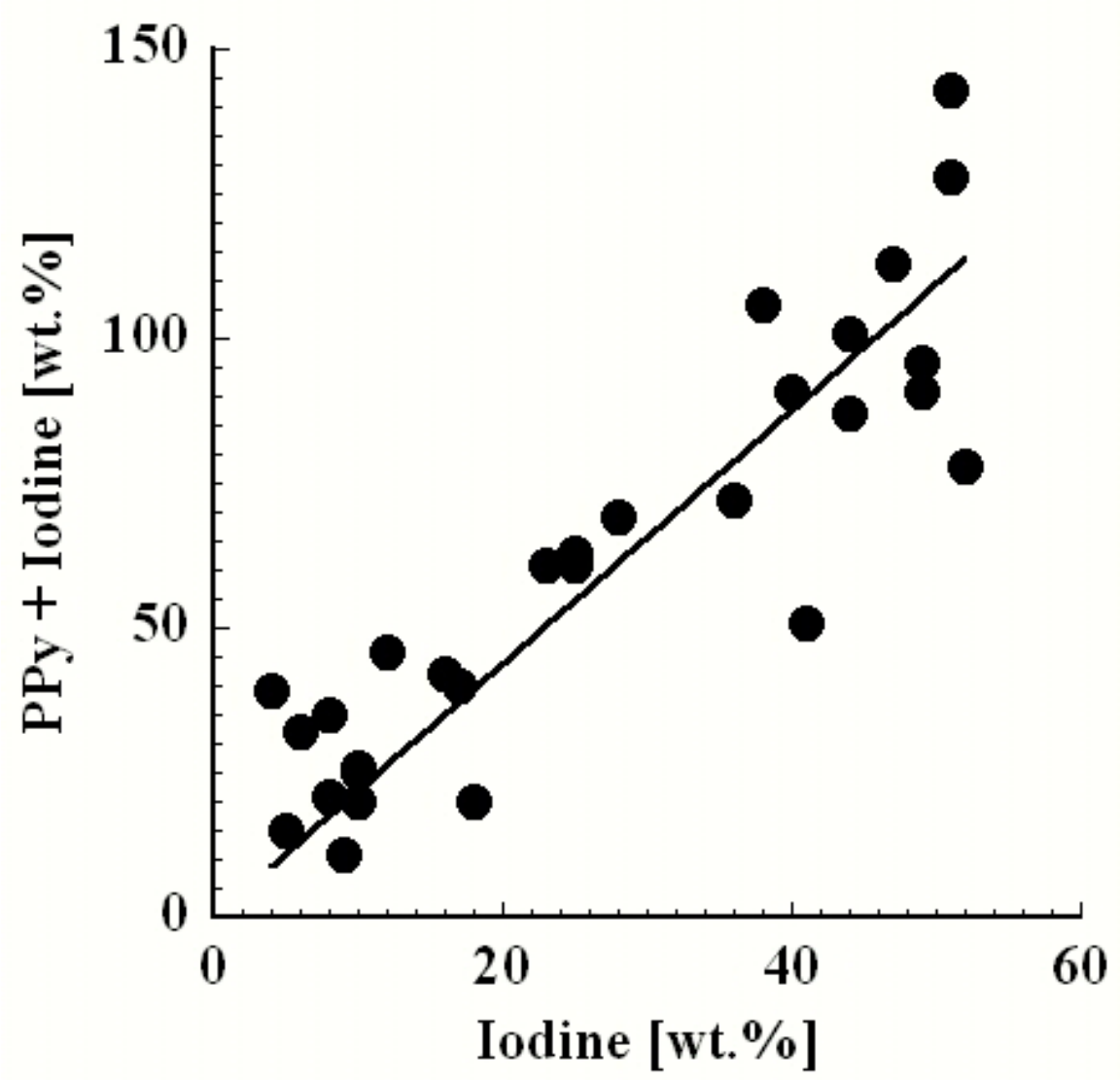

Figure 5-21. Amount of conductive PPy complex against amount of I_2 impregnated.

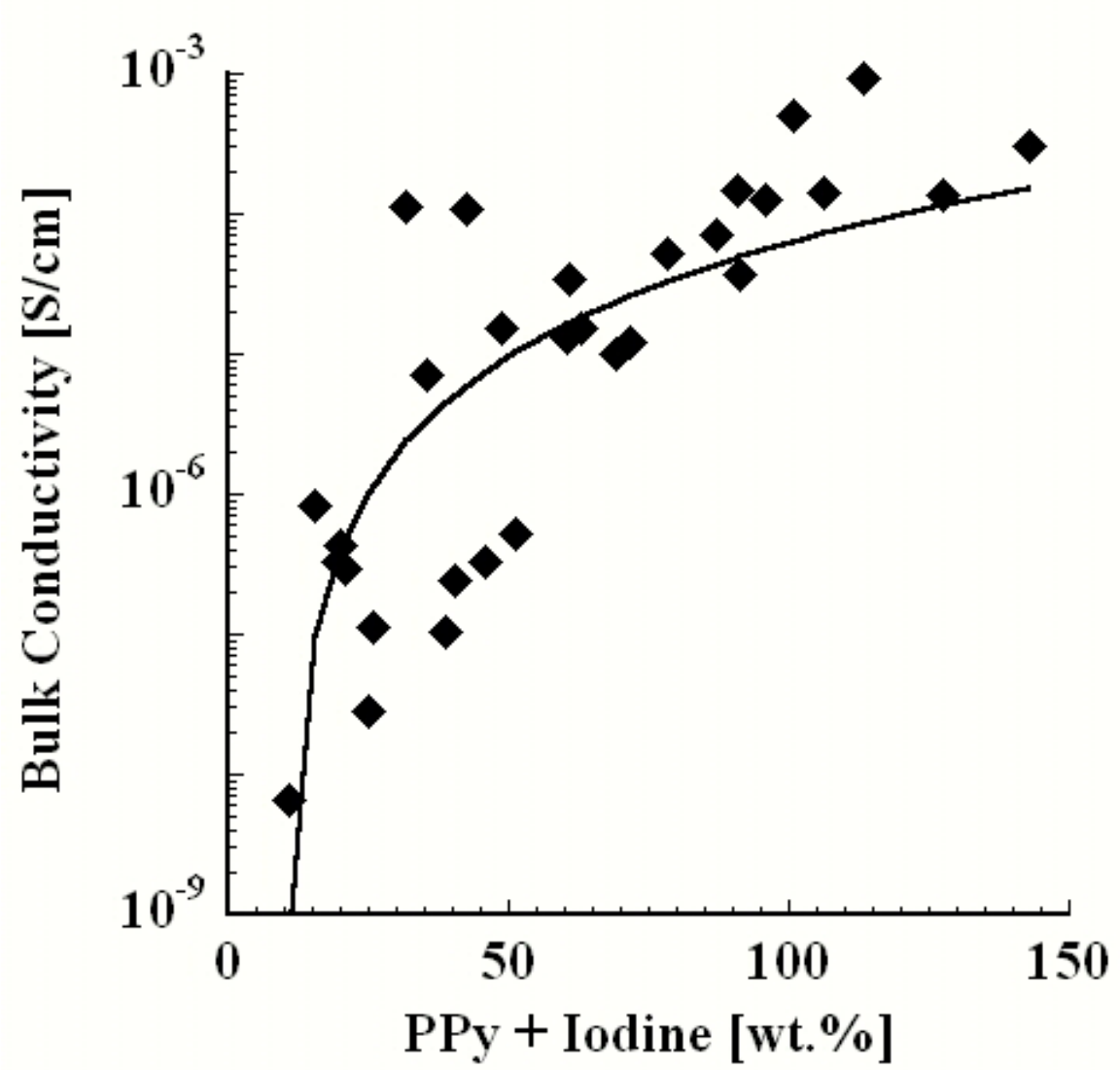

Figure 5-22. Bulk conductivity of PPy + I_2 composite.

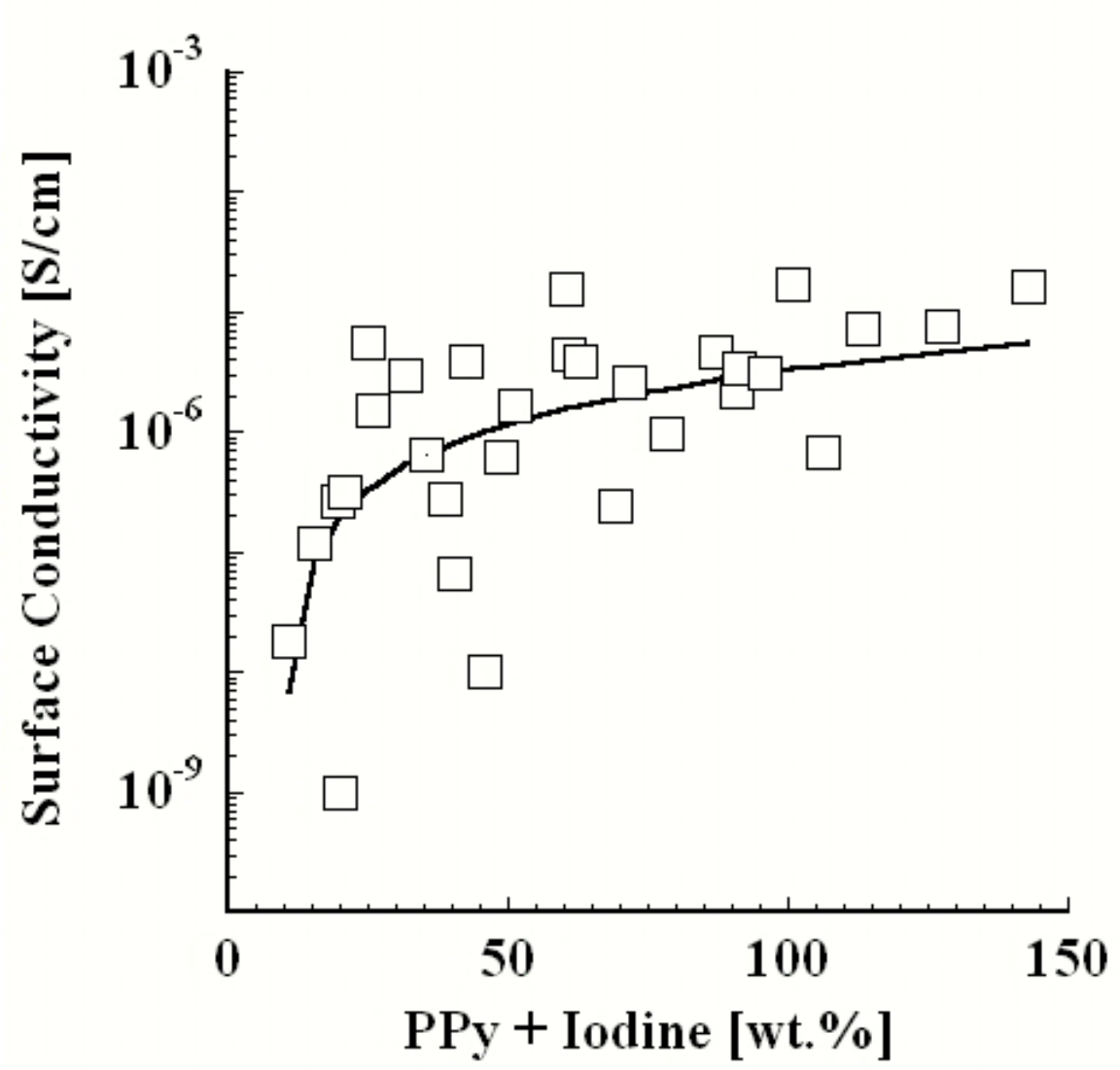

Figure 5-23. Surface conductivity of PPy + I_2 composite.

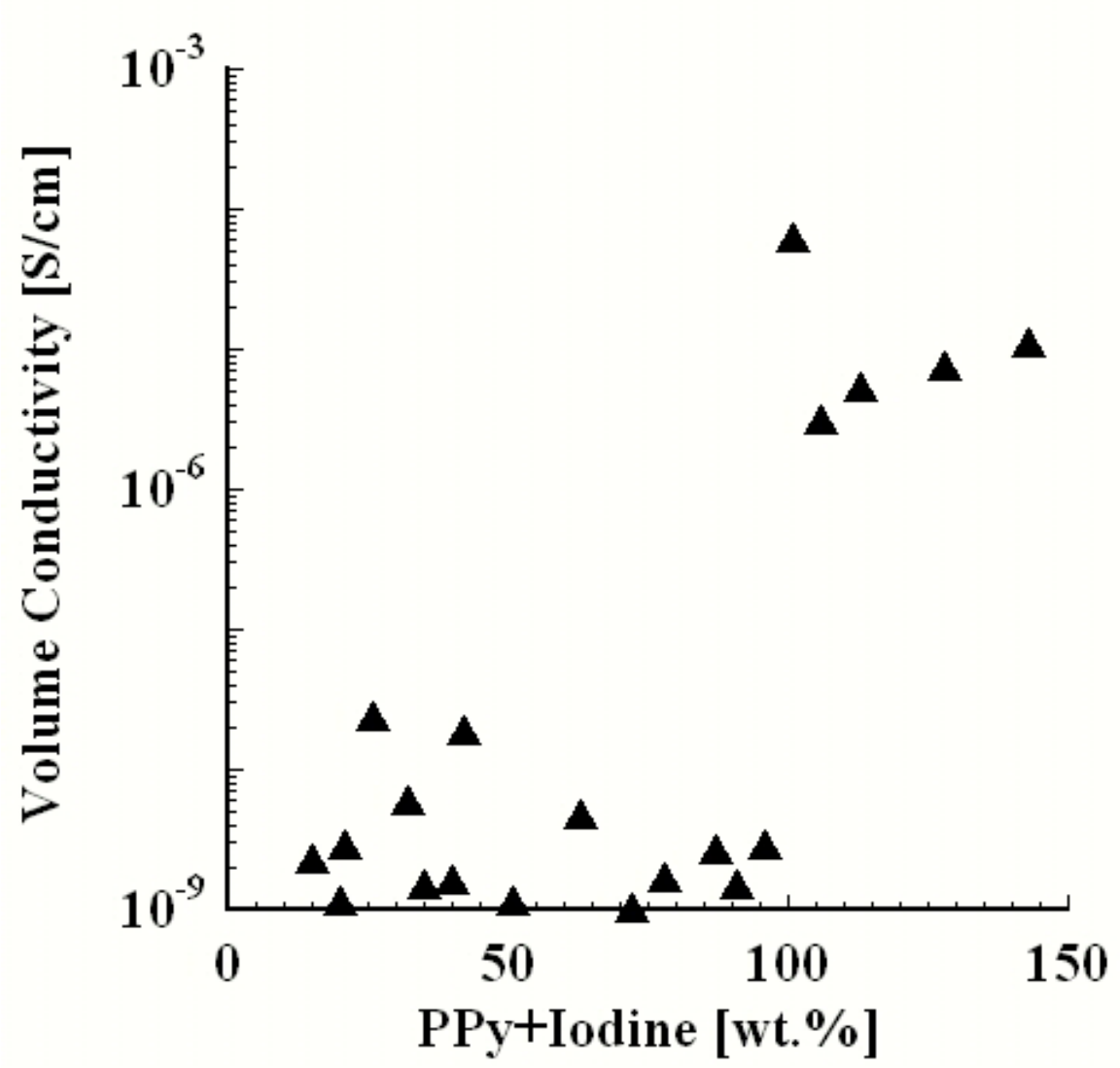

Figure 5-24. Volume conductivity of PPy + I_2 composite.

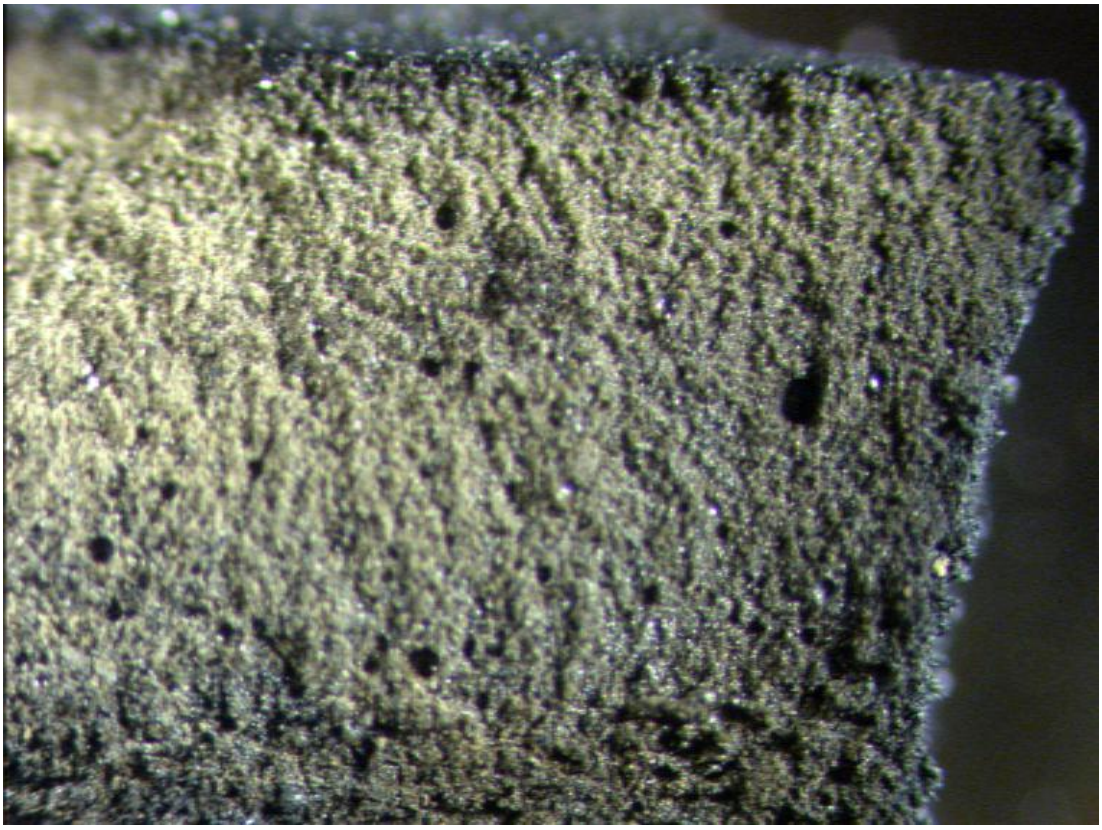

Figure 5-25. Optical micrograph of the cross-section of PPy + I_2 composite processed in $scCO_2$ (×25).

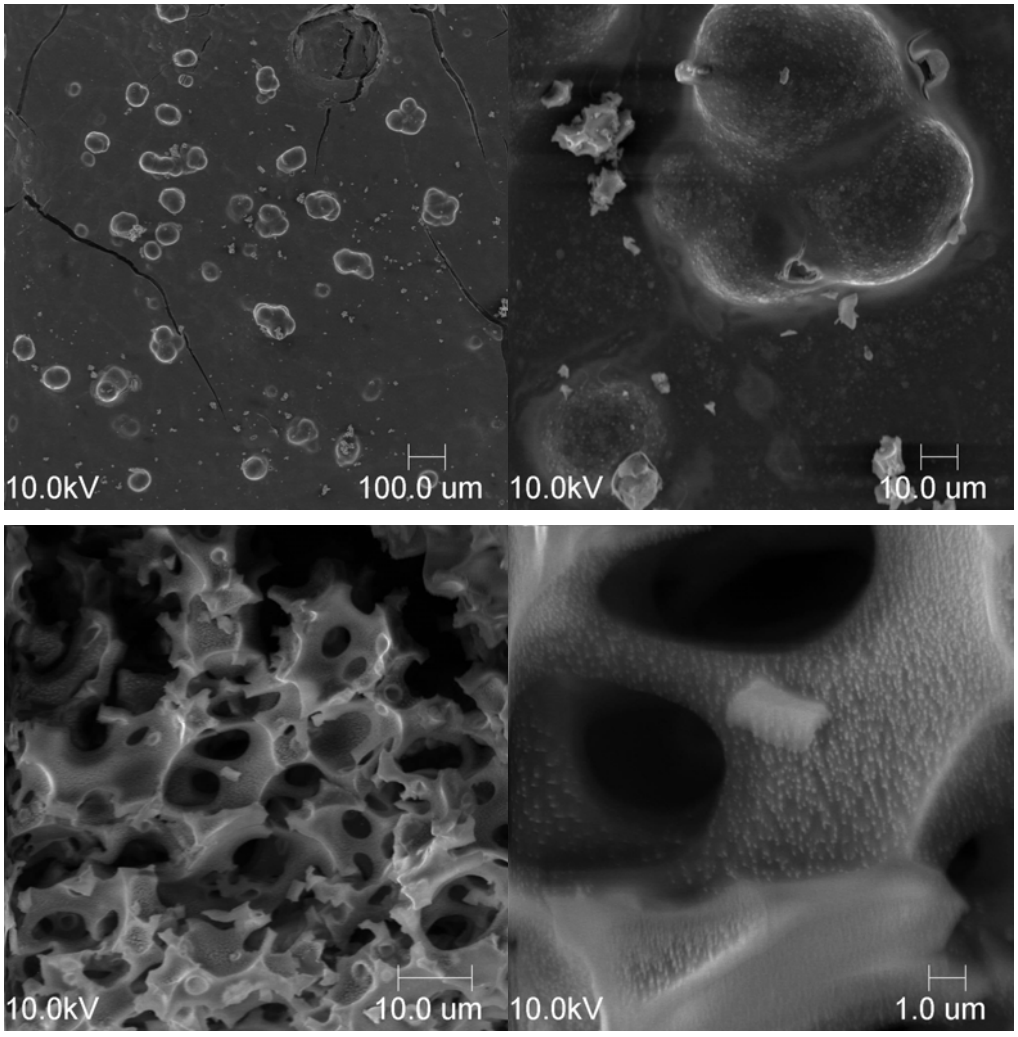

Figures 5-26(a)-(d). Optical micrograph of the surface (×50, 500) and cross-section (×1000, 5000) of PPy + I_2 composite processed in scCO_2.

5-4-4 **Pressure Effect on Partitioning between Substrate and Supercritical Fluid Phases**

The partition coefficient of I_2 in the PCPS substrate over the fluid phase was calculated from the experimental data in this work and the solubility data in the literature, and plotted as a function of CO_2 density in Figure 5-27. The partition coefficient decreases with CO_2 density because the solubility of I_2 increases as the CO_2 pressure increases (Fang *et al*., 1997), resulting in the preferential partitioning of I_2 into the fluid phase over the polymer phase. Additionally, the phase transition of I_2 at around 28 MPa should affect the change in the partition coefficient at higher pressures. The results in Figure 5-28 demonstrate that manipulating CO_2 pressure can lead to control of the level of electrical conductivity since the amount of the oxidant impregnated in the substrate is related to the amount of the PPy complex, and also to the level of electrical conductivity in the composite.

The observed effect of CO_2 pressure on partitioning is consistent with the experimentally obtained partition coefficients of azo-dyes in PMMA (West *et al*., 1998a; Ngo *et al*., 2003), polar liquids in crosslinked poly(dimethyl siloxane) (West *et al*., 1998b), polar and non-polar organic solids in crosslinked poly(dimethyl siloxane) (Condo *et al*., 1996) over the fluid phase. Kazarian *et al*. (1998) suggested that swelling of polymer by CO_2 might alter the specific interactions with solute and polymer, leading to the change in partitioning behavior.

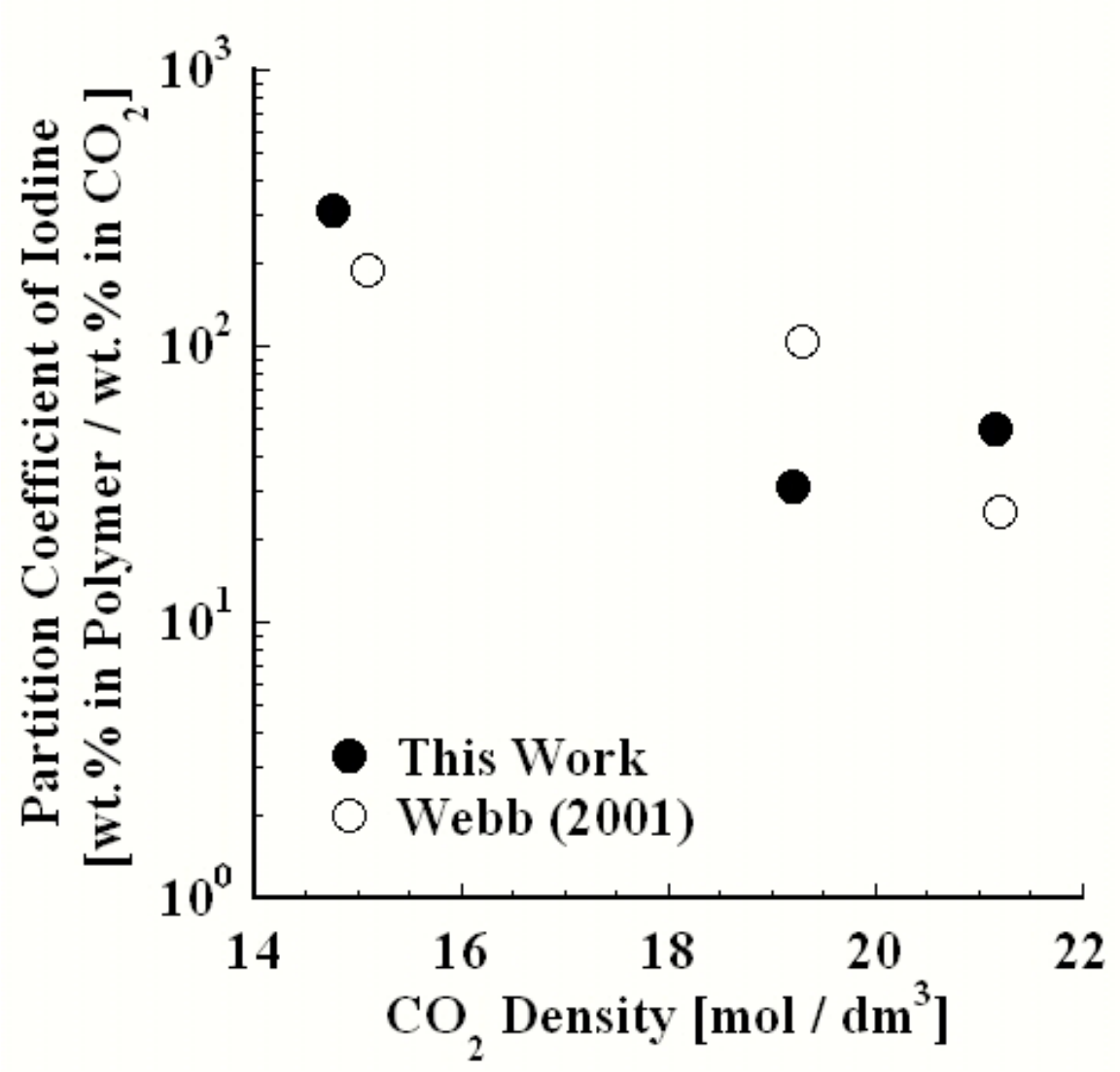

Figure 5-27. Dependence of I_2 partition coefficient on CO_2 density.

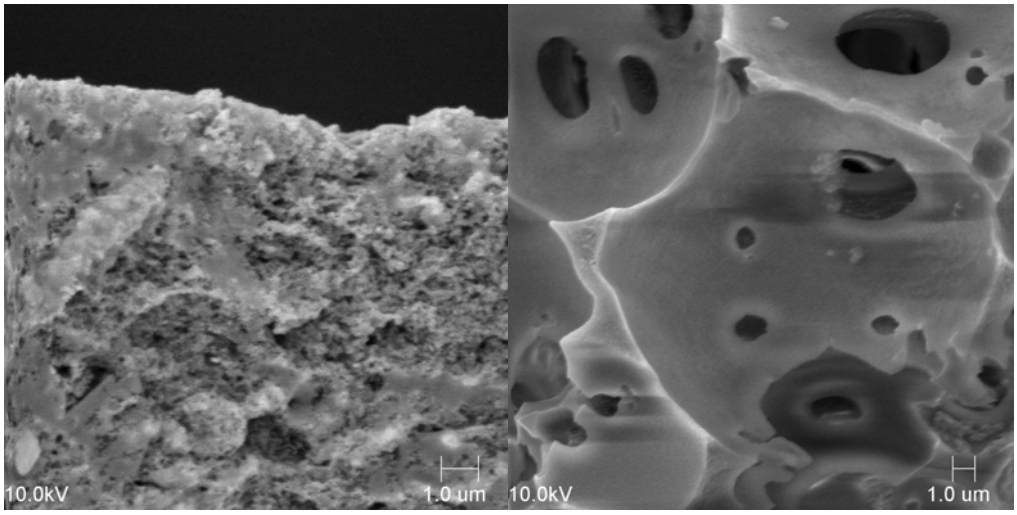

Figure 5-28(a) and (b). SEM pictures of the surface (×5000) and cross-section (×3000) of PPy + I_2 composite processed in reverse order.

5-4-5 **Reverse-Order Preparation**

The reverse procedure was also utilized to prepare conductive composites in $scCO_2$ where Py monomer is first impregnated in the host substrate, and the Py-impregnated substrate is in contact with I_2. The mass gain at each step was 83 and 49 wt. %, respectively. The decrease in weight can be attributed to the diffusion of Py monomer out of the substrate before the in-situ polymerization reaction takes place. In fact, after the second step, a thin film of PPy was obtained separately from the substrate surfaces. It is probably because the Py monomer absorbed was exuded out of the substrate, reacted with I_2 at the interface, and the resulting PPy film was peeled off. The SEM picture of the composite shows that dense layers of PPy were also formed near the surface of the composite (Figure 5-29(a)) whereas thin layers of PPy were deposited on the pore walls (Figure 5-29(b)). Although finite bulk and surface conductivities were observed, no volume conductivity was detected in the composite. Therefore, an interconnected network of PPy is not formed in the reverse-order preparation method.

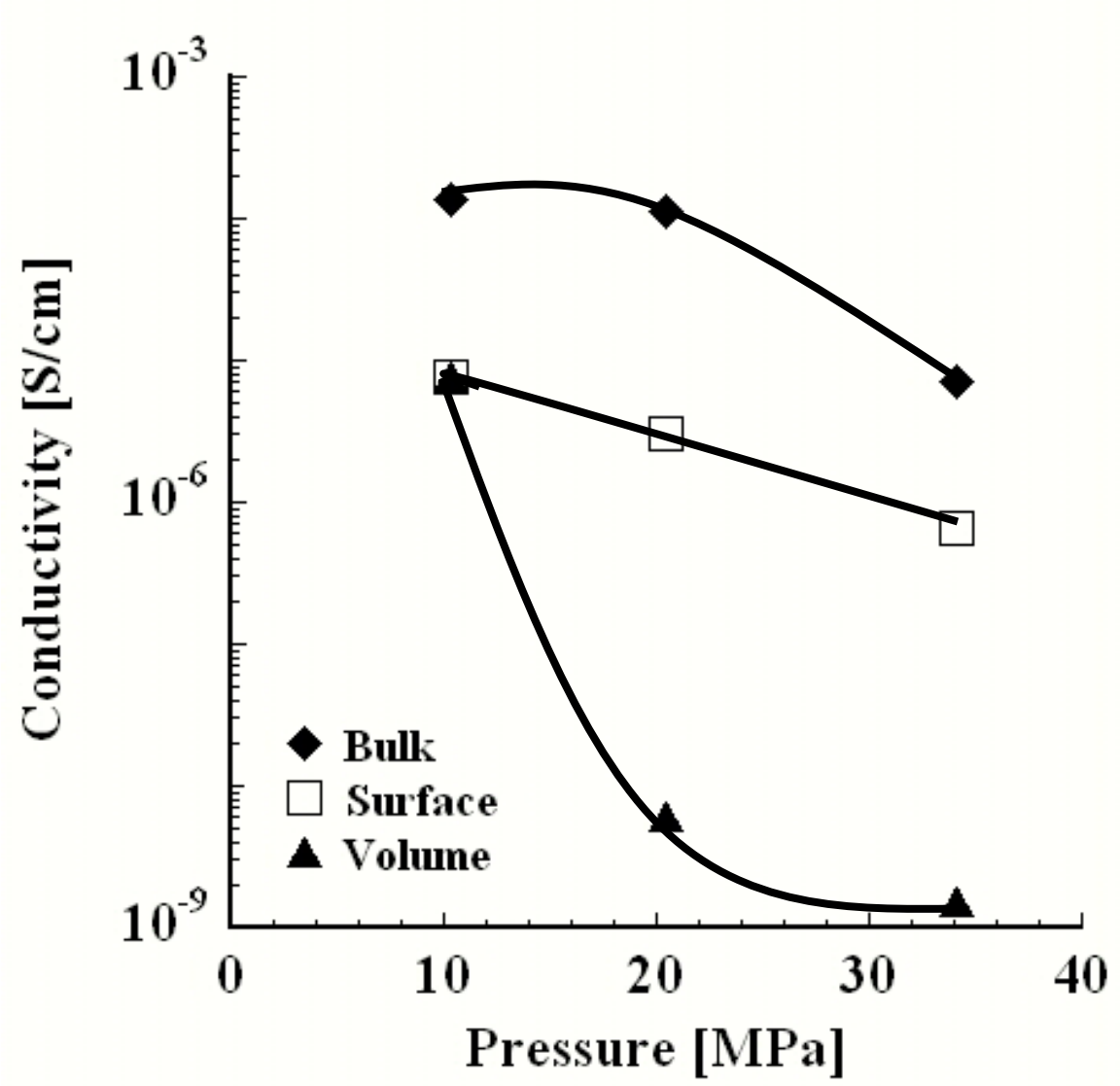

Figure 5-29. Control of electrical conductivity by manipulating CO_2 pressure.

5-5Electrical, Thermal, and Mechanical Properties of Composites

Selected conductive composites, PPy + I_2 in PMMA, PPy + $FeCl_3$ in PCPS and PPy + I_2 in PCPS, were further analyzed with respective to electrical, thermal, and mechanical properties. The composites selected generally exhibited the highest bulk conductivity.

5-5-1 **Thermal Stability**

Thermal stability of the host substrates and three composites was determined by the thermogravimetric method. The mass change of the samples is plotted as a function of temperature in Figures 5-30 and 5-31. The onset of weight loss in all the composites was near room temperature. The weight loss was ascribed to water vaporization since PPy is hygroscopic and can absorb water during storage (Bittihn *et al*., 1987). In addition, the PPy + I_2 composite with PMMA and PCPS exhibits a complex behavior of weight loss around 473 K, which may be ascribed to iodine vaporization. In the PPy + $FeCl_3$ composite in PCPS, on the other hand, the weight loss proceeded slightly and steadily. In all the composites, it was followed by steep weight loss, corresponding to substrate decomposition. The calculated decomposition temperatures are tabulated in Table 5-1. In this experiment, all the composites exhibit higher decomposition temperature of the substrate comparable to that reported in the literature (~ 660 K) by Omastova *et al*. (1998). The authors explained that the PPy layer covering the surface of the substrates partially prevents the decomposition of the substrate. Note that the PPy + $FeCl_3$

composite in PCPS has the highest thermal stability, which is consistent with its ordered structure of the conductive polymer than I_2 complex.

Using an assumption that each weight loss corresponds to either evaporation or decomposition, the composition of the composites was estimated from the thermogravimetric data. The calculated and actual weight values are compared in Table 5-2. The compositions of the PPy + I_2 composites in PMMA and PCPS are comparable to the weight data whereas the composition of the PPy + $FeCl_3$ composite in PCPS is overestimated. The data of the composites with I_2 complex suggests that etching of the aluminum pan by the formation of AlI_3 did not significantly affect the thermogravimetric data.

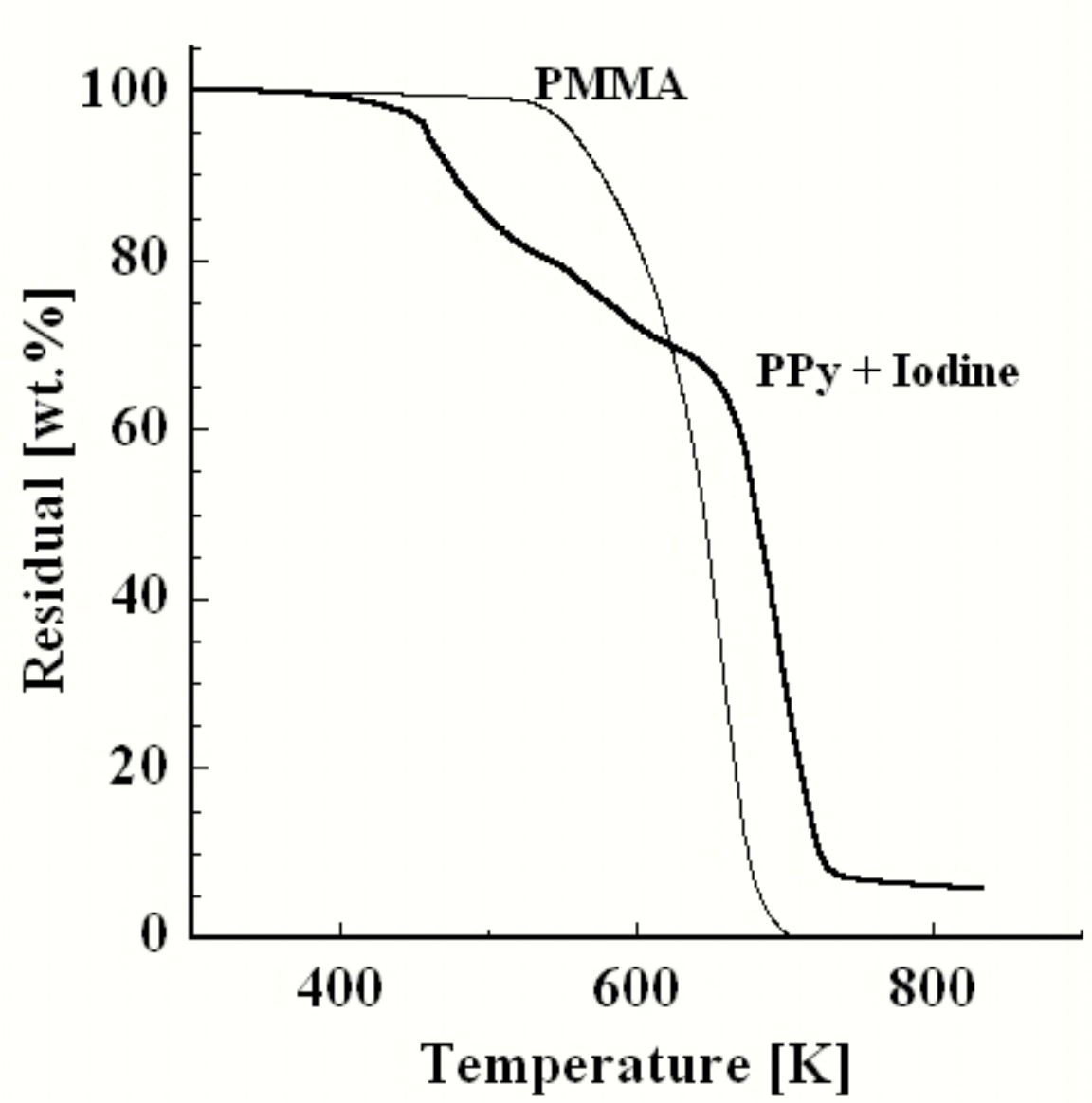

Figure 5-30. Thermogravimetric analysis of PMMA substrate and its composites.

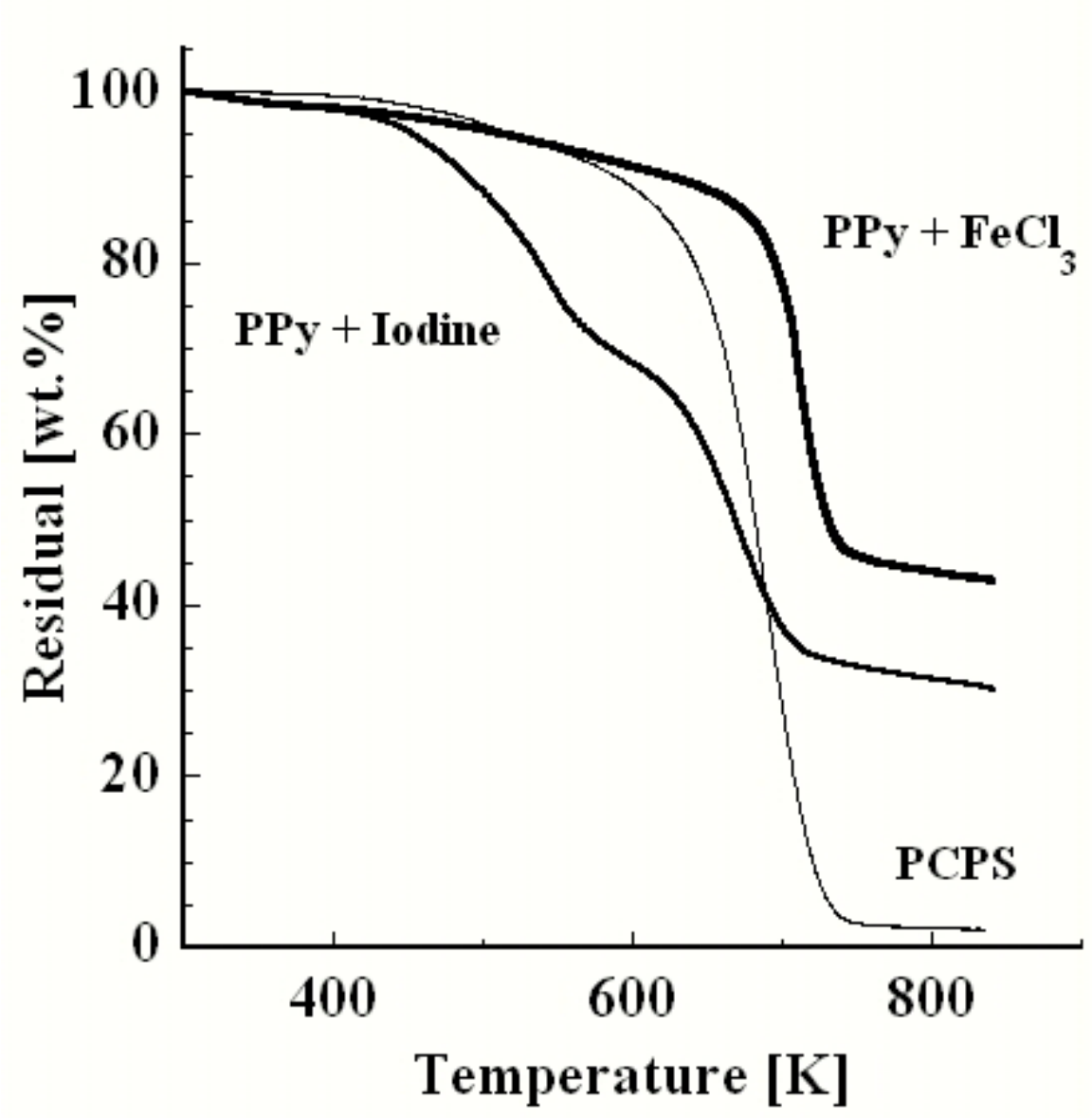

Figure 5-31. Thermogravimetric analysis of PCPS substrate and its composites.

Table 5-1. Decomposition temperature of host substrates and their composites.

Substrate	Oxidant	Decomposition [K]	Substrate	Oxidant	Decomposition [K]
PCPS	-	634	PMMA	-	562
PCPS	I_2	640	PMMA	I_2	663
PCPS	$FeCl_3$	689			

Table 5-2. Comparison of compositions of the composites.

	PPy + I_2		**PPy + I_2**			**PPy + $FeCl_3$**	
	PMMA		**PCPS**			**PCPS**	
	TG	**Actual**	**TG**	**Actual**		**TG**	**Actual**
I_2 [wt. %]	23	23	59	49	**PPy + $FeCl_3$ [wt. %]**	73	24
PPy [wt. %]	8	12	65	47			

5-5-2 **Compressive Mechanical Testing**

A mechanical tester was utilized to measure the compressive stress-strain relationship of the PCPS substrate and its composite as shown in Figure 5-32. The substrate has a yield point followed by a collapse plateau. The yield stress and strain of the substrate can be found around 2.1 MPa and 0.28, respectively. The observed yield stress values seem to correspond to those (0.9 – 2.5 MPa for polystyrene foams) calculated by the equation of Gibson and Ashby (1988) as discussed in Chapter 4. The PPy composites do not seem to exhibit a distinct yield point. However, at a small strain range (0.1 of strain), all the samples exhibit fluctuation in the curve. This may correspond to failure of weak cells. The lower yield stress and strain of the substrate can be found around 0.9 MPa and 0.15, respectively, which is the lower limit of yield stress in polystyrene foams.

Since each of the stress-strain curves includes a reasonably linear portion prior to yield, Young's modulus was calculated from the slope in the linear range, and the calculated data are summarized in Table 5-3. The magnitude of the compressive modulus indicates that the compressive properties depend on the type of oxidant. The PPy + $FeCl_3$ composite is the "hardest" whereas the PPy + I_2 composite is the "softest." The high compressive modulus of the former may be due to uniform coating of stiff and ordered PPy, and the low value of the latter may be due to continuous buckling, failure, and densification of pores with less rigid and random PPy coating. The difference in microstructure is reflected in their macroscopic deformation behavior.

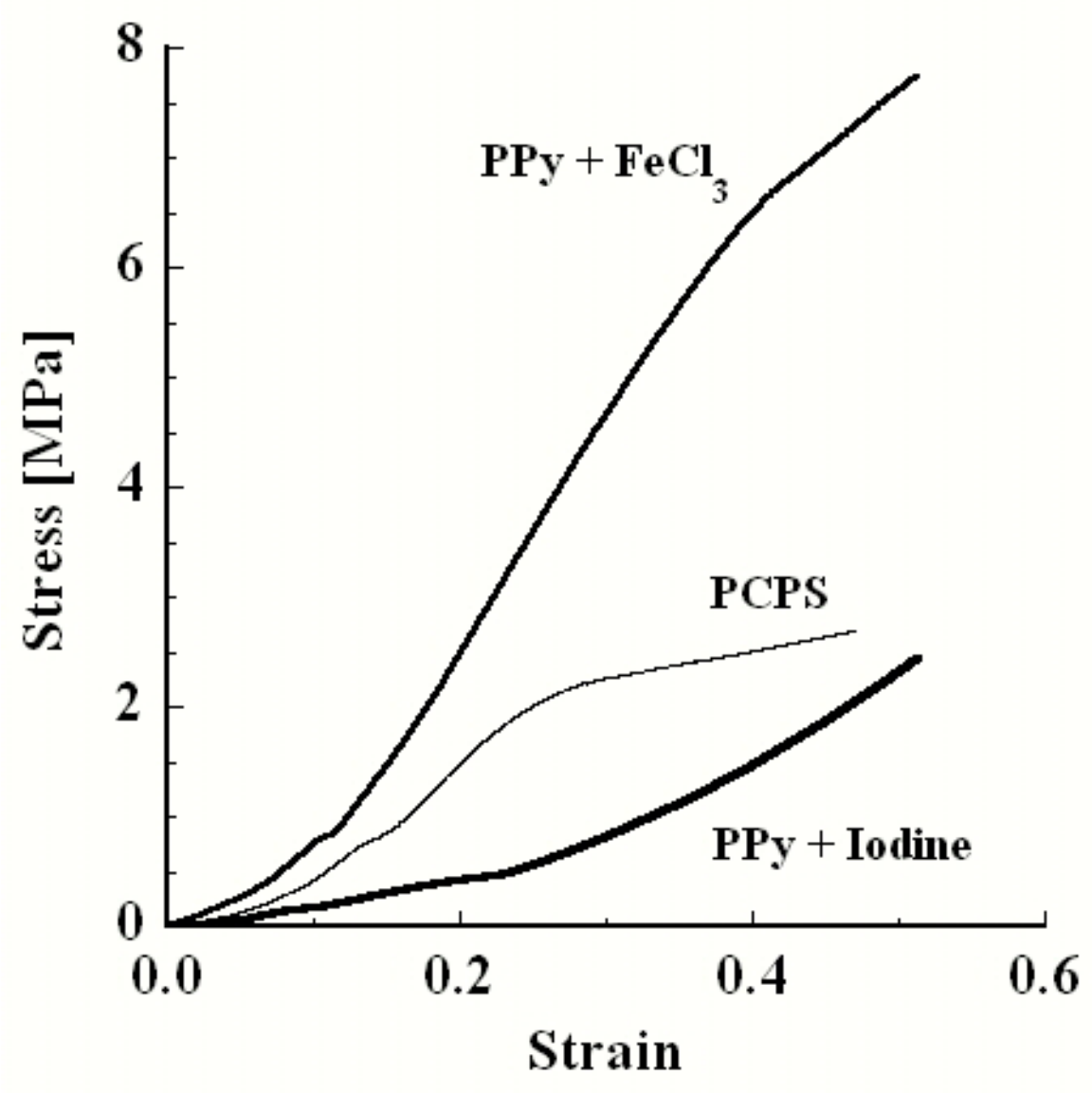

Figure 5-32. Compressive stress-strain curve of PCPS substrate and its composites.

Table 5-3. Summary of results in uniaxial compressive test.

Substrate	Oxidant	Young's modulus [MPa]	Yield stress [MPa]	Yield strain
PCPS	**-**	13.9	2.1	0.25
PCPS	**I_2**	9.5	-	-
PCPS	**$FeCl_3$**	22.7	-	-

5-5-3 **Temperature Effect on Electrical Conductivity**

Figures 5-33 and 5-34 show the temperature dependence of dc electrical conductivity in the three composites as a function of temperature and reciprocal temperature, respectively. The PMMA composite shows higher conductivity than the PCPS composite over the whole temperature range studied, which is consistent with the observation of the smooth conductive layer on the PMMA surface. In Figure 5-34, the slope of conductivity, σ, changes with reciprocal temperature, which means that the activation energy E_A depends on temperature:

$$E_A = -\frac{d \ln \sigma}{d(1/kT)} \qquad (5\text{-}4).$$

The temperature-dependent activation energy suggests that hopping conduction rather than band conduction may dominate the mechanism of conduction in the PPy composite (Singh *et al*., 1991a). Therefore, the applicability of the Mott's variable-range hopping (VRH) model (Mott and Davis, 1979) in the PPy composite was investigated. In the VRH model the temperature dependence of conductivity obeys the following function:

$$\sigma(T) \propto T^{1/2} \exp\left[-\left(\frac{T_0}{T}\right)^{-1/(n+1)}\right] \qquad (5\text{-}5)$$

where n (= 1, 2, and 3) is the number of dimensions in which the hopping occurs, and T_0 is a constant. The experimental and theoretical values of $\ln \sigma T^{1/2}$ as a function of $T^{-1/4}$ are plotted in Figures 5-35 for PPy + $FeCl_3$ composite in PCPS, PPy + I_2 composites in PCPS and PMMA. A better agreement of the VRH model is observed in PPy + $FeCl_3$ composite

when the $T^{-1/4}$ law is applied, indicating three-dimensional electronic transport. In the case of PPy + I_2 composite in PCPS, the correlation coefficient of the VRH model using a different temperature exponent did not vary. The correlation coefficient in PMMA composite is smaller than the above cases due to scatter in the experimental data. As an alternative electrical conduction model, the applicability of the charge-energy-limited tunneling (CELT) model (Sheng and Abeles, 1972; Sheng *et al*., 1973) was also evaluated; however, the CELT model failed to yield better results in either case than the VRH model in terms of the correlation coefficient. The correlation coefficients of the regression by the VRH model as a function of $T^{-1/4}$, $T^{-1/3}$, and $T^{-1/2}$ as well as those by the CELT model are tabulated in Table 5-4. For further analysis and comparison, the results with the $T^{-1/4}$ law were used, and are tabulated in Table 5-5. The values of $N(E_F)$, R, and W were calculated by taking the estimated value of $\alpha = 1$ $Å^{-1}$ (Singh *et al*., 1991a; Singh *et al*., 1991b). The calculated values are comparable to those of other PPy composites ($T_0 \sim 10^8$ K, $N(E_F) \sim 10^{20}$ eV^{-1} cm^{-3}, R ~ 25 Å, W ~ 0.1 eV) (Singh *et al*., 1991a; Singh *et al*., 1993; Aguilar-Hernandez and Potje-Kamloth, 2001).

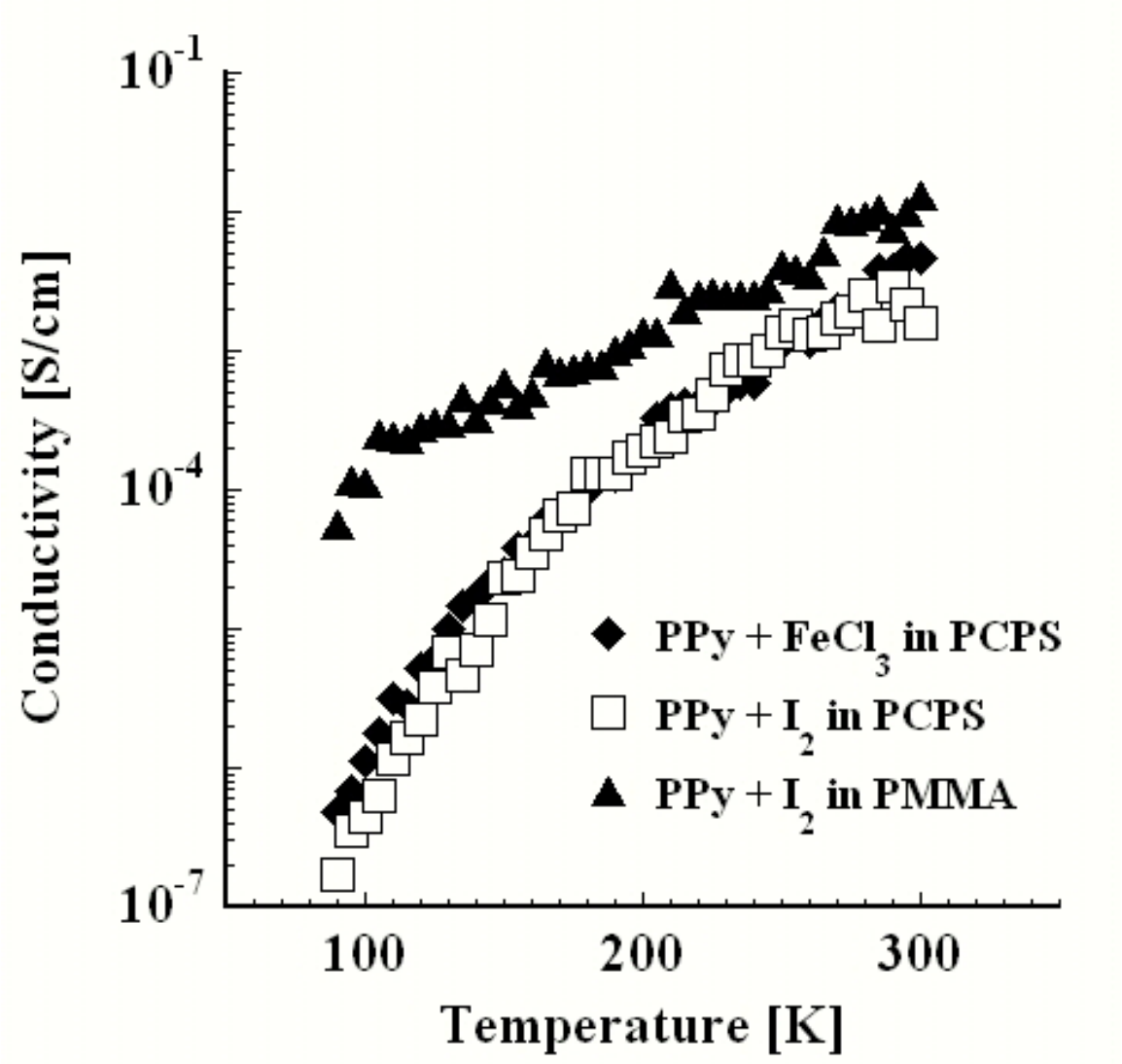

Figure 5-33. Temperature dependence of conductivity.

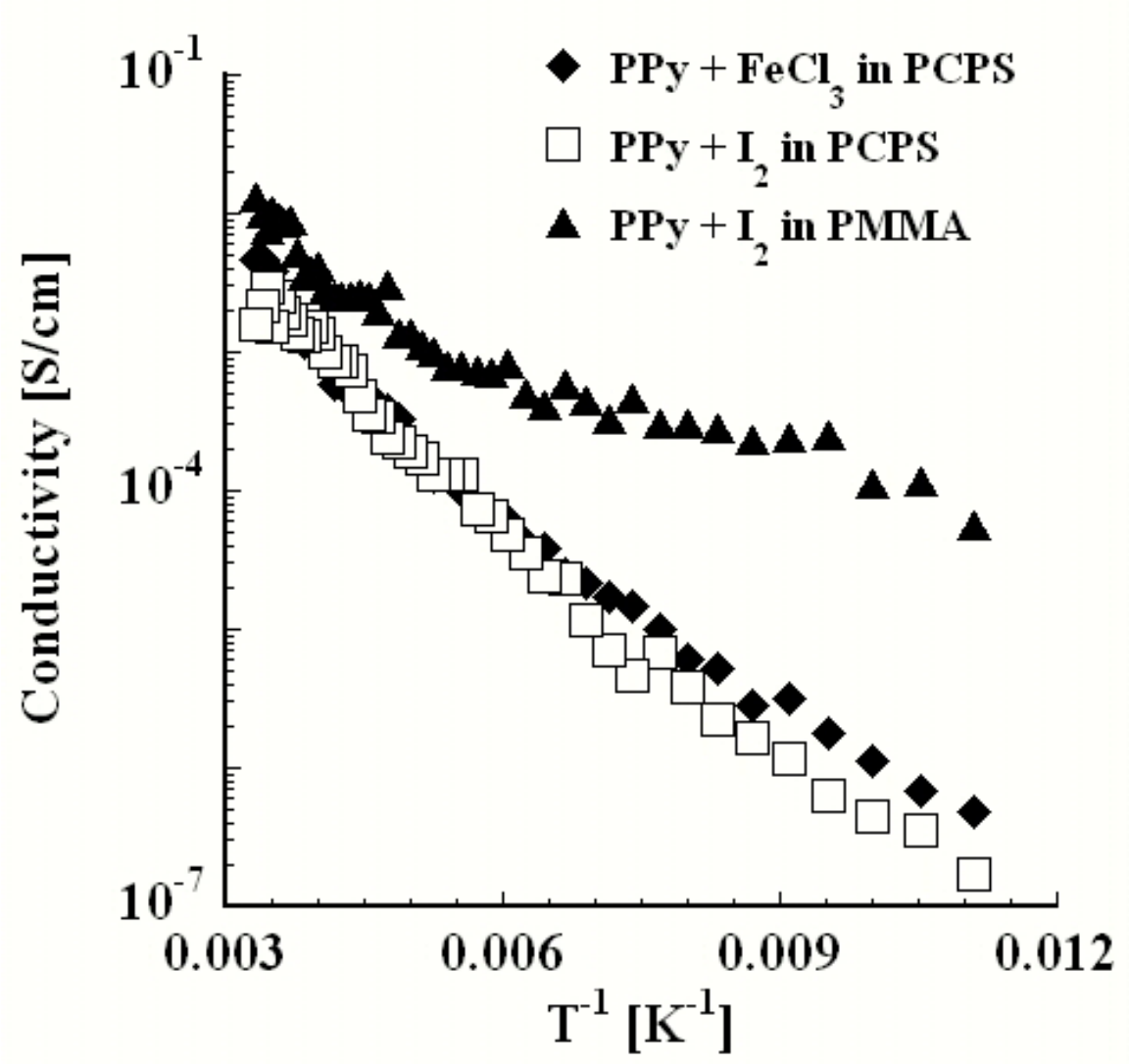

Figure 5-34. Arrehenius plot of conductivity.

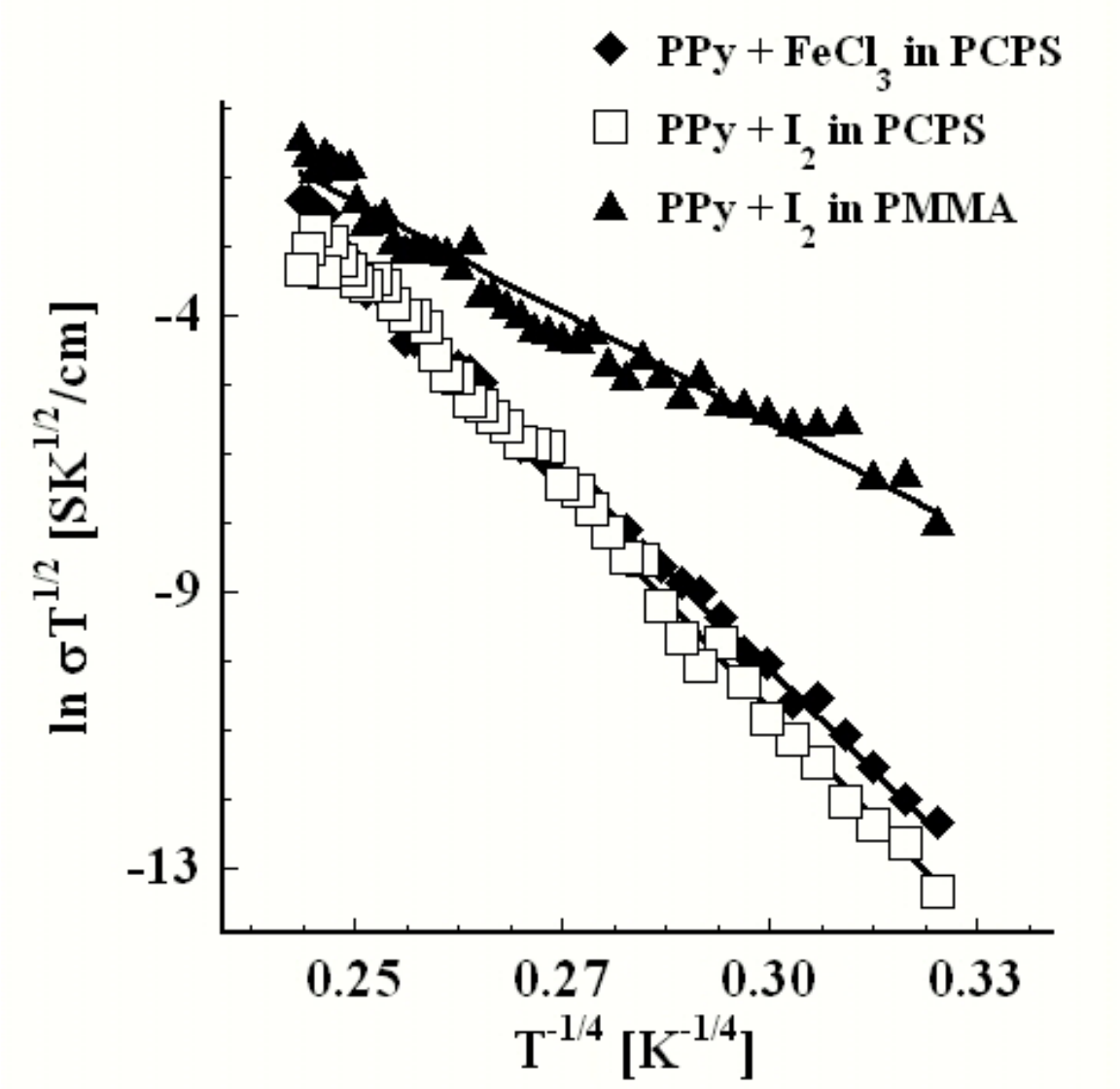

Figure 5-35. Plot of ln $\sigma T^{1/2}$ as a function of $T^{-1/4}$.

Table 5-4. Correlation coefficient in VRH and CELT models.

Substrate	Oxidant	$T^{-1/4}$	$T^{-1/3}$	$T^{-1/2}$	CELT
PCPS	**$FeCl_3$**	0.996	0.995	0.992	0.992
PCPS	**I_2**	0.993	0.994	0.994	0.993
PMMA	**I_2**	0.956	0.954	0.946	0.935

Table 5-5. Mott's parameters for PPy composite.

Substrate	Oxidant	T_0 [$10^7 \times K$]	K_0 [$S\ cm^{-1}\ K^{1/2}$]	$N(E_F)$ [$10^{20} \times cm^{-3}\ eV^{-1}$]	R [Å]	W [eV]
PCPS	**$FeCl_3$**	17.2	5.56×10^{10}	10.8	15.1	0.065
PCPS	**I_2**	23.1	5.99×10^{11}	8.03	16.2	0.070
PMMA	**I_2**	1.63	5.36×10^{5}	114	8.4	0.036

Assuming α of 1 $Å^{-1}$ at 100 K

CHAPTER 6

CONCLUSIONS AND RECOMMENDATIONS

6-1 ***Conclusions***

Thick composites (~ 3 mm in thickness) of PPy with electrically insulating porous (PCPS) and nonporous (PMMA) substrates were prepared using a two-step batch method. In the two-step method, impregnation of volatile (I_2) or nonvolatile ($FeCl_3$) oxidant in the substrate is followed by in-situ polymerization of pyrrole. Since the uniformity of conductivity in a thick conducting material determines the performance of the composite in practical applications, uniformity was determined via a new measurement - the volume conductivity - proposed in this work. The volume conductivity can provide a measure of spatial (three-dimensional) distribution of the conducting component in a composite, and therefore the level of conductivity that can be attained. This was verified by noting that volume conductivity data of this work were consistent with morphological observations. This suggests that the volume conductivity may be a useful characterization variable to consider in future investigations of thick composites.

Conductivities that attained values as high as 10^{-1} S/cm were obtained in this work in composites of PPy and PCPS when $FeCl_3$ was the oxidant. Use of the nonvolatile oxidant ($FeCl_3$) resulted in higher conducting polymer yield, and therefore composites with high conductivity. The mass gain of the PPy-$FeCl_3$ complex that was formed

increased linearly with the amount of $FeCl_3$ deposited in the substrate. Moreover, the behavior of the conductivity conformed to percolation behavior with respect to the amount of PPy formed. The percolation threshold was as low as 4 wt % suggesting that the stability and mechanical strength of the composites would approximately be that of the PCPS. This was verified by TGA and compressive strength measurements. The temperature behavior of the conductivity conformed with Mott's variable-range hopping (VRH) model suggesting three-dimensional electronic transport.

Use of the volatile oxidant (I_2) resulted in composites with conductivities that were slightly lower than in the case when $FeCl_3$ was the oxidant. However, I_2 is soluble in supercritical carbon dioxide and could be transported efficiently to the substrate. As a result, partitioning of the oxidant between the solvent phase and the polymer substrate, and hence the distribution of the oxidant in the substrate, could be controlled by manipulation of the pressure. The amount of PPy-I_2 complex formed was found to be linearly proportional to the amount of I_2 impregnated in the substrate. Since this amount is related to the level of conductivity in the composite, this work shows that the manipulation of pressure during the impregnation step can potentially be used to control the level of conductivity of the composite. The bulk and surface conductivities of the composite exhibited percolation behavior with respect to the amount of the PPy-I_2 complex formed. However, the percolation threshold was higher (~ 10 wt. %), and the bulk and surface conductivities lower by one or two orders of magnitude than those of the composite prepared with $FeCl_3$ at similar PPy concentrations. The volume conductivity exhibited a stepwise transition around 100 wt. % of PPy-I_2 complex with respect to the

substrate weight, when the degree of connectivity of the PPy network is apparently sufficient to have uniform conductivity in all directions.

A disadvantage of using iodine as the oxidant is that it tends to diffuse out of the substrate because of its volatility, a process that is accelerated in the presence of supercritical carbon dioxide. Thus, iodine was observed to diffuse out of the substrate when carbon dioxide was used to transport pyrrole to the substrate prior to the polymerization step of the process. This counter-diffusion led to the formation of a conducting surface layer, and hence a nonuniform distribution of PPy, even at low PPy concentrations.

The use of non-porous substrates such as PMMA requires a solvent that is able to swell the polymer appreciably in order for the oxidant to dissolve/diffuse into the substrate. Although carbon dioxide is an excellent swelling agent for PMMA, the limited diffusivity of the monomer and oxidant in the PMMA did not allow the desired interconnected network of conducting polymer throughout the composite to be attained in this work. Furthermore, the plasticization effect of supercritical carbon dioxide on the thermoplastic PMMA induced foaming during depressurization, leading to low integrity of the surface conducting phase of the composite. Therefore, a porous substrate offers the best means for obtaining thick conducting composites with a specified level of conductivity.

The hypothesis that the distribution of the oxidant controls the level of conductivity of a composite was verified. As a result, the two-step batch method in which supercritical carbon dioxide is used to facilitate transport and as a solvent for the oxidant

was found to be an effective method for the production of thick composites with uniform conductivity, thermal stability, and mechanical strength. Such composites are desired in important practical applications such as rechargeable battery electrodes and electromagnetic interference shielding materials.

6-2 ***Recommendations***

Hypercrosslinked polystyrene scaffolds (Steckle, Jr. *et al*., 1997) are expected to align conductive polymer chains along pore walls and therefore to enhance electrical conductivity by many orders of magnitude (Martin, 1994). The synthesis of a nano-structured polymer scaffold was carried out in this work. However, the trial failed due to the brittle nature of the substrate. This is a critical issue in the production of conductive composites because the mechanical strength of substrate determines that of its composite.

The intrinsic problem of the hypercrosslinked materials may be overcome through an elaborate synthetic technique for thermally-mended highly crosslinked polymeric materials (Chen *et al*., 2003). Alternatively, macroporous and nanoporous polymers may be used as ordered, open- porous templates with pores ranging from 50 - 500 nm in diameter by HF etching of silica beads (Jiang *et al*., 1999; Jiang *et al*., 2001), or with cylinders ranging 15 ~ 45 nm in diameter (Zalusky *et al*., 2002). Such templates with a well-defined structure would reveal the morphological-electrical conductivity relationship in the composite.

The counter-diffusion problem in the two-step batch processes may be overcome by immobilization of the oxidant. For example, bulky polymeric oxidants such as dodecylbenzenesulfonic acid and naphthalenesulfonic acid (Dutta and De, 2003), or ionic

oxidants such as $Fe(NO_3)_3$ can be trapped chemically in ion-exchange membranes (Li and Pickup, 1999) to prevent counter-diffusion altogether. The latter also allows the control of the properties of the conducting composite by manipulating the density or distribution of active reaction sites.

Based on a similar concept, nanoporous Vycor glass has also been used as a template (Zarbin *et al*., 1997; Zarbin *et al*., 1999; Sotomayor *et al*., 2001); however, the conductivity of the composite with 7 wt. % polypyrrole in the Vycor glass was as low as 10^{-7} S cm^{-1} (Maia *et al*., 1995). This may be attributed to an insufficient amount of reactive chemicals deposited in the pores. The use of $scCO_2$ is expected to enhance the diffusivity of chemicals in small pores and channels, which would result in uniform distribution of reagents within a practical period of time. Furthermore, "tunability" of $scCO_2$ properties by experimental variables may allow the optimization of processes for making conducting composites.

Potential studies that could be carried out in $scCO_2$ would include impregnation of pre-made conducting polymers in a templating substrate. High-pressure spectroscopic experiments have demonstrated that conjugated polymers of per-/semi-fluorinated 3-alkylthiophenes (Middlecoff and Collard, 1997; Hong *et al*., 2000) are soluble, and therefore, processable in $scCO_2$. The application of the solvent to crude CO_2-philic polymer products would also facilitate the development of an environmentally benign separation process for removal of inorganic catalysts used in the polymerization reaction. Ultimately, polymerization as well as processing steps in conducting composite production could be conducted in $scCO_2$.

APPENDIX A

COMPOSITE PRODUCTION DATA

All the experimental data in composite synthesis in this work are presented. M_i [wt. %] is the mass gain at step i with respective to the weight of substrate, S_B, S_S, and S_V [S/cm] are the bulk, surface, and volume conductivities, respectively, and d [cm] the thickness of substrate.

PMMA:

Table A-1. Impregnation of I_2 in CO_2 at 313 K and 10.3 MPa, polymerization of Py vapor at 297 K and 0.1 MPa for 48 h.

Step 1	M_1	Step 2	M_2	S_B	S_S	S_V	d
4 h	10		25	3.30×10^{-6}	1.09×10^{-6}	-	0.290
24 h	23		35	6.19×10^{-5}	8.11×10^{-5}	-	0.245

Table A-2. Impregnation of I_2 in CO_2 at 313 K and 10.3 MPa for 24 h, polymerization of Py in CO_2 at 313 K and 10.3 MPa for 24 h.

Step 1	M_1	Step 2	M_2	S_B	S_S	S_V	d
	18		82	1.32×10^{-4}	1.13×10^{-8}	-	0.400

PCPS:

Table A-3. Impregnation of $FeCl_3$ in CO_2 at 297 K and 0.1 MPa for 96 h, Polymerization of Py in CO_2 at 313 K and 10.3 MPa for 1h.

Step 1	M_1	Step 2	M_2	S_B	S_S	S_V	d
	27		37	3.36×10^{-3}	7.09×10^{-4}	-	0.285

Table A-4. Impregnation of $FeCl_3$ in CH_3CN at 297 K and 0.1 MPa for 1 h, vacuum overnight, polymerization of Py vapor at 313 K and 0.1 MPa for 24 h.

Step 1	M_1	Step 2	M_2	S_B	S_S	S_V	d
0.06 M	1		28	1.37×10^{-3}	1.52×10^{-5}	1.68×10^{-4}	0.275
0.25 M	22		84	4.96×10^{-3}	1.04×10^{-4}	1.92×10^{-4}	0.215
0.50 M	77		140	6.89×10^{-3}	1.28×10^{-4}	1.96×10^{-4}	0.225
0.75 M	101		198	7.07×10^{-3}	1.28×10^{-4}	7.45×10^{-4}	0.280
1.00 M	119		214	2.37×10^{-2}	6.60×10^{-5}	2.20×10^{-3}	0.245

Table A-5. Impregnation of $FeCl_3$ in CH_3CN at 297 K and 0.1 MPa for 24 h, vacuum overnight, polymerization of Py in CO_2 at 313 K and 10.3 MPa for 24 h.

Step 1	M_1	Step 2	M_2	S_B	S_S	S_V	d
0.01 M	3		5	9.65×10^{-9}	2.21×10^{-9}	5.43×10^{-9}	0.200
0.06 M	5		14	1.71×10^{-4}	4.21×10^{-6}	9.00×10^{-7}	0.270
0.25 M	4		24	1.35×10^{-2}	2.38×10^{-4}	2.05×10^{-5}	0.200
0.25 M	7		27	6.57×10^{-3}	1.09×10^{-3}	1.04×10^{-5}	0.225
0.50 M	42		72	7.79×10^{-3}	7.39×10^{-6}	2.13×10^{-4}	0.475
0.75 M	103		136	5.86×10^{-4}	7.69×10^{-5}	2.88×10^{-5}	0.280
1.00 M	215		258	4.14×10^{-3}	2.72×10^{-4}	1.37×10^{-3}	0.225

Table A-6. Impregnation of 0.25 M $FeCl_3$ in CH_3CN at 297 K and 0.1 MPa, vacuum overnight, polymerization of Py in CO_2 at 313 K and 10.3 MPa for 1 h.

Step 1	M_1	Step 2	M_2	S_B	S_S	S_V	d
1 h	18	0.1 h	40	6.58×10^{-3}	1.59×10^{-3}	6.72×10^{-4}	0.310
1 h	19		21	2.32×10^{-4}	4.74×10^{-6}	4.13×10^{-7}	0.420
1 h	39		54	7.73×10^{-3}	1.30×10^{-4}	7.09×10^{-6}	0.260
1 h	25		24	1.13×10^{-3}	1.22×10^{-2}	3.43×10^{-6}	0.200
4 h	26		24	1.46×10^{-3}	4.67×10^{-3}	1.51×10^{-6}	0.265
9 h	24		25	6.65×10^{-5}	2.11×10^{-3}	8.00×10^{-8}	0.280
16 h	27		28	1.02×10^{-3}	1.13×10^{-3}	5.62×10^{-5}	0.240
24 h	28		27	1.05×10^{-2}	6.74×10^{-4}	3.24×10^{-7}	0.295
24 h	18		43	3.65×10^{-4}	5.31×10^{-6}	2.88×10^{-5}	0.425

Table A-7. Impregnation of I_2 vapor at 313 K and 0.1 MPa, polymerization of Py vapor at 313 K and 0.1 MPa.

Step 1	M_1	Step 2	M_2	S_B	S_S	S_V	d
24 h	12	24 h	46	3.24×10^{-7}	1.02×10^{-8}	-	0.265
168 h	47	48 h	113	9.29×10^{-4}	7.28×10^{-6}	5.43×10^{-6}	0.200

Table A-8. Impregnation of I_2 in CO_2 at 313 K and 10.3 MPa, polymerization of Py vapor at 297 K and 0.1 MPa for 48 h.

Step 1	M_1	Step 2	M_2	S_B	S_S	S_V	d
1 h	9		11	6.69 e-9	1.80×10^{-8}	-	0.250
2 h	10		20	4.32×10^{-7}	1.00×10^{-9}	1.16×10^{-9}	0.235
2 h	5		15	8.32×10^{-7}	1.18×10^{-7}	2.35×10^{-9}	0.285
4 h	10		25	2.80×10^{-8}	5.66×10^{-6}	8.48×10^{-10}	0.225
4 h	17		40	2.44×10^{-7}	6.51×10^{-8}	1.68×10^{-9}	0.235
4 h	18		20	3.35×10^{-7}	2.65×10^{-7}	-	0.235
4 h	8		21	2.93×10^{-7}	3.18×10^{-7}	2.97×10^{-9}	0.265
4 h	10		26	1.14×10^{-7}	1.50×10^{-6}	2.39×10^{-8}	0.275
9 h	25		61	1.33×10^{-5}	1.55×10^{-5}	-	0.260
9 h	28		69	1.01×10^{-5}	2.45×10^{-7}	-	0.250
9 h	25		63	1.55×10^{-5}	3.86×10^{-6}	4.82×10^{-9}	0.245
16 h	51		143	3.04×10^{-4}	1.66×10^{-5}	1.12×10^{-5}	0.285
16 h	40		91	1.45×10^{-4}	2.13×10^{-6}	1.54×10^{-9}	0.260
16 h	44		101	4.99×10^{-4}	1.67×10^{-5}	6.38×10^{-5}	0.265
16 h	16		42	1.09×10^{-4}	3.85×10^{-6}	1.94×10^{-8}	0.290
16 h	38		106	1.43×10^{-4}	6.64×10^{-7}	3.11×10^{-6}	0.285
24 h	51		128	1.35×10^{-4}	7.69×10^{-6}	7.65×10^{-6}	0.175

Table A-9. Impregnation of I_2 in CO_2 at 313 K for 24 h, polymerization of Py vapor at 297 K and 0.1 MPa for 48 h.

Step 1	M_1	Step 2	M_2	S_B	S_S	S_V	d
20.5 MPa	6		32	1.12×10^{-4}	2.99×10^{-6}	6.11×10^{-9}	0.225
34.1 MPa	8		35	7.14×10^{-6}	6.62×10^{-7}	1.52×10^{-9}	0.200

Table A-10. Impregnation of I_2 in CO_2 at 313 K and 10.3 MPa for 24 h, polymerization of Py in CO_2 at 313 K and 10.3 MPa.

Step 1	M_1	Step 2	M_2	S_B	S_S	S_V	d
	41	1 h	51	5.31×10^{-7}	1.67×10^{-6}	1.19×10^{-9}	0.220
	52	4 h	78	5.16×10^{-5}	9.82×10^{-7}	1.71×10^{-9}	0.245
	49	9 h	91	3.72×10^{-5}	3.45×10^{-6}	6.59×10^{-10}	0.195
	44	16 h	87	7.07×10^{-5}	4.72×10^{-6}	2.69×10^{-9}	0.240
	49	24 h	96	1.25×10^{-4}	3.04×10^{-6}	2.98×10^{-9}	0.255
	36	24 h	72	1.22×10^{-5}	2.59×10^{-6}	1.06×10^{-9}	0.290

Table A-11. Impregnation of I_2 in CO_2 at 313 K and 20.5 MPa for 24 h, polymerization of Py in CO_2 at 313 K and 20.5 MPa for 24 h.

Step 1	M_1	Step 2	M_2	S_B	S_S	S_V	d
	4		39	1.02×10^{-7}	2.75×10^{-7}	-	0.385

Table A-12. Impregnation of Py in CO_2 at 313 K and 10.3 MPa for 24 h, polymerization with I_2 in CO_2 at 313 K and 10.3 MPa for 24 h.

Step 1	M_1	Step 2	M_2	S_B	S_S	S_V	d
	83		49	1.52×10^{-5}	6.33×10^{-7}	-	0.255

Table A-13. Impregnation of I_2 in CO_2 at 313 K and 10.3 MPa for 24 h, polymerization of Py in CO_2 at 313 K and 10.3 MPa for 24 h, doping with I_2 in CO_2 at 313 K and 10.3 MPa for 4 h.

Step 1	M_1	Step 2	M_2	S_B	S_S	S_V	d
	23		61	3.40×10^{-5}	4.47×10^{-6}	2.76×10^{-7}	0.270

APPENDIX B

BET MEASUREMENT REPORT

The specific surface area in porous, crosslinked polystyrene synthesized by a condensed emulsion polymerization (Ruckenstein and Park, 1988) was obtained via an isothermal gas absorption measurement with nitrogen as an adsorbent. The mass of the substrate was 0.1100 g after drying overnight under a vacuum of 4×10^{-3} Torr at 423 K. In the following pages, the analysis reports produced by the ASAP software are presented.

Full Report Set

ASAP 2010 V5.02 C Unit 1 Serial # 631 Page 1

Sample Id: PCPS1
Outgas Time /Temp
Submitter/Operator BCW
File Name: A:\PCPS1.SMP

Started: 9/17/2003 11:15:49AM Analysis Adsorptive: N2
Completed: 9/17/2003 2:20:17PM Analysis Bath: 77.19 K
Report Time: 9/18/2003 10:00:26AM Thermal Correction: No
Sample Weight: 0.1100 g Smoothed Pressures: No
Warm Freespace: 27.9452 cm³ ENTERED Cold Freespace: 89.2064 cm³
Equil. Interval: 10 secs Low Pressure Dose: None

Analysis Log

Relative Pressure	Pressure (mmHg)	Vol Adsorbed (cm³/g STP)	Elapsed Time (HR:MN)	Saturation Press.(mmHg)
			00:51	746.86804
0.011495872	8.58469	0.3451	00:59	
0.034212410	25.54721	0.9287	01:02	
0.059977712	44.78519	1.5159	01:04	
0.079892301	59.65326	1.9332	01:06	
0.100286195	74.87815	2.3146	01:08	
0.120245149	89.77724	2.7072	01:10	
0.140062537	104.56774	3.0152	01:13	
0.160294800	119.66851	3.3454	01:15	
0.180046775	134.40730	3.6708	01:18	
0.200351521	149.55980	3.9609	01:20	
0.250046364	186.64978	4.7735	01:22	
0.300340598	224.18456	5.5631	01:24	
0.350519761	261.62619	6.2902	01:27	
0.400489437	298.91278	6.9439	01:29	
0.450393162	336.14752	7.6309	01:31	
0.500716221	373.69260	8.2329	01:33	
0.550636849	410.92746	8.7348	01:36	
0.600545020	448.15698	9.3208	01:38	
0.650747967	485.60385	9.9413	01:40	
0.700890561	522.99384	10.4892	01:43	
0.750817333	560.22870	11.0079	01:45	
0.800899939	597.57721	11.5191	01:47	
0.821015274	612.56433	11.6771	01:49	
0.850934094	634.85339	12.0117	01:52	
0.876210238	653.68805	12.2730	01:54	
0.901182993	672.29504	12.4720	01:56	
0.926171580	690.91254	12.6694	01:58	
0.951206176	709.55054	12.9820	02:01	
0.976517518	728.40582	13.2161	02:03	
0.998809824	744.90289	15.0701	02:13	
0.974799624	726.95789	12.6895	02:16	
0.933363373	696.03223	11.8230	02:18	
0.908092166	677.15106	11.3299	02:21	
0.882955387	658.38373	10.9251	02:23	
0.857894412	639.66296	10.5549	02:26	
0.832954618	621.04547	10.1165	02:28	
0.807874469	602.32465	9.7700	02:30	
0.782737008	583.55212	9.4617	02:33	
0.732888044	546.36908	9.0340	02:35	
0.682757930	508.97906	8.4085	02:37	
0.632302516	471.34088	7.7801	02:40	

Figure B-1. Analysis log.

Full Report Set

ASAP 2010 V5.02 C Unit 1 Serial # 631 Page 2

Sample Id: PCPS1
Outgas Time /Temp
Submitter/Operator BCW
File Name: A:\PCPS1.SMP

Started: 9/17/2003 11:15:49AM Analysis Adsorptive: N2
Completed: 9/17/2003 2:20:17PM Analysis Bath: 77.19 K
Report Time: 9/18/2003 10:00:26AM Thermal Correction: No
Sample Weight: 0.1100 g Smoothed Pressures: No
Warm Freespace: 27.9452 cm³ ENTERED Cold Freespace: 89.2064 cm³
Equil. Interval: 10 secs Low Pressure Dose: None

Analysis Log

Relative Pressure	Pressure (mmHg)	Vol Adsorbed (cm³/g STP)	Elapsed Time (HR:MN)	Saturation Press.(mmHg)
0.582567007	434.25095	7.1033	02:42	
0.532363012	396.81442	6.4977	02:44	
0.482259513	359.45544	5.7647	02:46	
0.432139382	322.08102	5.0965	02:49	
0.381917006	284.63937	4.4292	02:51	
			02:53	745.26489
0.331899251	247.35286	3.6769	02:55	
0.281021455	209.43542	2.9759	02:58	
0.230934706	172.10753	2.2665	03:00	
0.180917384	134.83138	1.5070	03:02	
0.135799035	101.20625	0.7707	03:04	

Figure B-2. Analysis log.

Full Report Set

ASAP 2010 V5.02 C Unit 1 Serial # 631 Page 3

```
          Sample Id: PCPS1
    Outgas Time /Temp
  Submitter/Operator  BCW
          File Name: A:\PCPS1.SMP

            Started: 9/17/2003 11:15:49AM Analysis Adsorptive: N2
          Completed: 9/17/2003 2:20:17PM       Analysis Bath: 77.19 K
        Report Time: 9/18/2003 10:00:26AM  Thermal Correction: No
      Sample Weight: 0.1100 g              Smoothed Pressures: No
     Warm Freespace: 27.9452 cm³  ENTERED      Cold Freespace: 89.2064 cm³
     Equil. Interval: 10 secs               Low Pressure Dose: None
```

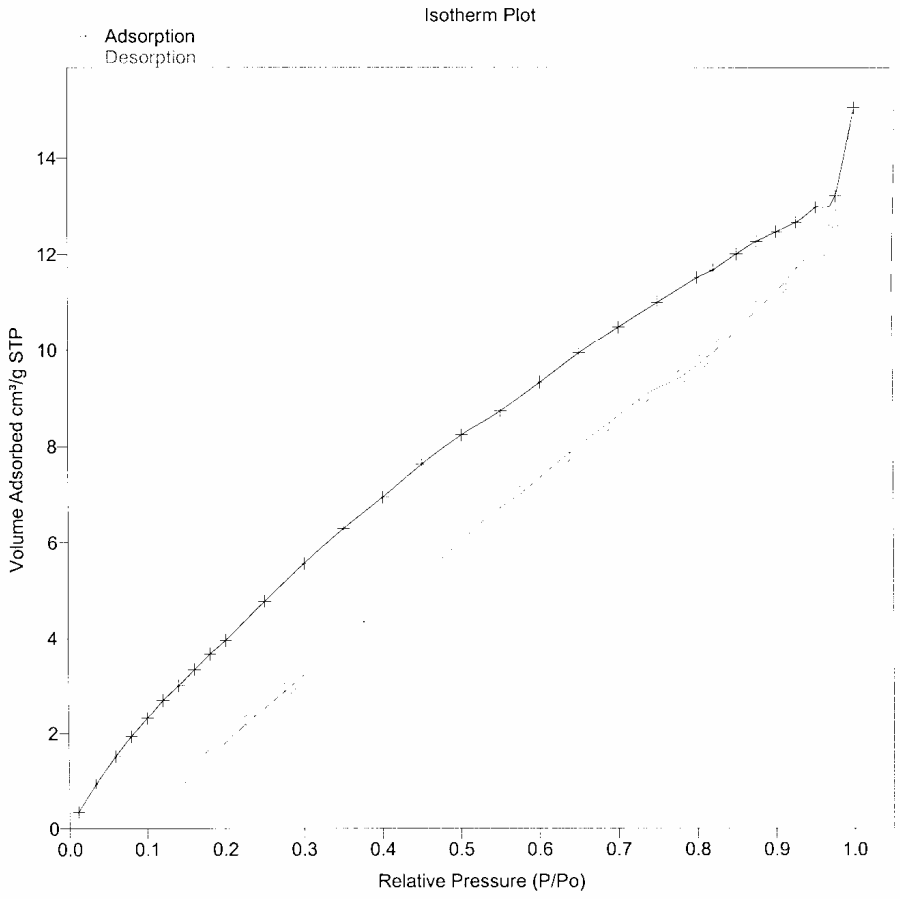

Figure B-3. Isotherm plot.

Sample Id: PCPS1
Outgas Time /Temp
Submitter/Operator BCW
File Name: A:\PCPS1.SMP

Started: 9/17/2003 11:15:49AM Analysis Adsorptive: N2
Completed: 9/17/2003 2:20:17PM Analysis Bath: 77.19 K
Report Time: 9/18/2003 10:00:26AM Thermal Correction: No
Sample Weight: 0.1100 g Smoothed Pressures: No
Warm Freespace: 27.9452 cm³ ENTERED Cold Freespace: 89.2064 cm³
Equil. Interval: 10 secs Low Pressure Dose: None

BET Surface Area Report

BET Surface Area:	23.7639	±	0.2562 m²/g
Slope:	0.150266	±	0.001956
Y-Intercept:	0.032919	±	0.000270
C:	5.564656		
VM:	5.458961	cm³/g STP	
Correlation Coefficient:	9.994920e-01		
Molecular Cross-section:	0.1620	nm²	

Relative Pressure	Vol Adsorbed (cm³/g STP)	1/ [VA*(Po/P - 1)]
0.059977712	1.5159	0.042089
0.079892301	1.9332	0.044915
0.100286195	2.3146	0.048158
0.120245149	2.7072	0.050488
0.140062537	3.0152	0.054018
0.160294800	3.3454	0.057062
0.180046775	3.6708	0.059819
0.200351521	3.9609	0.063256

Figure B-4. BET surface area report.

Sample Id: PCPS1
Outgas Time /Temp
Submitter/Operator BCW
File Name: A:\PCPS1.SMP

Started:	9/17/2003 11:15:49AM	Analysis Adsorptive:	N2
Completed:	9/17/2003 2:20:17PM	Analysis Bath:	77.19 K
Report Time:	9/18/2003 10:00:26AM	Thermal Correction:	No
Sample Weight:	0.1100 g	Smoothed Pressures:	No
Warm Freespace:	27.9452 cm³ ENTERED	Cold Freespace:	89.2064 cm³
Equil. Interval:	10 secs	Low Pressure Dose:	None

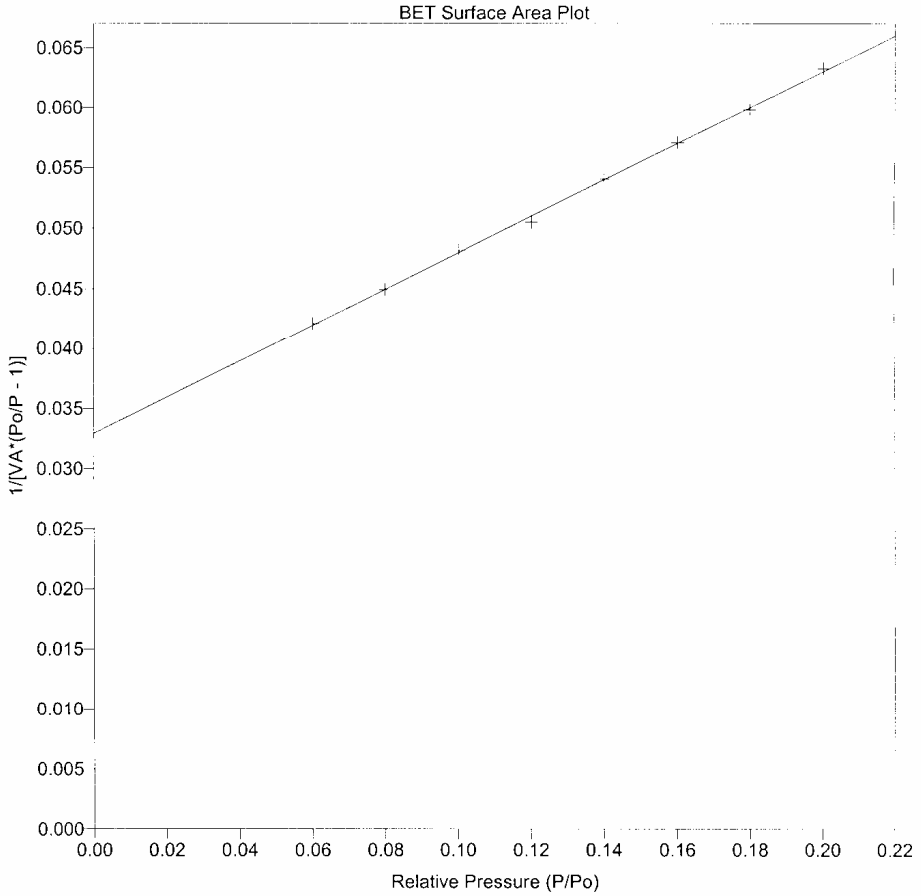

Figure B-5. BET surface area plot.

Sample Id: PCPS1
Outgas Time /Temp
Submitter/Operator BCW
File Name: A:\PCPS1.SMP

Started: 9/17/2003 11:15:49AM Analysis Adsorptive: N2
Completed: 9/17/2003 2:20:17PM Analysis Bath: 77.19 K
Report Time: 9/18/2003 10:00:26AM Thermal Correction: No
Sample Weight: 0.1100 g Smoothed Pressures: No
Warm Freespace: 27.9452 cm³ ENTERED Cold Freespace: 89.2064 cm³
Equil. Interval: 10 secs Low Pressure Dose: None

Langmuir Surface Area Report

Langmuir Surface Area:	55.7056	±	1.5451 m²/g
Slope:	0.078147	±	0.002168
Y-Intercept:	0.035159	±	0.000299
b:	0.449913		
VM:	12.796475	cm³/g STP	
Correlation Coefficient:	9.976999e-01		
Molecular Cross-section:	0.1620	nm²	

Relative Pressure	Vol Adsorbed (cm³/g STP)	1/ [VA*(Po/P)]
0.059977712	1.5159	0.039565
0.079892301	1.9332	0.041326
0.100286195	2.3146	0.043329
0.120245149	2.7072	0.044417
0.140062537	3.0152	0.046452
0.160294800	3.3454	0.047916
0.180046775	3.6708	0.049049
0.200351521	3.9609	0.050582

Figure B-6. Langmuir surface area report.

Sample Id: PCPS1
Outgas Time /Temp
Submitter/Operator BCW
File Name: A:\PCPS1.SMP

Started:	9/17/2003 11:15:49AM	Analysis Adsorptive:	N2
Completed:	9/17/2003 2:20:17PM	Analysis Bath:	77.19 K
Report Time:	9/18/2003 10:00:26AM	Thermal Correction:	No
Sample Weight:	0.1100 g	Smoothed Pressures:	No
Warm Freespace:	27.9452 cm³ ENTERED	Cold Freespace:	89.2064 cm³
Equil. Interval:	10 secs	Low Pressure Dose:	None

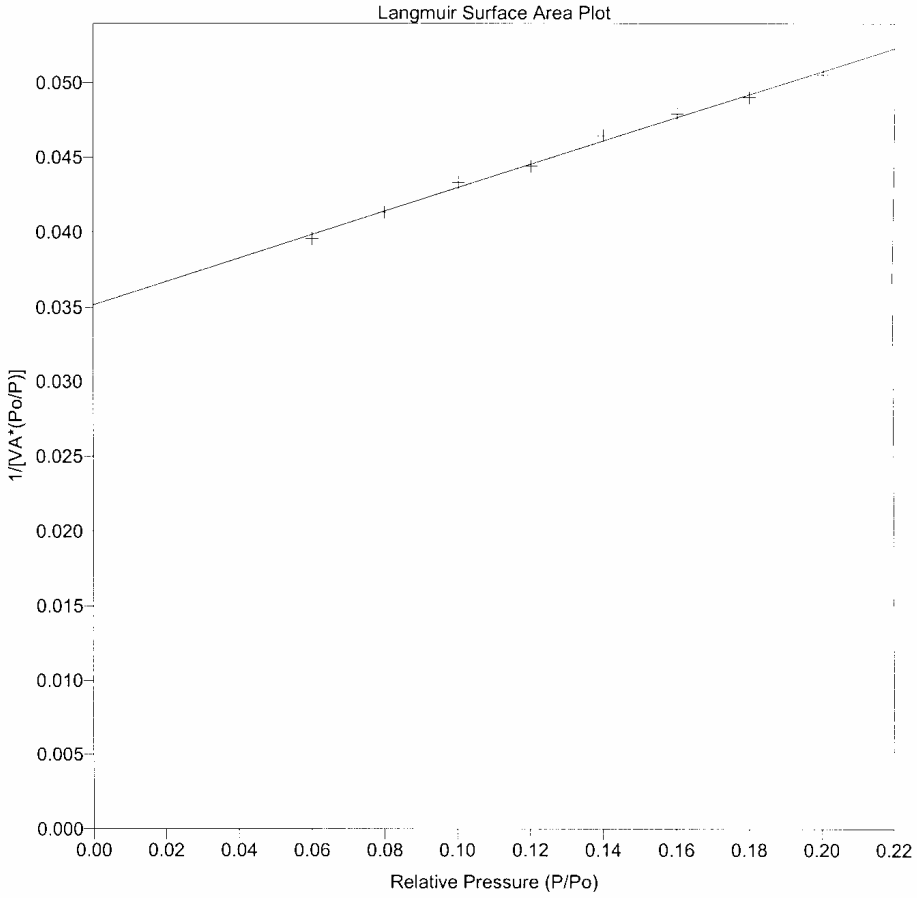

Figure B-7. Langmuir surface area plot.

Sample Id: PCPS1
Outgas Time /Temp
Submitter/Operator BCW
File Name: A:\PCPS1.SMP

Started: 9/17/2003 11:15:49AM Analysis Adsorptive: N2
Completed: 9/17/2003 2:20:17PM Analysis Bath: 77.19 K
Report Time: 9/18/2003 10:00:26AM Thermal Correction: No
Sample Weight: 0.1100 g Smoothed Pressures: No
Warm Freespace: 27.9452 cm³ ENTERED Cold Freespace: 89.2064 cm³
Equil. Interval: 10 secs Low Pressure Dose: None

---

t-Plot Report

Micropore Volume: -0.010110 cm³/g
Micropore Area: -13.4744 m²/g
External Surface Area: 37.2383 m²/g
Slope: 2.407442 ± 0.017127
Y-Intercept: -6.536320 ± 0.069646
Correlation Coefficient: 9.99848e-01
Thickness Range: 3.5000 to 5.0000 A

t = [13.9900 / (0.0340 - log(P/Po))] 0.5000

Surface Area Correction Factor: 1.00
Density Conversion Factor: 0.001547
Total Surface Area (by BET): 23.7639

Relative Pressure	Statistical Thickness (A)	Vol Adsorbed (cm³/g)
0.011495872	2.6625	0.3451
0.034212410	3.0541	0.9287
0.059977712	3.3374	1.5159
0.079892301	3.5163	1.9332
0.100286195	3.6805	2.3146
0.120245149	3.8296	2.7072
0.140062537	3.9699	3.0152
0.160294800	4.1078	3.3454
0.180046775	4.2388	3.6708
0.200351521	4.3711	3.9609
0.250046364	4.6902	4.7735
0.300340598	5.0144	5.5631
0.350519761	5.3472	6.2902
0.400489437	5.6946	6.9439
0.450393162	6.0643	7.6309
0.500716221	6.4680	8.2329
0.550636849	6.9084	8.7348
0.600545020	7.4003	9.3208
0.650747967	7.9638	9.9413

Figure B-8. t-plot report.

```
          Sample Id: PCPS1
    Outgas Time /Temp
  Submitter/Operator  BCW
          File Name: A:\PCPS1.SMP

            Started: 9/17/2003 11:15:49AM Analysis Adsorptive: N2
          Completed: 9/17/2003 2:20:17PM       Analysis Bath: 77.19 K
        Report Time: 9/18/2003 10:00:26AM  Thermal Correction: No
      Sample Weight: 0.1100 g              Smoothed Pressures: No
     Warm Freespace: 27.9452 cm³  ENTERED      Cold Freespace: 89.2064 cm³
    Equil. Interval: 10 secs               Low Pressure Dose: None
```

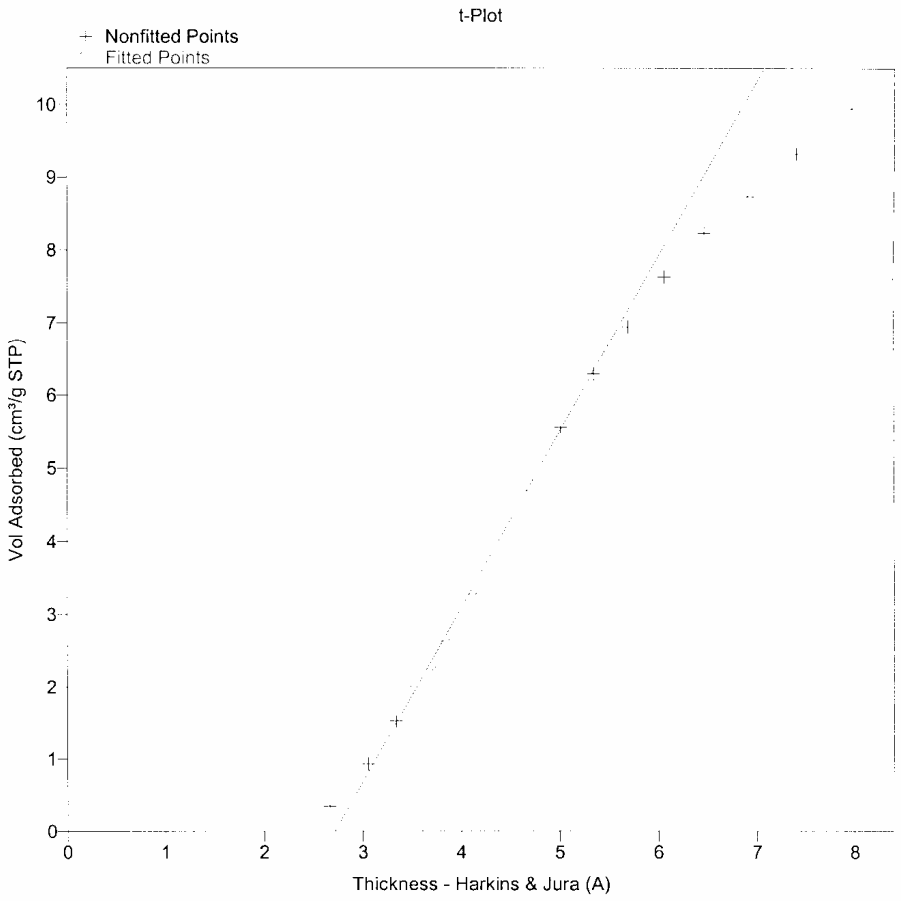

Figure B-9. t-plot.

Sample Id: PCPS1
Outgas Time /Temp
Submitter/Operator BCW
File Name: A:\PCPS1.SMP

Started: 9/17/2003 11:15:49AM Analysis Adsorptive: N2
Completed: 9/17/2003 2:20:17PM Analysis Bath: 77.19 K
Report Time: 9/18/2003 10:00:26AM Thermal Correction: No
Sample Weight: 0.1100 g Smoothed Pressures: No
Warm Freespace: 27.9452 cm³ ENTERED Cold Freespace: 89.2064 cm³
Equil. Interval: 10 secs Low Pressure Dose: None

BJH Adsorption Pore Distribution Report

$t = 3.5400 \times [-5.0000 / \ln(P/Po)]^{0.3330}$

Diameter Range: 17.0000 to 3000.0000 A
Adsorbate Property Factor: 9.530000 A
Density Conversion Factor: 0.001547
Fraction of Pores Open at Both Ends: 0.000

Pore Diameter Range (A)	Average Diameter (A)	Incremental Pore Volume (cm³/g)	Cumulative Pore Volume (cm³/g)	Incremental Pore Area (m²/g)	Cumulative Pore Area (m²/g)
16113.5- 838.9	877.6	0.003124	0.003124	0.142	0.142
838.9- 408.6	488.2	0.000336	0.003460	0.028	0.170
408.6- 271.7	312.7	0.000522	0.003982	0.067	0.237
271.7- 203.6	227.7	0.000331	0.004313	0.058	0.295
203.6- 162.7	178.4	0.000349	0.004661	0.078	0.373
162.7- 135.0	146.2	0.000483	0.005144	0.132	0.505
135.0- 112.2	121.4	0.000636	0.005780	0.210	0.715
112.2- 100.6	105.7	0.000294	0.006074	0.111	0.826
100.6- 79.6	87.5	0.001008	0.007082	0.461	1.287
79.6- 65.4	71.0	0.001048	0.008130	0.590	1.877
65.4- 55.1	59.3	0.001134	0.009265	0.765	2.642
55.1- 47.3	50.5	0.001323	0.010588	1.047	3.689
47.3- 41.0	43.7	0.001250	0.011838	1.144	4.834
41.0- 36.0	38.1	0.001042	0.012880	1.093	5.927
36.0- 31.7	33.5	0.001307	0.014187	1.559	7.486
31.7- 28.0	29.6	0.001532	0.015719	2.070	9.556
28.0- 24.8	26.2	0.001418	0.017136	2.163	11.719
24.8- 22.0	23.2	0.001593	0.018729	2.746	14.465
22.0- 19.3	20.5	0.001715	0.020444	3.352	17.818
19.3- 16.9	18.0	0.001693	0.022138	3.772	21.589

Figure B-10. BJH adsorption pore distribution report.

Sample Id: PCPS1
Outgas Time /Temp
Submitter/Operator BCW
File Name: A:\PCPS1.SMP

Started: 9/17/2003 11:15:49AM Analysis Adsorptive: N2
Completed: 9/17/2003 2:20:17PM Analysis Bath: 77.19 K
Report Time: 9/18/2003 10:00:26AM Thermal Correction: No
Sample Weight: 0.1100 g Smoothed Pressures: No
Warm Freespace: 27.9452 cm³ ENTERED Cold Freespace: 89.2064 cm³
Equil. Interval: 10 secs Low Pressure Dose: None

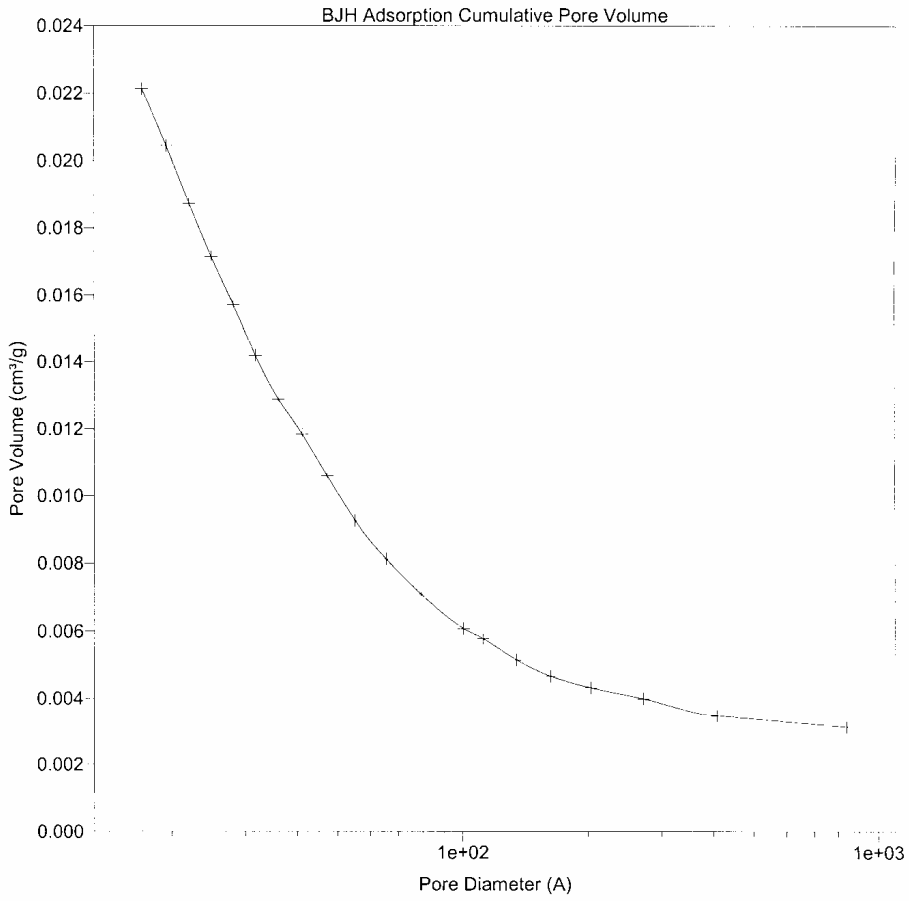

Figure B-11. BJH adsorption cumulative pore volume.

Sample Id: PCPS1
Outgas Time /Temp
Submitter/Operator BCW
File Name: A:\PCPS1.SMP

Started: 9/17/2003 11:15:49AM Analysis Adsorptive: N2
Completed: 9/17/2003 2:20:17PM Analysis Bath: 77.19 K
Report Time: 9/18/2003 10:00:26AM Thermal Correction: No
Sample Weight: 0.1100 g Smoothed Pressures: No
Warm Freespace: 27.9452 cm³ ENTERED Cold Freespace: 89.2064 cm³
Equil. Interval: 10 secs Low Pressure Dose: None

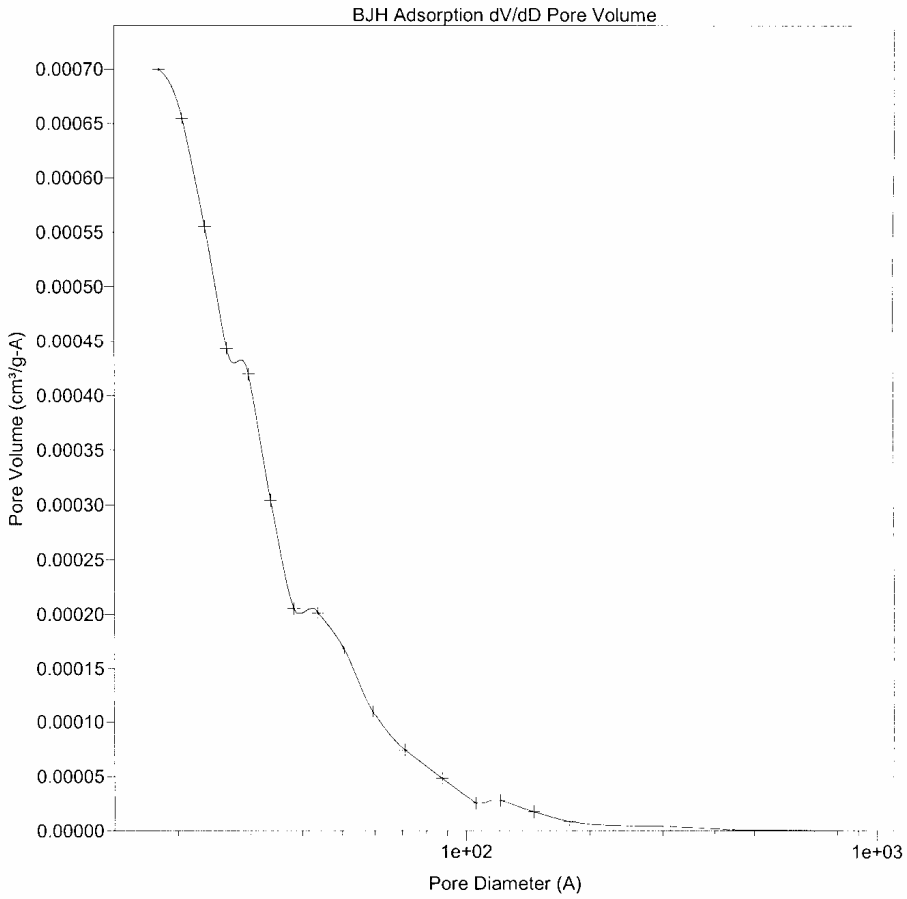

Figure B-12. BJH adsorption dV/dD pore volume.

Sample Id: PCPS1
Outgas Time /Temp
Submitter/Operator BCW
File Name: A:\PCPS1.SMP

Started: 9/17/2003 11:15:49AM Analysis Adsorptive: N2
Completed: 9/17/2003 2:20:17PM Analysis Bath: 77.19 K
Report Time: 9/18/2003 10:00:26AM Thermal Correction: No
Sample Weight: 0.1100 g Smoothed Pressures: No
Warm Freespace: 27.9452 cm³ ENTERED Cold Freespace: 89.2064 cm³
Equil. Interval: 10 secs Low Pressure Dose: None

BJH Desorption Pore Distribution Report

t = 3.5400 x [-5.0000 / ln(P/Po)]0.3330

Diameter Range: 17.0000 to 3000.0000 A
Adsorbate Property Factor: 9.530000 A
Density Conversion Factor: 0.001547
Fraction of Pores Open at Both Ends: 0.000

Pore Diameter Range (A)	Average Diameter (A)	Incremental Pore Volume (cm³/g)	Cumulative Pore Volume (cm³/g)	Incremental Pore Area (m²/g)	Cumulative Pore Area (m²/g)
16110.3- 779.3	813.0	0.003996	0.003996	0.197	0.197
779.3- 297.3	355.9	0.001389	0.005385	0.156	0.353
297.3- 215.5	243.3	0.000827	0.006212	0.136	0.489
215.5- 168.8	186.4	0.000687	0.006898	0.147	0.636
168.8- 138.4	150.5	0.000637	0.007535	0.169	0.805
138.4- 117.1	125.9	0.000779	0.008315	0.248	1.053
117.1- 101.1	107.8	0.000608	0.008922	0.225	1.278
101.1- 88.6	94.0	0.000539	0.009462	0.230	1.508
88.6- 70.7	77.6	0.000721	0.010183	0.372	1.879
70.7- 58.1	63.1	0.001140	0.011322	0.722	2.601
58.1- 48.7	52.6	0.001144	0.012466	0.870	3.471
48.7- 41.6	44.6	0.001241	0.013707	1.113	4.584
41.6- 35.8	38.3	0.001071	0.014778	1.119	5.704
35.8- 31.1	33.1	0.001325	0.016103	1.601	7.304
31.1- 27.0	28.8	0.001148	0.017251	1.597	8.901
27.0- 23.5	25.0	0.001105	0.018356	1.765	10.666
23.5- 20.5	21.8	0.001234	0.019591	2.264	12.930
20.5- 17.7	18.9	0.001039	0.020630	2.202	15.132

Figure B-13. BJH desorption pore distribution report.

```
          Sample Id: PCPS1
    Outgas Time /Temp
  Submitter/Operator  BCW
          File Name: A:\PCPS1.SMP

            Started: 9/17/2003 11:15:49AM Analysis Adsorptive: N2
          Completed: 9/17/2003 2:20:17PM        Analysis Bath: 77.19 K
        Report Time: 9/18/2003 10:00:26AM  Thermal Correction: No
      Sample Weight: 0.1100 g              Smoothed Pressures: No
     Warm Freespace: 27.9452 cm³  ENTERED      Cold Freespace: 89.2064 cm³
    Equil. Interval: 10 secs                Low Pressure Dose: None
```

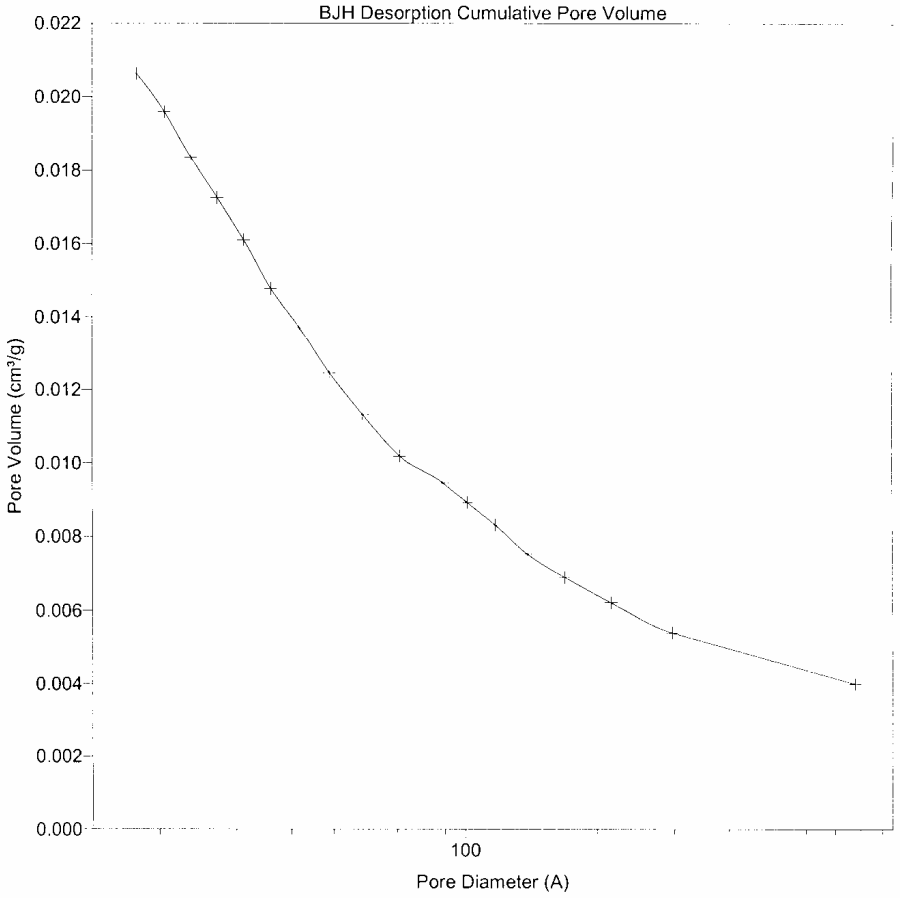

Figure B-14. BJH desorption cumulative pore volume.

```
          Sample Id: PCPS1
    Outgas Time /Temp
  Submitter/Operator  BCW
          File Name: A:\PCPS1.SMP

            Started: 9/17/2003 11:15:49AM Analysis Adsorptive: N2
          Completed: 9/17/2003 2:20:17PM       Analysis Bath: 77.19 K
        Report Time: 9/18/2003 10:00:26AM  Thermal Correction: No
      Sample Weight: 0.1100 g              Smoothed Pressures: No
     Warm Freespace: 27.9452 cm³  ENTERED      Cold Freespace: 89.2064 cm³
     Equil. Interval: 10 secs               Low Pressure Dose: None
```

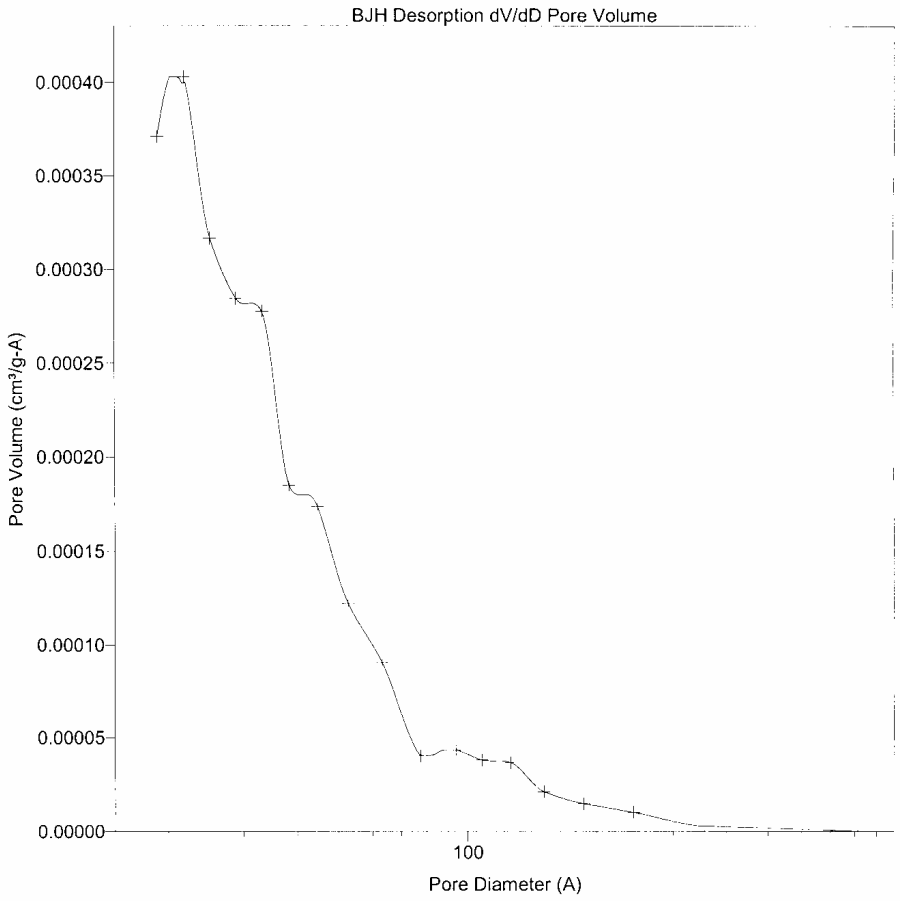

Figure B-15. BJH desorption dV/dD pore volume.

```
          Sample Id: PCPS1
    Outgas Time /Temp
  Submitter/Operator  BCW
          File Name: A:\PCPS1.SMP

            Started: 9/17/2003 11:15:49AM Analysis Adsorptive: N2
          Completed: 9/17/2003 2:20:17PM        Analysis Bath: 77.19 K
        Report Time: 9/18/2003 10:00:26AM  Thermal Correction: No
      Sample Weight: 0.1100 g              Smoothed Pressures: No
     Warm Freespace: 27.9452 cm³  ENTERED      Cold Freespace: 89.2064 cm³
    Equil. Interval: 10 secs                Low Pressure Dose: None
```

Options Report

Adsorptive Properties

```
                        Adsorptive: Nitrogen @ 77.35 K
             Maximum manifold pressure: 925.00 mmHg
                   Non-ideality factor: 0.000066
             Density conversion factor: 0.0015468
      Therm. tran. hard-sphere diameter: 3.860 A
         Molecular cross-sectional area: 0.162 nm²
```

Analysis Conditions

Analysis preparation options:

```
                      Fast evacuation: Yes
                      Evacuation time: 0.50 hours
                            Leak test: No
```

Free Space

```
                     Free space group: Entered
                      Warm free space: 27.9452 cm³
                      Cold free space: 89.2064 cm³
```

Equilibration options:

```
                Equilibration interval: 10 secs
  Min. equil. delay at P/Po >= 0.995: 600 secs
```

Sample backfill options:

```
       Backfill at start of analysis:Yes
         Backfill at end of analysis:Yes
                       Backfill Gas:Analysis gas
```

Target pressure options:

```
       Use first pressure fixed dose:No
        Use maximum volume increment: No
                    Target tolerance: 5.0 %  or 5.0 mmHg
                  Low pressure dosing: No
```

Po and Temperature options:

Figure B-16. Option report.

Full Report Set

ASAP 2010 V5.02 C Unit 1 Serial # 631 Page 17

Sample Id: PCPS1
Outgas Time /Temp
Submitter/Operator BCW
File Name: A:\PCPS1.SMP

Started: 9/17/2003 11:15:49AM Analysis Adsorptive: N2
Completed: 9/17/2003 2:20:17PM Analysis Bath: 77.19 K
Report Time: 9/18/2003 10:00:26AM Thermal Correction: No
Sample Weight: 0.1100 g Smoothed Pressures: No
Warm Freespace: 27.9452 cm³ ENTERED Cold Freespace: 89.2064 cm³
Equil. Interval: 10 secs Low Pressure Dose: None

Options Report

Po type: Measured
Temperature type: Calculated from measured Psat
Measurement interval: 120 minutes

Inside diameter of sample tube: 9.530 mm

Figure B-17. Option report.

Sample Id: PCPS1
Outgas Time /Temp
Submitter/Operator BCW
File Name: A:\PCPS1.SMP

Started: 9/17/2003 11:15:49AM Analysis Adsorptive: N2
Completed: 9/17/2003 2:20:17PM Analysis Bath: 77.19 K
Report Time: 9/18/2003 10:00:26AM Thermal Correction: No
Sample Weight: 0.1100 g Smoothed Pressures: No
Warm Freespace: 27.9452 cm^3 ENTERED Cold Freespace: 89.2064 cm^3
Equil. Interval: 10 secs Low Pressure Dose: None

Summary Report

Area

Single Point Surface Area at P/Po 0.20035152 : 13.7880 m^2/g

Volume

Single Point Adsorption Total Pore Volume of pores less than 844.1368 A Diameter at P/Po 0.97651752: 0.020443 cm^3/g

Pore Size

Adsorption Average Pore Diameter (4V/A by BET): 34.4095 A

Figure B-18. Summary report.

APPENDIX C

SQUID MEASUREMENT DATA

The constant-current van der Pauw technique was used to measure the resistivity where four isolated contacts (referred to 1, 2, 3, and 4) were placed on the periphery of the sample. The resistivity was determined by the formula in ASTM Method F76:

$$\rho = \frac{\rho_A + \rho_B}{2} \qquad \text{(C1)}$$

$$\rho_A = \frac{\pi}{4 \ln 2} \cdot \frac{f_A d}{I} \left[V_{21,34} - V_{12,34} + V_{32,41} - V_{23,41} \right] \qquad \text{(C2)}$$

$$\rho_B = \frac{\pi}{4 \ln 2} \cdot \frac{f_B d}{I} \left[V_{43,12} - V_{34,12} + V_{14,23} - V_{41,23} \right] \qquad \text{(C3)}$$

where ρ is the calculated resistivity [Ω cm], f the geometrical factor (assumed to be unity in this work), d the film thickness [cm], I the current magnitude [A], $V_{ij,kl}$ the measured potential difference between contact k and contact l when current enters contact i and exits contact j [V]. A total of eight measurements were made at one temperature to yield the averaged resistivity of the sample as shown in Figure C-1.

The thickness of the composites was 0.155 cm, 0.330 cm, 0.305 cm for PPy + $FeCl_3$ in PCPS, PPy + I_2 in PCPS, and PPy + I_2 in PMMA, respectively. The measured resistance of the composites is presented as a function of temperature below.

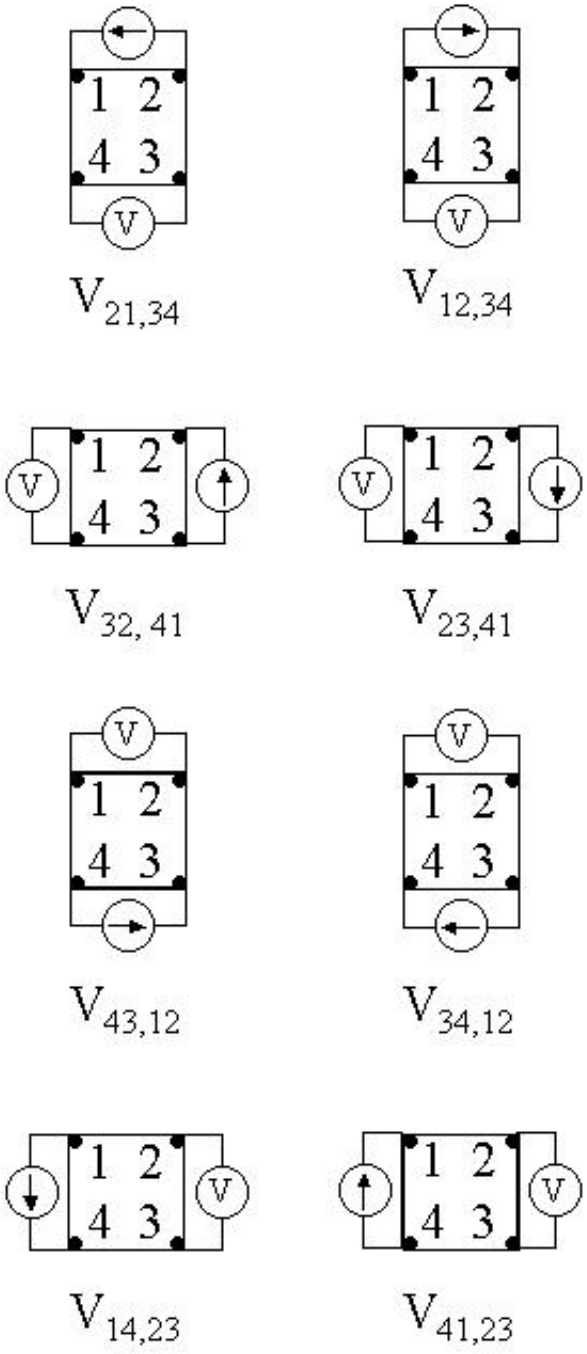

Figure C-1. van der Pauw resistivity measurement conventions.

Table C-1. Temperature dependence of conductivity in PPy + $FeCl_3$ in PCPS.

Temperature [K]	Resistivity [Ohm cm]	Conductivity [S/cm]
90.00	2.046009E+06	4.887563E-07
95.00	1.449987E+06	6.896615E-07
100.00	8.936961E+05	1.118949E-06
105.00	5.535937E+05	1.806379E-06
110.00	3.190815E+05	3.133996E-06
115.00	3.474655E+05	2.877983E-06
120.00	1.933644E+05	5.171584E-06
125.00	1.652548E+05	6.051261E-06
130.00	9.889770E+04	1.011146E-05
135.00	6.774563E+04	1.476110E-05
140.00	5.847671E+04	1.710083E-05
145.00	4.714981E+04	2.120899E-05
150.00	3.928751E+04	2.545338E-05
155.01	2.644492E+04	3.781444E-05
160.00	2.457141E+04	4.069771E-05
165.00	1.674814E+04	5.970813E-05
170.01	1.523017E+04	6.565916E-05
175.01	1.344241E+04	7.439141E-05
180.00	1.015900E+04	9.843492E-05
185.00	8.048110E+03	1.242528E-04
190.00	7.993826E+03	1.250965E-04
195.01	6.179680E+03	1.618207E-04
200.00	4.903278E+03	2.039452E-04
205.01	3.067231E+03	3.260269E-04
210.00	2.629288E+03	3.803311E-04
215.00	2.421900E+03	4.128990E-04
219.99	2.372619E+03	4.214752E-04
225.00	2.324002E+03	4.302923E-04
230.00	1.888914E+03	5.294048E-04
235.00	1.693400E+03	5.905280E-04
240.00	1.738843E+03	5.750951E-04
245.00	9.899252E+02	1.010177E-03
250.01	8.954350E+02	1.116776E-03
255.01	6.635226E+02	1.507108E-03
260.01	8.533541E+02	1.171847E-03
264.99	6.174795E+02	1.619487E-03
270.00	4.972660E+02	2.010996E-03
275.00	5.083754E+02	1.967051E-03
280.01	4.200836E+02	2.380478E-03
285.02	2.583990E+02	3.869985E-03
290.01	2.634465E+02	3.795837E-03
294.98	2.137425E+02	4.678526E-03
300.01	2.142195E+02	4.668110E-03

Table C-2. Temperature dependence of conductivity in PPy + I_2 in PCPS.

Temperature [K]	Resistivity [Ohm cm]	Conductivity [S/cm]
90.00	5.906875E+06	1.692943E-07
95.00	2.826415E+06	3.538051E-07
100.00	2.200750E+06	4.543906E-07
105.00	1.567435E+06	6.379851E-07
110.00	8.696097E+05	1.149941E-06
115.00	6.089830E+05	1.642082E-06
120.00	4.496276E+05	2.224063E-06
125.00	2.599694E+05	3.846606E-06
130.00	1.440610E+05	6.941505E-06
135.00	2.152639E+05	4.645461E-06
140.01	1.405082E+05	7.117024E-06
145.00	8.538902E+04	1.171111E-05
150.00	4.257591E+04	2.348746E-05
155.00	4.096501E+04	2.441108E-05
160.00	2.854868E+04	3.502789E-05
165.01	2.034118E+04	4.916136E-05
170.00	1.545312E+04	6.471185E-05
175.01	1.374989E+04	7.272788E-05
180.00	7.767771E+03	1.287371E-04
185.01	7.723838E+03	1.294693E-04
190.00	7.632158E+03	1.310245E-04
195.00	5.883296E+03	1.699727E-04
200.01	5.237031E+03	1.909479E-04
205.00	4.477823E+03	2.233228E-04
209.99	4.138114E+03	2.416560E-04
215.00	2.928334E+03	3.414911E-04
220.00	2.862030E+03	3.494024E-04
225.00	2.075372E+03	4.818414E-04
230.00	1.382973E+03	7.230798E-04
235.00	1.146718E+03	8.720542E-04
240.00	1.165263E+03	8.581754E-04
245.00	1.000170E+03	9.998298E-04
250.00	7.355581E+02	1.359512E-03
255.00	6.621608E+02	1.510207E-03
260.01	7.645470E+02	1.307964E-03
264.99	7.249480E+02	1.379409E-03
270.00	5.936631E+02	1.684457E-03
275.00	5.289445E+02	1.890558E-03
280.01	4.012262E+02	2.492360E-03
285.01	6.449424E+02	1.550526E-03
290.00	3.345801E+02	2.988821E-03
295.02	4.566339E+02	2.189938E-03
300.00	6.405178E+02	1.561237E-03

Table C-3. Temperature dependence of conductivity in PPy + I_2 in PMMA.

Temperature [K]	Resistivity [Ohm cm]	Conductivity [S/cm]
90.00	1.762676E+04	5.673192E-05
95.00	8.642938E+03	1.157014E-04
100.00	9.054212E+03	1.104458E-04
105.00	3.931670E+03	2.543449E-04
110.00	4.203440E+03	2.379004E-04
115.00	4.305798E+03	2.322450E-04
120.00	3.573612E+03	2.798289E-04
125.00	3.305502E+03	3.025260E-04
130.00	3.227559E+03	3.098317E-04
135.00	2.156123E+03	4.637954E-04
140.01	3.075342E+03	3.251670E-04
145.00	2.273368E+03	4.398759E-04
150.00	1.696278E+03	5.895261E-04
155.00	2.434723E+03	4.107244E-04
160.00	1.959620E+03	5.103029E-04
165.01	1.202960E+03	8.312829E-04
170.00	1.410422E+03	7.090076E-04
175.01	1.359871E+03	7.353636E-04
180.00	1.250806E+03	7.994845E-04
185.01	1.245261E+03	8.030443E-04
189.99	9.937553E+02	1.006284E-03
195.00	8.819740E+02	1.133820E-03
200.00	7.435470E+02	1.344905E-03
205.00	7.383535E+02	1.354365E-03
210.00	3.329023E+02	3.003884E-03
215.00	4.998444E+02	2.000623E-03
220.00	4.037997E+02	2.476475E-03
225.00	3.889924E+02	2.570744E-03
230.01	3.952446E+02	2.530079E-03
235.00	3.960690E+02	2.524812E-03
239.99	4.024557E+02	2.484745E-03
245.01	3.513725E+02	2.845982E-03
250.00	2.373373E+02	4.213412E-03
255.00	2.638368E+02	3.790222E-03
260.00	2.809331E+02	3.559566E-03
265.00	1.947072E+02	5.135917E-03
270.01	1.129183E+02	8.855964E-03
275.00	1.185174E+02	8.437578E-03
280.00	1.089154E+02	9.181437E-03
284.98	9.789103E+01	1.021544E-02
290.00	1.284766E+02	7.783516E-03
295.01	9.972063E+01	1.002801E-02
300.00	7.722499E+01	1.294918E-02

APPENDIX D

THERMOGRAVIMETRIC MEASUREMENT DATA

A Seiko Instruments Model TG/DTA 320 was utilized under nitrogen flow of 250 mL/min. The reference was an empty aluminum pan, and a small amount of fractured samples (5-15 mg) was placed in a sample aluminum pan. The temperature scan started from room temperature to 823 K, and the heating rate was set at 20 K/min. The weight data were converted into percentage of residual with respective to the initial weight. Selected data as a function of temperature every 10 K are listed in Table D-1. The onset temperature of decomposition is defined as a cross point of tangent lines before and after a steep weight change is observed.

Table D-1. Selected thermogravimetric data.

PMMA		PPy + I2 in PMMA		PCPS		PPy + I2 in PCPS		PPy + FeCl3 in PCPS	
Temperature [K]	Residual [wt.%]	Temperature [K]	Residual [wt.%]	Temperature [K]	Residual [wt.%]	Temperature [K]	Residual [wt.%]	Temperature [K]	Residual [wt.%]
300.98	100.00	301.10	100.00	301.21	100.00	301.13	100.00	301.17	100.00
310.11	100.02	310.05	100.02	310.04	100.11	310.02	99.90	310.12	99.89
320.11	100.02	320.12	100.01	320.13	100.04	320.22	99.56	320.09	99.64
330.27	100.01	330.24	99.99	330.15	100.02	330.18	99.18	330.13	99.37
340.25	100.00	340.13	99.96	340.26	99.99	340.13	98.85	340.15	99.10
350.31	99.98	350.12	99.89	350.05	99.93	350.03	98.57	350.07	98.86
360.16	99.96	360.01	99.82	360.30	99.85	360.18	98.37	360.11	98.67
370.31	99.94	370.18	99.73	370.17	99.81	370.26	98.21	370.18	98.53
380.20	99.91	380.12	99.61	380.09	99.76	380.10	98.06	380.23	98.44
390.29	99.88	390.31	99.42	390.24	99.66	390.10	97.94	390.19	98.31
400.18	99.83	400.14	99.20	400.02	99.58	400.12	97.82	400.05	98.16
410.20	99.78	410.16	98.91	410.30	99.45	410.28	97.60	410.04	98.03
420.37	99.73	420.31	98.56	420.15	99.30	420.15	97.28	420.28	97.87
430.12	99.68	430.31	98.14	430.31	99.05	430.37	96.81	430.19	97.63
440.05	99.63	440.14	97.65	440.32	98.75	440.31	96.16	440.22	97.42
450.30	99.56	450.10	96.84	450.24	98.43	450.27	95.32	450.18	97.15
460.27	99.51	460.19	94.66	460.27	98.13	460.23	94.26	460.02	96.90
470.37	99.44	470.04	91.90	470.04	97.75	470.28	93.01	470.29	96.60
480.02	99.37	480.22	89.19	480.24	97.33	480.07	91.64	480.17	96.30
490.02	99.29	490.26	86.99	490.24	96.85	490.13	90.08	490.32	95.98
500.09	99.20	500.26	85.13	500.25	96.23	500.27	88.39	500.28	95.61
510.08	99.09	510.07	83.44	510.18	95.67	510.31	86.52	510.08	95.27
520.30	98.92	520.06	82.04	520.07	95.00	520.35	84.42	520.38	94.83
530.17	98.55	530.08	80.97	530.08	94.45	530.00	82.10	530.27	94.47
540.29	97.72	540.24	80.07	540.08	93.84	540.03	79.35	540.11	94.02
550.32	96.43	550.23	79.16	550.13	93.23	550.13	76.37	550.28	93.61
560.04	94.36	560.12	77.79	560.27	92.58	560.10	73.91	560.16	93.14
570.14	91.80	570.09	76.40	570.01	91.79	570.27	72.07	570.20	92.71
580.05	88.95	580.07	75.11	580.04	90.96	580.24	70.63	580.27	92.26
590.09	85.72	590.04	73.67	590.11	89.95	590.05	69.41	590.24	91.79
600.14	82.03	600.07	72.25	600.18	88.83	600.34	68.28	600.24	91.36
610.27	77.40	610.38	71.08	610.25	87.45	610.16	67.17	610.27	90.86
620.33	71.63	620.30	70.16	620.16	85.74	620.12	65.82	620.21	90.37
630.22	64.81	630.24	69.30	630.29	83.45	630.16	63.95	630.11	89.87
640.04	56.11	640.20	68.28	640.31	80.42	640.17	61.40	640.27	89.26
650.04	43.76	650.10	66.70	650.30	76.21	650.17	58.11	650.02	88.64
660.09	28.85	660.22	64.15	660.24	70.40	660.14	54.13	660.14	87.79
670.03	15.46	670.20	59.82	670.21	62.28	670.10	49.62	670.03	86.67
680.53	6.31	680.20	51.44	680.21	51.87	680.01	45.06	680.05	85.06
690.32	2.55	690.27	42.15	690.07	39.97	690.31	40.76	690.31	82.23

Table D-1. Selected TG data (continued).

PMMA		PPy + I2 in PMMA		PCPS		PPy + I2 in PCPS		PPy + FeCl3 in PCPS	
Temperature [K]	Residual [wt.%]	Temperature [K]	Residual [wt.%]	Temperature [K]	Residual [wt.%]	Temperature [K]	Residual [wt.%]	Temperature [K]	Residual [wt.%]
700.07	0.68	700.16	30.76	700.23	27.98	700.24	37.51	700.25	77.38
710.08	-0.03	710.10	20.75	710.02	17.94	710.13	35.37	710.11	68.56
720.07	-0.06	720.12	12.55	720.34	10.04	720.23	34.20	720.07	57.40
730.09	-0.07	730.35	8.14	730.26	5.61	730.33	33.61	730.28	50.18
740.03	-0.08	740.01	7.19	740.27	3.47	740.01	33.21	740.26	46.94
750.23	-0.08	750.29	6.87	750.05	2.89	750.03	32.83	750.10	45.80
760.16	-0.08	760.30	6.67	760.24	2.66	760.11	32.49	760.13	45.28
770.12	-0.08	770.21	6.50	770.01	2.54	770.09	32.20	770.02	44.92
780.21	-0.08	780.09	6.37	780.15	2.48	780.12	31.89	780.22	44.56
790.00	-0.09	790.25	6.24	790.21	2.40	790.17	31.63	790.35	44.24
800.16	-0.09	800.09	6.12	800.30	2.34	800.14	31.36	800.22	43.99
810.19	-0.09	810.10	6.02	810.31	2.29	810.11	31.09	810.35	43.74
820.17	-0.09	820.18	5.91	820.30	2.20	820.09	30.85	820.28	43.50
830.25	-0.09	830.18	5.82	830.06	2.22	830.25	30.59	830.20	43.22
834.58	-0.09	832.72	5.80	834.69	2.15	840.05	30.22	839.76	42.77

APPENDIX E

TENSILE MEASUREMENT DATA

A uniaxial electromechanical testing device (TestResources, Model 650R) was used to measure the relationship between stress and strain of the PCPS substrate and its composite. Square specimens were cut out of the samples, and their initial dimensions were measured using a caliper. A preload of 5 N was applied to the samples before initiating compression testing at a rate of 0.5 mm/min. Samples were tested to a strain endpoint of 50 % of initial thickness. The stress-strain relationship of the sample was calculated from the measured load-displacement data and sample dimensions as follows:

$$\sigma = \frac{F}{S} \tag{F-1}$$

$$\delta = \frac{D}{d} \tag{F-2}$$

where σ is the stress [MPa], F the measured load [N], S the cross-sectional area of the sample [mm^2], δ the strain [-], D the measured displacement [mm], d the thickness of the sample [mm]. The sample dimensions are listed in Table E-1, and the calculated stress as a function of strain every 0.01 is listed in Table E-2. The yield point of the substrate was determined to be the intercept of two straight lines that are tangent to the stress-strain curve before and after yield. Compressive modulus was also determined from the largest slope in the linear elastic region of the stress-strain curve. The tangent lines are shown in Figure E-1.

Table E-1. Sample dimensions.

	Cross-sectional Area [mm^2]	Thickness [mm]
PCPS	95.6370	3.62
PPy + I_2	154.5048	1.56
PPy + $FeCl_3$	94.4965	2.73

Table E-2. Selected stress-strain data.

PCPS		PPy + I_2		PPy + $FeCl_3$	
Strain	Stress [MPa]	Strain	Stress [MPa]	Strain	Stress [MPa]
0.0100	0.0231	0.0103	0.0091	0.0100	0.0437
0.0200	0.0409	0.0201	0.0214	0.0201	0.0891
0.0300	0.0640	0.0300	0.0371	0.0300	0.1425
0.0401	0.0922	0.0401	0.0537	0.0401	0.2002
0.0501	0.1291	0.0500	0.0683	0.0501	0.2538
0.0600	0.1738	0.0602	0.0901	0.0600	0.3257
0.0700	0.2226	0.0701	0.1178	0.0700	0.4099
0.0801	0.2856	0.0800	0.1453	0.0800	0.5152
0.0900	0.3431	0.0900	0.1642	0.0900	0.6257
0.1000	0.4208	0.1001	0.1759	0.1001	0.7428
0.1100	0.5150	0.1100	0.1988	0.1101	0.8217
0.1201	0.6171	0.1202	0.2270	0.1200	0.9281
0.1300	0.7195	0.1300	0.2542	0.1300	1.1033
0.1401	0.7829	0.1402	0.2828	0.1401	1.2792
0.1501	0.8517	0.1501	0.3101	0.1500	1.4583
0.1600	0.9545	0.1601	0.3363	0.1600	1.6403
0.1700	1.0835	0.1702	0.3608	0.1700	1.8317
0.1801	1.2173	0.1800	0.3838	0.1800	2.0330
0.1900	1.3552	0.1902	0.4080	0.1900	2.2470
0.2000	1.4846	0.2001	0.4246	0.2000	2.4703
0.2101	1.6076	0.2102	0.4483	0.2100	2.6982
0.2200	1.7252	0.2202	0.4680	0.2200	2.9182
0.2300	1.8289	0.2300	0.4883	0.2300	3.1408
0.2401	1.9234	0.2402	0.5272	0.2401	3.3682
0.2500	2.0107	0.2500	0.5674	0.2501	3.5852
0.2600	2.0808	0.2602	0.6150	0.2600	3.8007
0.2700	2.1395	0.2700	0.6654	0.2700	4.0223
0.2801	2.1921	0.2800	0.7178	0.2801	4.2427
0.2901	2.2300	0.2902	0.7721	0.2900	4.4468
0.3000	2.2606	0.3000	0.8257	0.3000	4.6484
0.3101	2.2832	0.3101	0.8842	0.3101	4.8530
0.3200	2.3066	0.3201	0.9435	0.3201	5.0610
0.3300	2.3338	0.3301	1.0046	0.3300	5.2569
0.3400	2.3633	0.3403	1.0657	0.3401	5.4449
0.3501	2.3844	0.3501	1.1295	0.3500	5.6325
0.3600	2.4089	0.3600	1.1950	0.3601	5.8177
0.3701	2.4321	0.3703	1.2643	0.3700	5.9958
0.3800	2.4560	0.3800	1.3317	0.3801	6.1691
0.3901	2.4799	0.3902	1.4040	0.3900	6.3333
0.4000	2.5023	0.4002	1.4775	0.4000	6.4803
0.4100	2.5336	0.4101	1.5552	0.4101	6.6289
0.4200	2.5608	0.4203	1.6370	0.4200	6.7437
0.4300	2.5833	0.4302	1.7156	0.4300	6.8451
0.4400	2.6109	0.4402	1.7970	0.4400	6.9491

Table E-2. Selected stress-strain data (continued).

PCPS		PPy + I_2		PPy + $FeCl_3$	
Strain	Stress [MPa]	Strain	Stress [MPa]	Strain	Stress [MPa]
0.4500	2.6384	0.4500	1.8785	0.4500	7.0611
0.4601	2.6644	0.4602	1.9663	0.4601	7.1712
0.4695	2.6972	0.4700	2.0533	0.4700	7.2794
		0.4803	2.1450	0.4801	7.3924
		0.4901	2.2353	0.4900	7.5045
		0.5001	2.3294	0.5001	7.6096

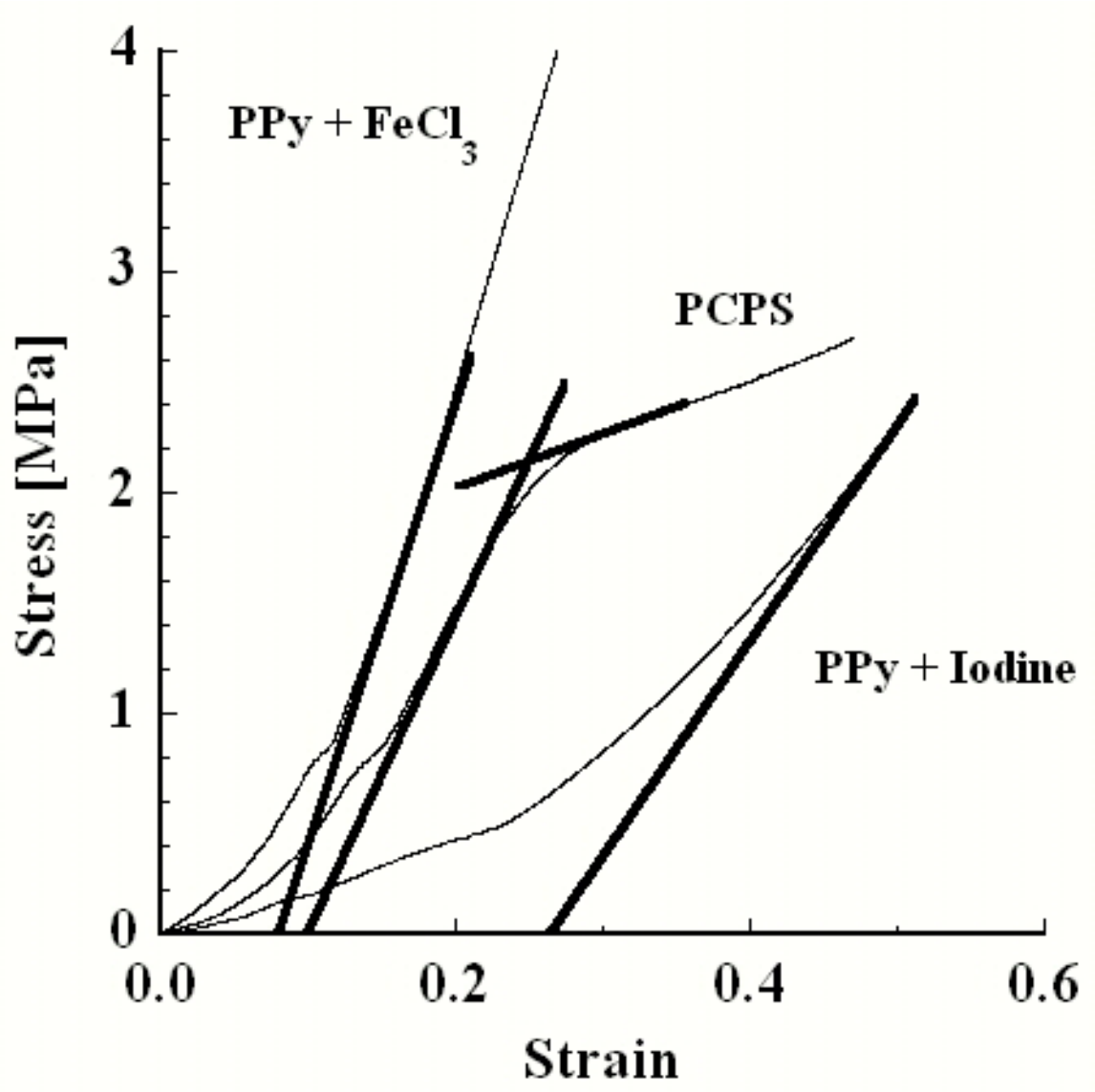

Figure E-1. Tangent lines for yield point and Young's Modulus.

APPENDIX F

FITTING PROGRAMS

Data fitting was conducted by a non-linear optimization technique using the C programming language. In this work, the Rosenbrock method (Rosenbrock, 1960) was adopted to optimize parameters in fitting functions for the minimization of the difference in input data and calculated values. One of the advantages is that the technique does not require a derivative of an objective function that would be necessary in most optimization models. The Gram-Schmit process was used for the orthonormalization of vectors to calculate the best solution in parametric fields.

The programs consists of main.c, sub.c, and header.h files. The main file contains main, conditional, and output functions with input data. The subroutine file includes the multidimensional objective and vector-rotational functions. In the header file, symbolic constants and function protocols are defined. The compile, linking, and execution of the programs were conducted on a Microsoft Visual C++ 6.0 software. As an example, the fitting programs and resulted output are presented in the following pages.

main.c

```
//*************************************************************************
*************************//
//
// Rosenbrock method
//
// Find p[N] to minimize f(p[N])
//
// N (# of parameters) is defined in "header.h" --> "Rebuit All" if you change any in the
file
//
// Fitting Function is defined in "sub.c"       --> Copy it to char fit[] in this file
//
//*************************************************************************
*************************//

#include <stdio.h>
#include <stdlib.h>
#include <string.h>
#include <math.h>
#include "header.h"

int main(void)
{
        // ### FITTING FUNCTION ###
        char fit[]="y=-2.5+(-17.+2.5)/(1.+exp(p[0]*(x-.04)))";

        // ### DATA INPUT ###
        const double yexp[]={-5.108969701,-8.015663813,-3.021169997,-6.032263074,-
2.897190463,-3.766489826,-1.903523049,-2.483423848,-3.634323066,-2.304127449,-
1.870061876,-2.948168325,-2.835079812,-4.17709664,-2.374137057,-1.978665376,-
2.182393853,-2.558957023,-2.991999894,-2.862637858,-1.895089881,-2.362017221,-
2.473668777,-2.78835509,-2.181879438,-3.438134852,-5.879836215,-8.655607726,-
5.632249213,-6.077890595,-3.838385007,-5.375290813,-2.384961752,-3.869326226,-
5.324309948,-3.495304078,-3.624223351,-1.911870882,-2.330449756,-2.674926654,-
3.196058278,-3.171160179,-2.963098199,-3.178619732,-2.945740524,-4.817274329,-
3.000163056,-2.418595839,-3.149600863,-5.594900491,-2.797752357,-5.274735642};
        const double xexp[]={0.041019956,0.045310016,0.065905097,
0.092821782,0.100677201,0.141299194,0.168051708,0.195809831,0.207026349,
0.214285714,0.238827839,0.239302694,0.243616287,0.249375,0.263480392,0.2681623
93,0.272082879,0.277948718,0.279639175,0.28436019,0.289042821,0.305595409,0.369
248036,0.399148936,0.400925212,0.431770469,0.041019956,0.045310016,0.065905097
,0.092821782,0.100677201,0.141299194,0.168051708,0.195809831,0.207026349,0.2142
85714,0.238827839,0.239302694,0.243616287,
```

```
0.249375,0.263480392,0.268162393,0.272082879,0.277948718,0.279639175,0.2843601
9,0.289042821,0.305595409,0.369248036,0.399148936,0.400925212,0.431770469};

        // ### DEFAULT FILE NAME ###
        char def[]="test.txt";
        FILE *fp;
        char buf[MAXCHARS+1], *fname;
        int i=0,j,k,m,flag,YEXP;
        int icar[N];
        double pini=0.0, sini=0.1, pnorm, f, f0, ycal;
        double p[N], p0[N], p1[N], s[N], s0[N], d[N], bnorm[N];
        double t[N][N], a[N][N], b[N][N];

        // Data Consistency Check
        YEXP=sizeof(yexp)/sizeof(yexp[0]);
        if(YEXP != sizeof(xexp)/sizeof(xexp[0])) {printf("# of data not
consistent!\n");exit(1);}

        // File Output
        printf("Input the file name (< %d characters)\nPress return for
default:",MAXCHARS);
        gets(buf);
        if(strlen(buf) != 0)
        {
                fname=(char *)malloc(strlen(buf)+1);
                strcpy(fname,buf);
        }
        else
        {
                fname=(char *)malloc(strlen(def)+1);
                strcpy(fname,def);
        }

        // OPEN THE OUTPUT FILE
        if(!(fp=fopen(fname,"w"))){printf("\nCan't open the file %s \n",fname);exit(1);}

        for(i=0;i<N;i++)
        {
                p0[i]=pini;
                s0[i]=sini;

                for(j=0;j<N;j++)
                {
                        t[j][i]=0.0;
                        if(i==j) t[j][i]=1.0;
                }
```

```
}

f0=.0;
for(i=0;i<YEXP;i++)
{
        ycal=f_p(p0,&xexp[i]);
        f0+=(yexp[i]-ycal)*(yexp[i]-ycal); // residual: yres+=(exp-calc)^2;
}
if(f0<EPSILON) // No parameter optimization
{
        i=0;j=0;pnorm=0.0;
        printf("\niteration(T=%d,S=%d)\nNorm in p's=%e\n",i,j,pnorm);
        fprintf(fp,"iteration(T=%d,S=%d)\nNorm in p's=%e\n",i,j,pnorm);
        printf("Residual in y's=%e\n\n",f0);
        fprintf(fp,"Residual in y's=%e\n\n",f0);
        printf("Fitting Function:\n%s\n\n",fit);
        fprintf(fp,"Fitting Function:\n%s\n\n",fit);
        for(i=0;i<N;i++) printf("p[%d]=%e\n",i,p0[i]);
        for(i=0;i<N;i++) fprintf(fp,"p[%d]=%e\n",i,p0[i]);
        printf("\n");
        fclose(fp);
        printf ("Output the datafile = %s \n\n",fname);
        return(0);
}

for(i=0;i<TMAX;i++)
{
        for(j=0;j<N;j++)
        {
                icar[j]=0;
                p1[j]=p0[j];
                s[j]=s0[j];
                d[j]=0.0;
        }

        for(j=0;j<SMAX;j++)
        {
                flag=1;

                for(k=0;k<N;k++)
                {
                        for(m=0;m<N;m++) p[m]=p0[m]+s[k]*t[m][k];
                        f=.0;
                        for(m=0;m<YEXP;m++)
                        {
                                ycal=f_p(p,&xexp[m]);
```

```
                                        f+=(yexp[m]-ycal)*(yexp[m]-ycal); // residual:
yres+=(exp-calc)^2;
                                }

                                if(f<f0)
                                {
                                        d[k]+=s[k];
                                        s[k]*=ALPHA;
                                        f0=f;
                                        for(m=0;m<N;m++) p0[m]=p[m];
                                        if(icar[k]==0) icar[k]=1;
                                }
                                else
                                {
                                        s[k]*=-BETA;
                                        if(icar[k]==1) icar[k]=2;
                                }
                                for(m=0;m<N;m++) if(icar[m]!=2) {flag=0;continue;}
                        }
                        if(flag) break; // break j-loop
                }

                pnorm=0.0;
                for(m=0;m<N;m++) pnorm+=(p0[m]-p1[m])*(p0[m]-p1[m]);
                pnorm=sqrt(pnorm);

                if(pnorm<EPSILON)
                {
                        printf("\niteration(T=%d,S=%d)\nNorm in p's=%e\n",i,j,pnorm);
                        fprintf(fp,"iteration(T=%d,S=%d)\nNorm in p's=%e\n",i,j,pnorm);
                        printf("Residual in y's=%e\n\n",f0);
                        fprintf(fp,"Residual in y's=%e\n\n",f0);
                        printf("Fitting Function:\n%s\n\n",fit);
                        fprintf(fp,"Fitting Function:\n%s\n\n",fit);
                        for(m=0;m<N;m++) printf("p[%d]=%e\n",m,p0[m]);
                        for(m=0;m<N;m++) fprintf(fp,"=%e\n",p0[m]);
                        printf("\n");
                        for(m=0;m<YEXP;m++)
fprintf(fp,"%f %f %f\n",xexp[m],yexp[m],-2.5+(-17.+2.5)/(1.+exp(p[0]*(xexp[m]-
.04))));
                        fclose(fp);
                        printf ("Output the datafile = %s \n\n",fname);
                        return(0);
                }
                if(j==SMAX) break;
                if(!(rotate(a,b,t,d,bnorm))) exit(0);
```

```
        }

        printf("\nError: iteration over MAX!\n");
        fprintf(fp,"Error: iteration over MAX!\n");
        printf("iteration(T=%d,S=%d)\nNorm in p's=%e\n",i,j,pnorm);
        fprintf(fp,"iteration(T=%d,S=%d)\nNorm in p's=%e\n",i,j,pnorm);
        printf("Residual in y's=%e\n\n",f0);
        fprintf(fp,"Residual in y's=%e\n\n",f0);
        printf("Fitting Function:\n%s\n\n",fit);
        fprintf(fp,"Fitting Function:\n%s\n\n",fit);
        for(i=0;i<N;i++) printf("p[%d]=%e\n",i,p0[i]);
        for(i=0;i<N;i++) fprintf(fp,"p[%d]=%e\n",i,p0[i]);
        printf("\n");

        // CLOSE THE OUTPUT FILE
        fclose(fp);
        printf ("Output the datafile = %s \n\n",fname);
        return(0);
}
// EOF
```

sub.c

```
// Header files
#include <stdio.h>
#include <stdlib.h>
#include <string.h>
#include <math.h>
#include "header.h"

//
// Subroutine functions
//
double f_p(double p[N],const double *xexp)
{
	double x,y;
	x=*xexp;

	// ### FITTING FUNCTION: Use p[]&x ###
	y=-2.5+(-17.+2.5)/(1.+exp(p[0]*(x-.04)));

	return y;
}
//
int rotate(double a[N][N],double b[N][N],double t[N][N],double d[N],double bnorm[N])
{
	int i,j,k,m;
	double work[2];

	for(i=0;i<N;i++)
	{
		for(k=0;k<N;k++)
		{
			a[k][i]=0.0;
			for(j=0;j<N;j++) a[k][i]+=d[j]*t[k][j];
		}
	}

	for(i=0;i<N;i++) b[i][0]=a[i][0];

	bnorm[0]=0.0;
	for(i=0;i<N;i++) bnorm[0]+=b[i][0]*b[i][0];
	bnorm[0]=sqrt(bnorm[0]);
	for(i=0;i<N;i++) t[i][0]=b[i][0]/bnorm[0];

	for(i=1;i<N;i++)
	{
```

```
                for(k=0;k<N;k++)
                {
                        work[1]=0.0;
                        for(j=0;j<i;j++)
                        {
                                work[0]=0.0;
                                for(m=0;m<N;m++) work[0]+=a[m][i]*t[m][j];
                                work[1]+=work[0]*t[k][j];
                        }
                        b[k][i]=a[k][i]-work[1];
                }
        }

        for(i=1;i<N;i++)
        {
                bnorm[i]=0.0;
                for(j=0;j<N;j++) bnorm[i]+=b[j][i]*b[j][i];
                if(bnorm[i]==0.0) bnorm[i]=1.0;
                bnorm[i]=sqrt(bnorm[i]);

                for(j=0;j<N;j++) t[j][i]+=b[j][i]/bnorm[i];
        }

        return(1);
}
//EOF
```

header.h

```
// header.h
#if defined( header_h )
#else
#define header_h

// Symbolic constants
#define N 1            // ### # of parameters to fit ###
#define EPSILON 1.0e-6  // ### Allowable error ###
#define SMAX 10000       // Iteration limits
#define TMAX 10000      // Iteration limits
#define ALPHA 3.0
#define BETA 0.5
#define MAXCHARS 80     // Limits of characters in file name

// Function prototype
double f_p(double p[N],const double *xexp);
int rotate(double a[N][N],double b[N][N],double t[N][N],double d[N],double bnorm[N]);

#endif
// EOF of header.h
```

test.txt

iteration(T=33,S=100000)
Norm in p's=2.980231e-009
Residual in y's=1.023008e+002

Fitting Function:
y=p[1]+p[0]*log10(x-.04)

=1.303717e+000
=-2.511928e+000
0.041020 -5.108970 -6.411892
0.045310 -8.015664 -5.477760
0.065905 -3.021170 -4.580425
0.092822 -6.032263 -4.177019
0.100677 -2.897190 -4.098519
0.141299 -3.766490 -3.808337
0.168052 -1.903523 -3.675645
0.195810 -2.483424 -3.564556
0.207026 -3.634323 -3.525197
0.214286 -2.304127 -3.501108
0.238828 -1.870062 -3.426515
0.239303 -2.948168 -3.425165
0.243616 -2.835080 -3.413041
0.249375 -4.177097 -3.397250
0.263480 -2.374137 -3.360336
0.268162 -1.978665 -3.348596
0.272083 -2.182394 -3.338950
0.277949 -2.558957 -3.324817
0.279639 -2.992000 -3.320809
0.284360 -2.862638 -3.309763
0.289043 -1.895090 -3.299016
0.305595 -2.362017 -3.262581
0.369248 -2.473669 -3.140941
0.399149 -2.788355 -3.091724
0.400925 -2.181879 -3.088931
0.431770 -3.438135 -3.042499
0.539092 -2.111560 -2.905415
0.550936 -3.630917 -2.892136
0.699495 -2.555576 -2.747625
0.719230 -2.108258 -2.730931
0.761044 -1.237513 -2.697105
0.835157 -2.304590 -2.641709
1.404240 -2.162001 -2.336068
2.136022 -1.625180 -2.092918
2.577147 -2.383013 -1.984775

0.041020 -5.879836 -6.411892
0.045310 -8.655608 -5.477760
0.065905 -5.632249 -4.580425
0.092822 -6.077891 -4.177019
0.100677 -3.838385 -4.098519
0.141299 -5.375291 -3.808337
0.168052 -2.384962 -3.675645
0.195810 -3.869326 -3.564556
0.207026 -5.324310 -3.525197
0.214286 -3.495304 -3.501108
0.238828 -3.624223 -3.426515
0.239303 -1.911871 -3.425165
0.243616 -2.330450 -3.413041
0.249375 -2.674927 -3.397250
0.263480 -3.196058 -3.360336
0.268162 -3.171160 -3.348596
0.272083 -2.963098 -3.338950
0.277949 -3.178620 -3.324817
0.279639 -2.945741 -3.320809
0.284360 -4.817274 -3.309763
0.289043 -3.000163 -3.299016
0.305595 -2.418596 -3.262581
0.369248 -3.149601 -3.140941
0.399149 -5.594900 -3.091724
0.400925 -2.797752 -3.088931
0.431770 -5.274736 -3.042499
0.539092 -3.886511 -2.905415
0.550936 -3.491655 -2.892136
0.699495 -3.268879 -2.747625
0.719230 -5.131232 -2.730931
0.761044 -0.692986 -2.697105
0.835157 -3.983529 -2.641709
1.404240 -3.892699 -2.336068
2.136022 -4.180761 -2.092918
2.577147 -3.565470 -1.984775

APPENDIX G

PRESSURE GAUGE CALIBRATION

A Heise pressure gauge (Model CM-51917) was used to measure the system pressure in the high-pressure experiments. The gauge was calibrated with a Budenberg dead-weight pressure gauge tester (Model 380H). According to the manual, the actual pressure of the dead-weight pressure tester, P_a, is given by:

$$P_a = P_n \frac{g}{9.80665}\left[1 + C(20 - T)\right]$$

where P_n is the nominal pressure, g is the gravitational acceleration at the calibration site, C is the temperature coefficient (2.3×10^{-5} for Model 380H), and T is the temperature in degrees Celsius. The temperature during the calibration was 24.1 degrees Celsius, and the local gravity was 9.795 m s^{-2}. The calibration data of the Heise pressure gauge with the dead-weight pressure gauge tester are shown in Table G-1. A least-square fit of the calibration data plotted in Figure G-1 was used to determine the actual pressure of the gauge. Note that the absolute pressure of the system is the sum of the actual pressure and atmospheric pressure.

Table G-1. Calibration data of Heise pressure gauge.

Pn [psi]	Pa [psi]	Model CM-51917 [psi]
10	10	10
200	200	200
50	50	50
1000	999	1004
100	100	100
2000	1997	2001
200	200	202
4000	3995	3999
300	300	302
400	399	403
500	499	503
600	599	604
700	699	704
800	799	803
900	899	904
1000	999	1003
1100	1099	1103
1200	1198	1204
1300	1298	1302
1400	1398	1405
1500	1498	1503
1600	1598	1603
1700	1698	1704
1800	1798	1803
1900	1898	1902
2000	1997	2001
2100	2097	2100
2200	2197	2200
2300	2297	2300
2400	2397	2400
2500	2497	2499
2600	2597	2598
2700	2697	2697
2800	2796	2798
2900	2896	2898
3000	2996	3000
3100	3096	3098
3200	3196	3199
3300	3296	3298

Table G-1. Calibration data of Heise pressure gauge (continued).

P_n [psi]	P_a [psi]	Model CM-51917 [psi]
3400	3396	3398
3500	3496	3499
3600	3595	3597
3700	3695	3698
3800	3795	3798
3900	3895	3897
4000	3995	3997
4100	4095	4096
4200	4195	4196
4300	4294	4296
4400	4394	4395

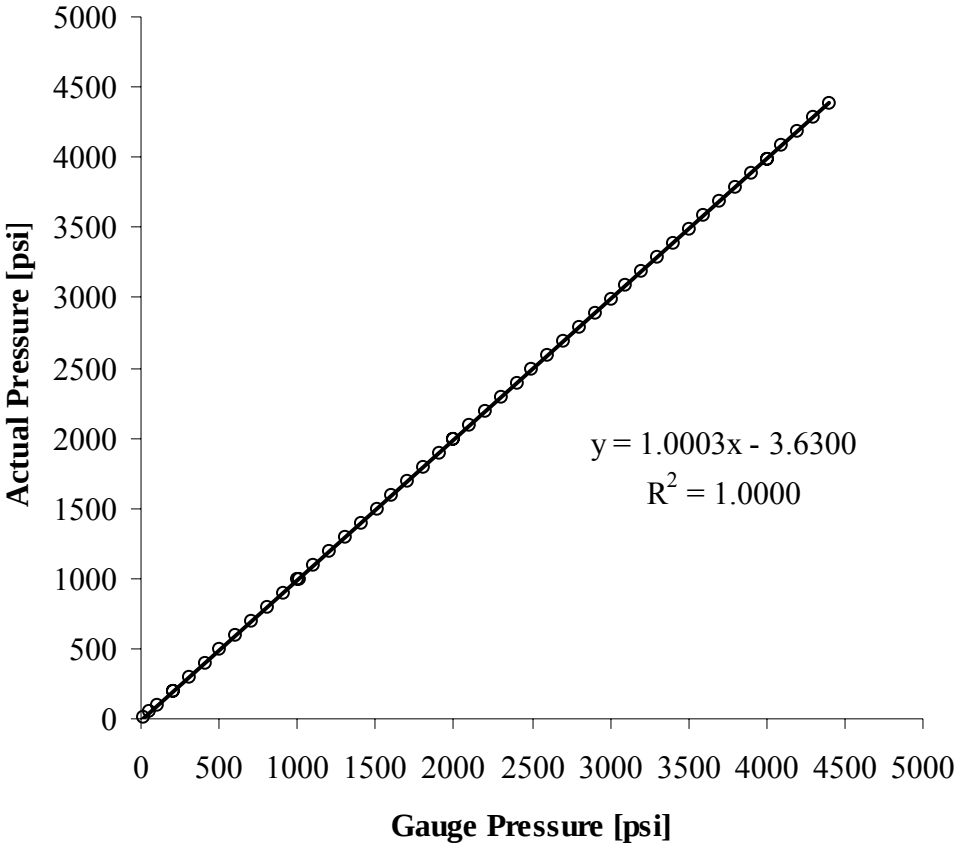

Figure G-1 Lease-square fit of the calibration data.

REFERENCES

Abbett, K. F.; Teja, A. S.; Kowalik, J.; Tolbert, L. "Polymerization of 3-Undecylbithiophene and Preparation of Poly(3-undecylbithiophene)/Polystyrene Composites in Supercritical Carbon Dioxide," *Macromolecules* 2003, 36, 3015-3019.

Aguilar-Hernandez, J.; Potje-Kamloth, K. "Evaluation of the Electrical Conductivity of Polypyrrole Polymer Composites," *Journal of Physics D, Applied Physics* 2001, 34, 1700-1711.

Ambegaokar, V.; Halperin, B. I.; Langer, J. S. "Hopping Conductivity in Disordered Systems," *Physical Review B* 1971, 4(8), 2612-2620.

Anderson, P. E.; Badlani, R. N.; Mayer, J.; Mabrouk, P. A. "Electrochemical Synthesis and Characterization of Conducting Polymers in Supercritical Carbon Dioxide," *Journal of the American Chemical Society* 2002, 124(35), 10284-10285.

Arbizzani, C.; Mastragostino, M.; Passerini, S.; Pillegi, R.; Scrosatt, B. "An Electrochromic Window Based on Polymethyl Thiophene and Nickel Oxide Electrodes," *Electrochimica Acta* 1991, 36(5/6), 837-840.

Arca, M.; Arca, E.; Yildiz, A.; Guven, O. "Thermal-Stability of Poly(pyrrole)," *Journal of Materials Science Letters* 1987, 6(9), 1013-1015.

Arora, K. A.; Lesser, A. J.; McCarthy, T. J. "Synthesis, Characterization, and Expansion of Poly(tetrafluoroethylene-*co*-hexafluoropropylene)/Polystyrene Blends Processed in Supercritical Carbon Dioxide," *Macromolecules* 1999, 32, 2562-2568.

Arora, K. A.; Lesser, A. J.; McCarthy, T. J. "Compressive Behavior of Microcellular Polystyrene Foams Processed in Supercritical Carbon Dioxide," *Polymer Engineering and Science* 1998, 38(12), 2055-2062.

Avlyanov, J. K.; Kuhn, H. H.; Josefowicz, J. Y.; MacDiarmid, A. G. "In-Situ Deposited Thin Films of Polypyrrole: Conformational Changes Induced by Variation of Dopant and Substrate Surface," *Synthetic Metals* 1997, 84, 153-154.

Baik, D. H.; Kim, G. L.; Park, Y. H.; Lee, Y.; Son, Y. "Effect of Polymer Blending on the Electrical Conductivity of Polypyrrole/Copolyester Composite Films," *Polymer Bulletin* 1998, 41, 713-719.

Balci, N.; Bayramli, E.; Toppare, L. "Conducting Polymer Composites: Polypyrrole and Poly(vinyl chloride-vinyl acetate) Copolymer," *Journal of Applied Polymer Science* 1997, 64, 667-671.

Beck, F.; Ruetschi, P. "Rechargeable Batteries with Aqueous Electrolytes," *Electrochimica Acta* 2000, 45(15/16), 2467-2482.

Bein, T.; Enzel, P. "Encapsulation of Polypyrrole Chains in Zeolite Channels," *Angewandte Chemie International Edition* 1989, 28(12), 1692-1694.

Benseddik, E.; Bonnet, A.; Lefrant, S. "Transport Properties in Polypyrrole Powders and in PPy-PVA Composites: Evidence for Bipolaronic Clusters," *Journal of Applied Polymer Science* 1998, 68, 709-713.

Benseddik, E.; Makhlouki, M.; Bernede, J. C.; Lefrant, S.; Pron, A. "XPS Studies of Environmental Stability of Polypyrrole-Poly(vinyl alcohol) Composites," *Synthetic Metals* 1995, 72, 237-242.

Bhattacharya, A.; De, A. "Conducting Composites of Polypyrrole and Polyaniline: A Review," *Progress in Solid State Chemistry* 1996, 24, 141-181.

Bittihn, R.; Ely, G.; Woeffler, F. "Polypyrrole As an Electrode Material for Secondary Lithium Cells," *Makromolekulare Chemie. Macromolecular Symposia* 1987, 8, 51-59.

Bleha, M.; Kudela, V.; Rosava, E. Yu.; Polotskaya, G. A.; Kozlov, A. G.; Elyashevich, G. K. "Synthesis and Characterization of Thin Polypyrrole Layers on Polyethylene Microporous Films," *European Polymer Journal* 1999, 35, 613-620.

Boinowitz, T; Sude, G. T.; Tormin, U.; Krohn, H.; Beck, F. "A Metal-Free Polypyrrole/ Graphite Secondary Battery with An Anion Shuttle Mechanism," *Journal of Power Sources* 1995, 56, 179-187.

Brahim, S.; Narinesingh, D.; Guiseppi-Elie, A. "Polypyrrole-Hydrogel Composites for the Construction of Clinically Important Biosensors," *Biosensors and Bioelectronics* 2002, 17(1-2), 53-59.

Bredas, J. L.; Themans, B.; Andre, J. M.; Chance, R. R.; Silbey, R. "The Role of Mobile Organic Radicals and Ions (Solitons, Polarons and Bipolarons) in the Transport Properties of Doped Conjugated Polymers," *Synthetic Metals* 1984a, 9, 265-274.

Bredas, J. L.; Scott, J. C.; Yakushi, K.; Street, G. B. "Polarons and Bipolarons in Polypyrrole: Evolution of the Band Structure and Optical Spectrum Upon Doping," *Physical Review B* 1984b, 30(2), 1023-1025.

Brunswick, A.; Cavanaugh, T. J.; Mathur, D.; Russo, A. P.; Nauman, E. B. "Experimental Confirmation of Computer-Aided Polymer Blend Designs," *Journal of Applied Polymer Science* 1998, 68, 339-343.

Cai, Z.; Martin, C. R. "Electronically Conductive Polymer Fibers with Mesoscopic Diameters Show Enhanced Electronic Conductivities," *Journal of the American Chemical Society* 1989, 111, 4138-4139.

Canelas, D. A.; Betts, D. E.; DeSimone, J. M. "Dispersion Polymerization of Styrene in Supercritical Carbon Dioxide: Importance of Effective Surfactants," *Macromolecules* 1996, 29, 2818-2821.

Cassignol, C.; Cavarero, M.; Boudet, A.; Ricard, A. "Mocrostructure-Conductivity Relationship in Conducting Polypyrrole/Epoxy Composites," *Polymer* 1999, 40, 1139-1151.

Castillo-Ortega, M. M.; Encinas, J. C.; Rodriguez, D. E.; Olayo, R. "Preparation and Characteristic of Electroconductive Polypyrrole-Thermoplastic Composites," *Journal of Applied Polymer Science* 2001, 81, 1498-1506.

Cepak, V. M.; Martin, C. R. "Preparation of Polymeric Micro- and Nanostructures Using a Template-Based Deposition Method," *Chemistry of Materials* 1999, 11(5), 1363-1367.

Chandrasekhar, P. "1. Basics of Conducting Polymers (CPs)," In *Conducting Polymers, Fundamentals and Applications: A Practical Approach*, Kluwer Academic Publishers, Massachusetts, 1999a, 3-22.

Chandrasekhar, P. "15. Batteries," In *Conducting Polymers, Fundamentals and Applications: A Practical Approach*, Kluwer Academic Publishers, Massachusetts, 1999b, 433-452.

Cheah, K.; Forsyth, M.; Truong, V.-T. "Ordering and Stability in Conducting Polypyrrole," *Synthetic Metals* 1998, 94, 215-219.

Chen, X.; Wudl, F.; Mal, A. K.; Shen, H.; Nutt, S. R. "New Thermally Remendable Highly Cross-Linked Polymeric Materials," *Macromolecules* 2003, 36, 1802-1807.

Chen, X.; Devaux, J.; Issi, J.-P.; Billaud, D. "Chemically Oxidized Polypyrrole: Influence of the Experimental Condictions on Its Electrical Conductivity and Morphology," *Polymer Engineering and Science* 1995, 35(8), 642-647.

Condo, P. D.; Sumpter, S. R.; Lee, M. L.; Johnston, K. P. "Partition Coefficients and Polymer-Solute Interaction Parameters by Inverse Supercritical Fluid Chromatography," *Industrial and Engineering Chemistry Research* 1996, 35, 1115-1123.

Condo, P. D.; Sanchez, I. C.; Panayiotou, C. G.; Johnston, K. P. "Glass Transition Behavior Including Retrograde Vitrification of Polymers with Compressed Fluid Diluents," *Macromolecules* 1992, 25, 6119-6127.

Cooper, A. I. "Polymer Synthesis and Processing Using Supercritical Carbon Dioxide," *Journal of Materials Chemistry* 2000, 10, 207-234.

Defieuw, G.; Samijin, R.; Hoogmartens, I.; Vanderzande, D.; Gelan, J. "Antistatic Polymer Layers Based on Poly(isothianaphthene) Applied from Aqueous Compositions," *Synthetic Metals* 1993, 57, 3702-3706.

DeJesus, M. C.; Weiss, R. A.; Hahn, S. F. "Synthesis of Conductive Nanocomposites by Selective In Situ Polymerization of Pyrrole within the Lamellar Microdomains of a Block Copolymer," *Macromolecules* 1998, 31, 2230-2235.

DeJesus, M. C.; Fu, Y.; Weiss, R. A. "Conductive Polymer Blends Prepared by In Situ Polymerization of Pyrrole: A Review," *Polymer Engineering and Science* 1997a, 37(12), 1936-1943.

DeJesus, M. C.; Weiss, R. A.; Chen, Y. "The Development of Conductive Composite Surfaces by a Diffusion-Limited In Situ Polymerization of Pyrrole in Sulfonated Polystyrene Ionomers," *Journal of Polymer Science, Part B, Polymer Physics* 1997b, 35, 347-357.

DeSimone, J. M. "Synthesis of Conductive Polymers in Liquid and Supercritical CO_2," *PCT WO* 98/43250.

DeSimone, J. M.; Guan, Z.; Elsbernd, C. S. "Synthesis of Fluoropolymers in Supercritical Carbon Dioxide," *Science* 1992, 257, 945-947.

Diaz, A. F.; Crowley, J.; Bargon, J.; Gardini, G. P.; Torrance, J. B. "Electrooxidation of Aromatic Oligomers and Conducting Polymers," *Journal of Electroanalytical Chemistry* 1981, 121, 355-361.

Diaz, A. F.; Kanazawa, K. K.; Gardini, G. P. "Electrochemical Polymerization of Pyrrole*," Journal of the Chemical Society, Chemical Communications* 1979, 8, 635-636.

Dutta, P.; De, S. K. "Electrical Properties of Polypyrrole Doped with β-Naphthalenesulfonicacid and Polypyrrole-Polymethyl Methacrylate Blends," *Synthetic Metals* 2003, 139, 201-206.

Epstein, A. J.; Rommelmann, H.; Bigelow, R.; Gibson, H. W.; Hoffmann, D. M.; Tanner, D. B. "Role of Solitons in Nearly Metallic Polyacetylene," *Physical Review Letters* 1983, 50(23), 1866-1869.

Falcao, E. H. L.; DeAzevedo, W. M. "Polyaniline-Poly(vinyl alcohol) Composite As an Optical Recording Material," *Synthetic Metals* 2002, 128, 149-154.

Fang, R.-B.; Zhang, S.-H.; Zhang, W.-H. "Determination of Solubilities of Iodine and Sulfur in Supercritical CO_2 Using Chromatographic Retention Method," *Chemical Journal of Chinese Universities* 1997, 18, 869-872

Fournier, J.; Boiteux, G.; Seytre, G.; Marichy, G. "Percolation Network of Polypyrrole in Conducting Polymer Composites," *Synthetic Metals* 1997, 84, 839-840.

Fu, Y.; Weiss, R. A.; Gan, P. P.; Bessette, M. D. "Conductive Elastomeric Foams Prepared by In Situ Vapor Phase Polymerization of Pyrrole and Copolymerization of Pyrrole and N-Methylpyrrole," *Polymer Engineering and Science* 1998, 38(5), 857-862.

Fu, Y.; Palo, D. R.; Erkey, C.; Weiss, R. A. "Synthesis of Conductive Polypyrrole/ Polyurethane Foams via a Supercritical Fluid Process," *Macromolecules* 1997, 30, 7611-7613.

Gangopadhyay, R.; De, A. "Conducting Polymer Nanocomposites: A Brief Overview," *Chemistry of Materials* 2000, 12, 608-622.

Gao, J.; Heeger, H.; Lee, J. Y.; Kim, C. Y. "Soluble Polypyrrole As the Transparent Anode in Polymer Light-Emitting Diodes," *Synthetic Metals* 1996, 82, 221-223.

Ghoshal, S. K. "Resonant Third-Order Optical Nonlinearity in Polypyrrole," *Chemical Physics Letters* 1989, 158, 65-69.

Gibson, L. J.; Ashby, M. F. "5 The Mechanics of Foams: Basic Results," In *Cellular Solids: Structure and Properties*, Pergamon Press, New York, 1988, 120-168.

Gilani, T. H.; Masui, T.; Logvenov, G. Y.; Ishiguro, T. "Low-Temperature Hall Effect and Thermoelectric Power in Metallic PF_6-Doped Polypyrrole," *Synthetic Metals* 1996, 78, 327-331.

Guernion, N.; Ewen, R. J.; Pihlainen, K.; Ratcliffe, N. M.; Teare, G. C. "The Frabrication and Characterisation of A Highly Sensitive Polypyrrole Sensor and Its Electrical Responses to Amines of Differing Basicity at High Humidities," *Synthetic Metals* 2002, 126, 301-310.

Gulsen, D.; Hacarloglu, P.; Toppare, L.; Yilmaz, L. "Effect of Preparation Parameters on the Performance of Conductive Composite Gas Separation Membranes," *Journal of Membrane Science* 2001, 182, 29-39.

Hatakeyama, T.; Quinn, F.-X. "4 Thermogravimetry," In *Thermal Analysis: Fundamentals and Applications to Polymer Science, Second Edition*, New York, Wiley, 1999, 45-71.

Higgins, R. A. "3 The Crystal," In *Properties of Engineering Materials, Second Edition*, Industrial Press Inc., New York, 1994, 33-65.

Hong, X. M.; Tyson, J. C.; Collard, D. M. "Controlling the Macromolecular Architecture of Poly(3-alkylthiophene)s by Alternating Alkyl and Fluoroalkyl Substituents," *Macromolecules* 2000, 33, 3502-3504.

Hotta, S.; Rughooputh, S. D. D. V.; Heeger, A. J.; Wudl, F. "Spectroscopic Studies of Soluble Poly(3-alkylthienylenes)," *Macromolecules* 1987, 20, 212-215.

Huang, J.-C. "EMI Shielding Plastics: A Review," *Advances in Polymer Technology* 1995, 14(2), 137-150.

Ikegame, M.; Tajima, K.; Aida, T. "Template Synthesis of Polypyrrole Nanofibers Insulated within One-Dimensional Silicate Channels: Hexagonal Versus Lamellar for Recombination of Polarons into Bipolarons," *Angewandte Chemie International Edition* 2003, 42(19), 2154-2157.

Isotalo, H.; Ahlskog, M.; Stubb, H.; Laakso, J.; Karna, T.; Jussila, M.; Oesterholm, J. E. "Stability of Processed Poly(3-octylthiophene) and Its Blends," *Synthetic Metals* 1993, 55-57, 3581-3586.

Iwasaki, K.; Fujimoto, H.; Matsuzaki, S. "Conformational Changes of Poly(3-alkylthiophene)s with Temperature and Pressure," *Synthetic Metals* 1994, 63, 101-108.

Jiang, P.; Ostojic, G. N.; Narat, R.; Mittleman, D. M.; Colvin, V. L. "The Fabrication and Bandgap Engineering of Photonic Multilayers," *Advanced Materials* 2001, 13(6), 389-393.

Jiang, P.; Hwang, K. S.; Mittleman, D. M.; Bertone, J. F.; Colvin, V. L. "Template-Directed Preparation of Macroporous Polymers with Oriented and Crystalline Arrays of Voids," *Journal of the American Chemical Society* 1999, 121, 11630-11637.

Jen, K.-Y.; Miller, G. G.; Elsenbaumer, R. L. "Highly Conducting, Soluble, and Environmentally-Stable Poly(3-alkylthiophenes)," *Journal of the Chemical Society, Chemical Communications* 1986, 1346-1347.

Jonas, F.; Heywang, G. "Technical Applications for Conductive Polymers," *Electrochimica Acta* 1994, 39(8/9), 1345-1347.

Kaiser, A. B. "Electronic Transport Properties of Conducting Polymers and Carbon Nanotubes," *Reports on Progress in Physics* 2001a, 64, 1-49.

Kaiser, A. B. "Systematic Conductivity Behavior in Conducting Polymers: Effects of Heterogeneous Disorder," *Advanced Materials* 2001b, 13(12-13), 927-941.

Kamada, K.; Kamo, J.; Motonaga, A.; Iwasaki, T.; Hosokawa, H. "Gas Permeation Properties of Conducting Polymer Porous-Media Composite Membranes: 1.," *Polymer Journal* 1994, 26(2), 141-149.

Kang, E. T.; Neoh, K. G.; Tan, T. C.; Ong, Y. K. "The Polymerization and Oxidation of Pyrrole by Halogens in Organic Solvents," *Journal of Macromolecular Science, Chemistry* 1987, A24(6), 631-644.

Kazarian, S. G.; Vincent, M. F.; West, B. L.; Eckert, C. A. "Partitioning of Solutes and Cosolvents between Supercritical CO_2 and Polymer Phases," *The Journal of Supercritical Fluids* 1998, 13, 107-112.

Kemp, N. T.; Kaiser, A. B.; Liu, C.-J.; Chapman, B.; Mercier, O.; Carr, A. M.; Trodahl, H. J.; Buckley, R. G.; Partridge, A. C.; Lee, J. Y.; Kim, C. Y.; Bartl, A.; Dunsch, L.; Smith, W. T.; Shapiro, J. S. "Thermoelectric Power and Conductivity of Different Types of Polypyrrole," *Journal of Polymer Science, Part B, Polymer Physics* 1999, 37, 953-960.

Kendall, J. L.; Canelas, D. A.; Young, J. L.; DeSimone, J. M. "Polymerizations in Supercritical Carbon Dioxide," *Chemical Reviews* 1999, 99, 543-563.

Kerton, F. M.; Lawless, G. A.; Armes, S. P. "First Example of a Conducting Polymer Synthesised in Supercritical Fluids," *Journal of Materials Chemistry* 1997, 7(10), 1965-1966.

Khor, E.; Li, H. C.; Wee, A. "In Situ Polymerization of Pyrrole in Animal Tissue in the Formation of Hybrid Biomaterials," *Biomaterials* 1995, 16, 657-661.

Kim, I. T.; Elsenbaumer, R. L. "Chemical Synthesis and Properties of Poly(1-alkyl 2,5-pyrrolylene)," *Synthetic Metals* 1997, 84, 157-158.

Kim, J.; Sohn, D.; Sung, Y.; Kim, E.-R. "Fabrication and Characterization of Conductive Polypyrrole Thin Film Prepared by In Situ Vapor-Phase Polymerization," *Synthetic Metals* 2003, 132, 309-313.

Kirby C. F.; McHugh, M. A. "Phase Behavior of Polymers in Supercritical Fluid Solvents," *Chemical Reviews* 1999, 99, 565-602.

Koezuka, H.; Tsumura, A. "Field-Effect Transistor Utilizing Conducting Polymers," *Synthetic Metals* 1989, 28, 753-760.

Kontturi, K.; Pentti, P.; Sundholm, G. "Polypyrrole As a Model Membrane for Drug Delivery," *Journal of Electroanalytical Chemistry* 1998, 453, 231-238.

Kopanski, J. J.; Marchiando, J. F.; Lowney, J. R. "Scanning Capacitance Microscopy Applied to Two-Dimensional Dopant Profiling of Semiconductors," *Materials Science and Engineering, B, Solid-State Materials for Advanced Technology* 1997, 44, 46-51.

Kossmehl, G.; Engelmann, G. "10 Application of Electrically Conductive Polythiophenes," In *Handbook of oligo- and polythiophenes*, Fichou, D. Ed., Wiley-VCH, Weinheim, 1999, 491-524.

Kowalik, J.; Tolbert, L. M.; Narayan, S.; Abhiraman, A. S. "Electrically Conducting Poly(undecylbithiophene)s. 1. Regioselective Synthesis and Primary Structure," *Macromolecules* 2001, 34, 5471-5479.

Kuhn, H. H.; Child, A. D. "35 Electrically Conducting Textiles," In *Handbook of Conducting Polymers, Second Edition, Revised and Expanded*, Skotheim, T. A.; Elsenbaumer, R. L.; Reynolds, J. R. Ed., Marcel Dekker, Inc., New York, 1998, 993-1013.

Kumar, D.; Sharma, R. C. "Advances in Conductive Polymers," *European Polymer Journal* 1998, 34(8), 1053-1060.

Kung, E.; Lesser, A. J.; McCarthy, T. J. "Composites Prepared by the Anionic Polymerization of Ethyl 2-Cyanoacrylate within Supercritical Carbon Dioxide-Swollen Poly(tetrafluoroethylene-*co*-hexafluoropropylene)," *Macromolecules* 2000, 33, 8192-8199.

Kung, E.; Lesser, A. J.; McCarthy, T. J. "Morphology and Mechanical Performance of Polystyrene/Polyethylene Composites Prepared in Supercritical Carbon Dioxide," *Macromolecules* 1998, 31, 4160-4169.

Lee, W.-J.; Kim, Y.-J.; Jung, M.-O.; Kim, D.-H.; Cho, D. L.; Kaang, S. "Preparation and Properties of Conducting Polypyrrole-Sulfonated Polycarbonate Composites," *Synthetic Metals* 2001, 123, 327-333.

Lee, H. S.; Hong, J. "Chemical Synthesis and Characterization of Polypyrrole Coated on Porous Membranes and Its Electrochemical Stability," *Synthetic Metals* 2000a, 113, 115-119.

Lee, Y. H.; Lee, J. Y.; Lee, D. S. "A Novel Conducting Soluble Polypyrrole Composite with A Polymeric Co-Dopant," *Synthetic Metals* 2000b, 114, 347-353.

Lee, J. Y.; Song, K. T.; Kim, S. Y.; Kim, Y. C.; Kim, D. Y.; Kim, C. Y. "Synthesis and Characterization of Soluble Polypyrrole," *Synthetic Metals* 1997a, 84, 137-140.

Lee, W. P.; Park, Y. W.; Choi, Y. S. "Metallic Electrical Transport of PF_6-Doped Polypyrrole: DC Conductivity and Thermoelectric Power," *Synthetic Metals* 1997b, 84, 841-842.

Lee, J. Y.; Kim, D. Y.; Kim, C. Y. "Synthesis of Soluble Polypyrrole of the Doped State in Organic Solvents," *Synthetic Metals* 1995, 74, 103-106.

Lei, J.; Martin, C. R. "Infrared Investigations of Pristine Polypyrrole: Is the Polymer Called Polypyrrole Really Poly(pyrrole-*co*-hydroxypyrrole)?" *Synthetic Metals* 1992, 48, 331-336.

Li, G.; Pickup, P. G. "Ion Transport in a Chemically Prepared Polypyrrole/Poly(styrene-4-sulfonate) Composite," *The Journal of Physical Chemistry* 1999, 103, 10143-10148.

Lin, A. S. P.; Barrows, T. H.; Cartmell, S. H.; Guldberg, R. E. "Microarchitectural and Mechanical Characterization of Oriented Porous Polymer Scaffolds," *Biomaterials* 2003, 24, 481-489.

Liu, Y.; Cui, T.; Varahramyan, K. "Fabrication and Characteristics of Polymeric Thin-Film Capacitor," *Solid-State Electronics* 2003, 47(5), 811-814.

Liu, J.; Wan, M. "Composites of Polypyrrole with Conducting and Ferromagnetic Behaviors," *Journal of Polymer Science, Part A, Polymer Chemistry* 2000, 38, 2734-2739.

Liu, J.-M.; Sun, L.; Yang, S. C. "Molecular Complex of Conductive Polymer and Polyelectrolyte; and A Process of Producing Same," *U. S. Patent* No. 5489400, 1996.

Lu, Y.; Shi, G.; Li, C.; Liang, Y. "Thin Polypyrrole Films Prepared by Chemical Oxidative Polymerization," *Journal of Applied Polymer Science* 1998, 70, 2169-2172.

Machida, S.; Miyata, S. "Chemical Synthesis of Highly Electrically Conductive Polypyrrole," *Synthetic Metals* 1989, 31, 311-318.

Maia, D. J.; Zarbin, A. J. G.; Alves, O. L.; DePaoli M.-A. "Glass-Encapsulated Molecular Wires: A Polypyrrole/Porous Glass Composite," *Advanced Materials* 1995, 7(9), 792-794.

Makhlouki, M.; Morsli, M.; Bonnet, A.; Conan, A.; Pron, A.; Lefrant, S. "Transport Properties in Polypyrrole-PVA Composites: Evidence for Hopping Condition," *Journal of Applied Polymer Science* 1992, 44, 443-446.

Malinauskas, A. "Chemical Deposition of Conducting Polymers," *Polymer* 2001, 42, 3957-3972.

Mano, V.; Felisberti, M. I.; Matencio, T.; DePaoli, M.-A. "Thermal, Mechanical and Electrochemical Behavior of Poly(vinyl chloride)/Polypyrrole Blends (PVC/PPy)," *Polymer* 1996, 37(23), 5165-5170.

Martin, C. R. "Nanomaterials: A Membrane-Based Synthetic Approach," *Science* 1994, 266, 1961-1966.

Martin, C. R.; Liang, W.; Menon, V.; Parthasarathy, R.; Parthasarathy, A. "Electronically Conductive Polymers As Chemically Selective Layers for Membrane-Based Separations," *Synthetic Metals* 1993, 57(1), 3766-3773.

Masubuchi, S.; Kazama, S.; Matsushita, R.; Matsuyama, T. "The Influence of Dopant Species on Transport Properties in As-Grown Polypyrrole Films Prepared by Electrochemical Method," *Synthetic Metals* 1995, 69, 345-346.

Mellor, W.; Wright, E.; Clift, R.; Azapagic, A.; Stevens, G. "A Mathematical Model and Decision-Support Framework for Material Recovery, Recycling, and Cascaded Use," *Chemical Engineering Science* 2002, 57, 4697-4713.

Middlecoff, J. S.; Collard, D. M. "Perfluoroalkyl Substituted Polythiophenes: Poly(2-(3-thienyl)ethyl perfluoroalkanoates)s," *Synthetic Metals* 1997, 84, 221-222.

Mohamed, A. B. H.; Miane, J. L.; Zangar, H. "Radiofrequency and Microwave (10 kHz-8 GHz) Electrical Properties of Polypyrrole and Polypyrrole-Poly(methyl methacrylate) Composites," *Polymer International* 2001, 50, 773-777.

Morsli, M.; Bonnet, A.; Samir, F.; Jousseaume, V.; Lefrant, S. "Electrical Conductivity and Thermoelectric Power of Polybithiophene-Polystyrene Composites," *Synthetic Metals* 1996, 76, 273-276.

Mott, N. F.; Davis, E. A. "2 Theory of Electrons in a Non-Crystalline Medium," In *Electronic Processes in Non-Crystalline Materials, Second Edition*, Clarendon Press, Oxford, 1979, 7-64.

Muth, O.; Hirth, Th.; Vogel, H. "Polymer Modification by Supercritical Impregnation," *The Journal of Supercritical Fluids* 2000, 17, 65-72.

Myers, R. E. "Chemical Oxidative Polymerization As a Synthetic Route to Electrically Conducting Polypyrroles," *Journal of Electronic Materials* 1986, 15, 61-69.

Narayan, S. "Synthesis and Characterization of Electrically Conducting Poly(undecyl bithiophene)s," *Ph. D. thesis*, Georgia Institute of Technology, 1999.

Newman, P. R.; Warren, Jr., L. F.; Witucki, E. F. "Process for Producing Electrically Conductive Composites and Composites Produces Therein," *U. S. Patent* No. 4617228, 1986.

Ngo, T. T.; Liotta, C. L.; Eckert, C. A.; Kazarian, S. G. "Supercritical Fluid Impregnation of Different Azo-Dyes into Polymer: In Situ UV/Vis Spectroscopic Study," *The Journal of Supercritical Fluids* 2003, 215-221.

Nikpour, M.; Chaouk, H.; Mau, A.; Chung, D. J.; Wallace, G. "Porous Conducting Membranes Based on Polypyrrole-PMMA Composites," *Synthetic Metals* 1999, 99, 121-126.

Novak, P. "Limitations of Polypyrrole Synthesis in Water and Their Causes," *Electrochimica Acta* 1992, 37, 1227-1230.

Ogasawara, M.; Funahashi, K.; Demura, T.; Hagiwara, T.; Iwata, K. "Enhancement of Electrical Conductivity of Polypyrrole by Stretching," *Synthetic Metals* 1986, 14, 61-69.

Ogasawara, M.; Funahashi, K.; Iwata, K. “Enhancement of Electric-Conductivity of Polypyrrole by Stretching,” *Molecular Crystals and Liquid Crystals* 1985, 118, 159-162.

Ojio, T.; Miyata, S. “Highly Transparent and Conducting Polypyrrole-Poly(vinyl alcohol) Composite Films Prepared by Gas State Polymerization,” *Polymer Journal* 1986,18(1), 95-98.

Omastova, M.; Simon, F. “Surface Characterizations of Conductive Poly(methyl methacrylate)/Polypyrrole Composites,” *Journal of Materials Science* 2000, 35, 1743-1749.

Omastova, M.; Chodak, I.; Pionteck, J. “Electrical and Mechanical Properties of Conducting Polymer Composites,” *Synthetic Metals* 1999, 102, 1251-1252.

Omastova, M.; Pavlinec, J.; Pionteck, J.; Simon, F.; Kosina, S. “Chemical Preparation and Characterization of Conductive Poly(methyl methacrylate)/ Polypyrrole Composites,” *Polymer* 1998, 39(25), 6559-6566.

Omastova, M.; Pavlinec, J.; Pionteck, J.; Simon, F. “Synthesis, Electrical Properties and Stability of Polypyrrole-Containing Conducting Polymer Composites,” *Polymer International* 1997, 43, 109-116.

Omastova, M.; Kosina, S.; Pionteck, J.; Janke, A.; Pavlinec, J. “Electrical Properties and Stability of Polypyrrole Containing Conducting Polymer Composites,” *Synthetic Metals* 1996a, 81, 49-57.

Omastova, M.; Pionteck, J.; Kosina, S. “Preparation and Characterization of Electrically Conductive Polypyropylene/ Polypyrrole Composites,” *European Polymer Journal* 1996b, 32(6), 681-689.

Onoda, M.; Moritake, T.; Matsuda, T.; Nakayama, H. “Physical Properties and Application of Conducting Polypyrrole-Silica Glass Composite Films Prepared by Electrochemical Polymerization,” *Synthetic Metals* 1995, 71, 2255-2256.

Park, J. S.; Ruckenstein, E. "Conducting Polyheterocycle Composites Based on Porous Host," *Journal of Electronic Materials* 1992, 21(2), 205-215.

Paul, D. K.; Mitra, S. S. "Evaluation of Mott's Parameters for Hopping Conduction in Amorphous Ge, Si, and Se-Si," *Physical Review Letters* 1973, 31(16), 1000-1003.

Pionteck, J.; Omastova, M.; Potscheke, P.; Simon, F.; Chodak, I. "Morphology, Conductivity, and Mechanical Properties of Polypyrrole-Containing Composites," *Journal of Macromolecular Science, Physics* 1999, B38(5/6), 737-748.

Pomerantz, M.; Tseng, J. J.; Zhu, H.; Sproull, S. J.; Reynolds, J. R.; Uitz, R.; Arnott, H. J. "Processable Polymers and Copolymers of 3-alkylthiophenes and Their Blends," *Synthetic Metals* 1991, 41-43, 825-830.

Pomposo, J. A.; Rodriguez, J.; Grande, H. "Polypyrrole-Based Conducting Hot Melt Adhesives for EMI Shielding Applications," *Synthetic Metals* 1999, 104, 107-111.

Powell, M. J. "Site Percolation in Randomly Packed Spheres," *Physical Review B* 1979, 20(10), 4194-4198.

Pron, A.; Fabianowski, W.; Budrowski, C.; Raynor, B.; Kucharski, Z.; Suwalski, J.; Lefrant, S.; Fatseas, G. "Polypyrrole Films Grown on the Surface of a Polyvinyl: Ferric Chloride Complex," *Synthetic Metals* 1987, 18, 49-52.

Przyluski, J.; Zagorska, M.; Conder, K.; Pron, A. "Electrochemical Synthesis of Polyacetylene Tetrachloroferrate $[CH(FeCl_4)_y]_x$ and tetrachloroaluminate $[CH(AlCl_4)_y]_x$," *Polymer* 1982, 23, 1872-1874.

Rajagopalan, P.; McCarthy, T. J. "Two-Step Surface Modification of Chemically Resistant Polymers: Blend Formation and Subsequent," *Macromolecules* 1998, 31, 4791-4797.

Ratcliffe, N. M. "Polypyrrole-Based Sensor for Hydrazine and Ammonia," *Analytica Chimica Acta* 1990, 239, 257-262.

Roberts, W. P.; Schulz, A. "Method of Forming Electrically Conductive Polymer Blends," *U. S. Patent* No. 4604427, 1986.

Rodeheaver, B. A. "Open-Celled Microcellular Themoplastic Foam," *M. S. thesis*, Georgia Institute of Technology, 2000.

Rosenbrock, H. H. "An Automatic Method for Finding the Greatest or Least Value of a Function," *Computer Journal* 1960, 3(3), 175-184.

Roy, R.; Sen, S. K.; Digar, M.; Bhattacharyya, S. N. "Conductivity and Thermoelectric Power in Conducting Polypyrrole Films," *Journal of Physics, Condensed Matter* 1991, 3, 7849-7856.

Ruckenstein, E.; Park, J. S. "New Method for the Preparation of Thick Conducting Polymer Composites," *Journal of Applied Polymer Science* 1991a, 42, 925-934.

Ruckenstein, E.; Park, J. S. "Polythiophene and Polythiophene-Based Conducting Composites," *Synthetic Metals* 1991b, 44, 293-306.

Ruckenstein, E.; Park, J. S. "Hydrophilic-Hydrophobic Polymer Composites," *Journal of Polymer Science, Part C, Polymer Letters* 1988, 26, 529-536.

Sarbu, T.; Styranec, T. J.; Beckman, E. J. "Design and Synthesis of Low Cost, Sustainable CO_2-philes," *Industrial and Engineering Chemistry Research* 2000, 39, 4678-4683.

Sarrazin, J.; Persin, M.; Cretin, M. "Conductive Polymer Membranes," *Macromolecular Symposia* 2002, 188, 1-12.

Sato, M.; Tanaka, S.; Kaeriyama, K. "Soluble Conducting Polythiophenes," *Journal of the Chemical Society, Chemical Communications* 1986, 873-874.

Saunders, B. R.; Fleming, R. J.; Murray, K. S. "Recent Advances in the Physical and Spectroscopic Properties of Polypyrrole Films, Particularly Those Containing Transition-Metal Complexes As Counteranions," *Chemistry of Materials* 1995, 7, 1082-1094.

Saurin, M.; Armes, S. P. "Study of the Chemical Polymerization of Pyrrole onto Printed Circuit Boards for Electroplating Applications," *Journal of Applied Polymer Science* 1995, 56, 41-50.

Scher, H.; Zallen, R. "Critical Density in Percolation Processes," *Journal of Chemical Physics* 1970, 53, 3759-3761.

Scott, J. C.; Pfluger, P.; Krounbi, M. T.; Street, G. B. "Electron-Spin-Resonance Studies of Pyrrole Polymers: Evidence for Bipolarons," *Physical Review B* 1983, 28(4), 2140-2145.

Selampinar, F.; Toppare, L.; Akbulut, U.; Yalcin, T.; Suzer, S. "A Conducting Composite of Polypyrrole, II. As A Gas Sensor," *Synthetic Metals* 1995, 68, 109-116.

Shacklette, L. W.; Colaneri, N. F.; Kulkarni, V. G.; Wessling, B. "EMI Shielding of Intrinsically Conductive Polymers," *Journal of Vinyl Technology* 1992, 14, 2, 118-122.

Sheng, P. "Fluctuation-Induced Tunneling Conduction in Disordered Materials," *Physical Review B* 1980, 21(6), 2180-2195.

Sheng, P.; Abeles, B.; Arie, Y. "Hopping Conductivity in Granular Metals," *Physical Review Letters* 1973, 31(1), 44-47.

Sheng, P.; Abeles, B. "Voltage-Induced Tunneling Conduction in Granular Metals at Low Temperatures," *Physical Review Letters* 1972, 28(1), 34-37.

Shenoy, S. L.; Cohen, D.; Weiss, R. A.; Erkey, C. "Supercritical Carbon Dioxide Aided Preparation of Conductive Polyurethane-Polypyrrole Composites," *The Journal of Supercritical Fluids* 2003, *in press*.

Shenoy, S. L.; Cohen, D.; Erkey, C.; Weiss, R. A. "A Solvent-Free Process for Preparing Conductive Elastomers by an In Situ Polymerization of Pyrrole," *Industrial and Engineering Chemistry Research* 2002, 41, 1484-1488.

Shenoy, S. L.; Kaya, I.; Erkey, C.; Weiss, R. A. "Synthesis of Conductive Elastomeric Foams by an In Situ Polymerization of Pyrrole Using Supercritical Carbon Dioxide and Ethanol Cosolvents," *Synthetic Metals* 2001, 123, 509-514.

Shirakawa, H.; Louis, E. J.; MacDiarmid, A. G.; Chiang, C. K.; Heeger, A. J. "Synthesis of Electrically Conducting Organic Polymers. Halogen Derivatives of Polyacetylene, $(CH)_X$," *Journal of the Chemical Society, Chemical Communications* 1977, 578-580.

Singh, R.; Chandra, S.; Singh, H. Narula, A. K.; Broor, S. "Conducting Polymer Membrane and A Process for the Preparation of the Same Membrane," *U. S. Patent* No. 6156202, 2000.

Singh, R.; Tandon, R. P.; Chandra, S. "Evidence of Small-Polaron Formation in Polypyrrole," *Journal of Physics, Condensed Matter* 1993, 5, 1313-1318.

Singh, R.; Tandon, R. P.; Chandra, S. "Mechanism of DC Conduction in Lightly Doped Polypyrrole Films," *Journal of Applied Physics* 1991a, 70(1), 243-245.

Singh, R.; Tandon, R. P.; Panwar, V. S.; Chandra, S. "Low-Frequency AC Conduction in Lightly Doped Polypyrrole Films," *Journal of Applied Physics* 1991b, 69(4), 2504-2511.

Sotomayor, P. T.; Raimundo, Jr., I. M.; Zarbin, A. J. G.; Rohwedder, J. J. R.; Neto, G. O.; DePaoli, M.-A.; Alves, O. L. "Construction and Evaluation of An Optical pH Sensor Based on Poyaniline-Porous Vycor Glass Nanocomposite," *Sensor and Actuators B* 2001, 71, 157-162.

Sree, U.; Yamamoto, Y.; Deore, B.; Shiigi, H.; Nagaoka, T. "Characterization of Polypyrrole Nano-Films for Membrane-Based Sensors," *Synthetic Metals* 2002, 131, 161-165.

Steckle, Jr., W. P.; Apen, P. G.; Mitchell, M. A. "Highly Cross-Linked Nanoporous Polymers," *U. S. Patent* No. 5629353, 1997.

Street, G. B.; Clarke, T. C.; Geiss, R. H.; Lee, V. Y.; Nazzal, A.; Pfluger, P.; Scott, J. C. "Characterization of Polypyrrole," *Journal de Physique* 1983, 44, C3, 599-606.

Tang, M.; Wen, T.-Y.; Du, T.-B.; Chen, Y.-P. "Synthesis of Electrically Conductive Polypyrrole-Polystyrene Composites Using Supercritical Carbon Dioxide: I. Effects of the Blending Conditions," *European Polymer Journal* 2003a, 39, 143-149.

Tang, M.; Wen, T.-Y.; Du, T.-B.; Chen, Y.-P. "Synthesis of Electrically Conductive Polypyrrole-Polystyrene Composites Using Supercritical Carbon Dioxide: II. Effects of the Doping Conditions," *European Polymer Journal* 2003b, 39, 151-156.

Teja, A. S.; Eckert, C. A. "Commentary on Supercritical Fluids: Research and Applications," *Industrial and Engineering Chemistry Research* 2000, 39, 4442-4444.

Thieblemont, J. C.; Planche, M. F.; Petrescu, C.; Bouvier, J. M.; Bidan, G. "Stability of Chemically Synthesized Polypyrrole Films," *Synthetic Metals* 1993, 59, 81-96.

Tishchenko, G.; Rosova, E.; Elyashevich, G. K.; Bleha, M. "Porosity of Microporous Polyethylene Membranes Modified with Polypyrrole and Their Diffusion Permeability to Low-Molecular Weight Substances," *Chemical Engineering Journal* 2000, 79, 211-217.

Uhlir, Jr., A. "The Potentials of Infinite Systems of Sources and Numerical Solutions of Problems in Semiconductor Engineering," *The Bell System Technical Journal* 1955, 34, 105-128.

van der Pauw, L. J. "A Method of Measuring Specific Resistivity and Hall Effect of Discs of Arbitrary Shape," *Philips Research Reports* 1958, 13(1), 1-9.

Walker, J. A.; Warren, L. F.; Witucki, E. F. "New Chemically Prepared Conducting Pyrrole Blacks," *Journal of Polymer Science, Part A, Polymer Chemistry* 1988, 26(5), 1285-1294.

Wallace, G. G.; Innis, P. C. "Inherently Conducting Polymer Nanostructures," *Journal of Nanoscience and Nanotechnology* 2002, 2(5), 441-451.

Wang, Y.; Sotzing, G. A.; Weiss, R. A. "Conductive Polymer Foams As Sensors for Valatile Amines," *Chemistry of Materials* 2003, 15, 375-377.

Watkins, J. J.; McCarthy, T. J. "Polymerization in Supercritical Fluid-Swollen Polymers: A New Route to Polymer Blends," *Macromolecules* 1994, 27, 4845-4847.

Wang, H. L.; Fernandez, J. E. "Conducting Polymer Blends: Polypyrrole and Poly(vinyl methyl ketone)," *Macromolecules* 1992, 25, 6179-6184.

Wang, H. L.; Toppare, L.; Fernandez, J. E. "Conducting Polymer Blends: Polythiophene and Polypyrrole Blends with Polystyrene and Poly(bisphenol A carbonate)," *Macromolecules* 1990, 23, 1053-1059.

Wang, W.-C. V.; Kramer, E. J.; Sachse, W. H. "Effects of High-Pressure CO_2 on the Glass Transition Temperature and Mechanical Properties of Polystyrene," *Journal of Polymer Science, Polymer Physics Edition* 1982, 20, 1371-1384.

Warren, L. F.; Klivans, D. S.; Maus, L. "Electrically Conductive Composites and Method of Preparation," *U. S. Patent* No. 4582575, 1986.

Watkins, J. J.; McCarthy, T. J. "Polymerization of Styrene in Supercritical CO_2-Swollen Poly(chlorotrifluoroethylene)," *Macromolecules* 1995, 28, 4067-4074.

Webb, K. F. "Synthesis, Blending, and Doping of Electrically Conducting Poly(3-undecylbithiophene) in Supercritical Carbon Dioxide," *Ph. D. thesis*, Georgia Institute of Technology, 2001.

Webb, K. F.; Teja, A. S. "Solubility and Diffusion of Carbon Dioxide in Polymers," *Fluid Phase Equilibria* 1999, 160, 1029-1034.

Webb, K. F. "Formation of Electrically Conductive Polymer Blends Using Supercritical Carbon Dioxide," *M. S. thesis*, Georgia Institute of Technology, 1998.

Weiss, R. A.; Shenoy, S. L.; Cohen, D. "Conductive Elastomeric Foams and Method of Manufacture Thereof," *PCT WO* 02/39464 A2.

Wessling, B. "19 Dispersion As the Key to Processing Conductive Polymers," In *Handbook of Conducting Polymers, Second Edition, Revised and Expanded*, Skotheim, T. A.; Elsenbaumer, R. L.; Reynolds, J. R. Ed., Marcel Dekker, Inc., New York, 1998, 467-530.

West, B. L.; Kazarian, S. G.; Vincent, M. F.; Brantley, N. H.; Eckert, C. A. "Supercritical Fluid Dyeing of PMMA Films with Azo-Dyes," *Journal of Applied Polymer Science* 1998a, 69, 911-919.

West, B. L.; Bush, D.; Brantley, N. H.; Vincent, M. F.; Kazarian, S. G.; Eckert, C. A. "Modeling the Effects of Cosolvent-Modified Supercritical Fluids on Polymers with a Lattice Fluid Equation of State," *Industrial and Engineering Chemistry Research* 1998b, 37, 3305-3311.

Wissinger, R. G.; Paulaitis, M. E. "Swelling and Sorption in Polymer-CO_2 Mixtures at Elevated Pressures," *Journal of Polymer Science, Part B, Polymer Physics* 1987, 25, 2497-2510.

Wong, P. T. C.; Chambers, B.; Anderson, A. P.; Wright, P. V. "Large Area Conducting Polymer Composites and Their Use in Microwave Absorbing Material," *Electronics Letters* 1992, 28(17), 1651-1653.

Xie, H.-Q.; Liu, C.-M.; Guo, J.-S. "Preparation of Conductive Polypyrrole Composites by In-Situ Polymerization," *Polymer International* 1999, 48, 1099-1107.

Yamamoto, T.; Zhou, Z.-H.; Ando, I.; Kikuchi, M. "Preparation of Poly(pyrrole) by Dehalogenation Polycondensation of 2,5-Dibromopyrrole with a Zero-Valent Nickel Complex and IR and Solid State 13C-NMR Spectra of the Polymer," *Makromolekulare Chemie, Rapid Communications* 1993, 14(12), 833-839.

Yang, J.; Yang, Y.; Hou, J.; Zhang, X.; Zhu, W.; Xu, M.; Wan, M. "Polypyrrole-Polypropylene Composite Films: Preparation and Properties," *Polymer* 1996, 37(5), 793-798.

Yin, W.; Yan, T.; Gan, L. M.; Chew, C. H.; Liu, H.; Gu, T. "Conductive Composite Flims Based on Polypyrrole and Crosslinked Poly(styrene/butyl acrylate/acrylic acid)," *European Polymer Journal* 1998a, 34(12), 1763-1766.

Yin, W.; Liu, H.; Yin, B.; Yan, T.; Gu, T. "Conducting Composite Films Based on Polypyrrole and Crosslinked Poly(methyl acrylate-*co*-hydroxyethyl acrylate)," *European Polymer Journal* 1998b, 34(5/6), 779-782.

Yin, W.; Liu, H.; Li, J.; Li, Y.; Gu, T. "Conducting Composite Films Based on Polypyrrole and Crosslinked Poly(styrene-butyl acrylate-hydroxyethyl acrylate)," *Journal of Applied Polymer Science* 1997, 64, 2293-2298.

Yoshioka, K.; Masubuchi, S.; Fukuhara, T.; Kazama, S. "Intrinsic Transport Properties in Polypyrrle," *Synthetic Metals* 1999, 101, 509-510.

Zalusky, A. S.; Olayo-Valles, R.; Wolf, J. H.; Hilmyer, M. A. "Ordered Nanoporous Polymers from Polystyrene-Polyactide Block Copolymers," *Journal of the American Chemical Society* 2002, 124, 12761-12773.

Zarbin, A. J. G.; DePaoli, M.-A.; Alves, O. L. "Nanocomposites Glass/Conductive Polymers," *Synthetic Metals* 1999, 99, 227-235.

Zarbin, A. J. G.; DePaoli, M.-A.; Alves, O. L. "New Polyaniline/Porous Glass Composite," *Synthetic Metals* 1997, 84, 107-108.

Zhou, D.; Too, C. O.; Wallace, G. G.; Hodges, A. M.; Mau, A. W. H. "Protein Transport and Separation Using Polypyrrole Coated, Platinised Poly(vinylidene fluoride) Membranes," *Reactive and Functional Polymers* 2000, 45(3), 217-226.

Zuppiroli, L.; Bussac, M. N.; Paschen, S.; Chauvet, O.; Forro, L. "Hopping in Disordered Conducting Polymers," *Physical Review B* 1994, 50(8), 5196-5203.

VITA

Shutaro Kurosawa was born in Tokyo, Japan in 1975. After graduation from Odawara High School in Spring 1994, he enrolled at School of Engineering, Tohoku University in Miyagi, Japan. He started his academic career in his senior year under Dr. Kunio Arai at Department of Biochemistry and Engineering, School of Engineering, Tohoku University.

After completing his Bachelor of Science in March, 1998, his admission to graduate school at Tohoku University was approved with the entrance exam waived due to his high class grade. He started graduate research under the direction of Dr. Hiroshi Inomata at Research Center of Supercritical Fluid Technology, Graduate School of Engineering, Tohoku University where he received his Masters of Science in March, 2000.

He went to Atlanta, Georgia to attend School of Chemical Engineering at the Georgia Institute of Technology. He started his doctoral research under Dr. Amyn S. Teja in August, 2000.

During his graduate career, he was awarded scholarship from The Japan Scholarship Foundation (1998-2000), Molecular Design Institute Graduate Student Research Fellowship/ Office of Naval Research 2002 and 2003. He was also honored for Outstanding Academic Achievement 2002-2003.

Publications

Sato, T.; Kurosawa, S.; Smith, R. L. Jr.; Adschiri, T.; and Arai, K.; "Water Gas Shift Reaction Kinetics under Noncatalytic Conditions in Supercritical Water," *The Journal of Supercritical Fluids*, In Press, Corrected Proof, Available online 24 April 2003,

Kurosawa, S.; Saito, D.; and Inomata, H.; "Viscosity Measurement of Molten Polystyrene in the Presence of Carbon Dioxide," *Proceedings of the 8th Fall Meeting, Japan Society of Polymer Processing*, p. 205-206, November 9th - 10th, 2000, Information Plaza of Hiroshima, Hiroshima, Japan.

Sato, T.; Kurosawa, S.; Adschiri, T.; Arai, K.; "Kinetics of the Water-Gas Shift Reaction in Supercritical Water," *Kagaku Kougaku Ronbunshu* 1999, 25(6), 993-997.

Adschiri, T.; Okazaki, S.; Mochiduki M.; Kurosawa, S.; and Arai, K.; "Hydrogenation through Partial Oxidation of Hydrocarbons in Supercritical Water," *International Journal of the Society of Material Engineering for Resources*, 1999, 7(2), 24-32.

Okazaki, S.; Kurosawa, S.; Adschiri, T.; and Arai, K.; "Catalytic Hydrogenation of Naphthalene through Water Gas Shift Reaction in Supercritical Water," *Proceedings of the 6th Japan-China Symposium on Coal and C1 Chemistry*, p. 192, October 13th - 17th, 1998, Zao Heights Hotel, Zao, Japan.

Okazaki, S.; Kurosawa, S.; Adschiri, T.; Arai, K; "Catalytic hydrogenation of naphthalene via water-gas-shift reaction in supercritical water," *34th Sekitan Kagaku Kaigi Happyo Ronbunshu* 1997, 61-63.

Presentations

Kurosawa, S.; Okazaki, S.; Adschiri, T.; and Arai, K.; "Catalytic Hydrogenation of Naphthalene through Water-Gas Shift Reaction in Supercritical Water," 31th Fall Meeting, The Society of Chemical Engineers, Japan, September 29th - October 1st, 1998, Yamagata University, Yonezawa, Japan.

Kurosawa, S.; Kowalik, J.; Tolbert, L.; and Teja, A. S.; "Supercritical Processing of Electrically Conducting Polymers," 2003 Annual Meeting, AIChE, November 16th-21th, San Francisco Hilton & Towers, San Francisco, California.